Title
The Role of SWI/SNF Chromatin Remodeling in Breast Tumorigenesis

Author
Stewart, Kathleen Marie

Publication Date
2010

Peer reviewed|Thesis/dissertation

The Role of SWI/SNF Chromatin Remodeling in Breast Tumorigenesis

by

Kathleen Marie Stewart

DISSERTATION

Submitted in partial satisfaction of the requirements for the degree of

DOCTOR OF PHILOSOPHY

in

Biomedical Sciences

in the

GRADUATE DIVISION

of the

UNIVERSITY OF CALIFORNIA, SAN FRANCISCO

Dedication

This work is dedicated to
my amazing husband, Jason

Acknowledgements

At times our own light goes out and is rekindled
by a spark from another person.
Each of us has cause to think with deep gratitude of those
who have lighted the flame within us.
Albert Schweitzer (1875 – 1965)

It is said that it takes a village to raise a child. Well, I believe the same adage holds true for graduate students and the many people that contribute to their education and training both in their professional and their personal lives. I could not have accomplished my graduate work without this bi-coastal village of mentors, advisors, labmates, classmates, friends and family to support me along the way.

First and foremost, I would like to thank my mentor Valerie Weaver. I am a stronger, more forthright woman at the end of this journey because of you and the lessons you have taught me that will aid in my professional and personal life I will carry with me forever. I would also like to thank the members of my thesis committee, Jayanta Debnath for his technical assistance and invaluable input, Nancy Boudreau for her support and guidance and last but certainly not least, Zena Werb, for her concise and frank suggestions and astute criticism.

Additionally, I would like to thank the Biomedical Science program administrators, Lisa Magargal, Kevin Luong and Monique Piazza for their incredible assistance in my transfer to UCSF and helping me adjust to my new academic setting. I would like to thank this great BMS team for always being a friendly face, an answer to all of my questions and a sage counselor on all things academic, career and personal.

There are many members of the Weaver lab, both past and present, which deserve mention for their contribution. Foremost, I would like to thank Johnathon Lakins for sharing his time and expertise and all of his hands on assistance with teaching me everything I know about molecular biology—I will try my best to not be a “Kit Scientist”! I would like to thank the current members of the Weaver lab for their scientific guidance and friendship including Christian Frantz, Matthew Paszek, Anna Kalousova, Janna Mouw and past members including, Penney Gilbert, Gabriela Rozenberg-McPhee, and Nastaran Zahir-Kuhn.

I would not have been able to survive living 3,000 miles away, isolated from all of my family and friends if not for the kindness and camaraderie I found in the Class of 2006 matriculates. I most enjoyed our monthly-ish get-togethers of the “Girls’ Book Club,” where neither books were read nor discussed with any frequency. It was an amazing place for us to vent, share triumphs and heartache, eat delicious epicurean delights and drink copious amounts of wine to unwind from our daily science life stresses. I would especially like to thank Kristen Coakley, Renee

Vanderlaan and Sarah Gierke for their unwavering support and amazing friendship. Especially, Kristen, my personal therapist, who rescued me from many days where I could not see a bright end in sight, your advice and encouragement, propelled me to the end of this long journey.

I also would like to thank the many students and faculty members at my former institution, University of Pennsylvania, where I began my scientific career. First and foremost I would like to thank my fellow CAMB classmates, Natasha Girgis, Rebecca Beerman and Stacie Dilks for their continued friendship and support, despite our inability to ever call at the right time (darn time zone differences!!). Lastly, I would like to thank my personal mentor, Dr. Brian Keith, who has always been a constant source of support, too kind words and great friendship—despite me leaving Penn almost three years ago!

No acknowledgement section would be complete without mentioning the friends who I call my family. To my good friend Tina Jiwatram, whom I met briefly while serving on the Social Events Committee of the Graduate and Professional Students' Association, yet ended up forming a life long friendship when we both serendipitously ended up living in San Francisco, thanks for always having a perfect and professional answer for all of my most pressing dilemmas, for being my ultimate style mentor/icon and for just being an incredibly giving and kind friend. To Dr. Sonal Desai, whom I met during her brief postdoc in the Weaver lab, thank you for being such a great source of laughter, creativity and great

recipes! To my good friends from my undergraduate/Animal Science days, Kimberly Such and Meryll Corbin, you toughed out this long journey with me, dealt with my infrequent phone calls and visits and remained such supportive and fun friends through it all—now Kim just has to graduate and we will all finally be done with school! To my best friend of over 20 years, Elizabeth Mullen, you are a sister to me and always will be and I look forward to another 20 years of excitement and fun with our burgeoning new families.

Last but certainly not least, I huge amount of gratitude goes to my family, sisters Kelly and Shannon, Mom and Dad and my loving husband Jason, for putting up with all of my emotional ups and downs on this long road. I honestly would have given up a long time ago if not for all of your encouraging words at every step and for at least pretending to be slightly interested in the science. I hope to make you all proud.

ABSTRACT OF THE DISSERTATION

The Role of SWI/SNF Chromatin Remodeling in Breast Tumorigenesis

Kathleen Marie Stewart

Doctor of Philosophy in Biomedical Sciences

UNIVERSITY OF CALIFORNIA, SAN FRANCISCO, 2010

Professor Valerie M. Weaver, Thesis Advisor

Mammary epithelial cell (MEC)-extracellular matrix (ECM) interactions are critical for normal breast tissue development, differentiation and homeostasis by engaging a repertoire of ECM adhesion receptors including integrins to activate signaling processes that control MEC differentiation, proliferation and survival. Malignant progression alters MEC responsiveness to ECM cues and is highlighted by the observation that the expression of integrins is altered during breast tumor progression. The molecular basis for altered integrins in breast tumors and the regulation of integrin changes during malignant transformation are less understood. The goal of my thesis is to test the hypothesis that oncogene-dependent transformation promotes breast tumor progression through regulating changes in ECM responsiveness via α5 integrin through targeting of the SWI/SNF chromatin remodeling protein BRM. I found that oncogene-driven transformation depends upon increased expression of α5 integrin to promote MEC growth and survival in three-dimensional (3D) cultures and implicates the SWI/SNF chromatin remodeling protein, Brahma (BRM) in the regulation of

tumor-driven ECM responsiveness changes. I also observed decreased BRM expression in breast cancer cell lines and abrogation of BRM in non-malignant MECs enhanced cell motility and anchorage independent growth and upregulated a gene program associated with breast tumor progression. Microarray analysis of breast cancer patient samples revealed that reduced BRM expression correlated with increased disease recurrence and morbidity. Whether BRM is a *bona fide* tumor suppressor in breast cancers and whether targeting the re-expression of BRM in breast tumors is a viable therapeutic target remains an area of active research. Nevertheless, regaining ECM responsiveness in breast tumor cells by manipulating chromatin is without precedent and forms the foundation for future investigations into the epigenetic mechanisms governing ECM responsiveness and may lead to the discovery of novel molecular targets in the treatment of breast cancer.

Table of Contents

List of Figures

Chapter One.

Chapter Two.

Chapter Three.

Chapter Four.

Chapter Five.

List of Tables

Chapter Three.

List of Abbreviations

AKT/PKB	Akv (Virus) transforming gene/protein kinase B
ATP	Adenosine-5'-triphosphate
BAF	BRM/BRG1 associated factors
BM	Basement membrane
BSA	Bovine serum albumin
CBP	CREB binding protein
C/EBPs	CCAAT-enhancer-binding proteins
Cdc42	Cell division cycle 42
CHD	Chromodomain helicase DNA-binding
CRC	Chromatin remodeling complexes
ChIP	Chromatin Immunoprecipitation
ECM	Extracellular Matrix
EGF	Epidermal growth factor
EGFR	Epidermal growth factor receptor
ERK	Extracellular response kinase
ErbB2/Her2	v-erb-b2 erthyroblastic leukemia viral oncogene homolog 2/ human epidermal growth factor receptor 2
FAK	Focal adhesion kinase
FGF	Fibroblast growth factor
FN	Fibronectin

HAT	Histone acetyltransferase
HDAC	Histone deacetyltransferase
HGF	Human growth factor
IP	Immunoprecipitation
ISWI	Imitation SWI group
JUN	Jun oncogene
MAPK	Mitogen-activated protein kinase
MEC	Mammary epithelial cell
MEK	MAP/ERK kinase
MTT	(3-(4,5-Dimethylthiazol-2-yl)-2,5-diphenyltetrazolium bromide, a tetrazole)
MYC	v-myc myelocytomatosis viral oncogene homolog
NSCLC	Non-small cell lung carcinoma
NF-κB	Nuclear factor of kappa light polypeptide gene enhancer in B-cells
p130Cas	Crk associated substrate 130
p53	Protein 53
Q RT-PCR	Quantitative real time polymerase chain reaction
Ras	Rat sarcoma viral oncogenes homolog
Rb	Retinoblastoma
Rho	Ras homolog gene family

SFK	Src Family Kinases
Shc	Src homologous and collagen protein
shRNA	Short hairpin RNA
siRNA	Small interfering RNA
SNF	Sucrose non-fermenting
Src	Sarcoma inducing gene
Syk	Spleen tyrosine kinase
SWI	Mate type SWItching
TGF-b	Transforming growth factor-beta
VEGF	Vascular endothelial growth factor
WB	Western blot

Chapter One
Introduction

Chapter 1: Introduction

Breast Cancer Biology

Breast cancer ranks second in the United States as a leading cause of cancer-related deaths in women [1]. The majority of these breast cancer-related deaths are due to treatment resistant, metastatic tumors [1, 2].

Breast cancer comprises an extraordinarily diverse group of diseases with a large amount of heterogeneity in regards to presentation, morphology, biological characteristics and clinical behavior [3]. The heterogeneity of breast cancer subtypes affects responsiveness to therapy and also clinical outcome [4]. Breast cancers can be divided into two main groups: Estrogen Receptor (ER) positive breast cancers and ER negative breast cancers. These groups can then be further divided into five distinct molecular subtypes: luminal A and luminal B (ER positive breast cancers) [5-7], and normal-like [8-10], HER2 [7, 11], and basal-like (ER negative breast cancers) [12-15]. The HER2 and basal-like subtypes are of particular interest because both have an aggressive clinical nature and are associated with elevated incidence of metastasis [4]. Therefore, understanding the molecular mechanisms behind aggressive, metastatic breast cancers like HER2 and basal-like breast cancers is paramount to curing breast cancer.

Oncogenic Signaling in Breast Cancer

The progression of a primary mammary epithelial cell (MEC) to a malignant phenotype involves multiple genetic events including the activation of oncogenes and the loss of functional tumor suppressor genes[16]. These genetic events drive malignant progression in part by inducing cell growth and enhancing cell survival through the alteration of cell cycle pathway regulators, cell stress response genes and apoptotic signaling factors [17-27].

One well studied example of oncogene activation is the amplification of expression of epidermal growth factor receptor tyrosine kinases (EGFR RTKs) which are implicated in the development and progression of several human cancers including breast cancer [23, 28-30]. The EGFR family comprises four closely related type 1 RTKs that include EGFR (ErbB1, HER1), ErbB2 (HER2/c-neu), ErbB-3 (HER3), and ErbB-4 (HER4) [31]. The traditional EGFR signaling pathway consists of several key transduction cascades, namely, phospholipase C-γ(PLC- γ)- Ca^{2+}dependent calmodulin kinase(CaMK)/protein kinase C(PKC), Ras-Raf-mitogen activated kinase(MAPK), phosphatidylinositol-3 kinase(PI-3K)-Akt-glycogen synthase kinase[32] and signal transducers and activators of transcription(STATs). Each of these pathways involves transduction of growth

factor signals from the cytoplasmic membrane, via activation of cascades of signaling molecules, to specific cytoplasmic targets and into the nucleus to direct gene expression to alter cell migration, adhesion, proliferation and survival (Figure 1.1; [24, 33-46]). In addition to oncogenic activation of EGFR, these downstream signaling cascades are also frequently deregulated in tumors, promoting tumor growth and survival, therapeutic resistance and tumor metastasis [47-58].

Amplified expression of EGFR family members occur in both primary breast cancers and their derived cell lines [59-63]. Specifically, increased ErbB2 receptor expression occurs in 20% to 25% of primary human breast cancers [24, 64, 65]. Moreover, the extent of overexpression of ErbB2 correlates with negative features such as tumor size, lymph node involvement, high nuclear grade, aneuploidy, increased disease recurrence and increased morbidity [36, 66, 67]. Therefore, understanding the molecular mechanisms by which oncogenic signaling via ErbB2 amplification drives tumor progression is critical to the study and treatment of aggressive and refractive breast cancers.

Role of Microenvironment in Tumor Progression

Early work by Mintz, Bissell and others demonstrate that elevated oncogene expression and/or loss of functional tumor suppressors per se are insufficient for tumorigenesis and that normal tissue architecture restricts malignant progression even in the face of gross genetic abnormalities [68-73]. A framework of connective tissue and cells, termed the stroma or microenvironment, supports

and maintains mammary epithelial tissue architecture. The stroma consists of a cellular component (i.e., fibroblasts, endothelial cells, adipocytes, pericytes, leukocytes) and a non-cellular component. The noncellular component includes not only pH and oxygen content, but also the extracellular matrix (ECM) [74]. In broad terms there are three major components of the ECM: fibrous elements such as collagens and elastins, link proteins such as fibronectin and laminin and space filling molecules such as glycosaminoglycans [75-78].

In a normal mammary gland, the stroma and its components regulate mammary epithelial tissue organization through cell-cell and cell-ECM interactions via adhesion receptors and these concerted interactions restrict malignant progression [79, 80]. Tumors by contrast, are characterized by an altered stroma defined by ECM remodeling, activated fibroblasts, angiogenesis and the presence of an inflammatory infiltrate that promote tumor progression by enhancing MEC growth and survival and by modifying the inflammatory response [76, 81]. Although the functions of the stroma in promoting breast tumor progression have been extensively reviewed [74, 76, 79-89] , my thesis focuses exclusively on the role of the MEC-ECM interactions and their role in breast tumorigenesis.

Transformation also alters MEC responsiveness to ECM microenvironmental cues [81, 83, 90]. Adhesion receptors which include integrins and syndecans mediate this ECM responsiveness [91-93]. The observation that the expression of these adhesion receptors are altered during breast tumor progression highlights the importance of these receptors in mammary tumor biology [93-95]. The best characterized adhesion receptor in control of ECM responsiveness is the integrin receptor and is the focus of my thesis research [96, 97].

Integrins: Mediators of ECM Signals

Integrin receptors are composed of non-covalently bound, type I transmembrane α and β subunits, each with a large extracellular domain, a single pass transmembrane domain and a cytoplasmic domain, or tail, that interacts directly or indirectly with cytoskeletal proteins such as talin, vinculin, tensin, paxillin, alpha-actinin, and filamin ([98-104]; Figure 1.1). Eighteen α integrin and eight β integrin subunits form up to 24 distinct heterodimers (Figure 1.2). These integrin heterodimers bind to an array of ECM proteins as depicted in Figure 1.2 and transduce ECM cues through adhesion complexes that regulate cytoskeletal organization and cellular responses such as proliferation, migration and survival (Figure 1.1; [92, 105-110]). Of note, αvβ3, α5β1 and αvβ6 integrins are usually

expressed at low or undetectable levels in most adult epithelia, but are upregulated in expression in tumors [111-117]. Furthermore, inhibition of β1 integrin, EGFR, and/or MAPK signaling is sufficient to suppress tumor growth and restore normal MEC architecture, termed phenotypic reversion, in both non-invasive and invasive breast cancer cell lines in three dimensional (3D) cultures [68, 72, 118-120]. Consistent with these observations, generation of a β1 integrin conditional knock-out mouse prevents breast tumor formation, and impairs MEC growth [121]. Whether oncogenes require changes in ECM responsiveness via integrins and by what mechanism are an area of active investigation and a focus of my thesis research [16, 68, 76, 81, 88, 122].

Coordinated Regulation of Tumor Growth & Survival

Integrins transduce many signals that impinge upon growth regulatory pathways (for review see Figure 1.2; [102, 123-127]). These include activation of tyrosine kinases such as focal adhesion kinase (FAK), $pp60^{src}$, and c-Abl; serine-threonine kinases such as MAPK, c-Jun N-terminal kinase [128], and PKC; intracellular ions such as protons (pH) and calcium; the small GTPase Rho; and lipid mediators such as phosphoinositides, diacylglycerol, and arachidonic acid metabolites. ECM adhesion is therefore critical for cell cycle progression through its ability to trigger both MAPK signaling through direct mechanisms and proliferation pathways via crosstalk with growth factor receptors [129, 130].

Invasive breast cancers may override dependence on integrin signaling for survival and evade apoptosis despite the absence of an exogenous basement membrane, this behavior *in vitro* is known as anchorage independent growth [109, 131-133]. Why epithelial tumors acquire anchorage independence for survival is not completely understood.

There is precedence that oncogenes upregulate integrins and/or increase secretion of ECM proteins thereby promoting anchorage-independent tumor cell growth and survival [121, 131, 134]. For example, breast cancer cells upregulate α6β4 integrin-laminin 5 secretion to promote their survival in a 3D culture system [134]. Oncogene-mediated increases in integrin-dependent signaling events provide a molecular explanation for the link between growth and adhesion. Interestingly, several integrins cooperate with oncogenes to enhance growth factor signaling [135, 136], recruit transducing proteins to membrane cytoskeletal complexes[137] and increase nuclear translocation of transcriptional regulators that control diverse cellular functions including cell cycle progression and cell death [138, 139].

For example, Ras-transformed MECs require α5 integrin for cell survival in 3D collagen gel morphogenesis assays [140, 141]. Notably, α5 integrin and its predominant ligand, fibronectin, are implicated in breast tumor progression because they positively associate with metastatic lesions and pro-angiogenic activities in breast cancers [140, 142-146]. How oncogene-mediated transformation increases α5 integrin levels to promote breast tumor growth and survival and the physiological relevance of this potential cross-talk to breast tumor progression are unclear and are the focus of my thesis work.

α5β1 Integrin Regulation

Given the critical role that integrins play in a variety of cell behaviors, it is not surprising that complex mechanisms regulate integrin expression and activity. Although α5β1 integrin regulation is not fully understood, some of the molecular mechanisms involved include its transcriptional activation [147], mRNA stability, translational control [148, 149], trafficking [110, 150] and receptor recycling[151, 152]. At the transcriptional level, the α5 integrin promoter contains both an AP-1 consensus site and a CCAAT/enhancer binding protein (c/EBP) binding site that enhances transcriptional activation [153-155]. RTK and Ras-mediated signaling regulate AP-1 sites and c/EBP-β activities via ERK/MAPK signaling pathways [156, 157]. Consistent with these findings, enhanced RTK or Ras signaling increases α5 integrin protein levels in transformed breast cancer cell lines [141]. The exact mechanism by which RTK and/or Ras signaling regulates α5 integrin levels however remains poorly understood.

Epigenetic modifications are the most recently suggested mechanism of integrin transcriptional regulation [158, 159]. For example, the loss of activity of the SWI/SNF chromatin remodeling complex protein BRG1 associates with increasing levels of α5 integrin in human fibroblasts [159]. Moreover, the expression of SWI/SNF complex proteins associates with c/EBP-β activity and Ras signaling, both of which are regulators of α5 integrin promoter activity [153-155, 160, 161]. **Therefore, my hypothesis is that oncogenic signaling drives tumor progression through the regulation of α5 integrin levels by altering the function and or expression of the SWI/SNF chromatin remodeling complex.**

SWI/SNF Chromatin Remodeling Complexes

The human SWI/SNF complex is a large multi-subunit complex approximately 2MDa in size that modifies the accessibility of DNA to transcriptional machinery and other factors [162, 163]. Although the exact subunit composition of the SWI/SNF complex varies greatly, each of these complexes contain one of two mutually exclusive ATPase subunits, Brahma (BRM) and Brahma-Related Gene 1 (BRG1) and eight to twelve accessory subunits termed BAFs (Brahma accessory factors) (Figure 1.3; [163-168].

The SWI/SNF complex utilizes the energy of ATP hydrolysis to modulate DNA accessibility to transcriptional machinery, and thus plays an important role in regulating gene expression [169-176]. In mammalian cells, SWI/SNFs control the activation and repression of a diverse set of genes depicted in Figure 1.3 [177-184]. The exact mechanism by which SWI/SNF remodels chromatin is not fully understood, although it is an area of active research [185-187].

Loss of BRM, BRG1 and several other SWI/SNF proteins occur in human cancer cell lines and tumor specimens of the lung, prostate, stomach, and the breast however the significance of this loss in tumorigenesis is unclear [188-194]. Despite the loss of expression of these twelve SWI/SNF proteins, only BRM shows prognostic significance in lung cancers [195]. Therefore, in my thesis, I begin to examine the possible functional relevance of BRM in breast tumorigenesis and explore potential mechanisms behind BRM loss in breast cancers. Regulation of BRM expression is largely a mystery except for the observation that kinase phosphorylation events, by an unidentified protein kinase, abolish BRM protein levels during mitosis[196]. Because oncogenes drive Ras and integrin-dependent signaling via activated ERK, JNK and additional kinases, we explore the possibility that oncogenic transformation downregulates BRM expression via adhesion-dependent kinase activity [197-199]. **Therefore, my modified hypothesis is that oncogenic signaling drives tumor progression through the regulation of α5 integrin levels by altering the function and or expression of the SWI/SNF BRM chromatin remodeling protein.**

Three-Dimensional Model Systems to Study Mammary Epithelial Cell Behavior

In this thesis, we explore the mechanisms governing ECM responsiveness during oncogenic transformation through application of three-dimensional (3D) culture techniques.

Mammary gland development occurs primarily postnatally and is marked by distinct periods of glandular remodeling and morphogenesis between the times of birth and puberty, pregnancy and lactation and also throughout breast tumor progression [200-203]. The most basic structural component of the mature mammary gland is an acinus: a hollow, polarized, sphere-shaped structure that is capable of milk production.

Each acinus is lined with secretory luminal epithelial cells associated with myoepithelial cells. These mammary epithelial cells (MECs) are surrounded by a basement membrane (BM), that not only functions to support mammary structure, but also serves as a communication bridge between MECs and their surrounding environment, or stroma (Figure 1.4; [83]).

3D organotypic culture systems improve our understanding of breast cancer biology, specifically the importance of cell-cell and cell-ECM interactions that dominantly interfere with the phenotypic expression of the tumorigenic state [68, 74, 81, 96, 122, 204, 205].

Under 3D culture conditions, non-malignant MECs, such as the MCF10A MECs in our studies, undergo a series of morphogenic changes resulting in the formation of a growth arrested, acinus-shaped structure containing a single layer of polarized cells surrounding a hollow lumen similar to their *in vivo* human breast counterparts [83, 90, 206, 207]. Clearance of centrally located cells in this model involves apoptosis, in a process termed anoikis, where the absence of survival signals from the ECM triggers cell death [198, 208-211]. Importantly, many early breast cancer lesions, such as ductal carcinoma *in situs* (DCIS), are characterized by suppression of anoikis and filling of the luminal space [212].

Moreover, re-expression of genes frequently lost in breast cancer, such as alpha-dystroglycan (alpha-DG) permit MECs to form acinar-like structures in 3D assays similar to those of non-malignant MEC structures [213]. In contrast, the overexpression of oncogenes or activated RTKs into non-transformed MECs, such as Ras^{V12} or ErbB2, leads to the formation of hyperproliferative structures with perturbed morphogenesis [206, 214].

Tissue-specific differentiation [215], stem cell behavior [216] and even microenvironmental control of malignant transformation and tumor dormancy [72, 217] is effectively studied through application of 3D culture models. The study of diverse tissues and cells including the salivary gland [218] , liver [219], lung [220]

and endometrial tissues[221] also utilize 3D systems, giving this emerging culture system broader appreciation and functionality. These data make it increasingly clear that 3D cultures can promote expression of tissue-specific functions by allowing cells to receive cues from their neighboring cells and the basement membrane, which cannot occur when cells are plated on tissue culture plastic or other two-dimensional (2D) substrata.

Outline of Thesis

The goal of this thesis is to test the hypothesis that oncogenic signaling drives changes in ECM responsiveness via targeting of BRM chromatin remodeling proteins to promote breast tumor progression. To test this hypothesis, we first studied the role of α5β1 integrin-FN interactions in reconstituted basement membrane (rBM)-directed MEC morphogenesis assays. We found that α5β1-FN interactions promoted a premalignant phenotype as assessed by altered morphology and increased proliferation and survival in nonmalignant MECs embedded in 3D culture assays (Chapter 2). To explore the molecular mechanism governing α5 integrin regulation and its potential epigenetic regulation, we developed a shRNA targeting system for the SWI/SNF BRM protein. We identified BRM as a negative regulator of α5β1-FN interactions, whereby shRNA-mediated knockdown of BRM increased α5β1 integrin-FN expression levels and other adhesion-dependent activities (Chapter 2).

To directly assess a possible relationship between BRM activity and oncogenic transformation, we re-introduced BRM into BRM-deficient transformed MEC lines and observed a phenotypic reversion in 3D culture assays coupled with repression of α5β1 integrin-FN interactions and reduced α5 integrin levels (Chapter 2).

Given the strong prognostic value of BRM in lung cancer, we conducted a series of preliminary studies to examine the role of BRM chromatin remodeling activity in breast tumorigenesis (Chapter 3). We found that BRM expression levels were decreased in human breast cancer cell lines and we observed increased cell motility and anchorage independent growth in the absence of BRM expression and/or chromatin remodeling activity in MECs (Chapter 3). Furthermore, min the absence of BRM expression, microarray analysis revealed an increase in breast tumor progression gene markers such as snail and vimentin (Chapter 3). Consistent with these *in vitro* findings, multivariate analysis of previously published microarrays showed that reduced BRM expression associated with increased recurrence and increased morbidity in human breast cancer patients (Chapter 3). To begin to explore the functional relevance of BRM expression *in vivo*, we first analyzed BRM expression in a small sample of murine and human breast cancer samples and this initial finding suggested BRM expression was reduced *in vivo* during breast tumor progression (Chapter 3). In Chapter 4, we address the overall conclusions of this thesis and speculate upon the possible mechanisms governing ECM responsiveness, cooperativity of integrin-RTK signaling and the regulation of epigenetic modifiers during breast cancer progression and propose future experiments to be completed to answer these questions for this project.

References

1. acs.org. *Facts and Figures 2009*. 2009; Available from: www.acs.org.
2. Research, A.C.S.S. *Facts and Figures 2009*. [www.acs.org] 2009.
3. Harris, J., Lippman, ME, Morrow, M, Hellman, S, *In: Diseases of the Breast,*. 1996, Philadelphia: Lippincott-Raven.
4. Perou, C.M., et al., *Molecular portraits of human breast tumours.* Nature, 2000. **406**(6797): p. 747-52.
5. Reis-Filho, J.S., C. Westbury, and J.Y. Pierga, *The impact of expression profiling on prognostic and predictive testing in breast cancer.* J Clin Pathol, 2006. **59**(3): p. 225-31.
6. Sorlie, T., et al., *Gene expression patterns of breast carcinomas distinguish tumor subclasses with clinical implications.* Proc Natl Acad Sci U S A, 2001. **98**(19): p. 10869-74.
7. Parker, J.S., et al., *Supervised risk predictor of breast cancer based on intrinsic subtypes.* J Clin Oncol, 2009. **27**(8): p. 1160-7.
8. Peppercorn, J., C.M. Perou, and L.A. Carey, *Molecular subtypes in breast cancer evaluation and management: divide and conquer.* Cancer Invest, 2008. **26**(1): p. 1-10.
9. Pusztai, L., M. Cristofanilli, and S. Paik, *New generation of molecular prognostic and predictive tests for breast cancer.* Semin Oncol, 2007. **34**(2 Suppl 3): p. S10-6.
10. Geyer, F.C., C. Marchio, and J.S. Reis-Filho, *The role of molecular analysis in breast cancer.* Pathology, 2009. **41**(1): p. 77-88.

11. Rouzier, R., et al., *Breast cancer molecular subtypes respond differently to preoperative chemotherapy.* Clin Cancer Res, 2005. **11**(16): p. 5678-85.
12. Reis-Filho, J.S., et al., *Metaplastic breast carcinomas are basal-like tumours.* Histopathology, 2006. **49**(1): p. 10-21.
13. Fulford, L.G., et al., *Specific morphological features predictive for the basal phenotype in grade 3 invasive ductal carcinoma of breast.* Histopathology, 2006. **49**(1): p. 22-34.
14. Livasy, C.A., et al., *Phenotypic evaluation of the basal-like subtype of invasive breast carcinoma.* Mod Pathol, 2006. **19**(2): p. 264-71.
15. Turner, N.C. and J.S. Reis-Filho, *Basal-like breast cancer and the BRCA1 phenotype.* Oncogene, 2006. **25**(43): p. 5846-53.
16. Hanahan, D. and R.A. Weinberg, *The hallmarks of cancer.* Cell, 2000. **100**(1): p. 57-70.
17. Pitot, H.C., *Factors Predisposing to Cancer.* Science, 1981. **213**(4505): p. 327.
18. Weinstein, I.B., et al., *Cellular targets and host genes in multistage carcinogenesis.* Fed Proc, 1984. **43**(8): p. 2287-94.
19. Varley, J.M., et al., *Alterations to either c-erbB-2(neu) or c-myc proto-oncogenes in breast carcinomas correlate with poor short-term prognosis.* Oncogene, 1987. **1**(4): p. 423-30.
20. Muthuswamy, S.K. and W.J. Muller, *Activation of the Src family of tyrosine kinases in mammary tumorigenesis.* Adv Cancer Res, 1994. **64**: p. 111-23.

21. Turner, N.C., et al., *BRCA1 dysfunction in sporadic basal-like breast cancer.* Oncogene, 2007. **26**(14): p. 2126-32.

22. Lohrisch, C. and M. Piccart, *HER2/neu as a predictive factor in breast cancer.* Clin Breast Cancer, 2001. **2**(2): p. 129-35; discussion 136-7.

23. Eccles, S.A., *The role of c-erbB-2/HER2/neu in breast cancer progression and metastasis.* J Mammary Gland Biol Neoplasia, 2001. **6**(4): p. 393-406.

24. Slamon, D.J., *Proto-oncogenes and human cancers.* N Engl J Med, 1987. **317**(15): p. 955-7.

25. Deming, S.L., et al., *C-myc amplification in breast cancer: a meta-analysis of its occurrence and prognostic relevance.* Br J Cancer, 2000. **83**(12): p. 1688-95.

26. Watson, P.H., et al., *Relationship of c-myc amplification to progression of breast cancer from in situ to invasive tumor and lymph node metastasis.* J Natl Cancer Inst, 1993. **85**(11): p. 902-7.

27. Nass, S.J. and R.B. Dickson, *Defining a role for c-Myc in breast tumorigenesis.* Breast Cancer Res Treat, 1997. **44**(1): p. 1-22.

28. Schlegel, J., et al., *Amplification and differential expression of members of the erbB-gene family in human glioblastoma.* J Neurooncol, 1994. **22**(3): p. 201-7.

29. Reissmann, P.T., et al., *Amplification and overexpression of the cyclin D1 and epidermal growth factor receptor genes in non-small-cell lung cancer. Lung Cancer Study Group.* J Cancer Res Clin Oncol, 1999. **125**(2): p. 61-70.

30. Livasy, C.A., et al., *EGFR expression and HER2/neu overexpression/amplification in endometrial carcinosarcoma.* Gynecol Oncol, 2006. **100**(1): p. 101-6.

31. Hynes, N.E. and D.F. Stern, *The biology of erbB-2/neu/HER-2 and its role in cancer.* Biochim Biophys Acta, 1994. **1198**(2-3): p. 165-84.

32. Wang, Z.P., et al., *Asthma, lung function, and bronchial responsiveness in welders.* Am J Ind Med, 1994. **26**(6): p. 741-54.

33. Shibata, T., et al., *Dominant negative inhibition of the association between beta-catenin and c-erbB-2 by N-terminally deleted beta-catenin suppresses the invasion and metastasis of cancer cells.* Oncogene, 1996. **13**(5): p. 883-9.

34. Yarden, Y., *Biology of HER2 and its importance in breast cancer.* Oncology, 2001. **61 Suppl 2**: p. 1-13.

35. Slamon, D.J., et al., *Studies of the HER-2/neu proto-oncogene in human breast and ovarian cancer.* Science, 1989. **244**(4905): p. 707-12.

36. Ross, J.S., et al., *The Her-2/neu gene and protein in breast cancer 2003: biomarker and target of therapy.* Oncologist, 2003. **8**(4): p. 307-25.

37. Simon, M.A., *Receptor tyrosine kinases: specific outcomes from general signals.* Cell, 2000. **103**(1): p. 13-5.

38. Ben-Levy, R., et al., *A single autophosphorylation site confers oncogenicity to the Neu/ErbB-2 receptor and enables coupling to the MAP kinase pathway.* EMBO J, 1994. **13**(14): p. 3302-11.

39. Blaikie, P.A., et al., *The role of the Shc phosphotyrosine interaction/phosphotyrosine binding domain and tyrosine phosphorylation sites in polyoma middle T antigen-mediated cell transformation.* J Biol Chem, 1997. **272**(33): p. 20671-7.

40. Campbell, K.S., et al., *Polyoma middle tumor antigen interacts with SHC protein via the NPTY (Asn-Pro-Thr-Tyr) motif in middle tumor antigen.* Proc Natl Acad Sci U S A, 1994. **91**(14): p. 6344-8.

41. Dankort, D.L., et al., *Distinct tyrosine autophosphorylation sites negatively and positively modulate neu-mediated transformation.* Mol Cell Biol, 1997. **17**(9): p. 5410-25.

42. Dilworth, S.M., et al., *Transformation by polyoma virus middle T-antigen involves the binding and tyrosine phosphorylation of Shc.* Nature, 1994. **367**(6458): p. 87-90.

43. Janes, P.W., et al., *Structural determinants of the interaction between the erbB2 receptor and the Src homology 2 domain of Grb7.* J Biol Chem, 1997. **272**(13): p. 8490-7.

44. Niemann, C., et al., *Reconstitution of mammary gland development in vitro: requirement of c-met and c-erbB2 signaling for branching and alveolar morphogenesis.* J Cell Biol, 1998. **143**(2): p. 533-45.

45. Pelicci, G., et al., *A novel transforming protein (SHC) with an SH2 domain is implicated in mitogenic signal transduction.* Cell, 1992. **70**(1): p. 93-104.

46. Ricci, A., et al., *Analysis of protein-protein interactions involved in the activation of the Shc/Grb-2 pathway by the ErbB-2 kinase.* Oncogene, 1995. **11**(8): p. 1519-29.

47. Hallberg, B., S.I. Rayter, and J. Downward, *Interaction of Ras and Raf in intact mammalian cells upon extracellular stimulation.* J Biol Chem, 1994. **269**(6): p. 3913-6.

48. Kikuchi, A. and L.T. Williams, *The post-translational modification of ras p21 is important for Raf-1 activation.* J Biol Chem, 1994. **269**(31): p. 20054-9.

49. Marshall, C.J., *Ras effectors.* Curr Opin Cell Biol, 1996. **8**(2): p. 197-204.

50. McCormick, F., *GTP-binding proteins as oncogenes in human tumors.* Environ Health Perspect, 1991. **93**: p. 17-8.

51. Rodriguez-Viciana, P., et al., *Activation of phosphoinositide 3-kinase by interaction with Ras and by point mutation.* EMBO J, 1996. **15**(10): p. 2442-51.

52. Troppmair, J., et al., *Mitogen-activated protein kinase/extracellular signal-regulated protein kinase activation by oncogenes, serum, and 12-O-tetradecanoylphorbol-13-acetate requires Raf and is necessary for transformation.* J Biol Chem, 1994. **269**(9): p. 7030-5.

53. Warne, P.H., P.R. Viciana, and J. Downward, *Direct interaction of Ras and the amino-terminal region of Raf-1 in vitro.* Nature, 1993. **364**(6435): p. 352-5.

54. Zheng, Y., S. Bagrodia, and R.A. Cerione, *Activation of phosphoinositide 3-kinase activity by Cdc42Hs binding to p85.* J Biol Chem, 1994. **269**(29): p. 18727-30.

55. Webster, M.A., et al., *Requirement for both Shc and phosphatidylinositol 3' kinase signaling pathways in polyomavirus middle T-mediated mammary tumorigenesis.* Mol Cell Biol, 1998. **18**(4): p. 2344-59.

56. Guy, C.T., et al., *Activation of the c-Src tyrosine kinase is required for the induction of mammary tumors in transgenic mice.* Genes Dev, 1994. **8**(1): p. 23-32.

57. Miyakis, S., G. Sourvinos, and D.A. Spandidos, *Differential expression and mutation of the ras family genes in human breast cancer.* Biochem Biophys Res Commun, 1998. **251**(2): p. 609-12.

58. Pylayeva, Y., et al., *Ras- and PI3K-dependent breast tumorigenesis in mice and humans requires focal adhesion kinase signaling.* J Clin Invest, 2009. **119**(2): p. 252-66.

59. Downs-Kelly, E., et al., *The influence of polysomy 17 on HER2 gene and protein expression in adenocarcinoma of the breast: a fluorescent in situ hybridization, immunohistochemical, and isotopic mRNA in situ hybridization study.* Am J Surg Pathol, 2005. **29**(9): p. 1221-7.

60. Klijn, J.G., et al., *The clinical significance of epidermal growth factor receptor (EGF-R) in human breast cancer: a review on 5232 patients.* Endocr Rev, 1992. **13**(1): p. 3-17.

61. Bucci, B., et al., *EGF-R expression in ductal breast cancer: proliferation and prognostic implications.* Anticancer Res, 1997. **17**(1B): p. 769-74.

62. Klijn, J.G., et al., *Clinical breast cancer, new developments in selection and endocrine treatment of patients.* J Steroid Biochem Mol Biol, 1992. **43**(1-3): p. 211-21.

63. Klijn, J.G., et al., *The prognostic value of epidermal growth factor receptor (EGF-R) in primary breast cancer: results of a 10 year follow-up study.* Breast Cancer Res Treat, 1994. **29**(1): p. 73-83.

64. Ross, J.S. and J.A. Fletcher, *HER-2/neu (c-erb-B2) gene and protein in breast cancer.* Am J Clin Pathol, 1999. **112**(1 Suppl 1): p. S53-67.

65. Slamon, D.J., et al., *Human breast cancer: correlation of relapse and survival with amplification of the HER-2/neu oncogene.* Science, 1987. **235**(4785): p. 177-82.

66. Andrulis, I.L., et al., *neu/erbB-2 amplification identifies a poor-prognosis group of women with node-negative breast cancer. Toronto Breast Cancer Study Group.* J Clin Oncol, 1998. **16**(4): p. 1340-9.

67. Slamon, D.J. and G.M. Clark, *Amplification of c-erbB-2 and aggressive human breast tumors?* Science, 1988. **240**(4860): p. 1795-8.

68. Wang, F., et al., *Phenotypic reversion or death of cancer cells by altering signaling pathways in three-dimensional contexts.* J Natl Cancer Inst, 2002. **94**(19): p. 1494-503.

69. Mintz, B. and K. Illmensee, *Normal genetically mosaic mice produced from malignant teratocarcinoma cells.* Proc Natl Acad Sci U S A, 1975. **72**(9): p. 3585-9.

70. Dolberg, D.S. and M.J. Bissell, *Inability of Rous sarcoma virus to cause sarcomas in the avian embryo.* Nature, 1984. **309**(5968): p. 552-6.

71. Howlett, A.R., et al., *Cellular growth and survival are mediated by beta 1 integrins in normal human breast epithelium but not in breast carcinoma.* J Cell Sci, 1995. **108 (Pt 5)**: p. 1945-57.

72. Weaver, V.M., et al., *Reversion of the malignant phenotype of human breast cells in three-dimensional culture and in vivo by integrin blocking antibodies.* J Cell Biol, 1997. **137**(1): p. 231-45.

73. Kirshner, J., et al., *CEACAM1-4S, a cell-cell adhesion molecule, mediates apoptosis and reverts mammary carcinoma cells to a normal morphogenic phenotype in a 3D culture.* Proc Natl Acad Sci U S A, 2003. **100**(2): p. 521-6.

74. Shekhar, M.P., et al., *Breast stroma plays a dominant regulatory role in breast epithelial growth and differentiation: implications for tumor development and progression.* Cancer Res, 2001. **61**(4): p. 1320-6.

75. Lochter, A. and M.J. Bissell, *Involvement of extracellular matrix constituents in breast cancer.* Semin Cancer Biol, 1995. **6**(3): p. 165-73.

76. Shekhar, M.P., R. Pauley, and G. Heppner, *Host microenvironment in breast cancer development: extracellular matrix-stromal cell contribution to*

neoplastic phenotype of epithelial cells in the breast. Breast Cancer Res, 2003. **5**(3): p. 130-5.

77. Nara, Y., et al., *Immunohistochemical localization of extracellular matrix components in human breast tumours with special reference to PG-M/versican.* Histochem J, 1997. **29**(1): p. 21-30.

78. Suwiwat, S., et al., *Expression of extracellular matrix components versican, chondroitin sulfate, tenascin, and hyaluronan, and their association with disease outcome in node-negative breast cancer.* Clin Cancer Res, 2004. **10**(7): p. 2491-8.

79. Haslam, S.Z., *Cell to cell interactions and normal mammary gland function.* J Dairy Sci, 1988. **71**(10): p. 2843-54.

80. Park, C.C., M.J. Bissell, and M.H. Barcellos-Hoff, *The influence of the microenvironment on the malignant phenotype.* Mol Med Today, 2000. **6**(8): p. 324-9.

81. Ronnov-Jessen, L., O.W. Petersen, and M.J. Bissell, *Cellular changes involved in conversion of normal to malignant breast: importance of the stromal reaction.* Physiol Rev, 1996. **76**(1): p. 69-125.

82. Christensen, L., *The distribution of fibronectin, laminin and tetranectin in human breast cancer with special attention to the extracellular matrix.* APMIS Suppl, 1992. **26**: p. 1-39.

83. Streuli, C.H. and M.J. Bissell, *Expression of extracellular matrix components is regulated by substratum.* J Cell Biol, 1990. **110**(4): p. 1405-15.

84. Pietras, K. and A. Ostman, *Hallmarks of cancer: Interactions with the tumor stroma.* Exp Cell Res.

85. Haslam, S.Z. and T.L. Woodward, *Host microenvironment in breast cancer development: epithelial-cell-stromal-cell interactions and steroid hormone action in normal and cancerous mammary gland.* Breast Cancer Res, 2003. **5**(4): p. 208-15.

86. Tlsty, T.D. and L.M. Coussens, *Tumor stroma and regulation of cancer development.* Annu Rev Pathol, 2006. **1**: p. 119-50.

87. Weaver, V.M. and P. Gilbert, *Watch thy neighbor: cancer is a communal affair.* J Cell Sci, 2004. **117**(Pt 8): p. 1287-90.

88. Wiseman, B.S. and Z. Werb, *Stromal effects on mammary gland development and breast cancer.* Science, 2002. **296**(5570): p. 1046-9.

89. van Roozendaal, C.E., et al., *Stromal influences on breast cancer cell growth.* Br J Cancer, 1992. **65**(1): p. 77-81.

90. Petersen, O.W., et al., *Differentiation and cancer in the mammary gland: shedding light on an old dichotomy.* Adv Cancer Res, 1998. **75**: p. 135-61.

91. Plantefaber, L.C. and R.O. Hynes, *Changes in integrin receptors on oncogenically transformed cells.* Cell, 1989. **56**(2): p. 281-90.

92. Desgrosellier, J.S. and D.A. Cheresh, *Integrins in cancer: biological implications and therapeutic opportunities.* Nat Rev Cancer. **10**(1): p. 9-22.

93. Carey, D.J., *Syndecans: multifunctional cell-surface co-receptors.* Biochem J, 1997. **327 (Pt 1)**: p. 1-16.

94. Stillfried, G.E., D.N. Saunders, and M. Ranson, *Plasminogen binding and activation at the breast cancer cell surface: the integral role of urokinase activity.* Breast Cancer Res, 2007. **9**(1): p. R14.

95. Henry, M.D. and K.P. Campbell, *Dystroglycan inside and out.* Curr Opin Cell Biol, 1999. **11**(5): p. 602-7.

96. Fata, J.E., Z. Werb, and M.J. Bissell, *Regulation of mammary gland branching morphogenesis by the extracellular matrix and its remodeling enzymes.* Breast Cancer Res, 2004. **6**(1): p. 1-11.

97. Giancotti, F.G. and E. Ruoslahti, *Integrin signaling.* Science, 1999. **285**(5430): p. 1028-32.

98. Nermut, M.V., et al., *Electron microscopy and structural model of human fibronectin receptor.* EMBO J, 1988. **7**(13): p. 4093-9.

99. Burridge, K. and M. Chrzanowska-Wodnicka, *Focal adhesions, contractility, and signaling.* Annu Rev Cell Dev Biol, 1996. **12**: p. 463-518.

100. Hynes, R.O., *Integrins: versatility, modulation, and signaling in cell adhesion.* Cell, 1992. **69**(1): p. 11-25.

101. Hynes, R.O., *The extracellular matrix: not just pretty fibrils.* Science, 2009. **326**(5957): p. 1216-9.

102. Zamir, E. and B. Geiger, *Components of cell-matrix adhesions.* J Cell Sci, 2001. **114**(Pt 20): p. 3577-9.

103. Cukierman, E., R. Pankov, and K.M. Yamada, *Cell interactions with three-dimensional matrices.* Curr Opin Cell Biol, 2002. **14**(5): p. 633-9.

104. Brakebusch, C. and R. Fassler, *The integrin-actin connection, an eternal love affair.* EMBO J, 2003. **22**(10): p. 2324-33.

105. Clark, E.A. and J.S. Brugge, *Integrins and signal transduction pathways: the road taken.* Science, 1995. **268**(5208): p. 233-9.

106. Riveline, D., et al., *Focal contacts as mechanosensors: externally applied local mechanical force induces growth of focal contacts by an mDia1-dependent and ROCK-independent mechanism.* J Cell Biol, 2001. **153**(6): p. 1175-86.

107. Humphries, M.J., et al., *Integrin structure: heady advances in ligand binding, but activation still makes the knees wobble.* Trends Biochem Sci, 2003. **28**(6): p. 313-20.

108. Newham, P. and M.J. Humphries, *Integrin adhesion receptors: structure, function and implications for biomedicine.* Mol Med Today, 1996. **2**(7): p. 304-13.

109. Reddig, P.J. and R.L. Juliano, *Clinging to life: cell to matrix adhesion and cell survival.* Cancer Metastasis Rev, 2005. **24**(3): p. 425-39.

110. Caswell, P.T. and J.C. Norman, *Integrin trafficking and the control of cell migration.* Traffic, 2006. **7**(1): p. 14-21.

111. Takayama, S., et al., *The relationship between bone metastasis from human breast cancer and integrin alpha(v)beta3 expression.* Anticancer Res, 2005. **25**(1A): p. 79-83.

112. Liapis, H., A. Flath, and S. Kitazawa, *Integrin alpha V beta 3 expression by bone-residing breast cancer metastases.* Diagn Mol Pathol, 1996. **5**(2): p. 127-35.

113. Sloan, E.K., et al., *Tumor-specific expression of alphavbeta3 integrin promotes spontaneous metastasis of breast cancer to bone.* Breast Cancer Res, 2006. **8**(2): p. R20.

114. Felding-Habermann, B., et al., *Integrin activation controls metastasis in human breast cancer.* Proc Natl Acad Sci U S A, 2001. **98**(4): p. 1853-8.

115. Shimizu, H., et al., *Aberrant expression of integrin and erbB subunits in breast cancer cell lines.* Int J Oncol, 2002. **21**(5): p. 1073-9.

116. Francis, S.E., et al., *Central roles of alpha5beta1 integrin and fibronectin in vascular development in mouse embryos and embryoid bodies.* Arterioscler Thromb Vasc Biol, 2002. **22**(6): p. 927-33.

117. Koukoulis, G.K., et al., *Distribution of tenascin, cellular fibronectins and integrins in the normal, hyperplastic and neoplastic breast.* J Submicrosc Cytol Pathol, 1993. **25**(2): p. 285-95.

118. Kenny, P.A. and M.J. Bissell, *Tumor reversion: correction of malignant behavior by microenvironmental cues.* Int J Cancer, 2003. **107**(5): p. 688-95.

119. Park, C.C., et al., *Beta1 integrin inhibitory antibody induces apoptosis of breast cancer cells, inhibits growth, and distinguishes malignant from normal phenotype in three dimensional cultures and in vivo.* Cancer Res, 2006. **66**(3): p. 1526-35.

120. Castello-Cros, R., et al., *Staged stromal extracellular 3D matrices differentially regulate breast cancer cell responses through PI3K and beta1-integrins.* BMC Cancer, 2009. **9**: p. 94.

121. White, D.E., et al., *Targeted disruption of beta1-integrin in a transgenic mouse model of human breast cancer reveals an essential role in mammary tumor induction.* Cancer Cell, 2004. **6**(2): p. 159-70.

122. Bissell, M.J., et al., *The organizing principle: microenvironmental influences in the normal and malignant breast.* Differentiation, 2002. **70**(9-10): p. 537-46.

123. Zaidel-Bar, R., et al., *Early molecular events in the assembly of matrix adhesions at the leading edge of migrating cells.* J Cell Sci, 2003. **116**(Pt 22): p. 4605-13.

124. Pankov, R., et al., *Integrin dynamics and matrix assembly: tensin-dependent translocation of alpha(5)beta(1) integrins promotes early fibronectin fibrillogenesis.* J Cell Biol, 2000. **148**(5): p. 1075-90.

125. Galbraith, C.G., K.M. Yamada, and M.P. Sheetz, *The relationship between force and focal complex development.* J Cell Biol, 2002. **159**(4): p. 695-705.

126. Katsumi, A., et al., *Integrin activation and matrix binding mediate cellular responses to mechanical stretch.* J Biol Chem, 2005. **280**(17): p. 16546-9.

127. Burridge, K. and K. Wennerberg, *Rho and Rac take center stage.* Cell, 2004. **116**(2): p. 167-79.

128. Elsik, C.G., et al., *The genome sequence of taurine cattle: a window to ruminant biology and evolution.* Science, 2009. **324**(5926): p. 522-8.

129. Taddei, I., et al., *Integrins in mammary gland development and differentiation of mammary epithelium.* J Mammary Gland Biol Neoplasia, 2003. **8**(4): p. 383-94.

130. Boudreau, N., et al., *Suppression of ICE and apoptosis in mammary epithelial cells by extracellular matrix.* Science, 1995. **267**(5199): p. 891-3.

131. Guo, W., et al., *Beta 4 integrin amplifies ErbB2 signaling to promote mammary tumorigenesis.* Cell, 2006. **126**(3): p. 489-502.

132. Simpson, C.D., K. Anyiwe, and A.D. Schimmer, *Anoikis resistance and tumor metastasis.* Cancer Lett, 2008. **272**(2): p. 177-85.

133. Uhm, J.H., et al., *Vitronectin, a glioma-derived extracellular matrix protein, protects tumor cells from apoptotic death.* Clin Cancer Res, 1999. **5**(6): p. 1587-94.

134. Zahir, N., et al., *Autocrine laminin-5 ligates alpha6beta4 integrin and activates RAC and NFkappaB to mediate anchorage-independent survival of mammary tumors.* J Cell Biol, 2003. **163**(6): p. 1397-407.

135. Miyamoto, S., et al., *Integrins can collaborate with growth factors for phosphorylation of receptor tyrosine kinases and MAP kinase activation: roles of integrin aggregation and occupancy of receptors.* J Cell Biol, 1996. **135**(6 Pt 1): p. 1633-42.

136. Short, S.M., G.A. Talbott, and R.L. Juliano, *Integrin-mediated signaling events in human endothelial cells.* Mol Biol Cell, 1998. **9**(8): p. 1969-80.

137. Del Pozo, M.A., et al., *Integrins regulate GTP-Rac localized effector interactions through dissociation of Rho-GDI.* Nat Cell Biol, 2002. **4**(3): p. 232-9.

138. Aplin, A.E., et al., *Integrin-mediated adhesion regulates ERK nuclear translocation and phosphorylation of Elk-1.* J Cell Biol, 2001. **153**(2): p. 273-82.

139. Hirsch, E., et al., *Defective Rac-mediated proliferation and survival after targeted mutation of the beta1 integrin cytodomain.* J Cell Biol, 2002. **157**(3): p. 481-92.

140. Spangenberg, C., et al., *ERBB2-mediated transcriptional up-regulation of the alpha5beta1 integrin fibronectin receptor promotes tumor cell survival under adverse conditions.* Cancer Res, 2006. **66**(7): p. 3715-25.

141. Maschler, S., et al., *Tumor cell invasiveness correlates with changes in integrin expression and localization.* Oncogene, 2005. **24**(12): p. 2032-41.

142. Imanishi, Y., et al., *Angiopoietin-2 stimulates breast cancer metastasis through the alpha(5)beta(1) integrin-mediated pathway.* Cancer Res, 2007. **67**(9): p. 4254-63.

143. Jia, Y., et al., *Integrin fibronectin receptors in matrix metalloproteinase-1-dependent invasion by breast cancer and mammary epithelial cells.* Cancer Res, 2004. **64**(23): p. 8674-81.

144. Murthy, M.S., et al., *The potential role of integrin receptor subunits in the formation of local recurrence and distant metastasis by mouse breast cancer cells.* J Surg Oncol, 1996. **63**(2): p. 77-86.

145. Valastyan, S., et al., *Concomitant suppression of three target genes can explain the impact of a microRNA on metastasis.* Genes Dev, 2009. **23**(22): p. 2592-7.

146. Boudreau, N.J. and J.A. Varner, *The homeobox transcription factor Hox D3 promotes integrin alpha5beta1 expression and function during angiogenesis.* J Biol Chem, 2004. **279**(6): p. 4862-8.

147. Delcommenne, M. and C.H. Streuli, *Control of integrin expression by extracellular matrix.* J Biol Chem, 1995. **270**(45): p. 26794-801.

148. Pabla, R., Weyrich, A., , Dixon, D., Bray, Paul F., McIntyre, T.M., Prescott S., Zimmerman, G., *Integrin-dependent Control of Translation: Engagement of Integrin {alpha}IIbβ3 Regulates Synthesis of Proteins in Activated Human Platelets.* j cell biology, 1999. **144**(1): p. 175.

149. FL Harwood, R.G., *Regulation of αvβ3 and α5β1 integrin receptors by basic fibroblast growth factor and platelet-derived growth factor-BB in intrasynovial flexor tendon cells.* Wound Repair and Regeneration, 2010. **7**(5): p. 381-388.

150. Caswell, P.T., S. Vadrevu, and J.C. Norman, *Integrins: masters and slaves of endocytic transport.* Nat Rev Mol Cell Biol, 2009. **10**(12): p. 843-53.

151. Fabbri, M., Fumagalli, L., Bossi, L., Bianchi, E., Bender, J. and R Pardi, *A tyrosine-based sorting signal in the beta2 integrin cytoplasmic domain mediates its recycling to the plasma membrane and is required for ligand-supported migration.* EMBO J, 1999. **18**(18): p. 4915-4925.

152. Pellinen, T., and Ivaska, J., *Integrin traffic.* J Cell Sci, 2006(119): p. 3723-3731.

153. Corbi, A.L., U.B. Jensen, and F.M. Watt, *The alpha2 and alpha5 integrin genes: identification of transcription factors that regulate promoter activity in epidermal keratinocytes.* FEBS Lett, 2000. **474**(2-3): p. 201-7.

154. Koria, P. and S.T. Andreadis, *KGF promotes integrin alpha5 expression through CCAAT/enhancer-binding protein-beta.* Am J Physiol Cell Physiol, 2007. **293**(3): p. C1020-31.

155. Birkenmeier, T.M., et al., *The alpha 5 beta 1 fibronectin receptor. Characterization of the alpha 5 gene promoter.* J Biol Chem, 1991. **266**(30): p. 20544-9.

156. Mechta, F., et al., *Transformation by ras modifies AP1 composition and activity.* Oncogene, 1997. **14**(7): p. 837-47.

157. Nakajima, T., et al., *Phosphorylation at threonine-235 by a ras-dependent mitogen-activated protein kinase cascade is essential for transcription factor NF-IL6.* Proc Natl Acad Sci U S A, 1993. **90**(6): p. 2207-11.

158. Uhm, K.O., et al., *Aberrant DNA methylation of integrin alpha4: a potential novel role for metastasis of cholangiocarcinoma.* J Cancer Res Clin Oncol. **136**(2): p. 187-94.

159. Hill, D.A., et al., *Inducible changes in cell size and attachment area due to expression of a mutant SWI/SNF chromatin remodeling enzyme.* J Cell Sci, 2004. **117**(Pt 24): p. 5847-54.

160. Muchardt, C., et al., *ras transformation is associated with decreased expression of the brm/SNF2alpha ATPase from the mammalian SWI-SNF complex.* EMBO J, 1998. **17**(1): p. 223-31.

161. Kowenz-Leutz, E. and A. Leutz, *A C/EBP beta isoform recruits the SWI/SNF complex to activate myeloid genes.* Mol Cell, 1999. **4**(5): p. 735-43.

162. Peterson, C.L. and J.L. Workman, *Promoter targeting and chromatin remodeling by the SWI/SNF complex.* Curr Opin Genet Dev, 2000. **10**(2): p. 187-92.

163. Wang, W., et al., *Purification and biochemical heterogeneity of the mammalian SWI-SNF complex.* EMBO J, 1996. **15**(19): p. 5370-82.

164. Wang, W., et al., *Diversity and specialization of mammalian SWI/SNF complexes.* Genes Dev, 1996. **10**(17): p. 2117-30.

165. Kingston, R.E. and G.J. Narlikar, *ATP-dependent remodeling and acetylation as regulators of chromatin fluidity.* Genes Dev, 1999. **13**(18): p. 2339-52.

166. Vignali, M., et al., *ATP-dependent chromatin-remodeling complexes.* Mol Cell Biol, 2000. **20**(6): p. 1899-910.

167. Mohrmann, L. and C.P. Verrijzer, *Composition and functional specificity of SWI2/SNF2 class chromatin remodeling complexes.* Biochim Biophys Acta, 2005. **1681**(2-3): p. 59-73.

168. Smith, C.L. and C.L. Peterson, *ATP-dependent chromatin remodeling.* Curr Top Dev Biol, 2005. **65**: p. 115-48.

169. Cote, J., C.L. Peterson, and J.L. Workman, *Perturbation of nucleosome core structure by the SWI/SNF complex persists after its detachment, enhancing subsequent transcription factor binding.* Proc Natl Acad Sci U S A, 1998. **95**(9): p. 4947-52.

170. Imbalzano, A.N., et al., *Facilitated binding of TATA-binding protein to nucleosomal DNA.* Nature, 1994. **370**(6489): p. 481-5.

171. Bortvin, A. and F. Winston, *Evidence that Spt6p controls chromatin structure by a direct interaction with histones.* Science, 1996. **272**(5267): p. 1473-6.

172. Kwon, H., et al., *Nucleosome disruption and enhancement of activator binding by a human SW1/SNF complex.* Nature, 1994. **370**(6489): p. 477-81.

173. Khavari, P.A., et al., *BRG1 contains a conserved domain of the SWI2/SNF2 family necessary for normal mitotic growth and transcription.* Nature, 1993. **366**(6451): p. 170-4.

174. Deuring, R., et al., *The ISWI chromatin-remodeling protein is required for gene expression and the maintenance of higher order chromatin structure in vivo.* Mol Cell, 2000. **5**(2): p. 355-65.

175. Muchardt, C. and M. Yaniv, *ATP-dependent chromatin remodelling: SWI/SNF and Co. are on the job.* J Mol Biol, 1999. **293**(2): p. 187-98.

176. Hassan, A.H., K.E. Neely, and J.L. Workman, *Histone acetyltransferase complexes stabilize swi/snf binding to promoter nucleosomes.* Cell, 2001. **104**(6): p. 817-27.

177. Trouche, D., et al., *RB and hbrm cooperate to repress the activation functions of E2F1.* Proc Natl Acad Sci U S A, 1997. **94**(21): p. 11268-73.

178. DelBove, J., et al., *Inactivation of SNF5 cooperates with p53 loss to accelerate tumor formation in Snf5(+/-);p53(+/-) mice.* Mol Carcinog, 2009. **48**(12): p. 1139-48.

179. Shanahan, F., et al., *Cyclin E associates with BAF155 and BRG1, components of the mammalian SWI-SNF complex, and alters the ability of BRG1 to induce growth arrest.* Mol Cell Biol, 1999. **19**(2): p. 1460-9.

180. Muchardt, C. and M. Yaniv, *The mammalian SWI/SNF complex and the control of cell growth.* Semin Cell Dev Biol, 1999. **10**(2): p. 189-95.

181. Barker, N., et al., *The chromatin remodelling factor Brg-1 interacts with beta-catenin to promote target gene activation.* EMBO J, 2001. **20**(17): p. 4935-43.

182. Sudarsanam, P. and F. Winston, *The Swi/Snf family nucleosome-remodeling complexes and transcriptional control.* Trends Genet, 2000. **16**(8): p. 345-51.

183. Wolffe, A.P., F.D. Urnov, and D. Guschin, *Co-repressor complexes and remodelling chromatin for repression.* Biochem Soc Trans, 2000. **28**(4): p. 379-86.

184. Wu, J. and M. Grunstein, *25 years after the nucleosome model: chromatin modifications.* Trends Biochem Sci, 2000. **25**(12): p. 619-23.

185. Polach, K.J. and J. Widom, *Mechanism of protein access to specific DNA sequences in chromatin: a dynamic equilibrium model for gene regulation.* J Mol Biol, 1995. **254**(2): p. 130-49.

186. Zofall, M., et al., *Chromatin remodeling by ISW2 and SWI/SNF requires DNA translocation inside the nucleosome.* Nat Struct Mol Biol, 2006. **13**(4): p. 339-46.

187. Owen-Hughes, T., *Colworth memorial lecture. Pathways for remodelling chromatin.* Biochem Soc Trans, 2003. **31**(Pt 5): p. 893-905.

188. Gregory, R.I. and R. Shiekhattar, *Chromatin modifiers and carcinogenesis.* Trends Cell Biol, 2004. **14**(12): p. 695-702.

189. Muchardt, C. and M. Yaniv, *When the SWI/SNF complex remodels...the cell cycle.* Oncogene, 2001. **20**(24): p. 3067-75.

190. Glaros, S., et al., *The reversible epigenetic silencing of BRM: implications for clinical targeted therapy.* Oncogene, 2007. **26**(49): p. 7058-66.

191. Glaros, S., et al., *Targeted knockout of BRG1 potentiates lung cancer development.* Cancer Res, 2008. **68**(10): p. 3689-96.

192. Yamamichi, N., et al., *The Brm gene suppressed at the post-transcriptional level in various human cell lines is inducible by transient HDAC inhibitor treatment, which exhibits antioncogenic potential.* Oncogene, 2005. **24**(35): p. 5471-81.

193. Yamamichi, N., et al., *Frequent loss of Brm expression in gastric cancer correlates with histologic features and differentiation state.* Cancer Res, 2007. **67**(22): p. 10727-35.

194. Reisman, D., S. Glaros, and E.A. Thompson, *The SWI/SNF complex and cancer.* Oncogene, 2009. **28**(14): p. 1653-68.

195. Fukuoka, J., et al., *Chromatin remodeling factors and BRM/BRG1 expression as prognostic indicators in non-small cell lung cancer.* Clin Cancer Res, 2004. **10**(13): p. 4314-24.

196. Muchardt, C., et al., *The hbrm and BRG-1 proteins, components of the human SNF/SWI complex, are phosphorylated and excluded from the condensed chromosomes during mitosis.* EMBO J, 1996. **15**(13): p. 3394-402.

197. Guo, W. and F.G. Giancotti, *Integrin signalling during tumour progression.* Nat Rev Mol Cell Biol, 2004. **5**(10): p. 816-26.

198. Boudreau, N., C. Myers, and M.J. Bissell, *From laminin to lamin: regulation of tissue-specific gene expression by the ECM.* Trends Cell Biol, 1995. **5**(1): p. 1-4.

199. Reginato, M.J., et al., *Integrins and EGFR coordinately regulate the pro-apoptotic protein Bim to prevent anoikis.* Nat Cell Biol, 2003. **5**(8): p. 733-40.

200. Silberstein, G.B. and C.W. Daniel, *Investigation of mouse mammary ductal growth regulation using slow-release plastic implants.* J Dairy Sci, 1987. **70**(9): p. 1981-90.

201. Imagawa, W., G.K. Bandyopadhyay, and S. Nandi, *Regulation of mammary epithelial cell growth in mice and rats.* Endocr Rev, 1990. **11**(4): p. 494-523.

202. Warburton, M.J., et al., *Distribution of myoepithelial cells and basement membrane proteins in the resting, pregnant, lactating, and involuting rat mammary gland.* J Histochem Cytochem, 1982. **30**(7): p. 667-76.

203. Taylor-Papadimitriou, J., *Monoclonal antibodies in the study of differentiation and malignancy in the human breast.* Anticancer Res, 1987. **7**(5B): p. 1069-70.

204. Weaver, V.M., et al., *The importance of the microenvironment in breast cancer progression: recapitulation of mammary tumorigenesis using a unique human mammary epithelial cell model and a three-dimensional culture assay.* Biochem Cell Biol, 1996. **74**(6): p. 833-51.

205. Butcher, D.T., T. Alliston, and V.M. Weaver, *A tense situation: forcing tumour progression.* Nat Rev Cancer, 2009. **9**(2): p. 108-22.

206. Muthuswamy, S.K., et al., *ErbB2, but not ErbB1, reinitiates proliferation and induces luminal repopulation in epithelial acini.* Nat Cell Biol, 2001. **3**(9): p. 785-92.

207. Debnath, J. and J.S. Brugge, *Modelling glandular epithelial cancers in three-dimensional cultures.* Nat Rev Cancer, 2005. **5**(9): p. 675-88.

208. Frisch, S.M. and H. Francis, *Disruption of epithelial cell-matrix interactions induces apoptosis.* J Cell Biol, 1994. **124**(4): p. 619-26.

209. Valentijn, A.J. and A.P. Gilmore, *Translocation of full-length Bid to mitochondria during anoikis.* J Biol Chem, 2004. **279**(31): p. 32848-57.

210. Meredith, J.E., Jr. and M.A. Schwartz, *Integrins, adhesion and apoptosis.* Trends Cell Biol, 1997. **7**(4): p. 146-50.

211. Debnath, J., et al., *The role of apoptosis in creating and maintaining luminal space within normal and oncogene-expressing mammary acini.* Cell, 2002. **111**(1): p. 29-40.

212. He, P., et al., *Identification of carboxypeptidase E and gamma-glutamyl hydrolase as biomarkers for pulmonary neuroendocrine tumors by cDNA microarray.* Hum Pathol, 2004. **35**(10): p. 1196-209.

213. Muschler, J., et al., *A role for dystroglycan in epithelial polarization: loss of function in breast tumor cells.* Cancer Res, 2002. **62**(23): p. 7102-9.

214. Lee, G.Y., et al., *Three-dimensional culture models of normal and malignant breast epithelial cells.* Nat Methods, 2007. **4**(4): p. 359-65.

215. Weaver, V.M., et al., *beta4 integrin-dependent formation of polarized three-dimensional architecture confers resistance to apoptosis in normal and malignant mammary epithelium.* Cancer Cell, 2002. **2**(3): p. 205-16.

216. Kasemeier-Kulesa, J.C., et al., *Reprogramming multipotent tumor cells with the embryonic neural crest microenvironment.* Dev Dyn, 2008. **237**(10): p. 2657-66.

217. Margulis, A., et al., *E-cadherin suppression accelerates squamous cell carcinoma progression in three-dimensional, human tissue constructs.* Cancer Res, 2005. **65**(5): p. 1783-91.

218. Kadoya, Y. and S. Yamashina, *Salivary gland morphogenesis and basement membranes.* Anat Sci Int, 2005. **80**(2): p. 71-9.

219. Berthiaume, F., et al., *Effect of extracellular matrix topology on cell structure, function, and physiological responsiveness: hepatocytes cultured in a sandwich configuration.* FASEB J, 1996. **10**(13): p. 1471-84.

220. Vaughan, M.B., et al., *A three-dimensional model of differentiation of immortalized human bronchial epithelial cells.* Differentiation, 2006. **74**(4): p. 141-8.

221. Park, D.W., et al., *A well-defined in vitro three-dimensional culture of human endometrium and its applicability to endometrial cancer invasion.* Cancer Lett, 2003. **195**(2): p. 185-92.

Figure Legends

Figure 1.1 Simplified Integrin-RTK Signaling in MEC Growth & Survival

Cooperative integrin-receptor tyrosine kinases (RTK) signaling mediates survival, proliferation, differentiation and apoptosis of cells. The major pathways of integrin- and growth factor (GF) receptor-mediated signaling relevant to this thesis are indicated by pink ovals. Most integrins recruit FAK as well as activating signaling to PI3K and AKT/protein kinase B (PKB). FAK functions as a phosphorylation-regulated scaffold to recruit Src family kinases (SFKs) to focal adhesions. SFKs along with other downstream effectors such as Rho interact with components of the cell cytoskeleton to alter migration, cell shape and cell rigidity. FAK also activates ERK/MAPK pathways via Ras to affect cellular proliferation, survival and differentiation. Most importantly, joint integrin–RTK signaling is required for cell proliferation and for optimal cell survival and cell migration/invasion and is the focus of my thesis research.

Figure 1.2 Integrin heterodimers and ligands

Composition of known integrin heterodimers and reported major ECM ligands [100]. Abbreviations are as follows: Coll: Collagen, FN: Fibronectin; LN: Laminin; uPar: Urokinase-type Plasminogen Activator Receptor; VN: Vitronectin.

Figure 1.3 SWI/SNF chromatin remodeling complex components, interacting proteins and cellular function

Schematic diagram of the SWI/SNF protein complex in contact with chromatin. SWI/SNF component proteins are shown as green and teal spheres. Genomic DNA is shown as a black ribbon winding around octamers of histones that constitute nucleosomes (yellow cylinders). SWI/SNF interacting partners (pink ovals) and their subsequent regulation of cellular activities are highlighted.

Figure 1.4 Mammary Gland Biology

The mature mammary gland is composed of 15-20 lobes, each lobe is subdivided into smaller lobules and each lobule contains a hollow sphere (alveolus or acinus) lined with milk-secreting luminal epithelial cells and surrounded by myoepithelial cells (pink inset). Surrounding each acinus is a specialized membrane, termed the basement membrane. To keep the correct polarized morphology of this branching-duct system requires another essential component –the extracellular matrix (ECM), which together with additional cell types including adipocytes, endothelial cells, fibroblasts and inflammatory cells, constitutes the stroma (green meshwork surrounding acinus).

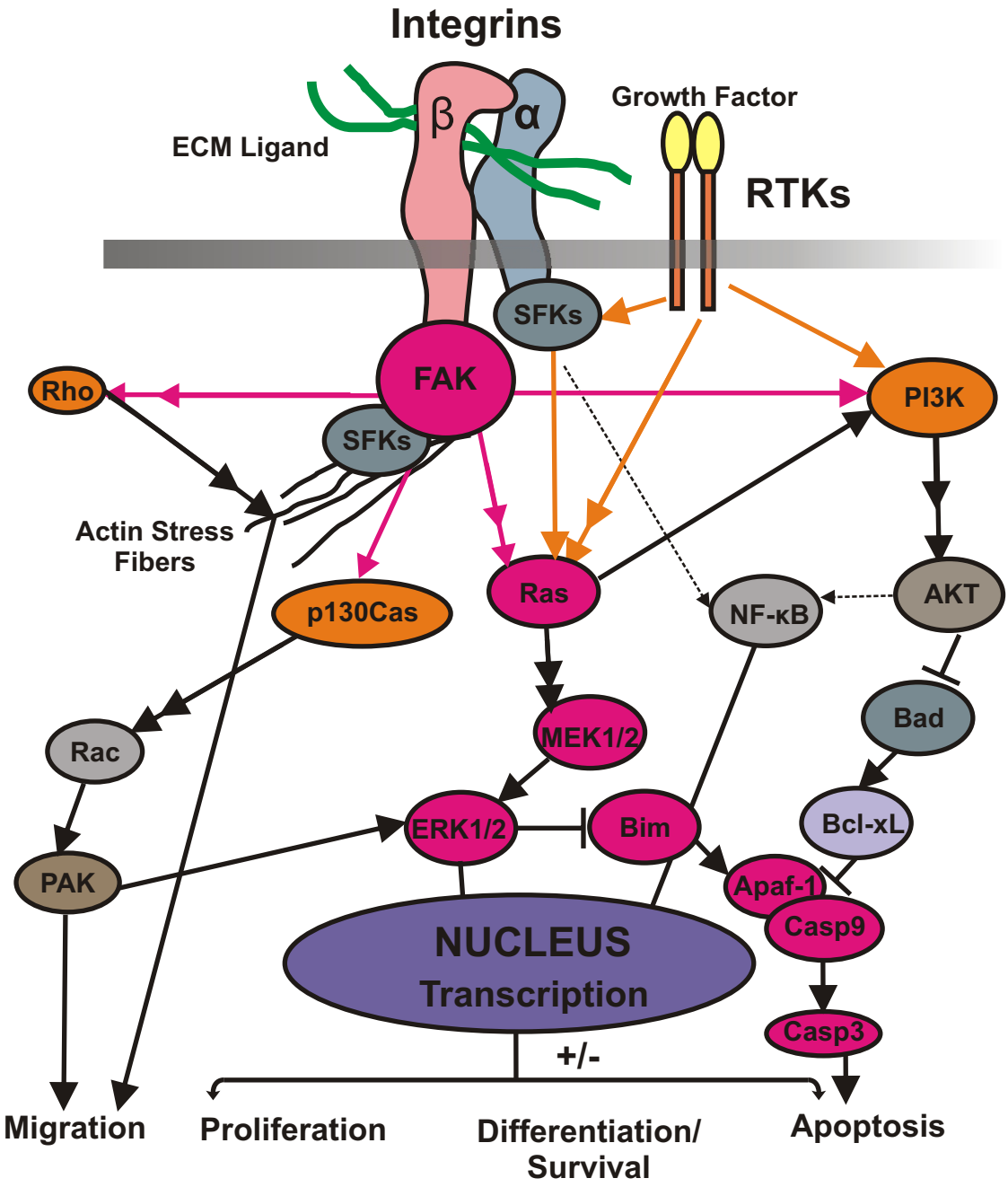

Figure 1.1 Simplified Integrin-RTK Signaling in MEC Growth & Survival

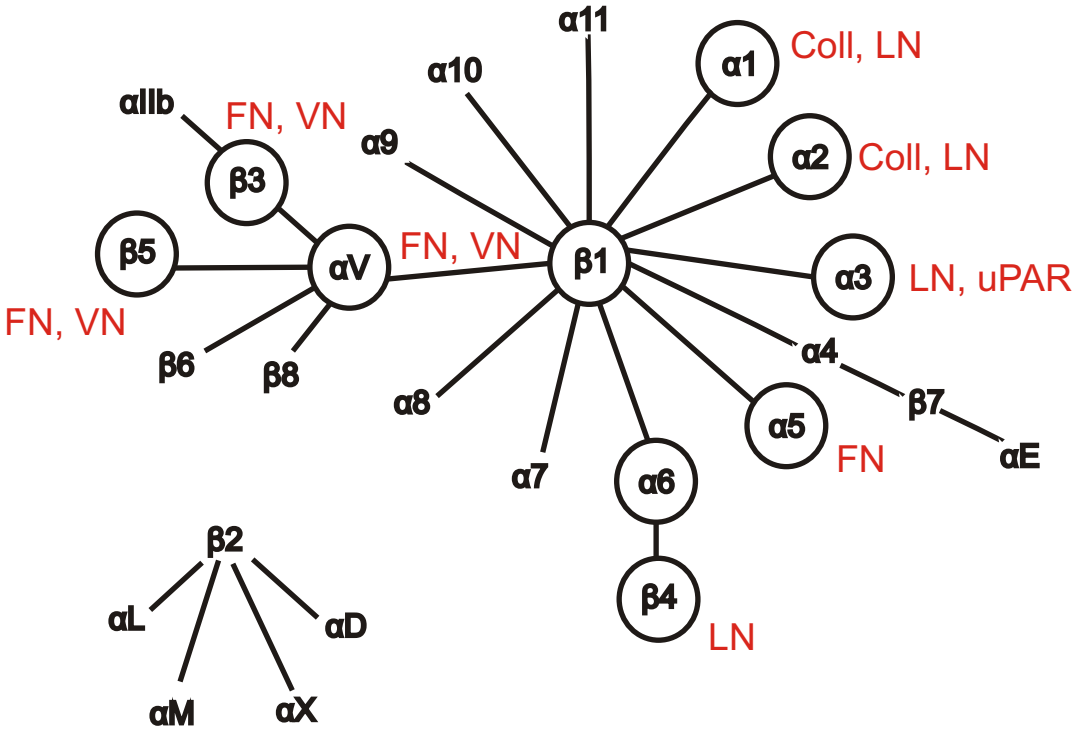

Figure 1.2 Integrin Heterodimers and Ligands

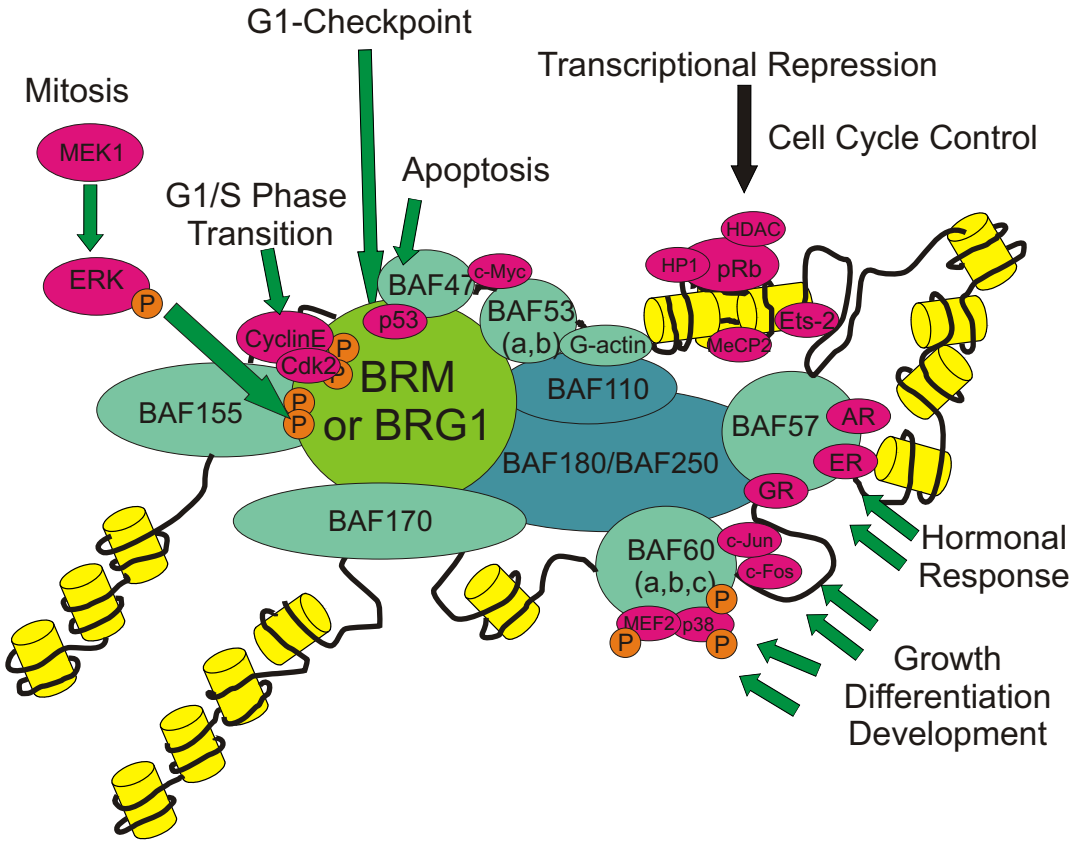

Figure 1.3 SWI/SNF chromatin remodeling complex components, interacting proteins and cellular function

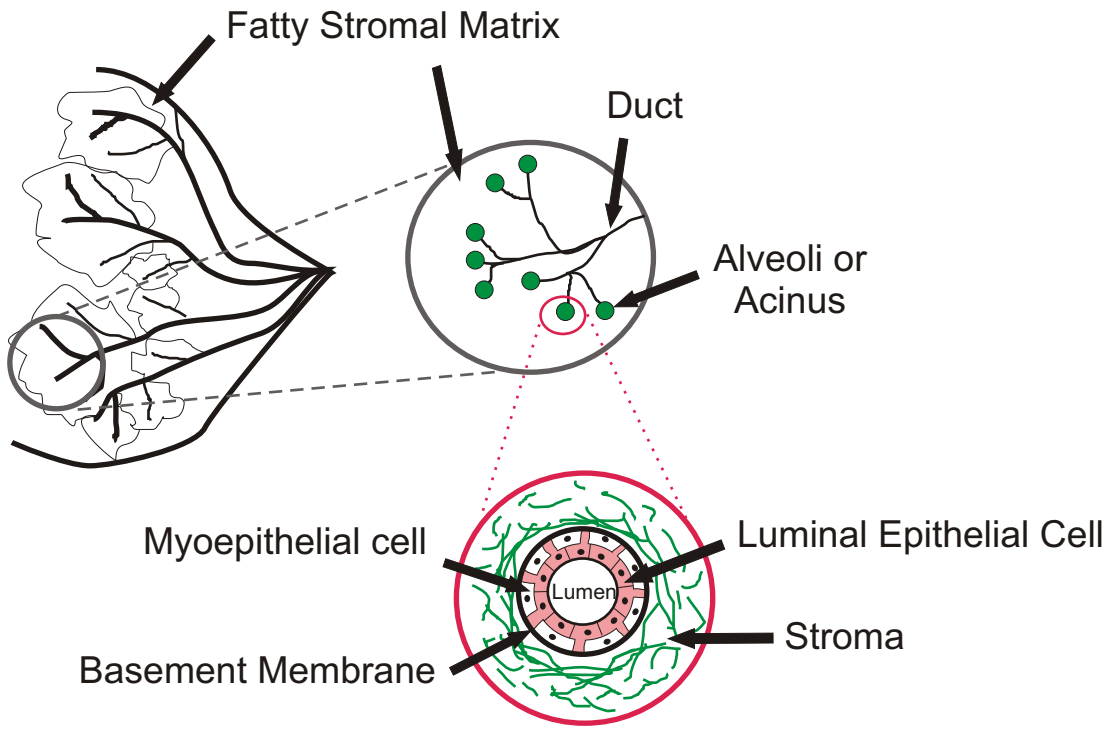

Figure 1.4 Mammary Gland Biology

Chapter Two
Oncogenic targeting of SWI/SNF BRM regulates α5 integrin to promote a tumor phenotype

Statement of Contribution

The execution of the studies contributing to the experimental findings reported in the manuscript entitled “Oncogenic targeting of the SWI/SNF BRM regulates α5 integrin to promote a tumor phenotype” were conducted primarily by Kathleen M. Stewart.

Dr. Nathalie Cohet generated and validated the BRM and Scramble shRNA targeting constructs and gave critical scientific feedback throughout the manuscript process. *Dr. Johnathon Lakins* generated and validated the following retroviral constructs: dominant negative BRM (K749R); wt BRM; and EGFP vector controls. Dr. Lakins also produced and validated the MCF10A wt ErbB2 over-expressing cell line used in this manuscript. Additionally, Dr. Lakins was of great technical assistance for all methodologies used in this manuscript. *Yekaterina Miroshinova* is currently completing experiments for the submission of this manuscript and all experiments requested by reviewers. *Dr. Jayanta Debnath* contributed the MCF10A Ras^{V12} cell line and its empty vector control to these studies and provided technical assistance, directed experiments and reviewed the scientific rigor of this manuscript. *Dr. David Reisman* manufactured the specific Anti-BRM antibody used in all of our experiments and contributed technical assistance to the production of this manuscript. *Drs. Jeffrey Nickerson and Anthony Imbalzano* first conducted the experiments characterizing and validating the dominant negative BRM (K749R) construct and provided great technical assistance and scientific feedback throughout the development of this project and writing of this manuscript.

Oncogenic targeting of SWI/SNF BRM regulates α5 integrin to promote a tumor phenotype

Kathleen M. Stewart[1], Nathalie Cohet[2], Yekaterina Miroshinova[1], Johnathon N. Lakins[1], Jayanta Debnath[3], David Reisman[4], Jeffrey A. Nickerson[2], Anthony N. Imbalzano[2], and Valerie M. Weaver[1, 5, 6]

[1]Department of Surgery and Center for Bioengineering and Tissue Regeneration, University of California San Francisco, San Francisco, CA 94143
[2]Department of Cell Biology, University of Massachusetts Medical School, Worcester, MA 01655
[3]Department of Pathology, University of California San Francisco, San Francisco, CA 94143
[4]Department of Medicine, Med-Hematology/Oncology Division, University of Michigan, Ann Arbor, MI 48109
[5]Department of Anatomy and Bioengineering and Therapeutic Sciences, Eli and Edythe Broad Center of Regeneration Medicine and Stem Cell Research and Helen Diller Family Comprehensive Cancer Center, University of California San Francisco, San Francisco, CA 94143

[6]Address correspondence to:

Valerie M. Weaver
University of California, San Francisco
Center for Bioengineering and Tissue Regeneration
Department of Surgery
513 Parnassus Avenue, S1364C-0456
San Francisco, CA 94143
Email: Valerie.Weaver@ucsfmedctr.org
Telephone: (415) 476-3826
Fax: (415) 476-3985

Abstract

Tumors typically exhibit modified integrin levels although the molecular basis for this phenotype remains unclear. In this study we examined the relationship between oncogene-dependent transformation and integrin levels in breast cancer. We found that oncogenic transformation promoted mammary epithelial cell growth and survival and disrupted mammary morphogenesis in three dimensional (3D) culture assays through increased α5 integrin levels. Furthermore, we discovered that a SWI/SNF chromatin remodeling enzyme, BRM, repressed α5 integrin levels in non-malignant MECs and BRM expression was reduced in oncogenically transformed MECs. Consistently, we observed that decreased BRM expression and/or activity in non-malignant MECs disrupted 3D mammary morphogenesis by increased α5 integrin levels. Furthermore, we found that re-expression of BRM in oncogenically-transformed MECs suppressed the malignant phenotype in 3D cultures via reduced α5 integrin expression. These findings underscore the reciprocal relationship between oncogenic transformation and altered ECM responsiveness and identify an epigenetic mechanism whereby oncogenes drive malignancy through the downregulation of the SWI/SNF BRM chromatin remodeling protein.

Introduction

Tumors are initiated by genetic alterations that modify the levels and function of key oncogenes and tumor suppressors [1]. Oncogenes and tumor suppressors drive malignant progression by inducing cell growth and enhancing cell survival through alterations of cell cycle pathway regulators, stress response genes and apoptotic signaling factors [2]. Tumors are also characterized by a desmoplastic response defined by extracellular matrix (ECM) remodeling, activated fibroblasts, angiogenesis and an inflammatory infiltrate [3]. This activated stroma can promote tumor progression by enhancing cell growth, increasing cell survival and modifying the inflammatory response and restricting tissue desmoplasia can impede malignancy. Interestingly, either oncogenic transformation or loss of tumor suppressor function modifies tumor cell responsiveness to ECM microenvironmental cues [4-6]. This suggests that genetic alterations that initiate tumors may drive malignancy by modifying mammary epithelial cell (MEC)-ECM interactions.

MEC-ECM interactions are mediated via adhesion receptors of which integrins are the best characterized [4-6]. Integrins are transmembrane receptors that transduce extracellular matrix (ECM) cues through adhesion complexes that regulate cytoskeletal organization and signaling factors to induce cell migration, growth, survival and tissue differentiation [7-12]. Furthermore, tumors frequently exhibit altered integrin profiles, increased focal adhesions, and enhanced integrin signaling [8, 13-17]. For instance, breast, colon and skin tumors have elevated

α6β4 integrin and secrete abundant Laminin-5 and α6β4 integrin-Laminin-5 interactions promote cell growth, survival and migration [8, 17-21]. In addition, breast, lung, and ovarian cancers show increased α5β1 integrin levels and its predominant ECM ligand, fibronectin [16, 19, 22, 23]. α5β1 integrin-fibronectin interactions support cell growth and survival and promote cell motility and angiogenesis in tumors [14, 16, 24, 25]. Moreover, α5β1 integrin-fibronectin interactions are often associated with more aggressive malignancies and current clinical studies are underway to evaluate the efficacy of α5β1 integrin monoclonal antibodies in the treatment of solid tumors [26, 27]. Consistently, ablating β1 integrin expression represses breast tumor progression and reducing integrin-mediated signaling likewise inhibits breast cancer [28-31]. Nevertheless, why α5β1 integrin expression and signaling are frequently deregulated in breast cancer needs to be clarified.

Given the critical role that integrins play in a variety of cell behaviors, it is not surprising that the strategies for integrin modulation are quite complex. While much work describes the biological function, activation and intracellular signaling of integrins, much less is known about the mechanisms which regulate integrin transcription although transcription factors and chromatin modifiers are implicated in this role [8, 14, 32]. Oncogenes, such as ErbB2, increase α5 integrin transcript levels in MECs, and Ha-Ras transformation associates with an increase in α5 integrin levels in non-malignant MECs [19, 33]. Given the established role of enhanced growth factor receptor signaling via ErbB2 in breast

cancers and its potential regulation of α5 integrin transcription, we explore the possibility that oncogenes promote cell growth and survival during tumor progression by increasing α5 integrin levels and if so, by what mechanism.

The α5 integrin promoter region contains both an AP-1 binding site and a CCAAT/enhancer binding protein (c/EBP) binding site that promote transcriptional activation. AP-1 and c/EBP-β transcriptional activities can be regulated through activated growth factor receptor and Ras-mediated signaling [14-17]. Interestingly, c/EBP-β activity and Ras signaling are implicated in coordinating activities of SWI/SNF chromatin remodeling complexes to regulate specific transcriptional targets [19 -21]. SWI/SNFs are chromatin remodeling proteins that are decreased in breast cancers and breast cancer cell lines but the functional relevance of their loss in breast cancer progression is unknown [34-36]. In this study, we explore the functional link between oncogenic signaling and altered MEC-ECM interactions via transcriptional regulation of α5 integrin by the SWI/SNF chromatin remodeling enzyme BRM during breast tumor progression.

Materials and Methods

Materials

We used commercial EHS matrix (Matrigel™) for the reconstituted basement membrane (rBM) assays; purified Rat tail Collagen I (BD Biosciences, San Jose, CA); Collagen IV (Collaborative Research Products, Bedford, MA), and purified Fibronectin and Laminin 1 (Sigma, St. Louis, MO) for the Cell Adhesion studies. Primary antibodies used for the studies were as follows: Goat antiserum: Lamin B1 [37]; Monoclonal mouse antibodies: α2 integrin, clone 10G11; α3 integrin, clone P15B; αv integrin, clone M9 (all from Millipore, Billerica, MA), β1 integrin, clone TS2/16; β4 integrin, clone 3E1 (all from ATCC, Manassus, VA), fibronectin, clone 3E3 (Millipore), Ki-67, clone 35 (BD Transduction Laboratories, San Jose, CA), Laminin-5 α3 chain specific, clone BM165 (gift from M.P. Marinkovich,[10]); Rabbit anti-serum: α5 integrin, ab1928 (Millipore); Brm (GST-purified protein, [34]) β-catenin [37]; Cleaved-Caspase 3 (Cell Signaling, Danvers, MA); Rat anti-serum: α6 integrin, clone GoH3 (Millipore), β1-integrin, clone AIIB2 (gift from C. Damsky, University of California, San Francisco; Weaver et al., 1997). Preservative free function blocking antibodies used for the studies were as follows: α2 integrin, clone BMA2.1 and α5 integrin, clone P1D6 (BD Biosciences), fibronectin, clone 3E3 (Millipore).

Secondary antibodies used for the studies were as follows: Cy-5-, FITC-, TRITC-nonconjugated anti-goat, mouse, rabbit, and rat antibodies (Jackson Immunoresearch Laboratories, West Grove, PA); ECL Horseradish peroxidase-conjugated anti-goat, mouse, rabbit and rat antibodies (Amersham Pharmacia Biotech, Pittsburgh, PA); Phycoerythrin-conjugated anti-goat, mouse, rabbit and rat antibodies [37].

Cell culture

MCF10A cells were obtained from ATCC and maintained in 2D monolayer cultures in DMEM:F12 (Invitrogen) supplemented with 5% donor horse serum (Invitrogen), 0.5µg/ml hydrocortisone [37], 100ng/ml cholera toxin [37], 10µg/ml insulin [37], 20ng/ml recombinant human epidermal growth factor (EGF, Peprotech, Rocky Hill, NJ) and 50 U/ml each of penicillin/streptomycin (Invitrogen). MCF10AT1 cells were obtained from the Barbara Ann Karmanos Institute (Detroit, MI), MCF10A Ras^{V12}, and MCF10A pBABE (empty vector control) (gift from J. Debnath, University of San Francisco, California) and MCF10A wt ErbB2 were previously generated and described [38]. For 3D morphogenesis assays, MECs were embedded (0.5-0.8 $x10^6$ cells/ml) within Matrigel, refed every 2 days and imaged for up to 30 days as previously described [39].

Vector Constructs and ectopic gene expression

Full length human BRM containing a single point mutation in the ATPase binding domain (K749R) was cloned into the pRet puro Tet IRES EGFP tetracycline-inducible vector. The shRNA for BRM and Scrambled Control (Scrm) were derived from siRNA previously designed [40] and were cloned into the pLVrtTRKRAB-NeoR tetracycline-inducible vector and expressed bicistronically with EGFP. Four myc tags were added to the C terminus of full-length BRM construct and cloned into the pLV puro TetO7mCMV tetracycline-inducible lentiviral vector and expressed biscistronically with eGFP. Full length human α5 integrin was cloned into the multiple cloning site of the lentiviral vector pLV puroTetO7mCMV tetracycline-inducible vector and expressed bicistronically with CHERRY. The preparation of virus and cell infection and selection have been described[13]. Target cells were infected with virus using 8ug/mL polybrene, and selected with puromycin (K749R), G148 (BRMi, Scrm) and Hygromycin (α5-Cherry, wt Brm).

Immunofluorescence

3D *in vitro* cultures were fixed using 2% paraformaldehyde, embedded in sucrose and frozen in Tissue-Tek OCT compound (Sakura Finetek, Torrance, CA) and sectioned using the Tissue-Tek Cryostat (Sakura Finetek) (6-10μm sections; [41]). Samples were incubated with primary antibodies followed by either AlexaFluor 488/594 or Cy5-conjugated secondary antibodies. Nuclei were counterstained with DAPI [37]. Slides were imaged using a scanning Zeiss

LSM510 confocal microscope and Zeiss LSM Imaging software (Thornwood, NY). Confocal images were recorded at 40x and conventional images were recorded at 10-40x. As previously described, colony size and morphology in 3D rBM assays were analyzed at indicated times and a minimum of 50 acini/images were taken per condition for statistical significance [13, 42].

Immunoblotting

Cells were lysed in Laemmli buffer containing 20mM sodium fluoride, 1mM sodium orthovanadate, and a cocktail of protease inhibitors. Protein concentration was determined using a bicinchoninic acid (BCA; Thermo Fisher Scientific, Rockford, IL) assay. Equal protein was separated on SDS-PAGE gels, immunoblotted, and visualized using an ECL system (Amersham). The chemiluminescent intensity of bands were calculated using the Image Analyzer LAS-1000 Plus system and the Image Reader LAS-1000 Pro version 1.0 software (Fuji, Tokyo, Japan).

Real-Time PCR

Random-primed cDNA was prepared from total isolated RNA (Trizol; Invitrogen, Carlsbad, CA). All primers of target genes and an internal control gene, 18S, were designed by Primer3 software (http://frodo.wi.mit.edu/primer3/; See Appendix). In each assay, target DNA sequences were quantified by real time PCR using SYBR Green detection system (Qiagen, Valencia, CA) and a Light Cycler Apparatus (Roche Applied Science; software version 3.5, Indianapolis,

IN). A singleplex reaction mix was prepared according to the manufacture's protocol, as described previously [11-13]. The thermal cycling conditions included an initial denaturation step at 95°C for 10 min, 40 cycles at 95°C for 15s and 60°C for one min. Fold change in expression were determined using the ΔCt method with normalization to total RNA [9].

Flow cytometry

Cells were isolated, nonspecific binding was blocked (60 min Dulbecco's PBS, 0.1% bovine serum albumin) and cells were incubated with saturating concentrations of primary mAb (1 hr), washed three times with Dulbecco's PBS and labeled with phycoerythrin-conjugated goat immunoglobulin [37]. Stained cells were washed three times and data was acquired on a FACScan™ (Becton Dickinson, Franklin Lakes, NJ). All manipulations were conducted at 4°C. A minimum of 20,000 gated events were collected to maximize statistical power. Histogram analysis was completed on FlowJo Analysis Software (Tree Star, Inc., Ashland, OR).

Adhesion assay

A modification to previously published methods [12, 13] was used to assess cell attachment to various extracellular matrix proteins. In brief, plates coated with either 0.05% Matrigel , 0.06mg/ml Collagen I, 10μg/ml Collagen IV, 10μg/ml Fibronectin, 10μg/ml Laminin I or 1% BSA (Amresco, Solon, OH) diluted in Dulbecco's PBS (Invitrogen). Wells were blocked (1h RT; 0.1% BSA), incubated

with target cells (30 min, 37^{o}C), washed (3x Dulbecco's PBS), and incubated with 0.5mg/ml MTT (4h, RT; Sigma). Cells were then lysed in DMSO and quantified using spectrophotometric assay of colored product using a Dynex Technologies MRX plate reader (Dyenx Technologies, Chantilly, VA).

Function-blocking studies

To inhibit integrin function or Fibronectin binding, cells were incubated with mAbs against α2 integrin (2-20 μg IgG/ml ECM), α5 integrin (2-20 μg IgG/ml ECM), fibronectin (2-20 μg IgG/ml ECM) or IgG isotype matched control mAbs (Jackson Immunoresearch) (2-20 μg IgG/ml ECM) at the time of cell embedment in 3D rBM morphogensis assays.

Statistical analysis

InStat software (Graphpad, LaJolla, CA) was used to conduct the statistical analysis of our data. Unless otherwise stated, two-tailed student *t*-tests were used for significance testing and two-tailed Pearson tests were used for correlation analysis. Means are presented as ±SEM of 3-5 independent experiments and statistical significance was considered $p< 0.05$. Unless otherwise noted, sample size was n=3.

Results

Oncogenic transformation is associated with increased α5β1 integrin levels.

We have demonstrated previously that normal and tumorigenic breast cell phenotypes can be effectively distinguished in the context of three dimensional (3D) reconstituted basement membrane (rBM) assays [43]. In 3D rBM assays, non-malignant MECs form polarized, growth-arrested, acinar structures, characterized by polarized β4 integrin localization and basal deposition of an endogenous basement membrane, composed mostly of laminin-5 (Figure 2.1A Control). Oncogenic transformation in the MCF10AT1, MCF10A-ErbB2 and MCF10A Ras^{V12} mammary epithelial cell lines (MECs) promoted MEC growth and survival and drove luminal filling to compromise MEC architecture in a 3D rBM assay (Figure 2.1A; [14]). Luminal filling and compromised MEC morphogenesis suggested oncogenic transformation perturbed MEC-ECM interactions to drive tumorigenesis. To explore possible functional links between MEC-ECM interactions and transformation, we examined integrin subunit levels in these transformed breast cancer cell lines. We found that oncogenic transformation was associated with a specific increase in total protein levels of the α5 integrin subunit and its predominant ECM ligand, fibronectin (Figure 2.1B).

We have previously shown that when transformed MECs were cultured in the presence of inhibitors of β1 integrin or epidermal growth factor receptor (EGFR), cells underwent “phenotypic reversion” to form near-normal growth-arrested acini similar to those formed by non-transformed MECs[43]. Therefore, we explored if inhibition of α5β1 integrin-fibronectin interactions using function blocking antibodies could cause phenotypic reversion of transformed MEC 3D cultures. We observed that α5 integrin or FN functional blocking antibodies phenotypically reverted transformed MEC 3D cultures (Figure 2.1C). In contrast, α2 integrin functional blocking antibody did not prevent compromised morphogenesis, suggesting specificity of altered MEC-ECM interactions via integrin subunit levels (Figure 2.1C). To determine if elevated α5β1 integrin-FN interactions are sufficient to promote MEC growth and survival and perturb 3D rBM-directed morphogenesis, we ectopically expressed α5 integrin in the non-malignant MCF10A cell line (Figure 2.8). We observed that increased α5 integrin levels per se did not perturb MEC morphogenesis. However in the presence of its ligand, fibronectin, increased α5 integrin levels supported a pre-malignant phenotype in 3D cultures as observed by luminal filling (Figure 2.1E). These data demonstrated that oncogenic transformation supported MEC growth and survival to perturb mammary morphogenesis in 3D cultures by increased α5β1 integrin-fibronectin interactions.

Brm is lost in transformed MECs and is associated with elevated α5β1 integrin levels

Little is known about the transcriptional regulation of specific integrin subunits. Interestingly, we observed that oncogenically transformed MECs not only modulated α5 integrin protein levels but that α5 integrin transcript levels were also significantly increased (Figure 2.2A).

Emerging evidence now implicates epigenetic mechanisms as potential transcriptional regulators of integrins [32, 44]. Abrogation of the activity of a SWI/SNF chromatin remodeling protein subunit associates with increasing α5 and αv integrin protein levels in human fibroblasts [32]. Therefore, we next asked whether the SWI/SNF protein BRM could be affected in transformed MECs. We found that BRM protein levels were significantly reduced in transformed MECs (Figure 2.2B). To further explore the relevance of BRM in oncogene-mediated integrin changes, we expressed an inducible BRM-specific shRNA construct in nonmalignant MCF10A MECs (Figure 2.2C). Depletion of BRM levels in MCF10A cells produced a consistent and specific upregulation of α5 integrin at the mRNA and at the protein levels (Figure 2.2D and Figure 2.2E).

Furthermore, BRM knockdown increased the amounts of α5β1 integrin subunits localized to the cell surface as observed by FACS analysis and this was associated with an increase in α5β1 integrin activity as observed by a robust ligation to fibronectin coated surfaces (Figure 2.2F, Figure 2.2G and Figure 2.12). These data demonstrate that BRM SWI/SNF chromatin remodeling activity modulates α5β1 integrin expression and activity in MECs.

Brm depletion promotes cell growth and survival of MECs in 3D rBM assay. Given that we only saw a minimal effect on the proliferation and morphology of MCF10A cells expressing shRNA-mediated BRM knockdown in 2D (Figure 2.11), we sought to further explore BRM-mediated regulation of cell growth and survival in the context of a 3D environment in MEC organotypic cultures. We observed a significant and early increase in colony area of BRM-depleted MEC cultures (Figure 2.3A and Figure 2.3B). Because we observed a significant increase in colony size similar to that of oncogenically transformed MECs, we next asked whether reduced BRM levels in MECs increased cell growth and survival in a 3D environment to perturb MEC morphogenesis. We observed a premalignant phenotype in BRM knockdown MECs, characterized by pronounced luminal filling, intact basement membrane as observed by Laminin-5 immunostaining and polarized 3D organoids as evidenced by β4 integrin immunostaining (Figure 2.3C and Figure 2.3D). Most notably, BRM-depleted MEC cultures showed a significant increase in the reactive stromal protein fibronectin, which is normally down regulated in 3D morphogenesis assays (Figure 2.3C; [45]).

The process of luminal clearance is executed by both cell growth and cell death regulators, therefore, we asked whether BRM-depleted structures inhibited cell death pathways and/or augmented cell growth pathways [46]. We observed reduced apoptotic activity as evident by cleaved Caspase-3 immunostaining (Figure 2.3E and Figure 2.3F). Staining for expression of Ki-67, a nuclear antigen expressed in late G1-M phase of the cell cycle, is a reliable indicator of cell cycle progression routinely used in this culture system [17, 22, 23]. Acini were cultured for 14 days, sufficient time for cells to exit the cell cycle and cease proliferation. Cells were stained with Ki-67 and co-stained with DAPI, and the percentage of Ki-67-positive cells in the widest confocal cross-section of each acinus was calculated. Results showed that reduced BRM levels in MCF10A cells induced a dramatic increase in the percentage of Ki-67–positive cells (Figure 2.3E and Figure 2.3G). Importantly, we were successful in replicating these data using 2 additional unique and specific shRNA targeting sequences to BRM in MCF10A cells (Figure 2.10). Together these data implicate BRM in the regulation of cell growth and survival in the development of 3D MEC acinar structures.

Brm ATPase activity is necessary to regulate MEC growth and survival in 3D.

The ATPase activity of BRM is essential for its chromatin remodeling function [17-19]. Therefore, we examined whether BRM-dependent effects on cell growth and survival rely on its chromatin remodeling function. We assessed this possibility by expressing a previously described inducible dominant negative BRM, containing a mutation in the ATP-binding site of its helicase-like domain (K749R), in MCF10A cells (Figure 2.4A; [47]). Consistent with BRM shRNA studies, reduced ATPase activity of BRM moderately increased proliferation in 2D (Figure 2.11) and showed a similar increase in colony size in 3D rBM morphogenesis assays (Figure 2.4B and Figure 2.4C). Moreover, expression of dominant negative BRM phenocopied the premalignant 3D phenotype and showed similar deposition of the reactive stromal marker fibronectin we observed in shRNA BRM cultures (Figure 2.4D). Furthermore, abrogation of BRM ATPase activity promoted luminal filling via increased proliferation as seen by Ki67 staining and reduced cell death as observed by activated Caspase-3 staining in 3D rBM studies (Figure 2.4G-I). These data indicate that the chromatin remodeling activities of BRM are necessary for the regulation of cell growth and survival in 3D.

BRM regulates premalignant behavior by modulating α5β1 integrin-FN interactions

We previously demonstrated that α5β1 integrin-FN interactions played a key role in promoting the aberrant growth and survival of transformed MEC in 3D rBM. Because we found that BRM modulated α5 integrin levels in MECs we asked whether blocking either α5 integrin or its ligand, fibronectin, could normalize the growth and survival of BRM shRNA MECs in 3D cultures. We observed that shRNA BRM MECs cultured in the presence of α5 integrin or fibronectin, but not α2 integrin, function blocking antibodies were sufficient to normalize the phenotype of BRM-depleted cultures in 3D (Figure 2.5A).

Specifically, we saw a pronounced decrease in filled lumens as observed by DAPI staining (Figure 2.5A and Figure 2.5B) and this was associated with a concordant decrease in cell proliferation as measured by Ki67 staining and an increase in apoptosis of the luminal cell population as observe by cleaved Caspase-3 immunostaining comparable to that of Scrambled control MECs (Figure 2.5A, Figure 2.5C and Figure 2.5D). Inhibition of α5β1 integrin-FN interactions in the context of BRM deficiency induced growth arrest and restored MEC architecture in 3D thereby functionally linking the activity of BRM in the regulation of α5β1 integrin-fibronectin interactions to restrict cell growth and survival.

Re-expression of BRM in transformed MECs elicits phenotypic reversion in 3D.

We previously showed that oncogenic transformation in MECs increased α5β1 integrin expression to drive tumor growth and survival and that this was associated with reduced BRM levels. Additionally, we showed that BRM promotes α5β1 integrin-fibronectin interactions to regulate MEC growth and survival. Therefore, to directly test if oncogene-mediated MEC transformation required BRM downregulation, we utilized an inducible lentiviral expression system to re-express wild type BRM to levels comparable to non-malignant MECs in ErbB2 and Ras^{V12} transformed MCF10A cells (Figure 2.6A). To determine if oncogenes regulate α5 integrin mRNA levels via BRM, we examined α5 integrin transcript levels upon re-expression of BRM in ErbB2 and Ras^{V12} transformed MCF10A cells. Consistently, we observed a repression of α5 integrin mRNA levels and also its protein levels with the re-expression of BRM in both ErbB2 and Ras transformed MCF10A cells (Figure 2.6B and Figure 2.6C).

We next asked whether re-expression of BRM would be sufficient to cause phenotypic reversion of oncogenically transformed MECs in 3D cultures. BRM-overexpressing ErbB2 and Ras^{V12} MECs and non-malignant MECs were embedded in 3D rBM gels. After 14 days, non-malignant MECs formed small, uniform, typical multicellular spheres with organized basement membranes and basally localized β4 integrin (Figure 2.6D). ErbB2 and Ras^{V12} MECs colonies (both unmodified and vector infected) continued to grow and formed large,

irregular, unpolarized colonies (Figure 2.6 D). In contrast, ErbB2 and Ras^{V12} transformed MECs re-expressing wt BRM underwent phenotypic reversion, forming control-like colonies that displayed appropriate cellular polarity similar to α5 integrin function blocking studies (Figure 2.6D, Figure 2.1C). Re-expression of wt BRM in transformed MECs also caused a significant reduction in proliferation as observed by Ki67 staining and promoted luminal clearance (Figure 2.6E and Figure 2.6F). These results indicate that re-expression of BRM at levels comparable with nonmalignant cells is sufficient not only to reduce the growth capacity of the tumor colonies but also to reinstate the polarized phenotype typical of normal breast epithelial acini.

BRM is a mediator of oncogene function in the regulation of α5β1 integrin to drive breast tumorigenesis

In this study we provided evidence that oncogenic signaling promoted MEC growth and survival through increased α5 integrin expression and decreased BRM expression (Figures 2.1 and 2.2). Re-expression of BRM and/or inhibition of α5β1 integrin-FN interactions in transformed MECs caused an almost complete reversion of breast tumor cell behavior to that of a non-malignant breast cell phenotype in 3D culture models as defined by the formation of growth arrested, hollow MEC acinar structures (Figures 2.5 and 2.6).

These data established a functional link between oncogene-mediated signaling, ECM responsiveness via α5β1 integrin-FN interactions and oncogenic targeting of an epigenetic modifier, BRM, to promote breast tumor progression. Based on the findings in this report we propose a model in which oncogenes drive growth and survival via augmented α5 integrin-fibronectin interactions through suppression of BRM expression and chromatin remodeling activities. Therefore, BRM serves as a mechanism by oncogenes function to regulate MEC-ECM interactions during malignant transformation (Figure 2.7).

Discussion

In this study we examined the relationship between oncogene-dependent transformation, integrin levels and expression of the epigenetic regulator BRM in breast cancer. We found that oncogenic transformation promoted mammary epithelial cell (MEC) growth and survival through increased α5 integrin levels and implicated BRM-directed chromatin remodeling changes as the mediator of these changes in ECM responsiveness in transformed MECs.

We found that increased α5β1 integrin-fibronectin (FN) interactions promoted MEC growth and survival to drive a pre-malignant phenotype, as evident by luminal filling, in 3D culture assays (Figure 2.1). These findings are consistent with prior studies which showed that ERBB2 signaling can transcriptionally upregulate α5 integrin levels in another breast cancer cell line, MCF-7 and provide an important mechanistic link[33]. Interestingly, Ras transformation in non-tumorigenic MECs increases levels of α5 integrin and α6 integrin protein levels and is associated with increased motility and enhanced tumor cell survival[19]. Furthermore, studies using various cell culture systems have suggested that α5β1 integrin is involved in many cellular processes including cell proliferation, angiogenesis and oncogenic transformation [16, 33, 48].

Expression of α5 integrin and fibronectin are largely absent in normal adult mammary tissue and their aberrant expression is associated with breast tumor progression and metastasis and also correlates with decreased survival of breast cancer patients [25, 26]. The findings in this report add to the growing body of literature that implicates α5β1 integrin in the pathogenesis of cancers [19, 23, 33, 49-51].

For example, in murine lung cancer cells, shRNA targeting of α5 integrin decreases tumor cell migration, proliferation and anchorage-independent growth [16]. Furthermore, knockdown of α5 integrin and not α2 integrin in lung cancer cells decreases tumor burden, reduces the number of metastatic lesions and increases animal survival in murine xenotransplant studies [16]. Moreover, we observed that increasing α5 integrin expression in non-malignant mammary epithelial cells in the context of its ligand, fibronectin, was sufficient to disrupt acinar morphogenesis and promoted MEC growth and survival. Our data supports a role of α5β1 integrin-fibronectin interactions in promoting MEC growth and survival in breast cancers.

These data may seem contradictory to other reports showing that malignant potential and metastatic ability appear to correlate with a decrease (not an increase) in α5β1 integrin and/or fibronectin expression [52-55]. For example, in murine mammary adenocarcinomas, downregulation of fibronectin gene transcription correlates with increased metastatic potential [55].Similarly, others

have suggested that tumor cells overexpressing α5β1 integrin are less tumorigenic than their parent cells [52] and that this integrin is not important in the context of spontaneous tumor formation [25, 56]. We believe that these seemingly disparate observations are explained by the types of tumors and tissues tested. Furthermore, it is likely that α5β1 integrin and fibronectin play different roles in malignant transformation, invasion, and metastases, processes that are linked mechanistically, but that are distinct from one another. α5β1 integrin may promote breast cancers once established by inducing intracellular signals that stimulate the expression of genes involved in cell cycle progression and inhibit apoptosis, while inhibiting genes involved in tumor suppression. On the other hand, a decrease in the expression of α5β1 integrin and/or fibronectin may be needed to promote detachment of tumor cells from their substrate and for effective tumor migration and invasion of MECs to other tissues thereby enhancing metastases.

We observed that reduced expression of a chromatin remodeling protein, BRM, associated with increased expression of α5 integrin mRNA and protein levels in non-malignant MECs. While traditional views of BRM activity refer to its transcriptional activation activities, this study bolsters the growing support of the transcriptional repression activities of the SWI/SNF complexes as well [58-60]. Additionally, previous experiments in human fibroblasts implicate the abrogation of SWI/SNF BRG-1 ATPase activity and upregulation of α5 and αv integrin total protein levels however, the potential effects of BRM ATPase activity on these

cells was never addressed or excluded. In our studies, we found that BRM specific shRNA targeting increased α5 integrin mRNA and protein levels whereas BRG-1 specific knockdown did not alter α5 integrin levels (Supplemental Figure 2.9). Whether BRM directly regulates the transcription of α5β1 integrin and/or fibronectin expression remains to be determined.

Identification of direct targets of BRM and BRG1-containing SWI/SNF complexes is currently underway, however, experiments are hampered by confounding variables such as the variation in the assembly of SWI/SNF complex accessory subunits, the high percent of sequence homology of BRM and BRG-1 requires rigorous validation of any targeting strategy, and the reports of compensatory upregulation and functional redundancy of BRM and BRG-1 subunits [61, 62].

We showed that decreased BRM expression and/or activity in non-malignant MECs disrupted 3D rBM-directed mammary morphogenesis via enhanced MEC survival (luminal filling) and aberrant secretion of FN. BRM is associated in the regulation of cellular proliferation through its repression activities on the cell cycle regulators pRb and Cyclin E, so it was not surprising that shRNA-mediated knockdown or expression of an ATPase dead BRM resulted in aberrant growth control in non-malignant MCF10A cells [20, 21, 39, 40]. However, we found that BRM also contributed to the regulation of MEC survival (i.e., luminal filling) in the context of a 3D culture environment. Importantly, premalignant breast diseases such as atypical hyperplastic lesions or carcinoma *in situs* are pathologically

identified by the presence of a partial or complete filled lumen [63]. Oncogenes, such as ErbB2, induce luminal filling in part by suppression of the pro-apoptotic protein Bim in an ERK-MAPK dependent manner, however the molecular mechanism behind Bim regulation is unclear [24, 25].

Whether BRM, α5 integrin and Bim are functionally linked in the regulation of MEC survival in 3D is an area of active investigation. Furthermore, our data provide a potential molecular mechanism for the previous observations that bulk chromatin remodeling changes associate with the maintenance and developmental changes that occur during the formation of MEC 3D cultures[64]. Certainly these observations implicate a functional relationship between chromatin remodeling and ECM responsiveness and suggest this is mediated via oncogenic signaling.

Our studies revealed that BRM expression is reduced in oncogenically transformed MECs and re-expression suppressed the malignant phenotype of 3D cultures and is associated with reduced α5 integrin mRNA and protein levels. We and others have shown that inhibition of either β1 integrin or receptor tyrosine kinase (RTK) signaling is sufficient to promote phenotypic reversion of ErbB1-transformed MECs in 3D culture assays [43, 65] Regardless of the inhibitory agent used phenotypic reversion is accompanied by down-regulation of both β1 integrin and EGFR proteins to levels observed in nonmalignant MECs[65]. The present studies suggest that BRM levels are also coordinately regulated by β1

integrin (via α5 integrin dimer) and RTK signaling through examination of BRM levels in transformed MECs and inhibitor studies in 3D cultures (Figure 2.2, Figure 2.5). Given that overexpression of BRM was also sufficient to cause phenotypic reversion of oncogenically transformed MECs, it is possible that BRM engages in an integrated cross-talk with the cell surface receptors β1 integrin and EGFR. Thus, oncogenic transformation of MECs would require the collective disruption of all of these coordinately regulated elements. If BRM expression is coupled to α5β1 integrin signaling pathways in MCF10A cells, we may expect upregulation of BRM levels with inhibition of α5 integrin signaling in 3D culture assays. BRM might also play a structural role in MECs. We reason that such a finding would explain why re-expression of BRM not only inhibited MEC proliferation but also enabled tissue reorganization in 3D cultures assays (Figure 2.6). To further explore the possible role BRM may plays in orchestrating tissue re-organization we have begun to examine mammary gland development in $BRM^{-/-}$ mice.

In the present study we ask whether enhanced oncogene-dependent signaling promotes tumorigenesis by altering MEC-ECM interactions and if so, how? We found that oncogenes such as ErbB2 and Ras^{V12} required α5β1 integrin-fibronectin interactions to drive MEC growth and survival in 3D cultures. We also identified a novel link between oncogene-dependent signaling and the function of chromatin remodeling agents (i.e.,BRM) in the transcriptional regulation of MEC-ECM α5β1 integrin-fibronectin interactions. These data implicate a novel

interaction between changes in the genome and changes in ECM responsiveness that combine to drive malignant progression. Additionally, since we observed changes in α5β1 integrin levels in relationship to BRM levels, and α5β1 integrin-FN interactions are strongly implicated in metastasis and angiogenesis, we are now investigating the role of BRM in breast tumor invasion and metastases.

While there are many genetic aberrations and epigenetic changes present in tumors, there are surprisingly are only a handful of conserved pathways that are altered in breast tumorigenesis [66]. Is this due to the fact that oncogenes must overcome or modify MEC-ECM restrictions to promote tumor growth and survival and if so, is this mediated via BRM activities? Together, these observations emphasize the overall need to explore the mechanisms and physiological relevance of MEC-ECM interactions in breast tumor progression.

Acknowledgements

We would like to thank Z. Werb, N. Boudreau and members of the Weaver lab for stimulating discussions. This work was supported by DODWX81XWH-05-1-0330.

References

1. Hanahan, D. and R.A. Weinberg, *The hallmarks of cancer.* Cell, 2000. **100**(1): p. 57-70.
2. Ronnov-Jessen, L. and O.W. Petersen, *ADP-ribosylation of actins in fibroblasts and myofibroblasts by botulinum C2 toxin: influence on microfilament morphology and migratory behavior.* Electrophoresis, 1996. **17**(11): p. 1776-80.
3. Radisky, E.S. and D.C. Radisky, *Stromal induction of breast cancer: inflammation and invasion.* Rev Endocr Metab Disord, 2007. **8**(3): p. 279-87.
4. Newham, P. and M.J. Humphries, *Integrin adhesion receptors: structure, function and implications for biomedicine.* Mol Med Today, 1996. **2**(7): p. 304-13.
5. Miranti, C.K. and J.S. Brugge, *Sensing the environment: a historical perspective on integrin signal transduction.* Nat Cell Biol, 2002. **4**(4): p. E83-90.
6. Giancotti, F.G. and E. Ruoslahti, *Integrin signaling.* Science, 1999. **285**(5430): p. 1028-32.
7. Gumbiner, B.M., *Cell adhesion: the molecular basis of tissue architecture and morphogenesis.* Cell, 1996. **84**(3): p. 345-57.
8. Guo, W. and F.G. Giancotti, *Integrin signalling during tumour progression.* Nat Rev Mol Cell Biol, 2004. **5**(10): p. 816-26.

9. Ridley, A.J., et al., *Cell migration: integrating signals from front to back.* Science, 2003. **302**(5651): p. 1704-9.

10. Zahir, N., et al., *Autocrine laminin-5 ligates alpha6beta4 integrin and activates RAC and NFkappaB to mediate anchorage-independent survival of mammary tumors.* J Cell Biol, 2003. **163**(6): p. 1397-407.

11. Reddig, P.J. and R.L. Juliano, *Clinging to life: cell to matrix adhesion and cell survival.* Cancer Metastasis Rev, 2005. **24**(3): p. 425-39.

12. Taddei, I., et al., *Integrins in mammary gland development and differentiation of mammary epithelium.* J Mammary Gland Biol Neoplasia, 2003. **8**(4): p. 383-94.

13. Paszek, M.J., et al., *Tensional homeostasis and the malignant phenotype.* Cancer Cell, 2005. **8**(3): p. 241-54.

14. Desgrosellier, J.S. and D.A. Cheresh, *Integrins in cancer: biological implications and therapeutic opportunities.* Nat Rev Cancer. **10**(1): p. 9-22.

15. Shimizu, H., et al., *Aberrant expression of integrin and erbB subunits in breast cancer cell lines.* Int J Oncol, 2002. **21**(5): p. 1073-9.

16. Roman, J., et al., *{alpha}5{beta}1 Integrin Expression is Essential for Tumor Progression in Experimental Lung Cancer.* Am J Respir Cell Mol Biol.

17. Diaz, L.K., et al., *Beta4 integrin subunit gene expression correlates with tumor size and nuclear grade in early breast cancer.* Mod Pathol, 2005. **18**(9): p. 1165-75.

18. Nikolopoulos, S.N., et al., *Integrin beta4 signaling promotes tumor angiogenesis.* Cancer Cell, 2004. **6**(5): p. 471-83.

19. Maschler, S., et al., *Tumor cell invasiveness correlates with changes in integrin expression and localization.* Oncogene, 2005. **24**(12): p. 2032-41.

20. Schofield, O., et al., *Abnormal expression of epiligrin and alpha 6 beta 4 integrin in basal cell carcinoma.* Dermatol Surg, 1998. **24**(5): p. 555-9.

21. Sordat, I., et al., *Differential expression of laminin-5 subunits and integrin receptors in human colorectal neoplasia.* J Pathol, 1998. **185**(1): p. 44-52.

22. Christensen, L., *The distribution of fibronectin, laminin and tetranectin in human breast cancer with special attention to the extracellular matrix.* APMIS Suppl, 1992. **26**: p. 1-39.

23. Sawada, K., et al., *Loss of E-cadherin promotes ovarian cancer metastasis via alpha 5-integrin, which is a therapeutic target.* Cancer Res, 2008. **68**(7): p. 2329-39.

24. Tani, N., et al., *Expression level of integrin alpha 5 on tumour cells affects the rate of metastasis to the kidney.* Br J Cancer, 2003. **88**(2): p. 327-33.

25. Taverna, D., et al., *A test of the role of alpha5 integrin/fibronectin interactions in tumorigenesis.* Cancer Res, 1998. **58**(4): p. 848-53.

26. Ng CM, B.S., Takimoto CH, Tang MT, Tolcher AW., *Mechanism-based receptor-binding model to describe the pharmacokinetic and pharmacodynamic of an anti-alpha(5)beta (1) integrin monoclonal antibody (volociximab) in cancer patients.* Cancer Chemother Pharmacol, 2009.

27. Garanger, E., D. Boturyn, and P. Dumy, *Tumor targeting with RGD peptide ligands-design of new molecular conjugates for imaging and therapy of cancers.* Anticancer Agents Med Chem, 2007. **7**(5): p. 552-8.

28. Park, C.C., et al., *Beta1 integrin inhibitory antibody induces apoptosis of breast cancer cells, inhibits growth, and distinguishes malignant from normal phenotype in three dimensional cultures and in vivo.* Cancer Res, 2006. **66**(3): p. 1526-35.

29. Pylayeva, Y., et al., *Ras- and PI3K-dependent breast tumorigenesis in mice and humans requires focal adhesion kinase signaling.* J Clin Invest, 2009. **119**(2): p. 252-66.

30. Wang, F., et al., *Phenotypic reversion or death of cancer cells by altering signaling pathways in three-dimensional contexts.* J Natl Cancer Inst, 2002. **94**(19): p. 1494-503.

31. White, D.E., et al., *Targeted disruption of beta1-integrin in a transgenic mouse model of human breast cancer reveals an essential role in mammary tumor induction.* Cancer Cell, 2004. **6**(2): p. 159-70.

32. Hill, D.A., et al., *Inducible changes in cell size and attachment area due to expression of a mutant SWI/SNF chromatin remodeling enzyme.* J Cell Sci, 2004. **117**(Pt 24): p. 5847-54.

33. Spangenberg, C., et al., *ERBB2-mediated transcriptional up-regulation of the alpha5beta1 integrin fibronectin receptor promotes tumor cell survival under adverse conditions.* Cancer Res, 2006. **66**(7): p. 3715-25.

34. Reisman, D.N., et al., *Concomitant down-regulation of BRM and BRG1 in human tumor cell lines: differential effects on RB-mediated growth arrest vs CD44 expression.* Oncogene, 2002. **21**(8): p. 1196-207.

35. Glaros, S., et al., *The reversible epigenetic silencing of BRM: implications for clinical targeted therapy.* Oncogene, 2007. **26**(49): p. 7058-66.

36. van de Vijver, M.J., et al., *A gene-expression signature as a predictor of survival in breast cancer.* N Engl J Med, 2002. **347**(25): p. 1999-2009.

37. Park, J.W., et al., *Rationale for biomarkers and surrogate end points in mechanism-driven oncology drug development.* Clin Cancer Res, 2004. **10**(11): p. 3885-96.

38. Levental, K.R., et al., *Matrix crosslinking forces tumor progression by enhancing integrin signaling.* Cell, 2009. **139**(5): p. 891-906.

39. Reginato, M.J., et al., *Integrins and EGFR coordinately regulate the pro-apoptotic protein Bim to prevent anoikis.* Nat Cell Biol, 2003. **5**(8): p. 733-40.

40. Cohet, N., Stewart, K.M., Mudhasani, R., Asirvatham, A., Mallappa, C., Imbalzano, K., Weaver, V.M., Imbalzano, A.N., Nickerson, J.A., *SWI/SNF chromatin remodeling enzyme ATPases promote cell proliferation in normal mammary epithelial cells.* accepted, 2010.

41. Weaver, V.M., et al., *beta4 integrin-dependent formation of polarized three-dimensional architecture confers resistance to apoptosis in normal and malignant mammary epithelium.* Cancer Cell, 2002. **2**(3): p. 205-16.

42. Debnath, J., S.K. Muthuswamy, and J.S. Brugge, *Morphogenesis and oncogenesis of MCF-10A mammary epithelial acini grown in three-dimensional basement membrane cultures.* Methods, 2003. **30**(3): p. 256-68.

43. Weaver, V.M., et al., *Reversion of the malignant phenotype of human breast cells in three-dimensional culture and in vivo by integrin blocking antibodies.* J Cell Biol, 1997. **137**(1): p. 231-45.

44. Uhm, K.O., et al., *Aberrant DNA methylation of integrin alpha4: a potential novel role for metastasis of cholangiocarcinoma.* J Cancer Res Clin Oncol. **136**(2): p. 187-94.

45. Williams, C.M., et al., *Fibronectin expression modulates mammary epithelial cell proliferation during acinar differentiation.* Cancer Res, 2008. **68**(9): p. 3185-92.

46. Mailleux, A.A., M. Overholtzer, and J.S. Brugge, *Lumen formation during mammary epithelial morphogenesis: insights from in vitro and in vivo models.* Cell Cycle, 2008. **7**(1): p. 57-62.

47. Muchardt, C., et al., *ras transformation is associated with decreased expression of the brm/SNF2alpha ATPase from the mammalian SWI-SNF complex.* EMBO J, 1998. **17**(1): p. 223-31.

48. Bhaskar, V., et al., *A function blocking anti-mouse integrin alpha5beta1 antibody inhibits angiogenesis and impedes tumor growth in vivo.* J Transl Med, 2007. **5**: p. 61.

49. Murillo, C.A., P.G. Rychahou, and B.M. Evers, *Inhibition of alpha5 integrin decreases PI3K activation and cell adhesion of human colon cancers.* Surgery, 2004. **136**(2): p. 143-9.

50. Hsu, S.L., et al., *Proteolysis of integrin alpha5 and beta1 subunits involved in retinoic acid-induced apoptosis in human hepatoma Hep3B cells.* Cancer Lett, 2001. **167**(2): p. 193-204.

51. Morozevich, G.E., et al., *Implication of alpha5beta1 integrin in invasion of drug-resistant MCF-7/ADR breast carcinoma cells: a role for MMP-2 collagenase.* Biochemistry (Mosc), 2008. **73**(7): p. 791-6.

52. Zhou, G.F., et al., *Over expression of integrin alpha 5 beta 1 in human hepatocellular carcinoma cell line suppresses cell proliferation in vitro and tumorigenicity in nude mice.* Mol Cell Biochem, 2000. **207**(1-2): p. 49-55.

53. Kuwada, S.K., J. Kuang, and X. Li, *Integrin alpha5/beta1 expression mediates HER-2 down-regulation in colon cancer cells.* J Biol Chem, 2005. **280**(19): p. 19027-35.

54. Varner, J.A., D.A. Emerson, and R.L. Juliano, *Integrin alpha 5 beta 1 expression negatively regulates cell growth: reversal by attachment to fibronectin.* Mol Biol Cell, 1995. **6**(6): p. 725-40.

55. Urtreger, A.J., et al., *Fibronectin is distinctly downregulated in murine mammary adenocarcinoma cells with high metastatic potential.* Oncol Rep, 2006. **16**(6): p. 1403-10.

56. Zutter, M.M., G. Mazoujian, and S.A. Santoro, *Decreased expression of integrin adhesive protein receptors in adenocarcinoma of the breast.* Am J Pathol, 1990. **137**(4): p. 863-70.

57. Busk, M., R. Pytela, and D. Sheppard, *Characterization of the integrin alpha v beta 6 as a fibronectin-binding protein.* J Biol Chem, 1992. **267**(9): p. 5790-6.

58. Wang, L., S. Pal, and S. Sif, *Protein arginine methyltransferase 5 suppresses the transcription of the RB family of tumor suppressors in leukemia and lymphoma cells.* Mol Cell Biol, 2008. **28**(20): p. 6262-77.

59. Dai, Y., et al., *Prohibitin and the SWI/SNF ATPase subunit BRG1 are required for effective androgen antagonist-mediated transcriptional repression of androgen receptor-regulated genes.* Carcinogenesis, 2008. **29**(9): p. 1725-33.

60. Schnitzler, G.R., S. Sif, and R.E. Kingston, *A model for chromatin remodeling by the SWI/SNF family.* Cold Spring Harb Symp Quant Biol, 1998. **63**: p. 535-43.

61. Muchardt, C. and M. Yaniv, *ATP-dependent chromatin remodelling: SWI/SNF and Co. are on the job.* J Mol Biol, 1999. **293**(2): p. 187-98.

62. Coisy-Quivy, M., et al., *Role for Brm in cell growth control.* Cancer Res, 2006. **66**(10): p. 5069-76.

63. Harris, J., Lippman, ME, Morrow, M, Hellman, S, *In: Diseases of the Breast,*. 1996, Philadelphia: Lippincott-Raven.

64. Plachot, C., Lelièvre, S.A., *DNA methylation control of tissue polarity and cellular differentiation in the mammary epithelium.* Exp Cell Res, 2004. **298**(1): p. 122-32.

65. Wang, F., et al., *Reciprocal interactions between beta1-integrin and epidermal growth factor receptor in three-dimensional basement membrane breast cultures: a different perspective in epithelial biology.* Proc Natl Acad Sci U S A, 1998. **95**(25): p. 14821-6.

66. Chen, H.M., et al., *AZU-1: a candidate breast tumor suppressor and biomarker for tumor progression.* Mol Biol Cell, 2000. **11**(4): p. 1357-67.

67. Mechta, F., et al., *Transformation by ras modifies AP1 composition and activity.* Oncogene, 1997. **14**(7): p. 837-47.

Figure Legends

Figure 2.1. Oncogenic-dependent malignant progression is associated with elevated α5 integrin expression.

(A) Top scheme: representation of 3D MEC morphologies observed. Top Panel: Micrographs of MCF10A (Parental), MCF10AT1 (AT1), MCF10A-wt ErbB2 (ErbB2) and MCF10ARas^{V12} (Ras ^{V12}) cells that were grown in reconstituted membrane (rBM) for 14 days, Scale bar represents 200 μm, higher magnification inset scale bar represents 100μm. Bottom Panel: Immunofluorescence for Polarity Markers: β4 Integrin and β-catenin (green and red respectively), nuclei were visualized with DAPI (blue). White dashed circles indicate cleared lumens, asterisk indicates absence of a lumen. Scale bar represents 25μm. (B) Representative immunoblot of total cellular α integrin subunits and fibronectin in MCF10A cell lines and total Lamin B1 (loading control). Relative protein levels were calculated by densitometric analysis of immunoblots; each sample was normalized to its internal loading control (Lamin B1) (C) Top Panel: Micrographs of ErbB2 cells treated with either α2 integrin, α5 integrin, fibronectin (FN) functional blocking antibodies (Abblk mAbs) or non-immunogenic isotype control IgG antibody (IgG) and grown in rBM (14 days).Scale bar represents 200 μm, higher magnification inset scale bar represents 100μm. Bottom Panel: Immunofluorescence for Polarity Marker: β4 Integrin (red), nuclei were visualized with DAPI (blue). Scale bar represents 25μm. (D) Histogram of cell lines in Panel (C) that were scored for the presence of a filled lumen at day 14. n>50 acini per sample; ***, p< 0.001. (E) Left Panel: Ectopic expression of α5 integrin in

MCF10A cells in 3D morphogenesis assays Right Panel: Ectopic expression of α5 integrin (+α5 integrin) with the addition of fibronectin ligand (+ FN). Top Panel: Micrographs of MECs grown in rBM for 14 days, Scale bar represents 200 μm, higher magnification inset scale bar represents 100μm. Bottom Panel: Immunostaining for polarity markers β4 Integrin and β-catenin (red) nuclei were visualized with DAPI (blue). Scale bar represents 25μm. (F) Colony area of MCF10A + α5 integrin for 14 days in 3D rBM with or without addition of FN., n>50 acini per sample.***, p< 0.001.). Results are the mean ± S.E.M. of 3 separate experiments. ***, p<0.001.

Figure 2.2 BRM is lost in transformed breast cancer cell lines and is associated with elevated α5β1 integrin expression and activity

(A) Histogram of integrin subunit mRNA levels in MCF10A cell lines normalized to 18S transcript levels. Results are the mean ± S.E.M. of 3 separate RNA isolations. **, p< 0.005, ***, p< 0.001. (B) Representative immunoblot of total cellular BRM and Lamin B1 (loading control) levels in MEC parental and transformed cell lines. Histogram is of relative BRM levels were calculated by densitometric analysis of immunoblots as compared to parental MCF10A cells and each sample was normalized to its internal loading control (Lamin B1). Results are the mean ± S.E.M. of 3 separate experiments. ***, p<0.001. (C) Representative immunoblot of BRM and BRG1 levels in MCF10A cells expressing either a doxycycline (Dox +/-) inducible shRNA-mediated Scrambled (Scrm) or BRM (BRMi) knockdown construct. Histogram is of percent normalized

protein levels calculated by densitometric analysis of immunoblots for either BRG1 or BRM, (non-induced,(-)) as compared to induced (+) levels in MCF10As. Each sample was normalized to the internal loading control (Lamin B1). Results are the mean ± S.E.M. of 5 separate experiments. ***, p< 0.001. (D) Histogram of integrin subunit mRNA levels in Scrm or BRMi cells normalized to 18S transcript levels. Results are the mean ± S.E.M. of 3 separate RNA isolations. ***, p< 0.001. (E) Representative immunoblot of integrin subunits in Scrm and BRMi cells. LaminB1 was used as an internal loading control. Histogram is of immunblot analysis of integrin subunit total protein levels normalized to Scrm levels. Results are the mean ± S.E.M. of 3 separate experiments.***, p< 0.001. (F) Representative histogram plots of 3 separate FACS analyses of cell surface integrin levels in Scrm and BRMi cells (G) Histogram of cellular attachment assay to extracellular matrix ligands in Scrm and BRMi cells. Results are the mean ± S.E.M. of 6 separate experiments. **, p< 0.05;***, p< 0.001.

Figure 2.3. Loss of Brm in nonmalignant MEC enhances survival in 3D organotypic cultures.

(A) Representative micrograph images of Scrambled (Scrm) and Brm shRNA (BRMi) MCF10A cells in a 3D rBM morphogenesis assay. Size bar represents 25 μm. (B) Colony area of MECs grown for 12 days in 3D rBM. Results are the mean ± S.E.M. of at least 3 separate experiments. ***, p< 0.001. (C) Representative micrographs of 3D rBM colonies (day 14). Left panel: Phase contrast micrographs of MEC acini, scale bar represents 25μm. Right panel: Immunofluorescence (red) for integrin subunits α5 integrin and β4 integrin and their respective ECM ligands fibronectin (FN) and Laminin-5 (LM5); nuclei were visualized with DAPI (blue). Scale bar represents 25μm. White dashed circles indicate cleared lumens, asterisk indicates absence of a lumen. (D) Histogram of 3-D colonies from Panel (C) that were scored for the presence of a filled lumen at day 14. Results are the mean ± S.E.M. of at least 6 separate experiments. n>50 acini per sample; ,***, p< 0.001. (E) Immunofluorescence (red) of Scrm and BRMi 3-D colonies for an apoptosis marker: Activated Caspase-3 and a cell proliferation marker: Ki67 ;nuclei were visualized using DAPI (blue). Scale bar represents 25μm. (F) Histogram of percent Caspase-3 positive nuclei within the lumen per colony of Scrm or BRMi cultures (Day 14). Results are the mean ± S.E.M. of 3 separate experiments. n>50 acini per sample; ,***, p< 0.001. (G) Histogram of percent Ki67 positive nuclei at day 14 from Scrm or BRMi 3D cultures. Results are the mean ± S.E.M. of 5 separate experiments. n>50 acini per sample; ,***, p< 0.001.

Figure 2.4. Loss of Brm ATPase remodeling activity is necessary to enhance MEC survival in 3D.

(A) Immunoblot analysis of total cellular BRM, BRG1 and Lamin B1 (loading control) levels in MCF10A cells expressing a tetracycline inducible retroviral ATPase dead BRM mutant (K749R) Histogram is of percent normalized protein levels which were calculated by densitometric analysis of immunoblots for either BRG1 or BRM (non-induced Control (Ctrl), +) values divided by BRG1 or BRM levels in cells grown in the absence of tetracycline (induced, K749R, -) after normalization to internal loading control (Lamin B1). Results are the mean ± S.E.M. of 3 separate experiments. ***, $p < 0.001$. (B) Representative micrographs Ctrl and K749R cells grown in 3D rBM. Scale bar represents 25μm. (C) Colony area of MECs grown for 12 days in 3D rBM. Results are the mean ± S.E.M. of at least 5 separate experiments,***, $p < 0.001$. (D) Representative micrographs of 3D colonies (day 14).). Left panel: Phase contrast micrographs of MEC acini, scale bar represents 25μm. Right panel: Immunofluorescence (red) for integrin subunits α5 integrin and β4 integrin and their respective ECM ligands fibronectin (FN) and Laminin-5 (LM5); nuclei were visualized with DAPI (blue). Scale bar represents 25μm. White dashed circles indicate cleared lumens, asterisk indicates absence of a lumen.

(E) Histogram of 3-D colonies that were scored for the presence of a filled lumen at day 14. Results are the mean ± S.E.M. of at least 6 separate experiments. n>50 acini per sample; ***, p< 0.001. (F) Immunofluorescence (red) of Ctrl and K749R 3-D colonies for an apoptosis marker: Activated Caspase-3 and a cell proliferation marker: Ki67 ; nuclei were visualized using DAPI (blue). Scale bar represents 25μm. (F) Histogram of percent Caspase-3 positive nuclei within the lumen per colony of Ctrl and K749R cultures (Day 14). Results are the mean ± S.E.M. of 3 separate experiments. n>50 acini per sample; ***, p< 0.001. (G) Histogram of percent Ki67 positive nuclei at day 14 from Ctrl and K749R 3D cultures. Results are the mean ± S.E.M. of 5 separate experiments. n>50 acini per sample; ***, p< 0.001.

Figure 2.5. Brm regulates malignant transformation by modulating α5β1 integrin-FN interactions

(A) Representative micrographs of shRNA-mediated BRM knockdown in MCF10A cells (BRMi) treated with either α2 integrin, α5 integrin, fibronectin (FN) functional blocking antibodies (Abblk mAbs) or non-immunogenic isotype control IgG antibody (IgG) and grown in rBM (14 days), Scrambled MCF10A were used as control cultures (Scr). Immunofluorescence for polarity marker: β4 Integrin, cell proliferation marker: Ki67, and Apoptosis marker: Caspase-3, (red); nuclei were visualized with DAPI (blue). Scale bar represents 25μm. White dashed circles indicate cleared lumens, asterisk indicates absence of a lumen. (B) Histogram representing Scrm cells treated with IgG antibodies (Ctrl) and Brmi

cells treated with either non-immunogenic isotype control IgG antibody (BRMi) or α5 integrin, α2 integrin or Fibronectin function blocking antibodies (α5 mAb; α2 mAb, FN mAb, respectively) that were scored for the presence of a filled lumen at day 14 from panel (A). Results are the mean ± S.E.M. of 3 separate experiments. n>50 acini per sample; ***, p< 0.001. (C) Histogram of percent Ki67 positive nuclei of day 14 colonies from panel (A) Results are the mean ± S.E.M. of 3 separate experiments. n>50 acini per sample; ***, p< 0.001. (D) Histogram of percent Caspase-3 positive nuclei within the lumen per colony of panel (A) Results are the mean ± S.E.M. of 3 separate experiments. n>50 acini per sample; ,***, p< 0.001.

Figure 2.6. Re-expression of BRM in oncogenically transformed MECs reverts malignant behavior in 3D

(A) Representative immunoblot of total cellular BRM levels in parental MCF10A cells (Ctrl), MCF10A wt ErbB2 cells uninduced (ErbB2) and induced to express wild type BRM (ErbB2 + wt BRM) and MCF10ARas^{V12} cells uninduced (Ras^{V12}) and induced to express wild type BRM (Ras^{V12} + wt BRM). (A') Histogram of relative protein levels which were calculated by densitometric analysis of immunoblots for BRM normalized to an internal loading control (Lamin B1). Results are the mean ± S.E.M. of 3 separate experiments. ***, p< 0.001. (B) Histogram of relative mRNA levels of integrin subunits and fibronectin with the induction of wild-type BRM in transformed MCF10A cells. (C) Representative immunoblot of total cellular integrin subunit and fibronectin levels with induction

of wild-type BRM in transformed MCF10A cells. Histogram is of relative protein levels which were calculated by densitometric analysis of immunoblots for integrin subunits and fibronectin and were normalized to an internal loading control (Lamin B1). Results are the mean ± S.E.M. of 3 separate experiments. ***, $p< 0.001$. (D) Top panel: Micrographs of Ctrl, ErbB2, ErbB2 + wt BRM and Ras^{V12}, and Ras^{V12} + wt BRM were grown in 3D rBM for 14 days. Scale bar represents 200μm; high magnification inset scale bar represents 50μm. Bottom Panel: Immunofluorescence of polarity marker: β4 integrin, proliferation marker: Ki67, and reactive stromal marker: Fibronectin (red); nuclei were visualized by DAPI (blue). Scale bar represents 25μm. White dashed circles indicate cleared lumens, asterisk indicates absence of a lumen. (E) Histogram of 3D colonies from panel (D) that were scored for the presence of a filled lumen at day 14 Results are the mean ± S.E.M. of 3 separate experiments. n>50 acini per sample; ,***, $p< 0.001$. (F) Histogram of percent Caspase-3 positive nuclei within the lumen per colony of panel (D) Results are the mean ± S.E.M. of 3 separate experiments. n>50 acini per sample; ,***, $p< 0.001$. (G) Histogram of percent Ki67 positive nuclei at day 14 from panel (D) Results are the mean ± S.E.M. of 3 separate experiments. n>50 acini per sample; ***, $p< 0.001$.

Figure 2.7. Proposed model of oncogene-mediated cell growth and survival in tumor progression.

Hypothetical model of the molecular mechanism of oncogene-mediated promotion of cell growth and survival during tumor progression. Aberrant oncogene activity suppresses BRM expression and also increases α5 integrin-FN interactions to promote cell growth and survival. BRM deficiency increases growth and survival by increasing α5 integrin-FN interactions. We propose changes in integrin α5 subunit expression and activity are regulated by BRM and functionally linked to oncogene-dependent transformation in MECs.

Figure 2.8. Verification of α5 integrin overexpression.

(A) Top panel: Representative micrographs of uninduced (Ctrl) and induced α5 integrin overexpressing MCF10A cells (+α5 integrin). Scale bar represents 200 μm. Bottom panel: TRITC excitation of control and α5-integrin overexpressing MCF10A cells in 2D. Scale bar represents 200 μm, higher magnification inset scale bar represents 25μm. (B) Representative immunoblot of total cellular α5 integrin levels and Lamin B1 (loading control) levels in uninduced (Ctrl) and induced α5-overexpressing MCF10A cells (+α5 integrin). Relative α5 integrin levels were calculated by densitometric analysis of immunoblots as compared to Ctrl MCF10A cells and each sample was normalized to its internal loading control (Lamin B1). Results are the mean ± S.E.M. of 3 separate experiments. ***, $p<0.001$.

Figure 2.9. BRG1 depletion does not alter α5 integrin levels.

(A) Histogram of relative α5 integrin levels. Protein levels were calculated by densitometric analysis of immunoblots as compared to uninduced BRG1 shRNA mediated knockdown cells and each sample was normalized to its internal loading control (Lamin B1). Results are the mean ± S.E.M. of 3 separate experiments. ***, $p<0.001$.

Figure 2.10 Verification of alternative BRM shRNA targeting sequences.

(A) Representative immunoblot of total cellular BRM levels and Lamin B1 (loading control) levels in Scrambled (Scrm) and BRM knockdown constructs #2 and #3 in MCF10A cells. (A') Relative BRM levels were calculated by densitometric analysis of immunoblots as compared to Scrambled MCF10A cells and each sample was normalized to its internal loading control (Lamin B1). Results are the mean ± S.E.M. of 3 separate experiments. ***, $p<0.001$. (B) Micrographs of mammary epithelial cell [67] lines grown in reconstituted membrane (rBM) for 14 days, Scale bar represents 200 μm, higher magnification inset scale bar represents 100μm. Bottom Panel: Immunofluorescence for polarity marker, β4 Integrin, nuclei were visualized with DAPI (blue).

White dashed circle notes the presence of a cleared lumen, asterisk notes the absence of a lumen. Scale bar represents 25μm. (C) Histogram of 3-D colonies that were scored for the presence of a filled lumen at day 14 (defined in the Methods). Results are the mean ± S.E.M. of 3 separate experiments. n>50 acini per sample; ,***, p< 0.001.

Figure 2.11. 2D effects of BRM depletion in nonmalignant MECs.

(A) Representative micrographs of uninduced (Ctrl), dominant negative induced (K749), scrambled (Scr) and BRM knockdown (BRMi) expressing MCF10A cells in 2D. Scale bar represents 200 μm. (B) Cell number in 2D cultures of Scrambled and BRM-knockdown MCF10A cells. Results are the mean ± S.E.M. of 3 separate experiments. ***, p<0.001. (C) Cell number in 2D cultures of control and dominant negative BRM expressing MCF10A cells. Results are the mean ± S.E.M. of 3 separate experiments. ***, p<0.001.

Figure 2.12 FACS analysis of integrin subunits with reduced BRM expression or activity

(A) Representative histogram plots of 3 separate FACS analyses of cell surface integrin levels in Scrambled or BRM knockdown MCF10A cells (B) Representative histogram plots of 3 separate FACS analyses of additional integrin subunits, Left panel: Scrambled versus BRM knockdown expressing MCF10A cells; Right panel: Control versus dominant negative BRM expressing MCF10A cells.

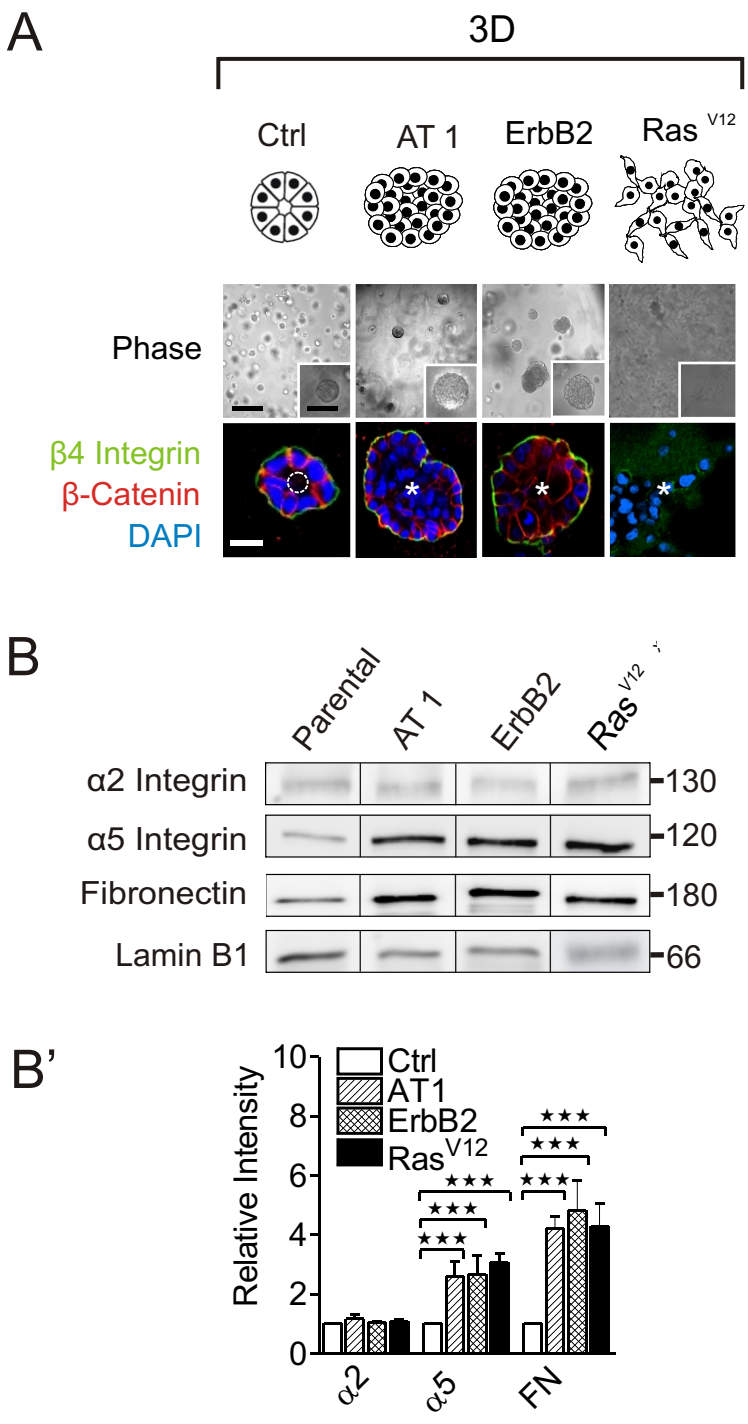

Figure 2.1. Oncogenic-dependent malignant progression is associated with elevated α5 integrin expression.

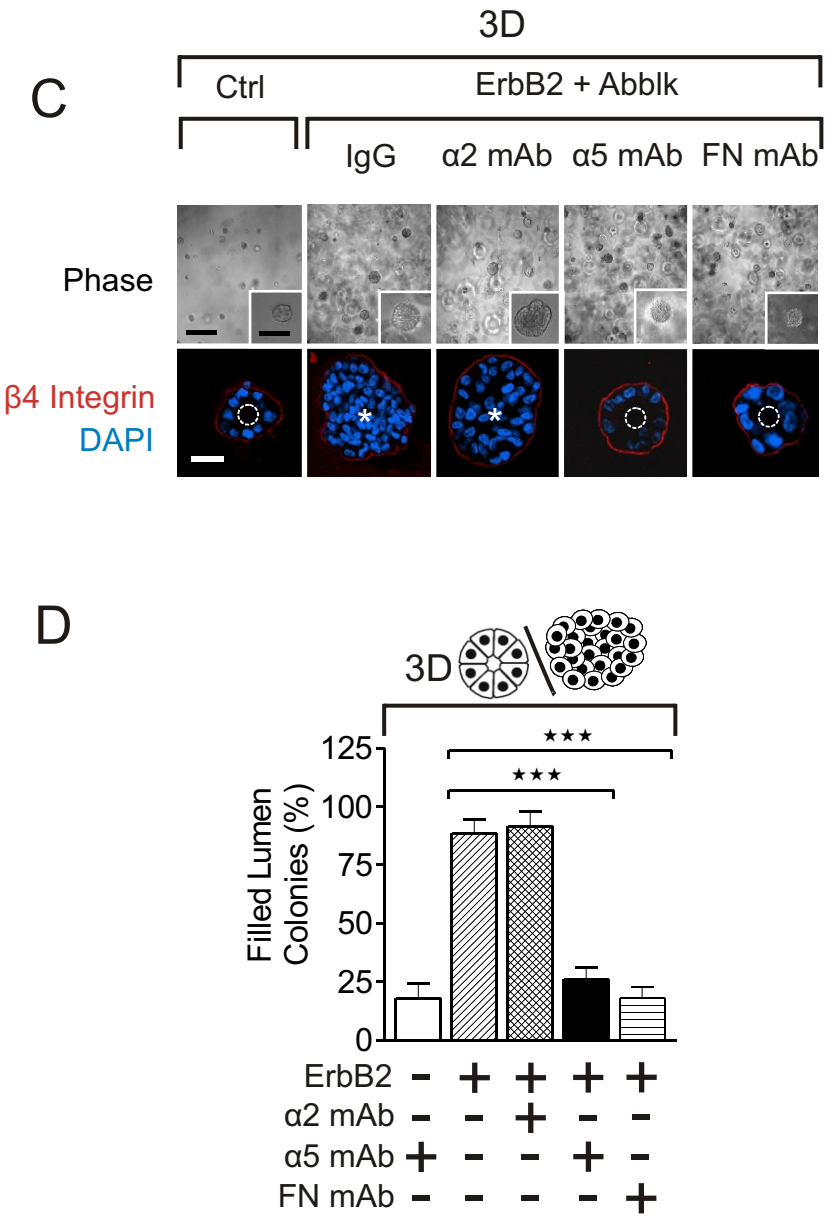

Figure 2.1. Oncogenic-dependent malignant progression is associated with elevated α5 integrin expression.

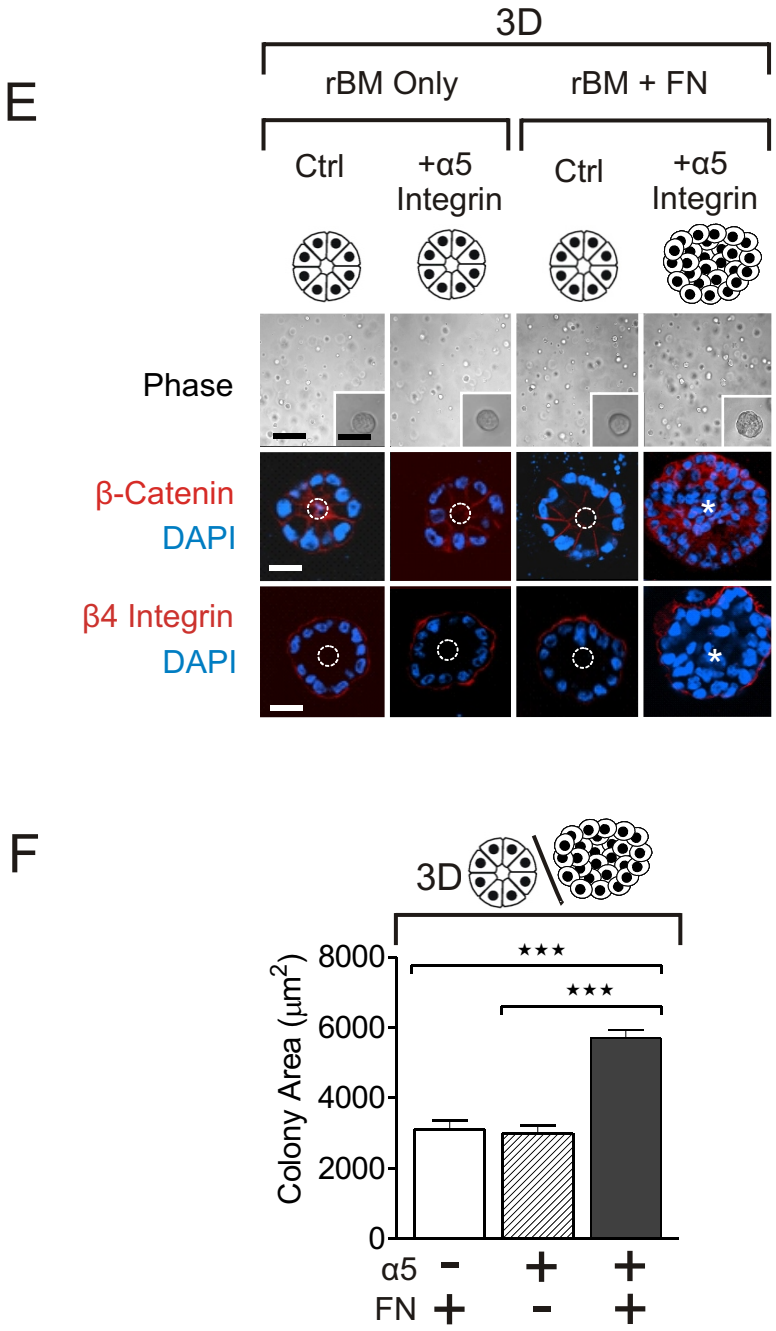

Figure 2.1. Oncogenic-dependent malignant progression is associated with elevated α5 integrin expression.

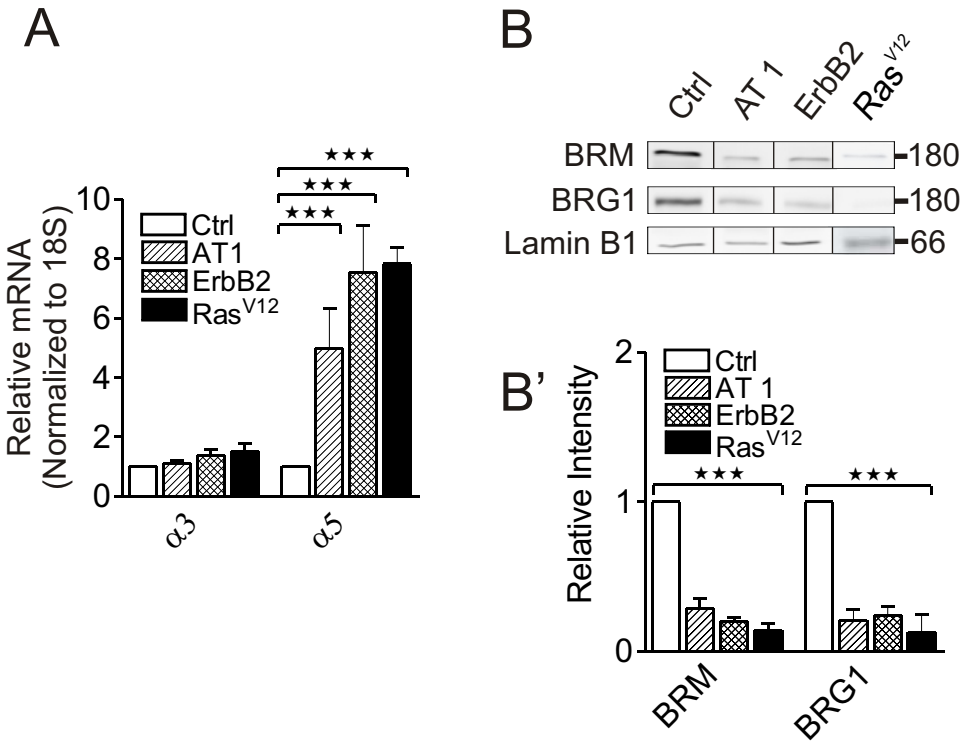

Figure 2.2 BRM is lost in transformed breast cancer cell lines and is associated with elevated α5β1 integrin expression and activity

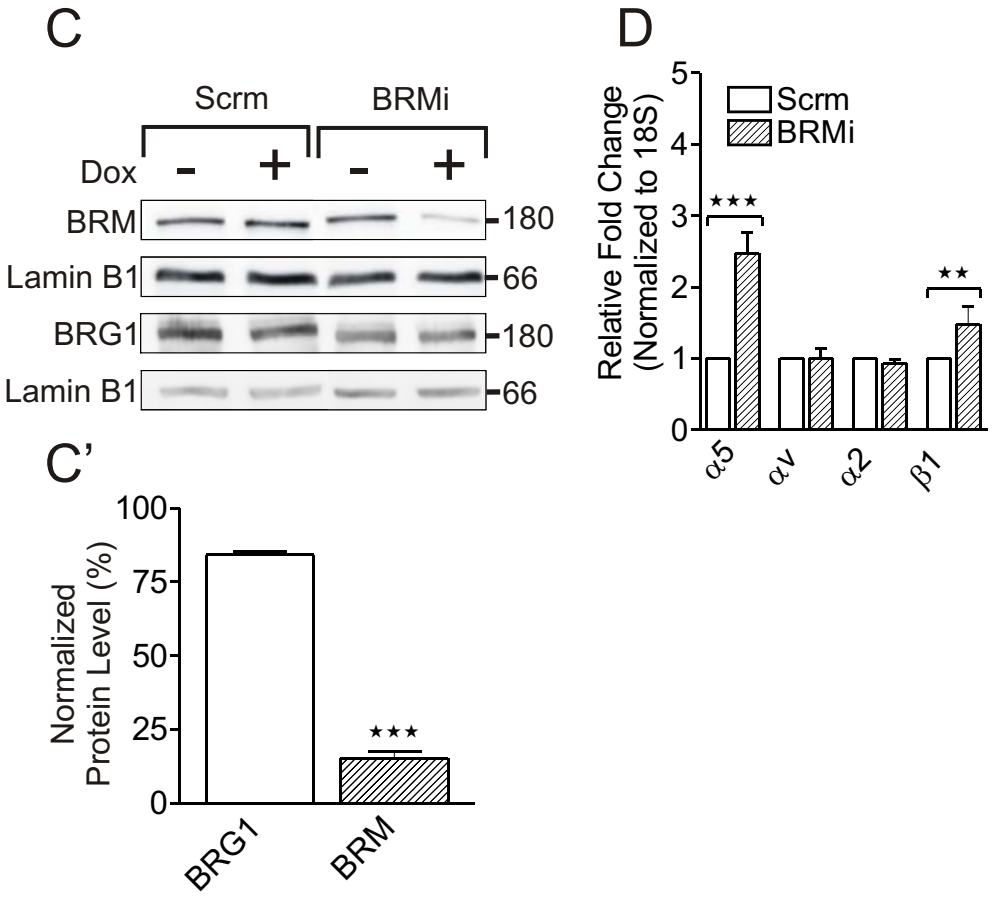

Figure 2.2 BRM is lost in transformed breast cancer cell lines and is associated with elevated α5β1 integrin expression and activity

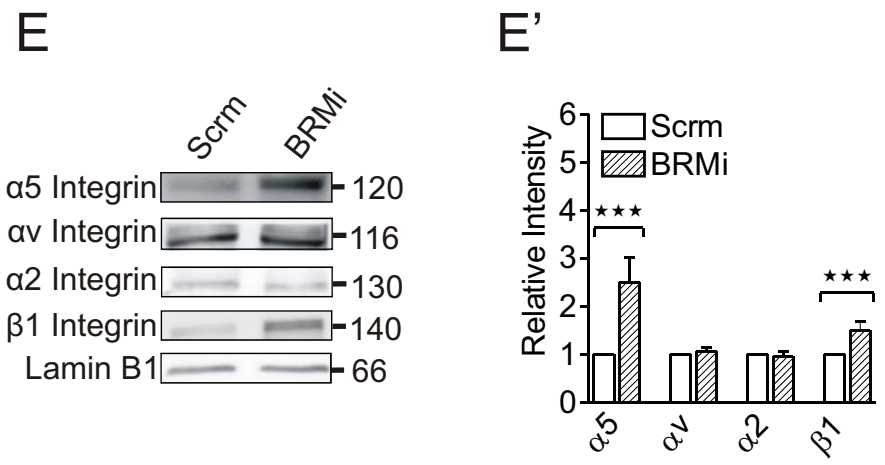

Figure 2.2 BRM is lost in transformed breast cancer cell lines and is associated with elevated α5β1 integrin expression and activity

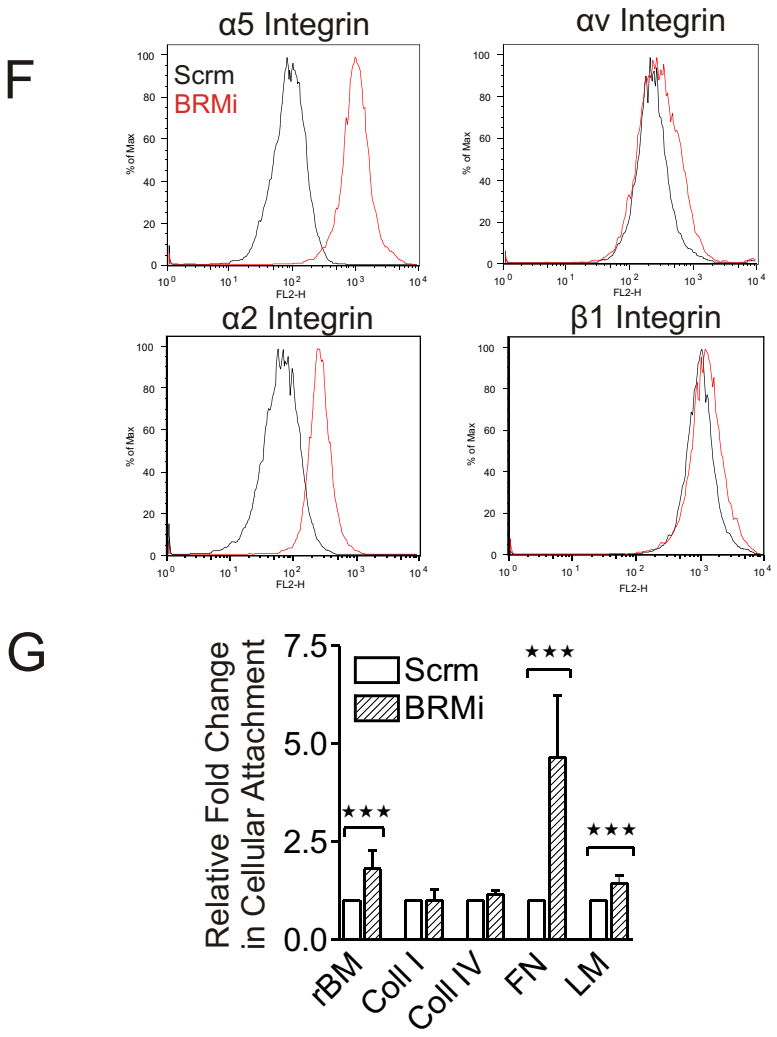

Figure 2.2 BRM is lost in transformed breast cancer cell lines and is associated with elevated α5β1 integrin expression and activity

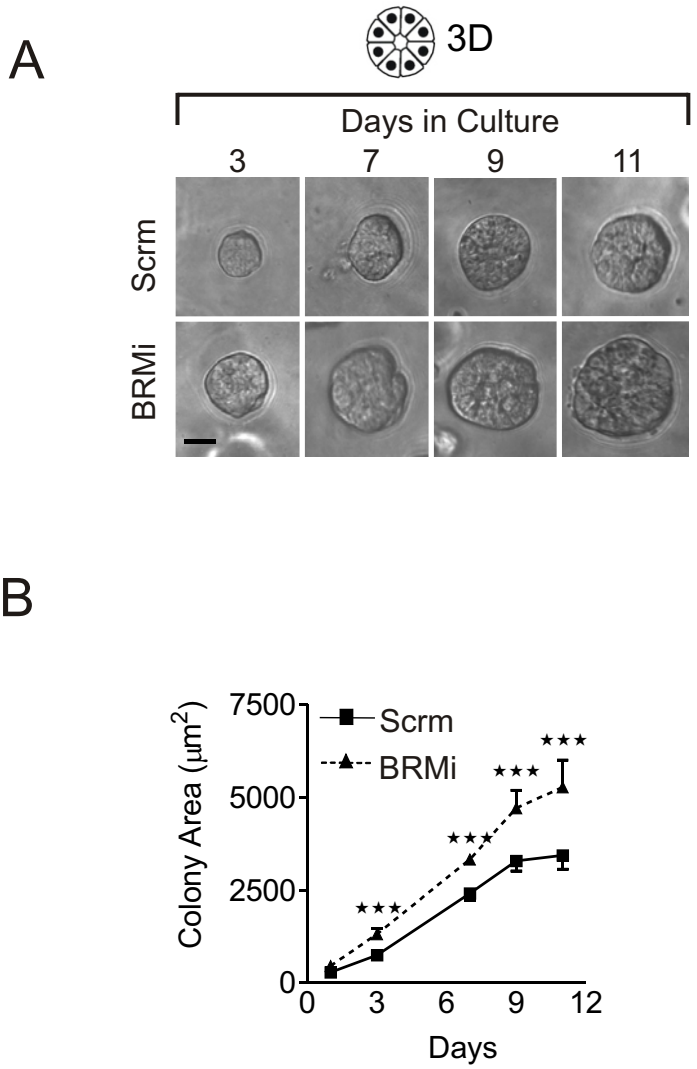

Figure 2.3. Loss of Brm in nonmalignant MEC enhances survival in 3D organotypic cultures.

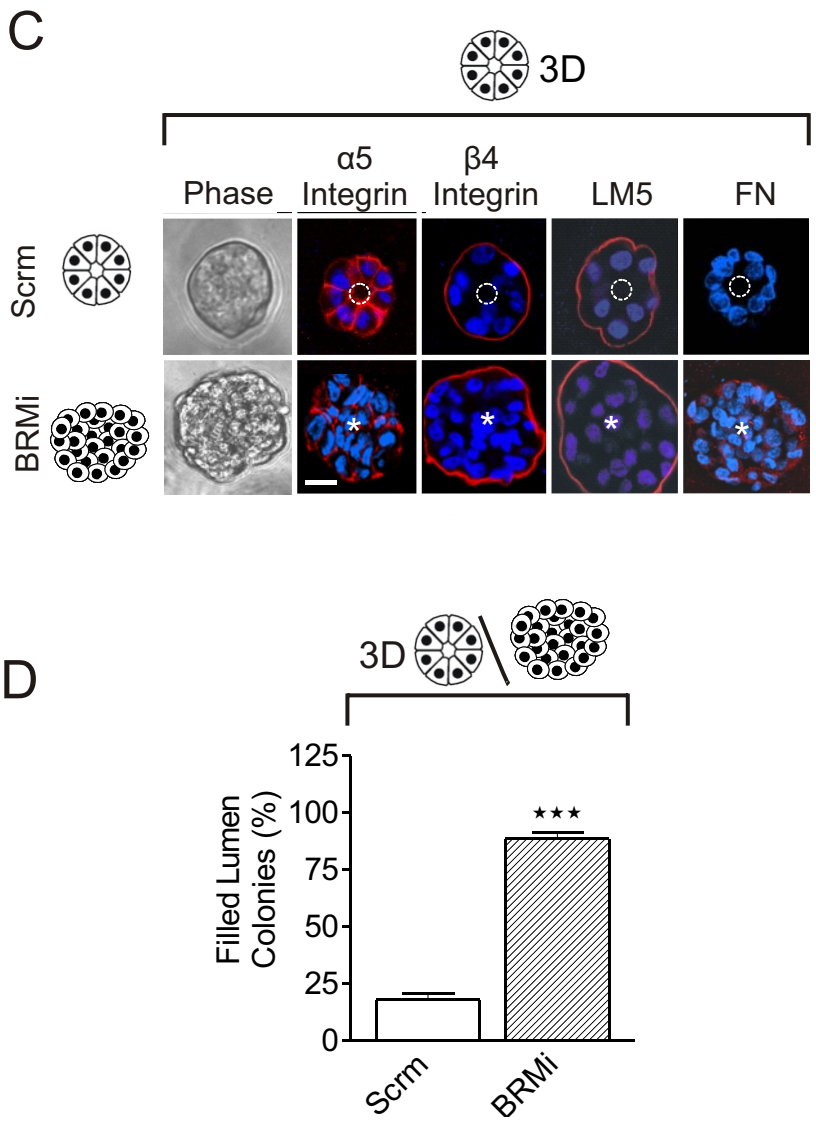

Figure 2.3. Loss of Brm in nonmalignant MEC enhances survival in 3D organotypic cultures.

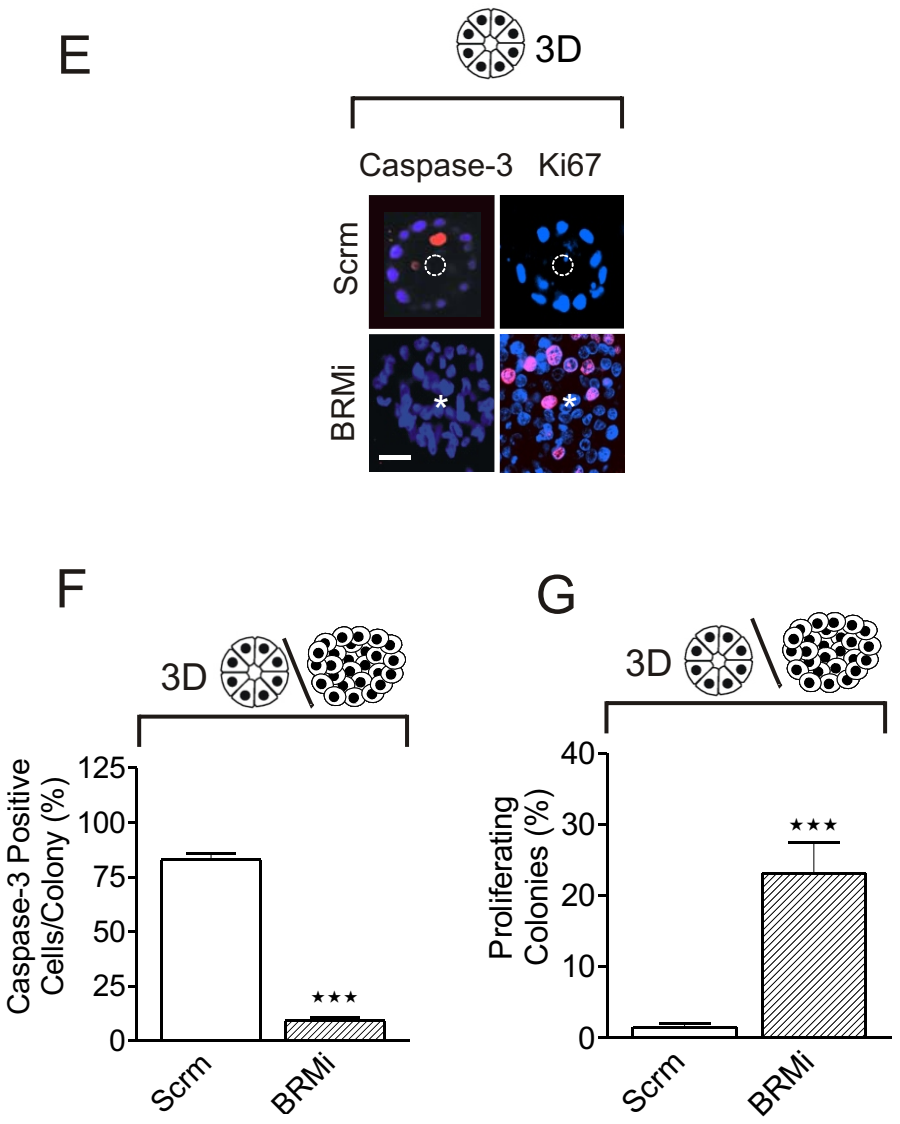

Figure 2.3. Loss of Brm in nonmalignant MEC enhances survival in 3D organotypic cultures.

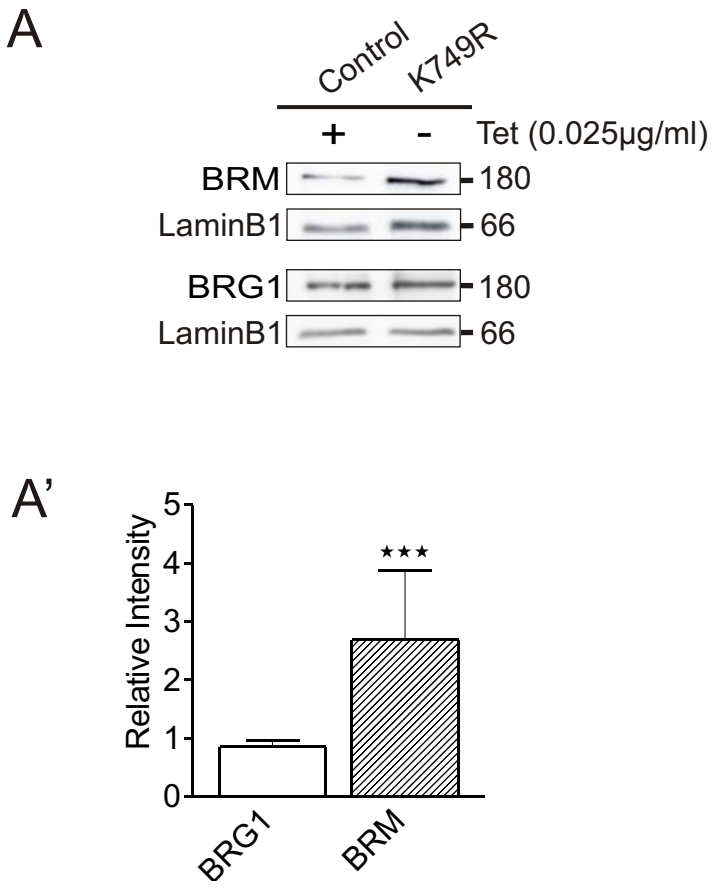

Figure 2.4. Loss of Brm ATPase remodeling cctivity is necessary to enhance MEC survival in 3D.

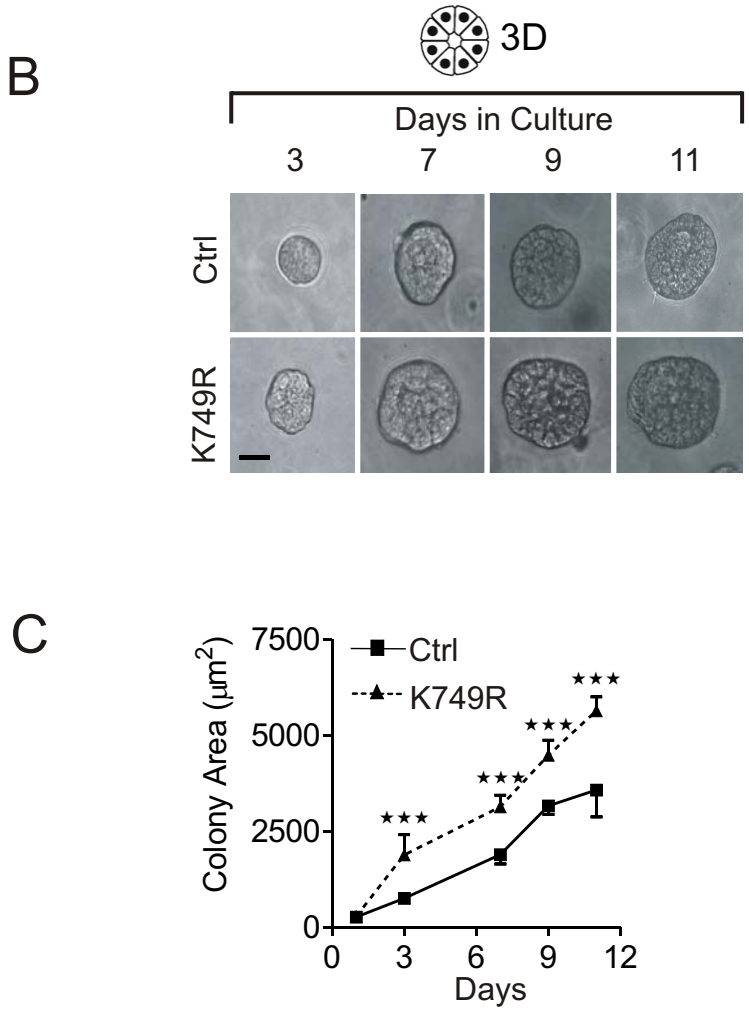

Figure 2.4. Loss of Brm ATPase Remodeling Activity is necessary to enhance MEC survival in 3D.

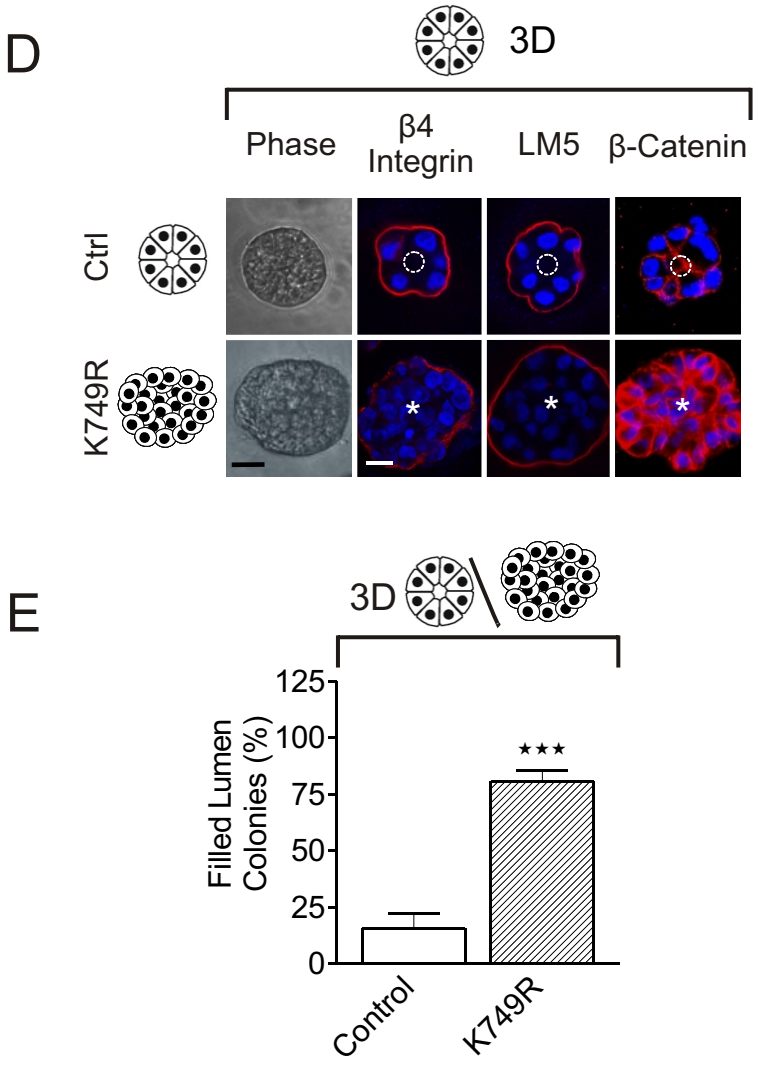

Figure 2.4. Loss of Brm ATPase Remodeling Activity is necessary to enhance MEC survival in 3D.

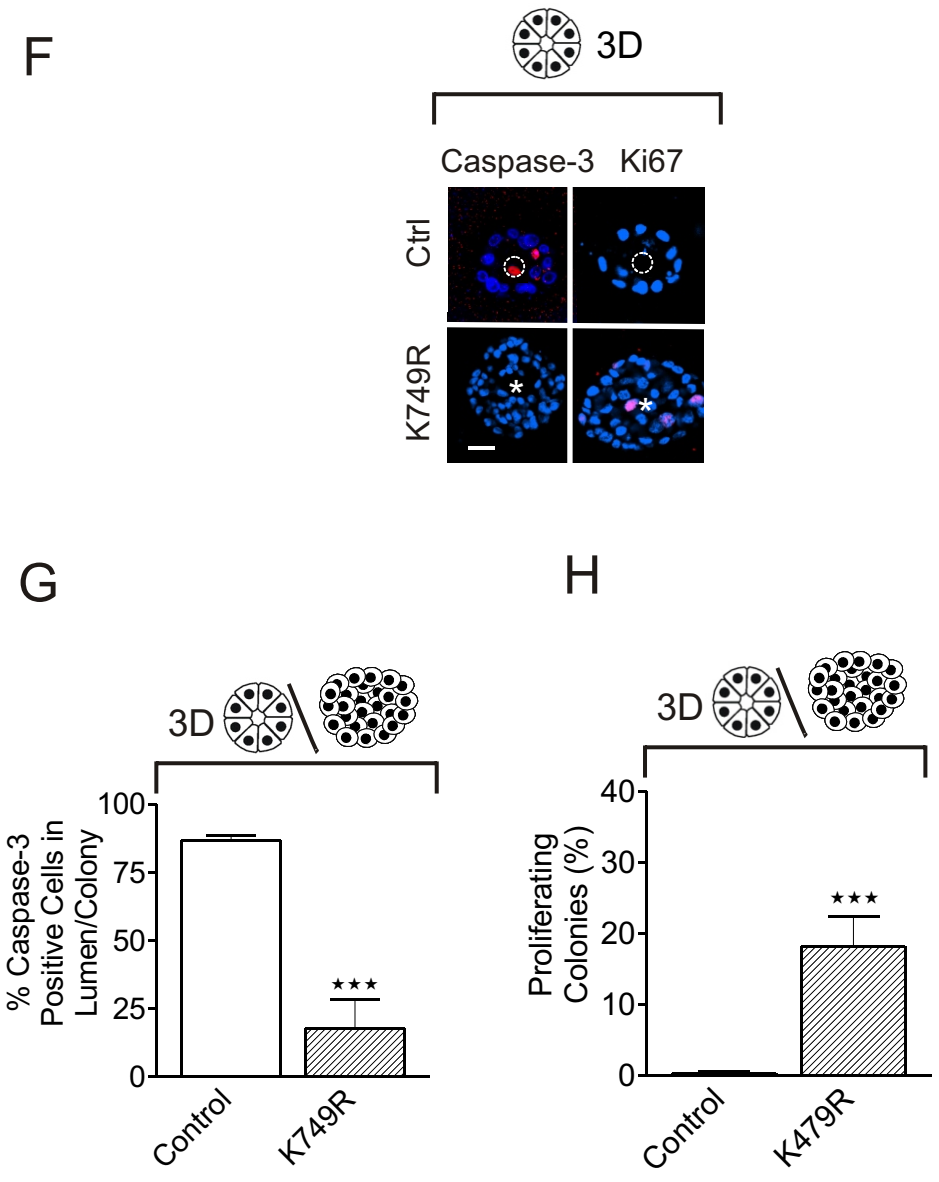

Figure 2.4. Loss of Brm ATPase Remodeling Activity is necessary to enhance MEC survival in 3D.

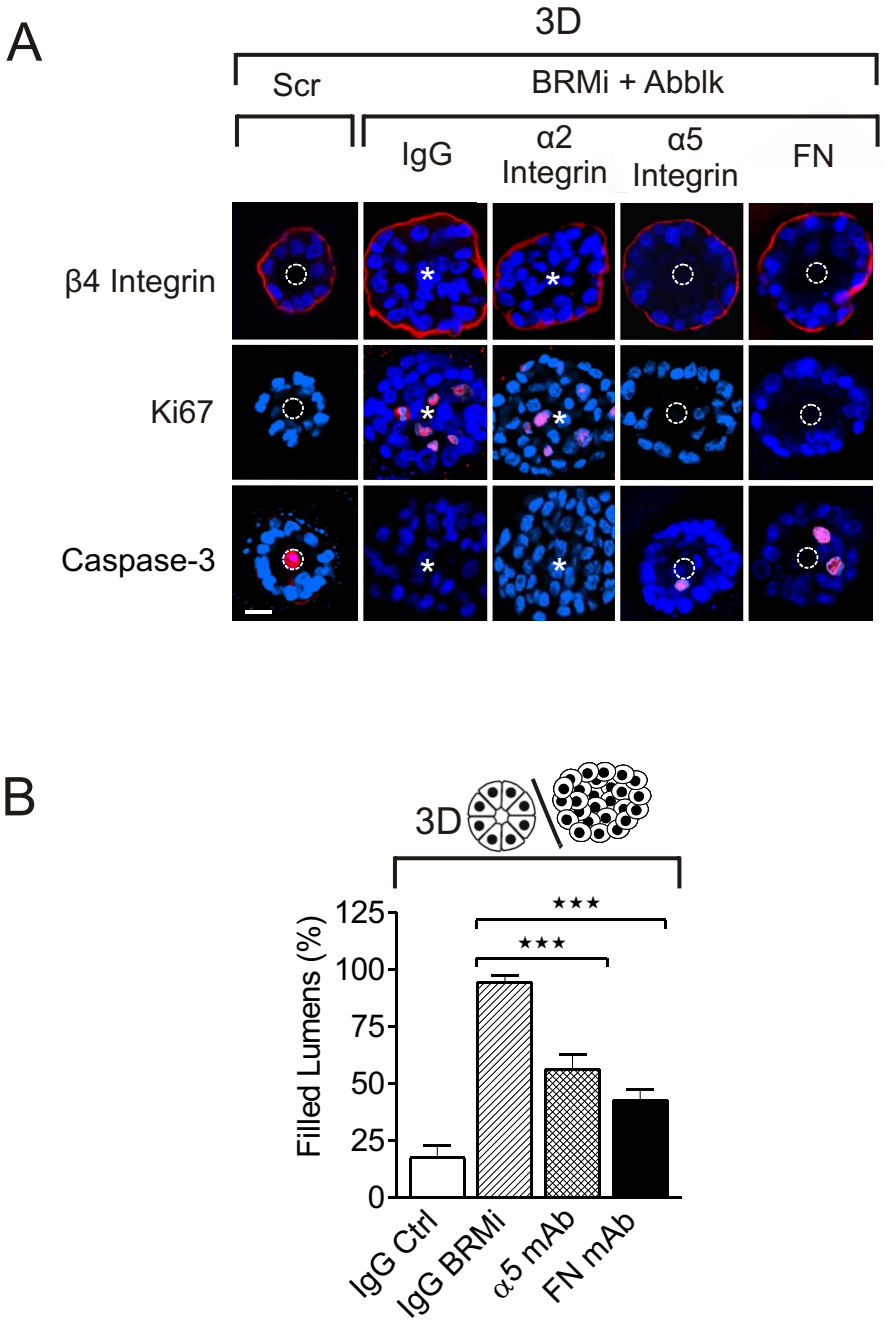

Figure 2.5. Brm regulates malignant transformation by modulating α5β1 integrin-FN interactions

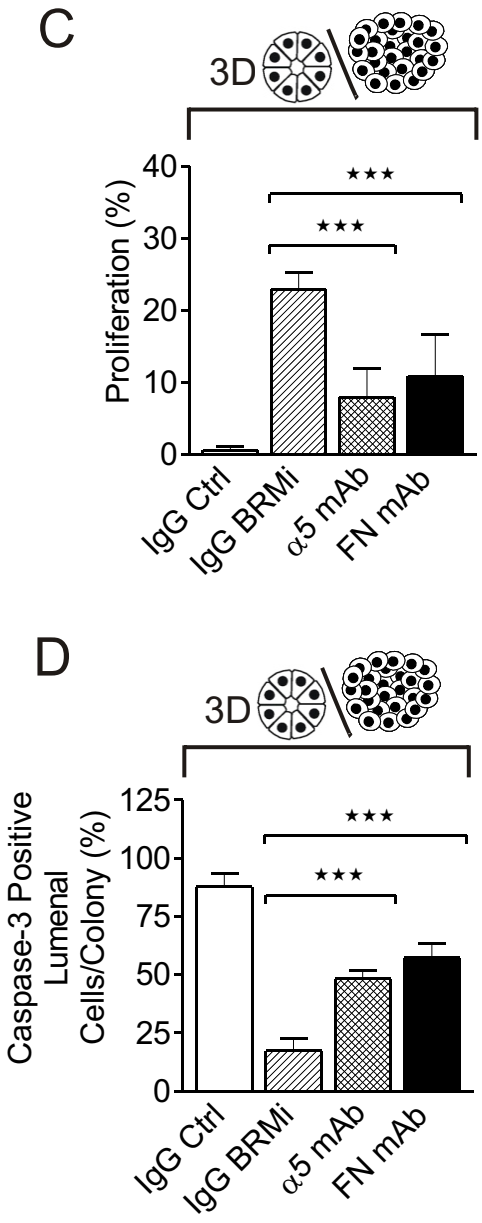

Figure 2.5. Brm regulates malignant transformation by modulating α5β1 integrin-FN interactions

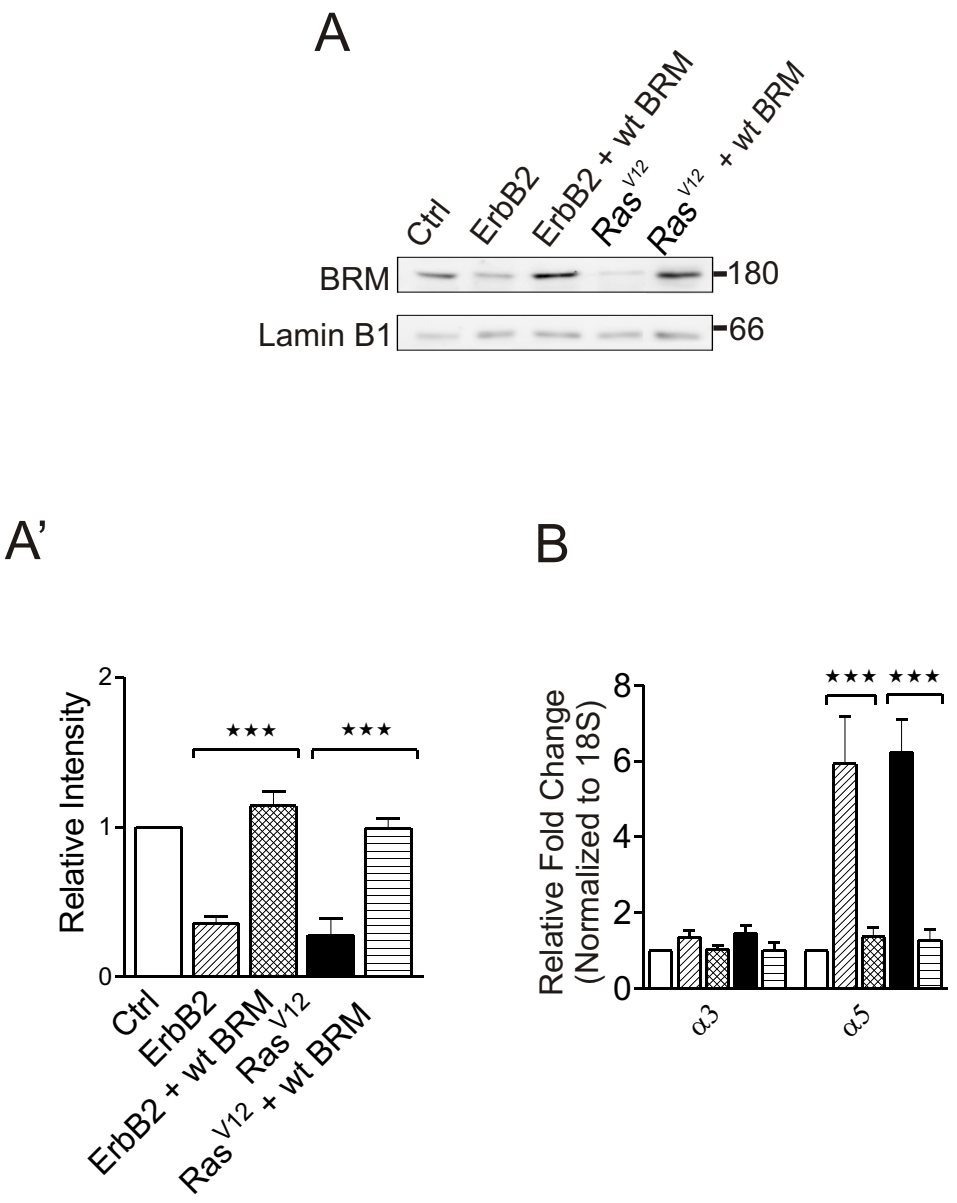

Figure 2.6. Re-expression of BRM in oncogenically transformed MECs reverts malignant behavior in 3D

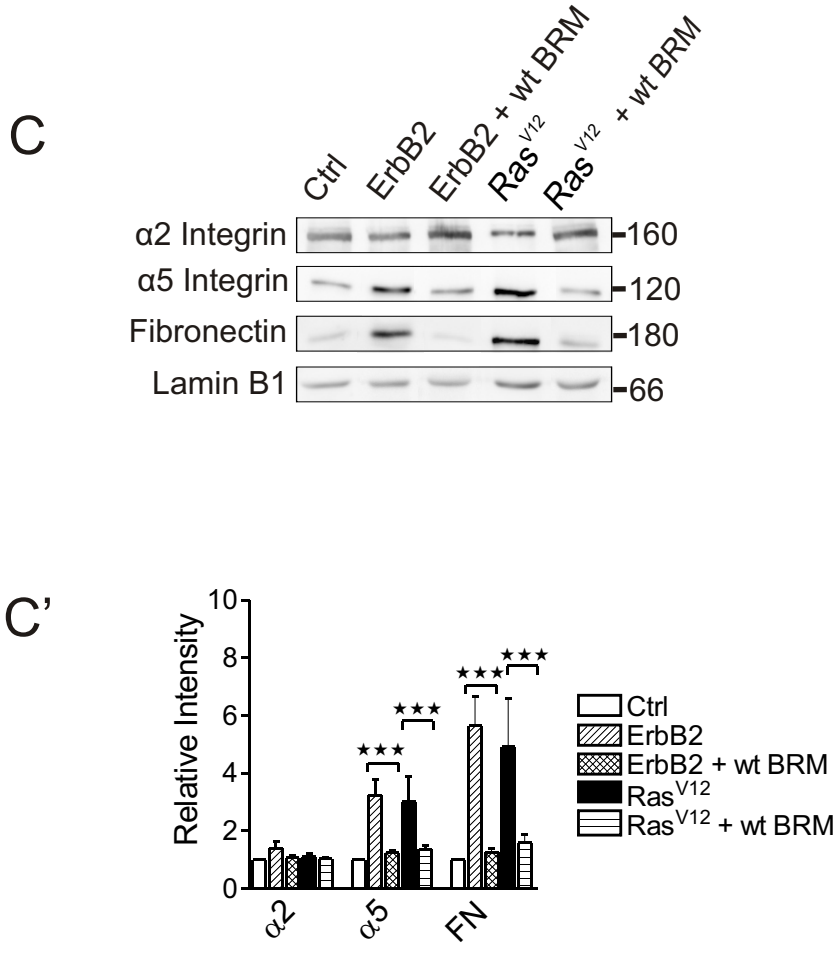

Figure 2.6. Re-expression of BRM in oncogenically transformed MECs reverts malignant behavior in 3D

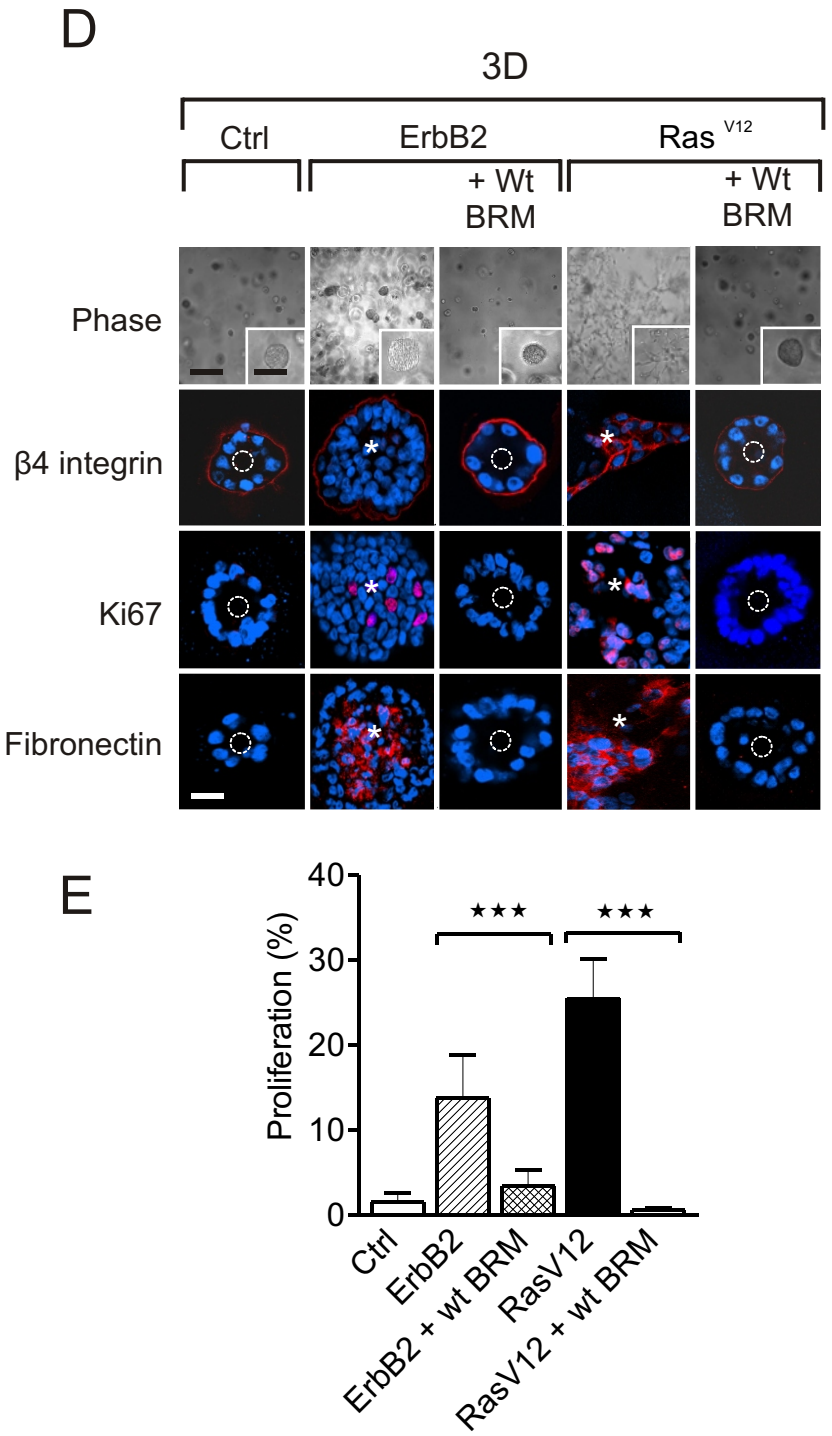

Figure 2.6. Re-expression of BRM in oncogenically transformed MECs reverts malignant behavior in 3D

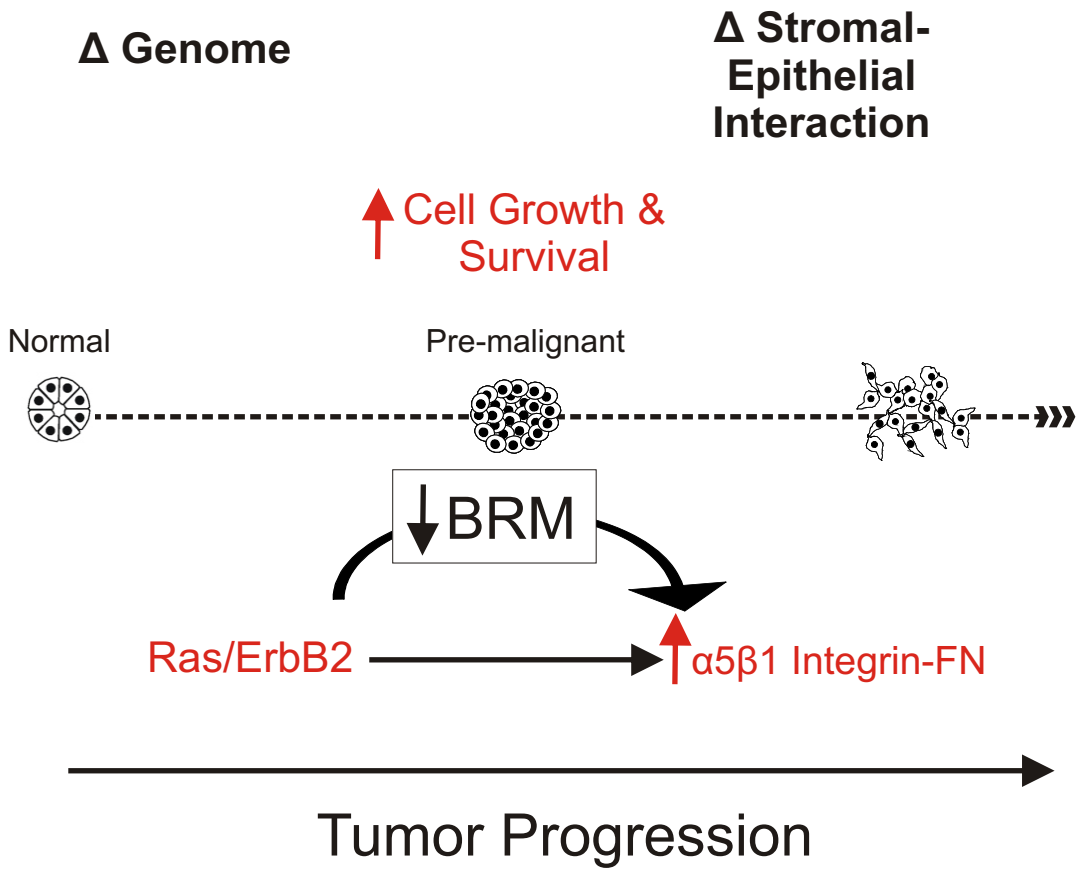

Figure 2.7. Proposed model of oncogene-integrin dialogue via BRM Chromatin Remodeling

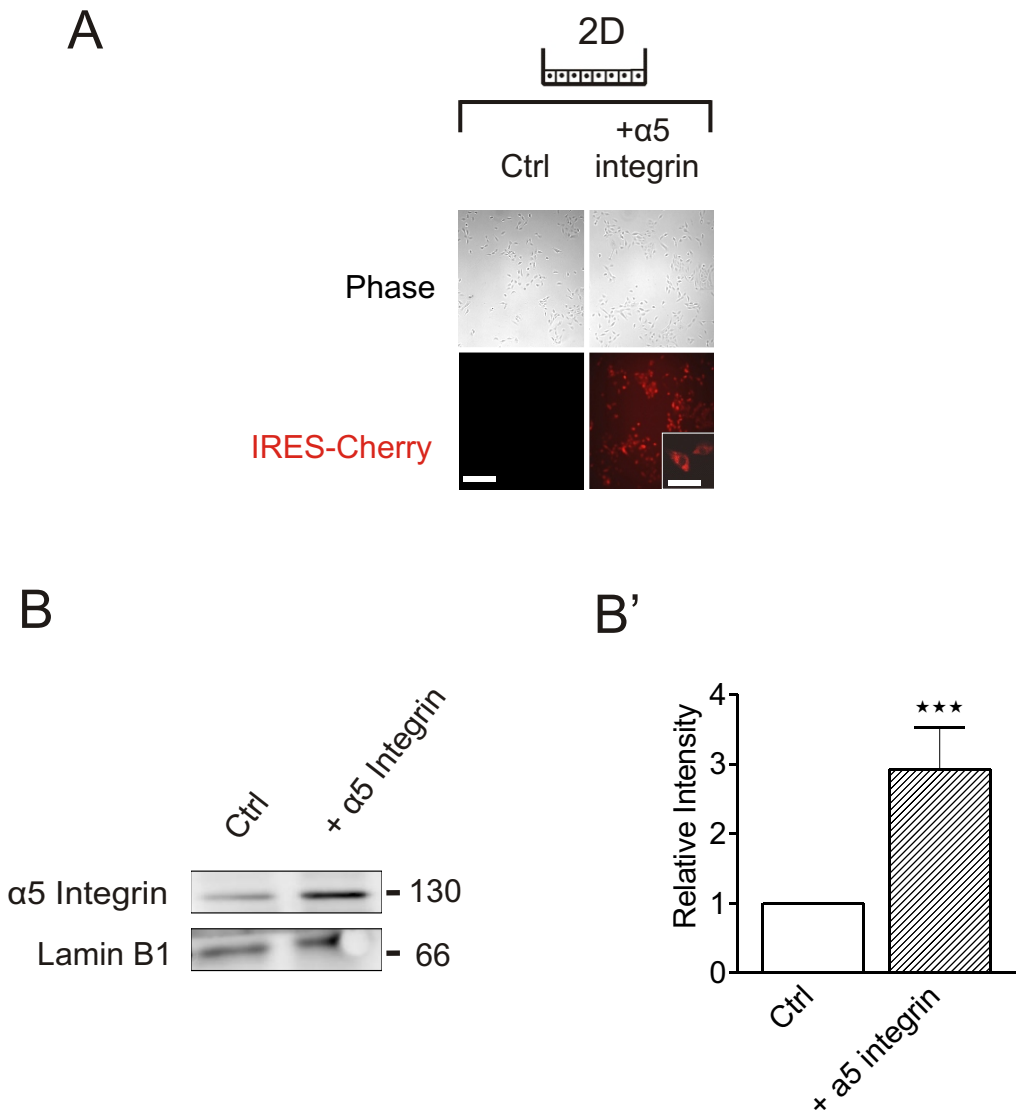

Figure 2.8 Verification of α5 integrin overexpression.

A

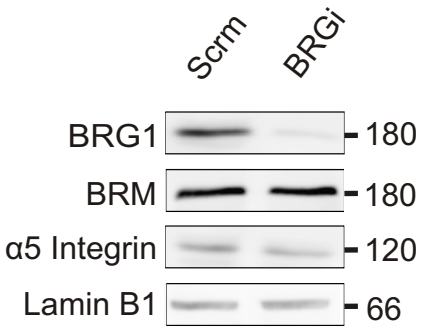

A’

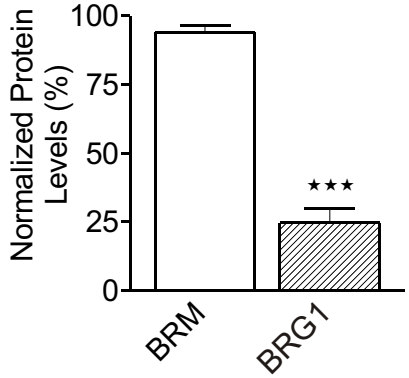

Figure 2.9 BRG1 depletion does not alter α5 integrin levels

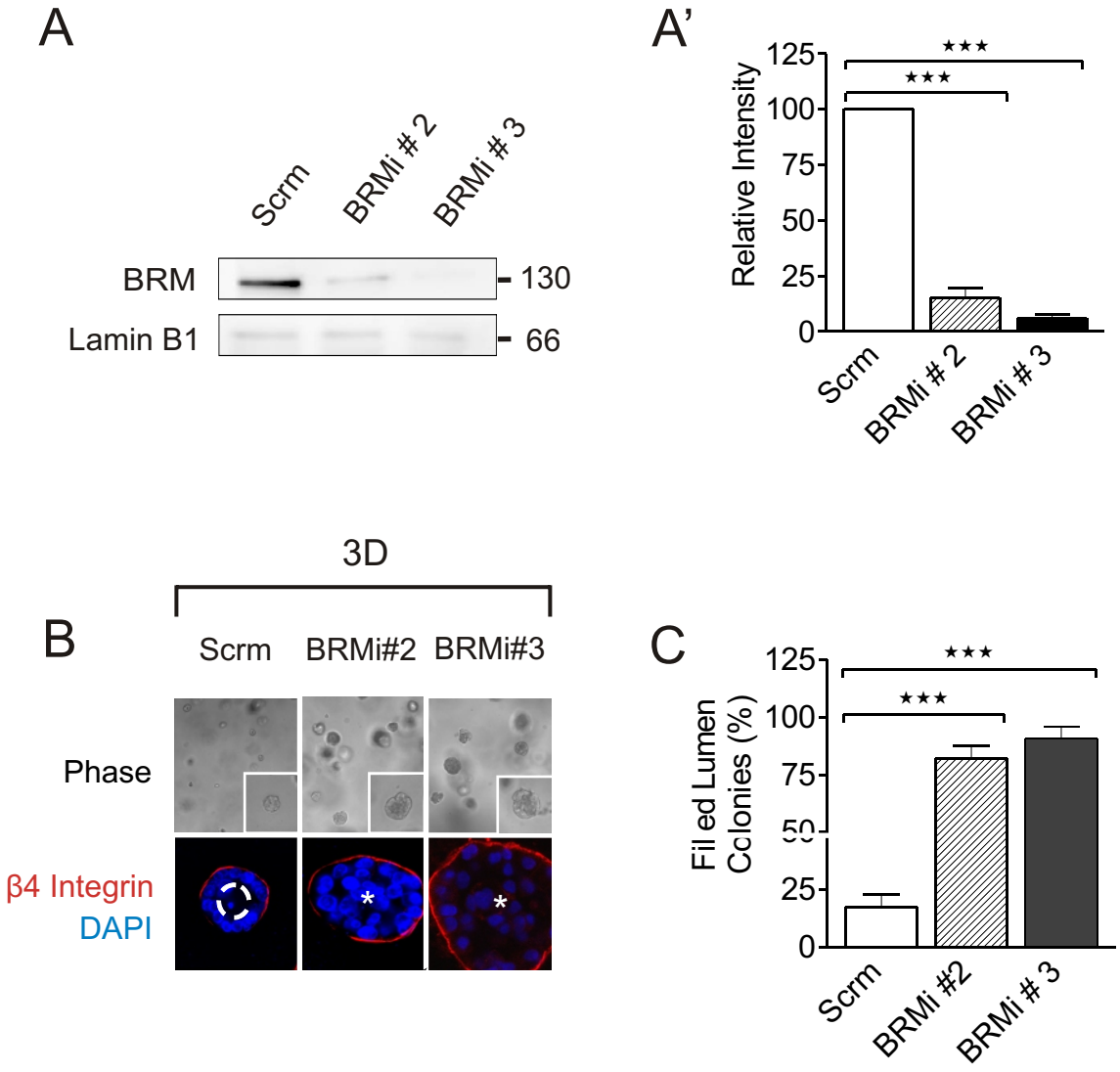

Figure 2.10 Verification of alternative BRM shRNA targeting sequences

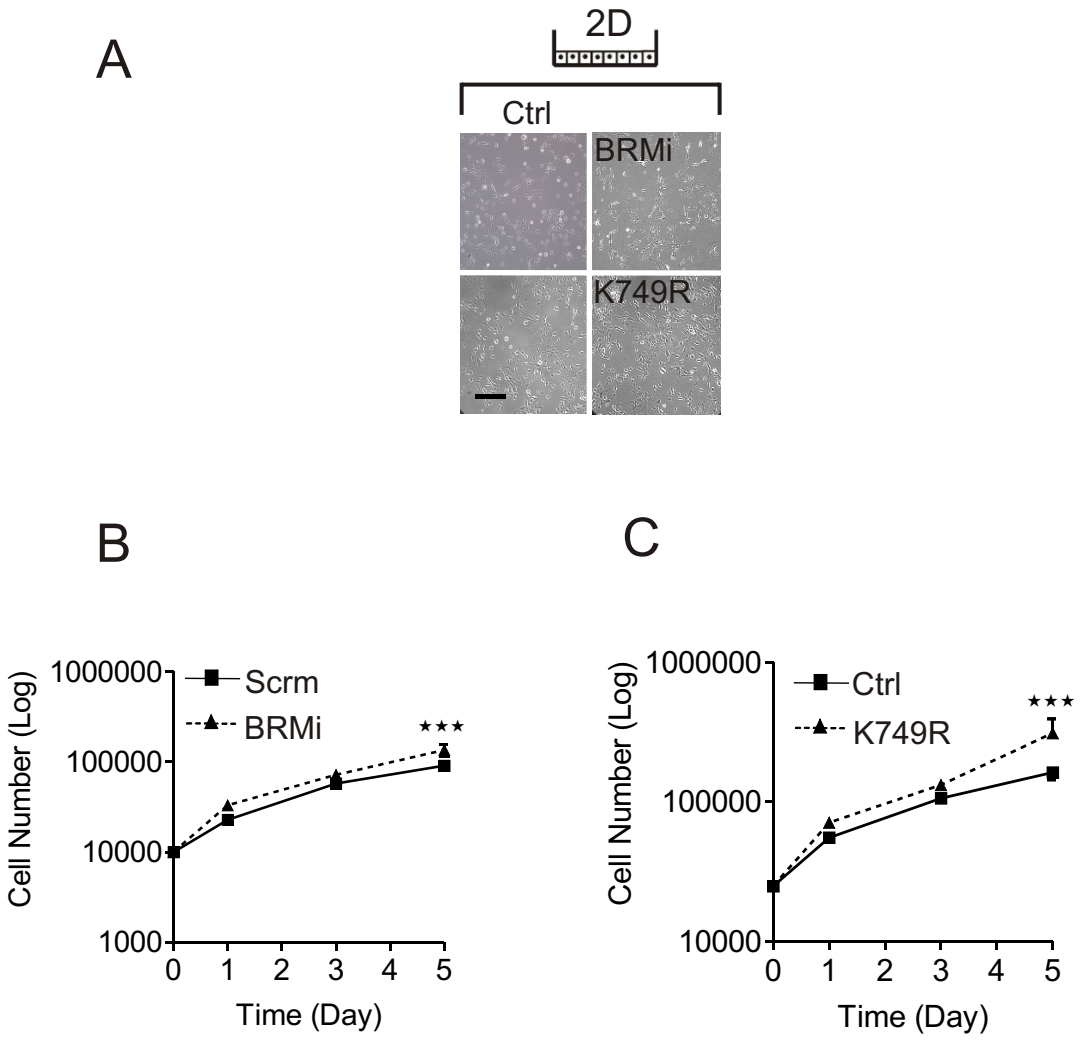

Figure 2.11 Decreased BRM expression or activity does not alter morphology or proliferation in 2D.

A

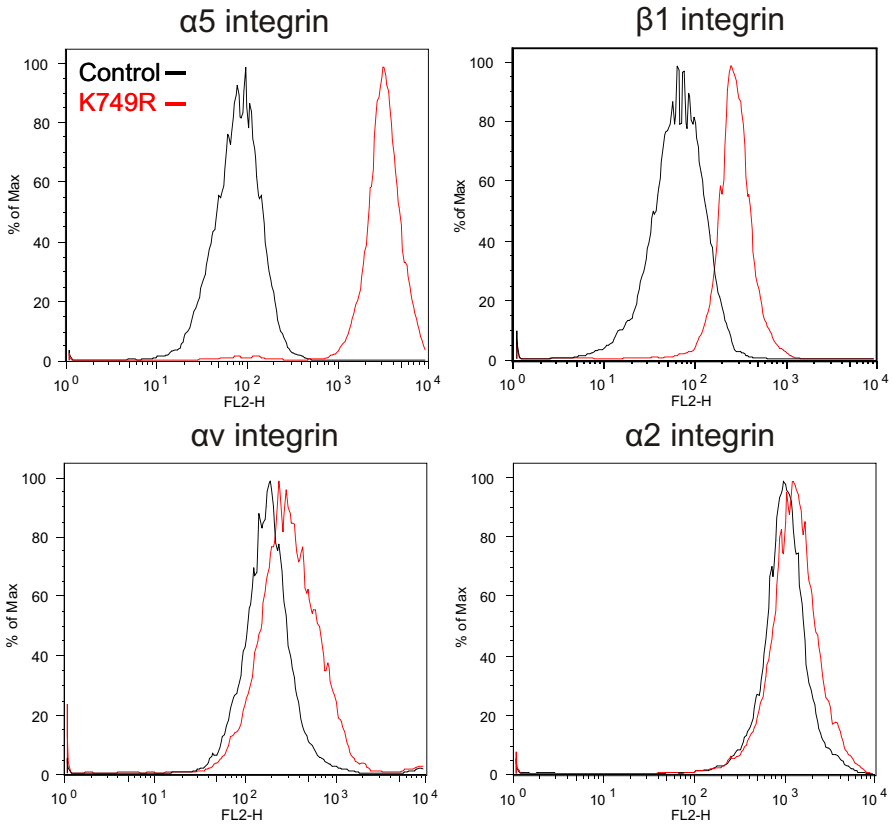

Figure 2.12 FACS Analysis of integrins with reduced Brm expression or activity

B

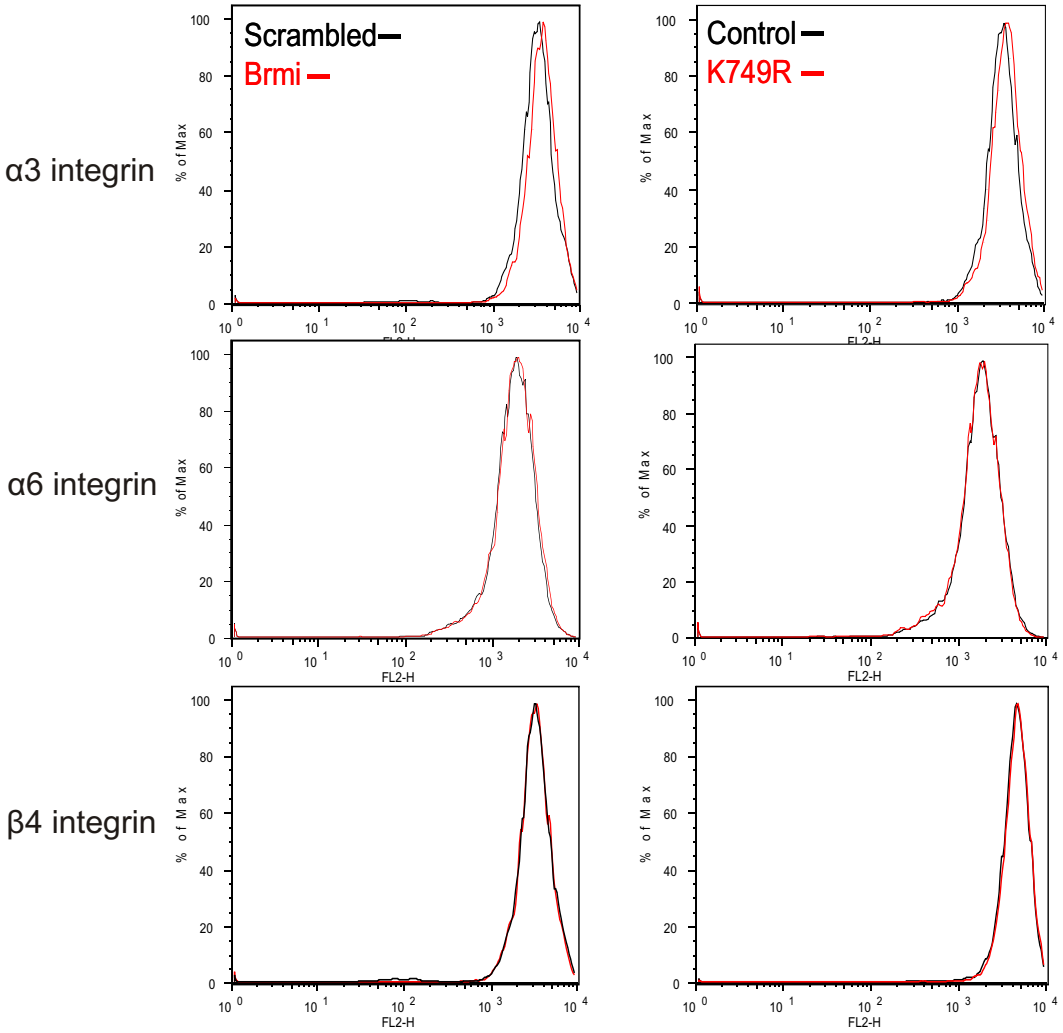

Figure 2.12 FACS Analysis of integrins with reduced Brm expression or activity

Chapter Three
Exploring the role of BRM in breast tumor progression

Statement of Contribution:

Kathleen M. Stewart primarily conducted the execution of the studies contributing to the experimental findings reported in this chapter.

Dr. Nathalie Cohet generated and validated the BRM and Scramble shRNA targeting constructs and gave critical scientific feedback throughout the manuscript process. *Dr. Johnathon Lakins* generated and validated the following retroviral constructs: dominant negative BRM (K749R) and EGFP vector controls. Additionally, Dr. Lakins was of great technical assistance for all methodologies used in this manuscript. *Dr. Kelvin Tsai* performed the multivariate analysis of BRM levels in previously published microarray data sets. *Dr. David Reisman* manufactured the specific Anti-BRM antibody used in all of our experiments and contributed technical assistance to the production of this chapter and in animal experiments. Dr. Reisman also provided $BRM^{-/-}$ mice to be used for future analysis. *Dr. Lisa Coussens* provided FVB/n wild type control mice for analysis in this chapter and also for future back-cross experiments to the Sv129/BL 6 $BRM^{-/-}$ strain.

Dr. Yunn-Yi Chen donated the human breast samples analyzed in this chapter. *Dr. Hongmei Yu* performed breeding and genotyping of the FVB-TgN MMTV-Neu mouse strain, monitored and collected breast tumors from these mice for this chapter. *Renee VanderLaan* assisted in the sectioning and mmunohistochemistry of mouse and human breast samples. *Drs. Frank McCormack and Susan Fisher* donated the MCF-7 breast cancer cell line and the MDA-MB-231 and HCC1143 breast cancer cell lines respectively. *Drs. Jeffrey Nickerson and Anthony Imbalzano* first conducted the experiments characterizing and validating the dominant negative BRM (K749R) construct and performed BRM knockdown microarray studies and analysis. They also provided great technical assistance and scientific feedback throughout the development of this project.

Chapter 3

Exploring the role of BRM in breast tumor progression

Abstract

A major problem in the treatment of breast cancer is metastatic disease. Metastasis requires mammary epithelial cell (MEC)-extracellular matrix interactions (ECM) to support tumor invasion and motility from the primary site and to promote efficient growth and survival at the secondary site. Identifying the mechanisms that modify MEC-ECM interactions during breast tumor progression is paramount in the treatment of metastatic disease. We have previously shown that oncogenic signaling in mammary epithelial cells increases α5β1 integrin-FN interactions and implicates an epigenetic modifier, BRM, in the regulation of these interactions. In the present study, we begin to explore the possible implications of BRM expression and/or activity in breast tumor progression. MEC *in vitro* culture studies suggested that loss of BRM expression and/or activity increased motility, contributed to anchorage independent growth and survival and correlated with increased expression of a set of genes implicated in breast tumor progression. Analysis of previously published microarrays showed that decreased BRM expression correlated with an increase in breast cancer recurrence and a decrease in overall patient survival. Preliminary exploration into BRM expression levels *in vivo* suggest that BRM expression may be reduced in human and murine breast cancer models. These initial studies provide

compelling evidence to support further research into the possibility that oncogene-driven downregulation of BRM contributes to breast tumor progression through regulation of adhesion-dependent cell behaviors.

Introduction

Despite improvements in detecting and treating primary breast tumors, long-term survival is often compromised by the appearance of metastatic tumors in unrelated tissues such as the brain or bone [1]. Metastasis is a multi-step process that requires dynamic changes in mammary epithelial cell (MEC)-extracellular matrix (ECM) interactions to support invasion and motility from the primary site and to promote efficient growth and survival at the secondary site [2-4]. Therefore, identifying the mechanisms that impact ECM responsiveness during tumor progression is important in the efforts to cure breast cancer.

Alterations in MEC responsiveness to ECM microenvironmental cues are mediated by adhesion receptors, of which integrins are the best characterized [5-12]. Breast tumors exhibit increased expression of α6β4, αvβ3 and/or α5β1 integrin although the molecular basis for this phenotype remains unclear [10, 13, 14]. Additionally, several integrins are implicated in the invasive and migratory functions of breast tumors [15-19]. For example, the first step in tumor progression is the acquisition of an invasive phenotype, which requires the disruption of cells' interactions with their neighboring cells, a process based on the loss of E-cadherin-mediated cell–cell adhesion [20, 21]. Loss of E-cadherin is associated with upregulation of α5 integrin levels in ovarian cancer cells and inhibition of α5 integrin in an ovarian cancer xenotransplant models shows reduced tumor burden, metastatic lesions and increased survival [22].

Interestingly, our previous studies show that oncogenic transformation promotes MEC growth and survival and disrupts mammary tissue architecture in three dimensional (3D) culture assays through increased levels of α5 integrin[23]. α5β1 integrin-fibronectin interactions are increased in expression in pancreatic, lung, liver, skin and breast tumors and are also strongly implicated in the successful formation of tumor metastases[15, 22, 24-31]. The molecular basis for altering α5 integrin levels in tumors and metastases remains an area of active investigation although studies have recently implicated epigenetic modifiers of the SWI/SNF chromatin remodeling complex family as potential regulators of α5 integrin levels [32].

Consistent with this hypothesis, we observe that reduced expression and/or activity of the SWI/SNF chromatin remodeling enzyme, BRM, increases α5 integrin protein and mRNA levels in non-malignant MECs and this is associated with disruption of mammary tissue architecture in 3D culture assays[23].
Loss of BRM, BRG1 and several other SWI/SNF proteins occur in human cancer cell lines and tumor specimens of the lung, prostate, stomach, and the breast however the significance of this loss in tumorigenesis needs to be addressed [33-39]. Despite the loss of expression of these twelve SWI/SNF proteins, only BRM shows prognostic significance in lung cancers [40].

Moreover, we observe that re-expression of BRM in transformed MECs that normally express low levels of BRM, restricts a malignant phenotype in 3D cultures [23]. These studies suggest that BRM can exert additional effects on MEC behavior that may or may not be dependent upon α5 integrin expression and/or activity and are the focus of this chapter [23].

Furthermore, our previous studies fail to address the physiological relevance of BRM in the developing mammary gland *in vivo*[23]. In addition to receiving cues from the microenvironment, the behavior of normal and malignant MECs is regulated by neighboring cells, stromal cells, soluble factors and physical forces which are variables not included in the parameters of our 3D rBM morphogenesis assays [7]. Therefore, in order to more faithfully recapitulate the histological complexity of the normal breast and breast cancers, we begin to examine BRM expression levels in a small set of whole animal systems of breast gland development and tumorigenesis and also of human breast cancer samples. In this chapter, I begin to explore the possible functional relevance of BRM in breast tumorigenesis and provide a rationale to support future experiments on this subject.

Materials and Methods

Materials

Primary antibodies used for the studies were as follows: Rabbit anti-serum: Brm (GST-purified protein,[41]); Goat antiserum: Lamin B1 [42]. Secondary antibodies used for the study were as follows: ECL Horseradish peroxidase-conjugated rabbit and goat whole antibodies (Amersham Pharmacia Biotech, Pittsburgh, PA); and Biotin-conjugated rabbit whole antibodies (Jackson Immunoresearch, West Grove, PA). Reagents used were Toluidine Blue O (Sigma; St. Louis, MO), MTT (Thiazolyl Blue Tetrazolium Bromide; Sigma), and Crystal Violet [42].

Human Samples

Human breast tissue samples were obtained from Dr. Yunn-Yi Chen, University of California, San Francisco, Department of Pathology and Laboratory medicine in accordance with Institutional Review Board approval. Reductive mammoplasty tissue or primary breast tumor samples were blinded during analysis and sample identification was revealed at the conclusion of the experiment.

Cell culture

MCF10A, MCF10AneoT (MCF10AT), and MCF10Ca1 were obtained from ATCC (Manassas, Virginia) and maintained in 2D monolayer cultures in DMEM:F12 (Invitrogen, Carlsbad, CA) supplemented with 5% donor horse serum (Invitrogen), 0.5µg/ml hydrocortisone [42], 100ng/ml cholera toxin [42], 10µg/ml insulin [42], 20ng/ml recombinant human epidermal growth factor (EGF,

Peprotech, Rocky Hill, NJ) and 50 U/ml each of penicillin/streptomycin (Invitrogen). The MCF-7 cell line was a generous gift from F. McCormack, UCSF, San Francisco, CA, and the MDA-MB 231 and HCC1143 cell lines were generous gifts of S. Fisher, UCSF, San Francisco, CA. These cell lines were maintained in DMEM:F12 supplemented with 10% FBS.

Mouse model

FVB-TgN MMTV -Neu (wild-type rat Neu gene expressed under the mouse mammary tumor virus LTR, referred to as MMTV-Neu in the text, (obtained from Jackson Laboratory) were maintained in specific pathogen-free conditions in accordance with the guidelines of the Institutional Animal Care and Use Committee at the University of California, San Francisco, California (previously described [43, 44]). Mice were sacrificed at 7–7.5 months of age, mammary glands were excised, formalin fixed, sectioned and immunohistochemistry was performed.

Vector Constructs and ectopic gene expression

Full length human BRM containing a single point mutation in the ATPase binding domain (K749R) was cloned into the pRet puro Tet IRES EGFP tetracycline-inducible vector. The shRNA for BRM and Scrambled Control (Scrm) were derived from siRNA previously designed [45, 46] and were cloned into the

pLVrtTRKRAB-NeoR tetracycline-inducible vector and expressed bicistronically with EGFP. Retrovirus and lentivirus were produced in 293 and 293T cells, respectively. Target cells were infected with virus using 8μg/mL polybrene, and selected with puromycin (K749R) or G148 (BRMi, Scrm).

Microarray Hybridization and Analysis

Affymetrix U74Av2 microarrays were used for the hybridization of biotin-labeled cDNA probes synthesized from 5 μg of total RNA or 1 μg poly(A)+ RNA using Superscript double–strand cDNA synthesis kit (Invitrogen), Bioarray High Efficiency RNA transcript labeling kits and Mg-catalyzed fragmentation kit (Enzo) according to the manufacturers' instruction. Microarrays were stained with phycoerythrin-streptavidin (Molecular Probes), scanned with Affymetrix GeneChip scanner and analyzed with Affymetrix Microarray Analysis Suite (MAS) version 5.0. BRB ArrayTools Version 3.0 (http://linus.nci.nih.gov./BRB-ArrayTools.html) was used for the analysis of the MAS 5.0 data set. A log base 2 transformation was applied to the data set before arrays were normalized. Each array was normalized using median values of gene expression over the entire array (global normalization). A median array was selected as the reference array for normalization and results were thresholded at 1.5 fold change.

Meta-Analysis of Published Data

We performed multivariate analysis of the NKI data set [47]. The Genebank ID of BRM used to interrogate the NKI data set was: SMARCA2: NM_003070. The NKI data set used Agilent two-color oligo microarrays for analysis of gene expression, with a total patient number of 295. All statistical analyses were performed in R statistical programming software (version 2.0.1; http://www.r-project.org/). The probabilities of overall survival were estimated according to the Kaplan-Meier method[48]. Significance of difference among subclasses of BRM expression quartiles were determined by log-rank test [49].

Immunohistochemistry

H&E staining was performed using standard methodologies. For BRM immunohistochemistry, formalin fixed, paraffin-embedded tissue samples were deparaffinized, and antigens were retrieved using 0.1M Citrate buffer (pH 6.0; 95C for 20 min, 25C for 20 min), incubated in 3% H_2O_2 for 15 min to block endogenous peroxidase activity and stained with antisera for BRM. Visualization was performed using the Vectastain Elite ABC system and 3,3'-diaminobenzidine (Vector Laboratories, Burlingame, CA) . Slides were then lightly counterstained in Mayer's hematoxylin, rinsed, dehydrated, cleared, and mounted. For mouse studies, n=3 slides per condition were analyzed; human samples, n=2 slides per condition were analyzed.

Immunoblotting

Cells were lysed in Laemmli buffer containing 20mM sodium fluoride, 1mM sodium orthovanadate, and a cocktail of protease inhibitors and the protein concentration determined using a bicinchoninic acid (BCA; Thermo Fisher Scientific, Rockford, IL) assay. Equal protein was separated on SDS-PAGE gels, immunoblotted, and visualized using an ECL system (Amersham). The chemiluminescent intensity of bands was digitized using the Image Analyzer LAS-1000 Plus system and the Image Reader LAS-1000 Pro version 1.0 software (Fuji, Tokyo, Japan).

Real-Time PCR

Random-primed cDNA was prepared from total isolated RNA (Trizol; Invitrogen, Carlsbad, CA). All primers of target genes and an internal control gene 18S were designed by Primer3 software (http://frodo.wi.mit.edu/primer3/; see Appendix III). In each assay, target DNA sequences were quantified by real time PCR using a SYBR Green and a Light Cycler Apparatus (Roche Applied Science; software version 3.5, Indianapolis, IN). A singleplex reaction mix was prepared according to the manufacture's protocol, as described previously [50, 51]. The thermal cycling conditions included an initial denaturation step at 95°C for 10 min, 40 cycles at 95°C for 15s and 60°C for one min. Fold change in expression were determined using the ΔCt method with normalization to total RNA [52].

Soft Agar Colony Assay

5,000 cells were plated in 0.7% agar layered on top of 1% agar in a 6 well plate. After 2 weeks, colonies were stained with 0.005% crystal violet. Colony number and size was determined by analysis of images from 3 independent experiments (n=50 images per experiment) which were taken with a Nikon Eclipse E600 standard epifluorescent microscope equipped with a QICAM camera. Colony size was determined by Spot™ Imaging software (Nikon Instruments Inc., Melville, NY; Q Imaging, Surrey, BC; Spot Imaging, Diagnostic Instruments Inc., Sterling Heights, MI).

Migration Studies

Cell migration was assessed using a monolayer wound healing assay [53]. Briefly, confluent cells were ‘wounded’ with a pipette tip and the healing of the wound was then imaged (n=50 images per trial; n=6 independent experiments) and wound distance was measured over time (0, 6, 9, and 12 hours) at 40x magnification using a Nikon Eclipse E600 standard epifluorescent microscope equipped with a QICAM camera and analyzed with Spot™ Imaging software. Data was represented as percent wound closure.

Statistical analysis

InStat software (Graphpad, LaJolla, CA) was used to conduct the statistical analysis of our data. Unless otherwise stated, two-tailed student *t*-tests were used for significance testing, and two-tailed Pearson tests for correlation analysis. Means are presented as ±SEM of 3-5 independent experiments and statistical significance was considered $p < 0.05$. Unless otherwise noted, sample size is n=3.

Results

Reduced BRM levels correlated with malignant behavior in human breast cancer cell lines

We previously showed that ErbB2- and Ras^{V12}- transformed mammary epithelial cell (MEC) lines exhibited decreased BRM protein levels[23]. Moreover, we found that BRM expression was lowest in the more aggressive Ras^{V12}- transformed cell line[23]. To further explore the relationship between BRM expression levels as a function of tumor aggression, we examined BRM levels in non-malignant MECs (MCF10As) and in a series of increasingly transformed breast cancer cell lines MCF-7, MDA-MB-231 and HCC1143 (in order of increasing malignancy) [54-57]. Immunoblotting showed a significant decrease in total BRM protein levels in the transformed MECs compared to MCF10As (Figure 3.1A). Additionally, we observed BRM protein levels inversely correlated with the degree of phenotypic malignancy of these breast cancer cell lines, i.e. BRM expression was the lowest in the most aggressive tumorigenic cell line (HCC1143) compared to other transformed MECs (Figure 3.1A).

To further explore the functional relationship between BRM levels and malignant behavior of breast cancer cells, we examined BRM expression in the molecularly defined MCF10A cell line series (MCF10A: non-malignant, parental cell line; MCF10AT: pre-malignant, H-ras transformed; and MCF10Ca1: malignant)[54, 58, 59]. BRM levels were reduced in MCF10AT and MCF10Ca1 cell lines and BRM expression appeared to be associated with tumor aggressiveness (Figure

3.1B). As BRM levels were associated with tumor aggressiveness, we next asked whether decreased BRM expression impacted adhesion-dependent behaviors characteristic of invasive tumors.

Absence of BRM and/or its remodeling activity promoted anchorage independent growth and survival

Tumor metastasis is controlled not only by enhanced growth and survival but also requires cell motility and invasion in order to disseminate to other sites in the body[60]. Therefore, we next asked whether reduced BRM expression and/or activity was sufficient to drive anchorage independent growth and survival. Soft colony agar studies revealed that loss of BRM expression or activity robustly increased colony formation and increased the general size of individual colonies as compared to nonmalignant MECs (Figure 3.2). The number and size of colonies generated from BRM-depleted MECS were similar to those of metastatic MDA-MB 231 cells that served as a positive control for these assays (Figure 3.2). These data demonstrated that decreased BRM expression or ATPase activity promoted anchorage independent growth and survival..

Reduced BRM chromatin remodeling activity increased cell motility

To explore the potential effects of BRM chromatin remodeling on MEC motility, we asked whether abrogation of BRM activity via overexpression of an ATPase-dead BRM mutant increased the migratory behavior of nonmalignant MECs. Using a 12-24 hour wound healing assay, we showed that reducing BRM

ATPase chromatin remodeling activity significantly increased cell motility in MCF10A cells (Figure 3.3). In contrast, non-malignant MCF10A cells did not migrate and failed to close the artificial wound (Figure 3.3). These data suggested that BRM chromatin remodeling activity may regulate MEC migration behavior through its ATPase-dependent activities.

Loss of BRM associated with upregulation of tumor-promoting genes

To address the possibility that downregulation of BRM could promote tumor progression and enhance tumor aggression, we analyzed the transcriptional profile of the non-malignant MCF10A cell line, in which BRM expression was knocked down by shRNA targeting. As summarized in Table 3.1, reduced BRM expression was associated with increased expression of genes implicated in breast tumor progression which is consistent with the fact that BRM loss could drive an entire program of genes that promote tumor progression. Specifically, we observed increased expression in ECM remodeling genes such as the matrix metalloproteinase-2 (MMP-2) and lysyl-oxidase-like protein 2 (LOXL2) as well as increased expression of reactive stromal-associated genes such as vimentin and SNAIL; all of which were implicated in tumor migration and invasion [61-68]. These findings suggested that BRM modulated an entire program of genes implicated in tumor aggression.

BRM was reduced and associated with poor clinical prognosis in human breast cancers. Poor clinical prognosis in human breast cancers associated with BRM reduction.

To validate our preliminary *in vitro* findings, we began to explore the relevance of BRM levels in human breast cancer samples by analyzing previously published microarray data sets [47]. We found that reduced BRM expression was associated with a significant increase in tumor recurrence and decrease in patient survival (Figure 3.4). These data implicated BRM as a potential marker of tumor progression and clinical outcome in human breast cancers.

Preliminary findings on BRM levels in the Murine Breast Cancer model MMTV-Neu

To validate our preliminary microarray analysis findings, we next explored the functional relevance of BRM in the FVB mouse mammary tumor virus (MMTV)-neu mouse model in which 70-80% of tumor-bearing mice develop metastatic breast cancer disease [43, 69]. Using a BRM-specific antibody, we performed immunohistochemistry analysis for BRM levels on an extremely limited population size of mice (2 mammary glands per condition) and found decreased BRM levels in the tumorigenic mammary gland samples (Figure 3.5).

By contrast, mammary epithelial cell populations of control mice abundantly expressed BRM in our small study (Figure 3.5). These preliminary findings suggested that the expression of BRM in murine breast cancer models should be further explored.

Preliminary Findings on BRM levels in human breast cancer samples

In addition to examining BRM levels in murine breast cancer models, we also began to analyze BRM levels in human breast cancer samples. We examined the levels of BRM in just two samples of each condition: normal breast tissue (taken from reductive mammoplasty procedure), premalignant breast tissue (ductal carcinoma *in situ*) and malignant breast tissue (invasive ductal carcinoma). Using a BRM-specific antibody, we noted that normal breast tissue had robust BRM positive staining (Figure 3.6). Furthermore, BRM expression appeared to be reduced in a subset of premalignant and malignant tumor cells however, these studies require further examination before BRM expression levels in human breast cancer samples can be determined (Figure 3.6).

Discussion

In this report, we have begun to explore the potential relationship between BRM SWI/SNF mediated chromatin remodeling and breast tumor progression *in vitro* and *in vivo*. We found that reduced BRM expression correlated with breast cancer cell line malignant behavior, enhanced MEC motility and anchorage independent growth and increased expression of genes associated with tumor progression. Furthermore, a preliminary investigation into BRM levels in murine and human breast cancer samples suggested that BRM expression may be reduced in tumors *in vivo* but requires further investigation.

In this study, we found that BRM expression is decreased in breast cancer cell lines and correlated with tumor aggressiveness (Figure 3.1). This observation is consistent with previous reports showing reduced SWI/SNF BRM protein levels in various cancer cell lines, including the MCF-7 breast cancer cell line we analyzed (Figure 3.1; [35, 70, 71]). The observation that BRM protein levels were reduced in the molecularly defined MCF10A cell line progression series adds further support to a tentative relationship between BRM levels and breast tumor progression (Figure 3.1). Because these cell lines share common genetic origins, our observed differences in gene expression patterns between these cells are likely indicative of changes that influence tumorigenic progression rather than differences in genetic backgrounds.

We demonstrated that in the absence of BRM chromatin remodeling activity and/or expression, non-malignant MECs became more motile and supported enhanced anchorage independent growth and survival in *in vitro* studies (Figures 3.4; 3.5). Breast tumor progression is functionally linked to the migration of transformed MECs across their endogenous basement membrane [78] and also to their growth and survival in the surrounding interstitial stroma [11, 79, 80]. Consistent with a putative role for BRM in the regulation of breast tumor progression, microarray analysis of BRM shRNA MECs revealed an increase in expression of a program of genes associated with breast tumor progression such as vimentin, SNAIL and fibronectin (Table 3.1; [26, 81, 82]).

While acquiring anchorage independent growth is not necessarily indicative of MEC invasion or tumorigenic behaviors, previous reports suggest it may represent promotion of a pre-malignant phenotype [83]. To address the question of MEC invasive behavior, we could examine the effects of BRM knockdown on: MEC invasion in Boyden chamber invasion assays, the expression/secretion of ECM degrading enzymes that would enable MEC invasion and *in vivo* xenotransplant studies.

We extended these initial *in vitro* findings by completing a multivariate analysis of the largest and longest published microarray data set for breast cancers, the Netherlands Cancer Institute data set (NKI) (Figure 3.5). We found that patients with the lowest BRM expression have increased tumor recurrence and reduced overall survival (Figure 3.5). The molecular basis for reduced BRM expression in breast cancers however remains unanswered.

We found that BRM expression appears to be reduced in mammary tissues of MMTV-Neu transformed mice and in human pre-malignant and invasive breast cancers (Figures 3.1; 3.2). Previous findings in prostate, gastric and lung cancer reveal reduced BRM expression in tumors [39, 84]. Furthermore, BRM loss is reported in approximately 10-30% of patients [35, 71]. However, due to the limited sample size, we cannot draw any finite conclusions on the expression of BRM in breast cancers. Despite the fact that these studies must be interpreted cautiously, nevertheless they do indicate that BRM levels in *in vivo* models of breast cancer need to be further explored.

Our preliminary exploration into the role of BRM in breast tumor progression suggests that BRM levels may be reduced in human breast cancer cell lines and murine and human breast cancer tissues. Furthermore, these initial studies provide compelling evidence to support further research into the possibility that reduced BRM levels contribute to breast tumor progression and metastasis.

References

1. Carlson, R.W., et al., *Breast cancer. Clinical practice guidelines in oncology.* J Natl Compr Canc Netw, 2009. **7**(2): p. 122-92.
2. Wiseman, B.S. and Z. Werb, *Stromal effects on mammary gland development and breast cancer.* Science, 2002. **296**(5570): p. 1046-9.
3. Spencer, V.A., R. Xu, and M.J. Bissell, *Extracellular matrix, nuclear and chromatin structure, and gene expression in normal tissues and malignant tumors: a work in progress.* Adv Cancer Res, 2007. **97**: p. 275-94.
4. Hanahan, D. and R.A. Weinberg, *The hallmarks of cancer.* Cell, 2000. **100**(1): p. 57-70.
5. Petersen, O.W., et al., *Differentiation and cancer in the mammary gland: shedding light on an old dichotomy.* Adv Cancer Res, 1998. **75**: p. 135-61.
6. Streuli, C.H. and M.J. Bissell, *Expression of extracellular matrix components is regulated by substratum.* J Cell Biol, 1990. **110**(4): p. 1405-15.
7. Ronnov-Jessen, L., O.W. Petersen, and M.J. Bissell, *Cellular changes involved in conversion of normal to malignant breast: importance of the stromal reaction.* Physiol Rev, 1996. **76**(1): p. 69-125.
8. Plantefaber, L.C. and R.O. Hynes, *Changes in integrin receptors on oncogenically transformed cells.* Cell, 1989. **56**(2): p. 281-90.
9. Desgrosellier, J.S. and D.A. Cheresh, *Integrins in cancer: biological implications and therapeutic opportunities.* Nat Rev Cancer. **10**(1): p. 9-22.

10. Carey, D.J., *Syndecans: multifunctional cell-surface co-receptors.* Biochem J, 1997. **327 (Pt 1)**: p. 1-16.

11. Fata, J.E., Z. Werb, and M.J. Bissell, *Regulation of mammary gland branching morphogenesis by the extracellular matrix and its remodeling enzymes.* Breast Cancer Res, 2004. **6**(1): p. 1-11.

12. Giancotti, F.G. and E. Ruoslahti, *Integrin signaling.* Science, 1999. **285**(5430): p. 1028-32.

13. Stillfried, G.E., D.N. Saunders, and M. Ranson, *Plasminogen binding and activation at the breast cancer cell surface: the integral role of urokinase activity.* Breast Cancer Res, 2007. **9**(1): p. R14.

14. Henry, M.D. and K.P. Campbell, *Dystroglycan inside and out.* Curr Opin Cell Biol, 1999. **11**(5): p. 602-7.

15. Zeng, Z.Z., et al., *alpha(5)beta(1) Integrin Ligand PHSRN Induces Invasion and alpha(5) mRNA in Endothelial Cells to Stimulate Angiogenesis.* Transl Oncol, 2009. **2**(1): p. 8-20.

16. Reinmuth, N., et al., *Alphavbeta3 integrin antagonist S247 decreases colon cancer metastasis and angiogenesis and improves survival in mice.* Cancer Res, 2003. **63**(9): p. 2079-87.

17. Ruoslahti, E., *Cell adhesion and tumor metastasis.* Princess Takamatsu Symp, 1994. **24**: p. 99-105.

18. Roman, J., et al., *{alpha}5{beta}1 Integrin Expression is Essential for Tumor Progression in Experimental Lung Cancer.* Am J Respir Cell Mol Biol.

19. Hsia, D.A., et al., *Differential regulation of cell motility and invasion by FAK.* J Cell Biol, 2003. **160**(5): p. 753-67.

20. Cavallaro, U. and G. Christofori, *Cell adhesion and signalling by cadherins and Ig-CAMs in cancer.* Nat Rev Cancer, 2004. **4**(2): p. 118-32.

21. Margulis, A., et al., *E-cadherin suppression accelerates squamous cell carcinoma progression in three-dimensional, human tissue constructs.* Cancer Res, 2005. **65**(5): p. 1783-91.

22. Sawada, K., et al., *Loss of E-cadherin promotes ovarian cancer metastasis via alpha 5-integrin, which is a therapeutic target.* Cancer Res, 2008. **68**(7): p. 2329-39.

23. Stewart, K.M., Cohet, N., Miroshinova, Y., Lakins, J., Debnath, J., Reisman, D., Nickerson, J.A., Imbalzano, A.N., Weaver, V.M., *Oncogenic-targeting of chromatin remodeling regulates stromal-epithelial interactions to promote malignant progression*

in preparation, 2010.

24. Maschler, S., et al., *Tumor cell invasiveness correlates with changes in integrin expression and localization.* Oncogene, 2005. **24**(12): p. 2032-41.

25. Ryschich, E., et al., *Promotion of tumor cell migration by extracellular matrix proteins in human pancreatic cancer.* Pancreas, 2009. **38**(7): p. 804-10.

26. Meng, X.N., et al., *Characterisation of fibronectin-mediated FAK signalling pathways in lung cancer cell migration and invasion.* Br J Cancer, 2009. **101**(2): p. 327-34.

27. Jha, R.K., et al., *Relationship of fibronectin and CD44v6 expression with invasive growth and metastasis of liver cancer.* Cancer Invest, 2009. **27**(3): p. 324-8.

28. Marasa, L., S. Marasa, and G. Sciancalepore, *Collagen IV, laminin, fibronectin, vitronectin. Comparative study in basal cell carcinoma. Correlation between basement membrane molecules expression and invasive potential.* G Ital Dermatol Venereol, 2008. **143**(3): p. 169-73.

29. Labat-Robert, J., *Fibronectin in malignancy.* Semin Cancer Biol, 2002. **12**(3): p. 187-95.

30. Kim, S., et al., *TMPRSS4 induces invasion and epithelial-mesenchymal transition through upregulation of integrin alpha5 and its signaling pathways.* Carcinogenesis. **31**(4): p. 597-606.

31. Qian, F., et al., *Interaction between integrin alpha(5) and fibronectin is required for metastasis of B16F10 melanoma cells.* Biochem Biophys Res Commun, 2005. **333**(4): p. 1269-75.

32. Hill, D.A., et al., *Inducible changes in cell size and attachment area due to expression of a mutant SWI/SNF chromatin remodeling enzyme.* J Cell Sci, 2004. **117**(Pt 24): p. 5847-54.

33. Gregory, R.I. and R. Shiekhattar, *Chromatin modifiers and carcinogenesis.* Trends Cell Biol, 2004. **14**(12): p. 695-702.

34. Muchardt, C. and M. Yaniv, *When the SWI/SNF complex remodels...the cell cycle.* Oncogene, 2001. **20**(24): p. 3067-75.

35. Glaros, S., et al., *The reversible epigenetic silencing of BRM: implications for clinical targeted therapy.* Oncogene, 2007. **26**(49): p. 7058-66.

36. Glaros, S., et al., *Targeted knockout of BRG1 potentiates lung cancer development.* Cancer Res, 2008. **68**(10): p. 3689-96.

37. Yamamichi, N., et al., *The Brm gene suppressed at the post-transcriptional level in various human cell lines is inducible by transient HDAC inhibitor treatment, which exhibits antioncogenic potential.* Oncogene, 2005. **24**(35): p. 5471-81.

38. Yamamichi, N., et al., *Frequent loss of Brm expression in gastric cancer correlates with histologic features and differentiation state.* Cancer Res, 2007. **67**(22): p. 10727-35.

39. Reisman, D., S. Glaros, and E.A. Thompson, *The SWI/SNF complex and cancer.* Oncogene, 2009. **28**(14): p. 1653-68.

40. Fukuoka, J., et al., *Chromatin remodeling factors and BRM/BRG1 expression as prognostic indicators in non-small cell lung cancer.* Clin Cancer Res, 2004. **10**(13): p. 4314-24.

41. Reisman, D.N., et al., *The expression of the SWI/SNF ATPase subunits BRG1 and BRM in normal human tissues.* Appl Immunohistochem Mol Morphol, 2005. **13**(1): p. 66-74.

42. Park, J.W., et al., *Rationale for biomarkers and surrogate end points in mechanism-driven oncology drug development.* Clin Cancer Res, 2004. **10**(11): p. 3885-96.

43. Guy, C.T., et al., *Expression of the neu protooncogene in the mammary epithelium of transgenic mice induces metastatic disease.* Proc Natl Acad Sci U S A, 1992. **89**(22): p. 10578-82.

44. Muller, W.J., et al., *Synergistic interaction of the Neu proto-oncogene product and transforming growth factor alpha in the mammary epithelium of transgenic mice.* Mol Cell Biol, 1996. **16**(10): p. 5726-36.

45. Rosson, G.B., et al., *BRG1 loss in MiaPaCa2 cells induces an altered cellular morphology and disruption in the organization of the actin cytoskeleton.* J Cell Physiol, 2005. **205**(2): p. 286-94.

46. Cohet, N., Stewart, K.M., Mudhasani, R., Asirvatham, A., Mallappa, C., Imbalzano, K., Weaver, V.M., Imbalzano, A.N., Nickerson, J.A., *SWI/SNF chromatin remodeling enzyme ATPases promote cell proliferation in normal mammary epithelial cells.* accepted, 2010.

47. van de Vijver, M.J., et al., *A gene-expression signature as a predictor of survival in breast cancer.* N Engl J Med, 2002. **347**(25): p. 1999-2009.

48. Kaplan, E.L., Meier, P., *Nonparametric estimation from incomplete observations.* J Amer Statist Assn, 1958. **53**: p. 457-481.

49. Mantel, N., *Evaluation of survival data and two new rank order statisticcs arising in its consideration.* Cancer Chemother Rep, 1966. **50**(3): p. 163-170.

50. Chou, Q., *Minimizing deletion mutagenesis artifact during Taq DNA polymerase PCR by E. coli SSB.* Nucleic Acids Res, 1992. **20**(16): p. 4371.

51. Kellogg, D.E., et al., *TaqStart Antibody: "hot start" PCR facilitated by a neutralizing monoclonal antibody directed against Taq DNA polymerase.* Biotechniques, 1994. **16**(6): p. 1134-7.

52. Bustin, S.A., *Absolute quantification of mRNA using real-time reverse transcription polymerase chain reaction assays.* J Mol Endocrinol, 2000. **25**(2): p. 169-93.

53. Zahir, N., et al., *Autocrine laminin-5 ligates alpha6beta4 integrin and activates RAC and NFkappaB to mediate anchorage-independent survival of mammary tumors.* J Cell Biol, 2003. **163**(6): p. 1397-407.

54. Soule, H.D., et al., *Isolation and characterization of a spontaneously immortalized human breast epithelial cell line, MCF-10.* Cancer Res, 1990. **50**(18): p. 6075-86.

55. Lippman, M., G. Bolan, and K. Huff, *The effects of androgens and antiandrogens on hormone-responsive human breast cancer in long-term tissue culture.* Cancer Res, 1976. **36**(12): p. 4610-8.

56. Cailleau, R., M. Olive, and Q.V. Cruciger, *Long-term human breast carcinoma cell lines of metastatic origin: preliminary characterization.* In Vitro, 1978. **14**(11): p. 911-5.

57. Gazdar, A.F., et al., *Characterization of paired tumor and non-tumor cell lines established from patients with breast cancer.* Int J Cancer, 1998. **78**(6): p. 766-74.

58. Heppner, G.H., F.R. Miller, and P.M. Shekhar, *Nontransgenic models of breast cancer.* Breast Cancer Res, 2000. **2**(5): p. 331-4.

59. Miller, F.R., et al., *MCF10DCIS.com xenograft model of human comedo ductal carcinoma in situ.* J Natl Cancer Inst, 2000. **92**(14): p. 1185-6.

60. Guarneri, V. and P. Conte, *Metastatic breast cancer: therapeutic options according to molecular subtypes and prior adjuvant therapy.* Oncologist, 2009. **14**(7): p. 645-56.

61. Dietrich, C. and B. Kaina, *The aryl hydrocarbon receptor (AhR) in the regulation of cell-cell contact and tumor growth.* Carcinogenesis.

62. Jezierska, A. and T. Motyl, *Matrix metalloproteinase-2 involvement in breast cancer progression: a mini-review.* Med Sci Monit, 2009. **15**(2): p. RA32-40.

63. Duffy, M.J., et al., *CA 15-3: a prognostic marker in breast cancer.* Int J Biol Markers, 2000. **15**(4): p. 330-3.

64. Hollosi, P., et al., *Lysyl oxidase-like 2 promotes migration in noninvasive breast cancer cells but not in normal breast epithelial cells.* Int J Cancer, 2009. **125**(2): p. 318-27.

65. Akiri, G., et al., *Lysyl oxidase-related protein-1 promotes tumor fibrosis and tumor progression in vivo.* Cancer Res, 2003. **63**(7): p. 1657-66.

66. Mendez, M.G., S.I. Kojima, and R.D. Goldman, *Vimentin induces changes in cell shape, motility, and adhesion during the epithelial to mesenchymal transition.* FASEB J.

67. Chen, W.J., et al., *Propylthiouracil, independent of its antithyroid effect, promotes vascular smooth muscle cells differentiation via PTEN induction.* Basic Res Cardiol. **105**(1): p. 19-28.

68. Olmeda, D., et al., *Snail silencing effectively suppresses tumour growth and invasiveness.* Oncogene, 2007. **26**(13): p. 1862-74.

69. Guy, C.T., R.D. Cardiff, and W.J. Muller, *Induction of mammary tumors by expression of polyomavirus middle T oncogene: a transgenic mouse model for metastatic disease.* Mol Cell Biol, 1992. **12**(3): p. 954-61.

70. Decristofaro, M.F., et al., *Characterization of SWI/SNF protein expression in human breast cancer cell lines and other malignancies.* J Cell Physiol, 2001. **186**(1): p. 136-45.

71. Reisman, D.N., et al., *Concomitant down-regulation of BRM and BRG1 in human tumor cell lines: differential effects on RB-mediated growth arrest vs CD44 expression.* Oncogene, 2002. **21**(8): p. 1196-207.

72. Weaver, V.M., et al., *Degradation of nuclear matrix and DNA cleavage in apoptotic thymocytes.* J Cell Sci, 1996. **109 (Pt 1)**: p. 45-56.

73. Chen, W.T. and J.Y. Wang, *Specialized surface protrusions of invasive cells, invadopodia and lamellipodia, have differential MT1-MMP, MMP-2, and TIMP-2 localization.* Ann N Y Acad Sci, 1999. **878**: p. 361-71.

74. Bowden, E.T., P.J. Coopman, and S.C. Mueller, *Invadopodia: unique methods for measurement of extracellular matrix degradation in vitro.* Methods Cell Biol, 2001. **63**: p. 613-27.

75. Clark, G.J., et al., *Overexpression of the Ras-related TC21/R-Ras2 protein may contribute to the development of human breast cancers.* Oncogene, 1996. **12**(1): p. 169-76.

76. Miyakis, S., G. Sourvinos, and D.A. Spandidos, *Differential expression and mutation of the ras family genes in human breast cancer.* Biochem Biophys Res Commun, 1998. **251**(2): p. 609-12.

77. Muchardt, C., et al., *ras transformation is associated with decreased expression of the brm/SNF2alpha ATPase from the mammalian SWI-SNF complex.* EMBO J, 1998. **17**(1): p. 223-31.

78. Ouhara, K., et al., *Actinobacillus actinomycetemcomitans outer membrane protein 100 triggers innate immunity and production of beta-defensin and the 18-kilodalton cationic antimicrobial protein through the fibronectin-integrin pathway in human gingival epithelial cells.* Infect Immun, 2006. **74**(9): p. 5211-20.

79. Johnson, K.R., J.L. Leight, and V.M. Weaver, *Demystifying the effects of a three-dimensional microenvironment in tissue morphogenesis.* Methods Cell Biol, 2007. **83**: p. 547-83.

80. Fernandez, M., et al., *Small-angle x-ray scattering studies of human breast tissue samples.* Phys Med Biol, 2002. **47**(4): p. 577-92.

81. Chen, W.J., et al., *Multidrug resistance in breast cancer cells during epithelial-mesenchymal transition is modulated by breast cancer resistant protein.* Chin J Cancer. **29**(2): p. 151-7.

82. Martin, M., P. Pujuguet, and F. Martin, *Role of stromal myofibroblasts infiltrating colon cancer in tumor invasion.* Pathol Res Pract, 1996. **192**(7): p. 712-7.

83. Bian, J., et al., *Suppression of in vivo tumor growth and induction of suspension cell death by tissue inhibitor of metalloproteinases (TIMP)-3.* Carcinogenesis, 1996. **17**(9): p. 1805-11.

84. Weissman, B. and K.E. Knudsen, *Hijacking the chromatin remodeling machinery: impact of SWI/SNF perturbations in cancer.* Cancer Res, 2009. **69**(21): p. 8223-30.

85. van 't Veer, L.J., et al., *Gene expression profiling predicts clinical outcome of breast cancer.* Nature, 2002. **415**(6871): p. 530-6.

Figure Legends

Figure 3.1 Reduced BRM levels correlated with malignant behavior in human breast cancer cell lines

(A) Left Panel: Representative immunoblot of total cellular BRM in mammary epithelial cell lines and total Lamin B1 (loading control). Right Panel:Relative BRM levels were calculated by densitometric analysis of immunoblots as compared to non-malignant MCF10A cells and each sample was normalized to its internal loading control (Lamin B1). Results are the mean ± S.E.M. of 3 separate experiments. ***, $p<0.001$. (B) Left Panel: Representative immunoblot of total cellular BRM in MCF10A breast cancer progression series and total Lamin B1 (loading control). Right Panel: Relative BRM levels were calculated by densitometric analysis of immunoblots as compared to Parental MCF10A cells and each sample was normalized to its internal loading control (Lamin B1). Results are the mean ± S.E.M. of 3 separate experiments. ***, $p<0.001$.

Figure 3.2 Absence of BRM and/or its remodeling activity promoted anchorage independent growth and survival

(A) Histogram of quantification of colonies present after 14 days of Control (Ctrl) and K749R MCF10A cells and Scrambled (Scrm) and shRNA BRM (BRMi) MCF10A cells being embedded in agar. Anchorage independent MDA-MB 231 cells were used a positive control for colony formation. Results are the mean ± S.E.M. of 3 separate experiments. ***, $p<0.001$. (B) Representative micrographs

of colony sizes in control and BRM depleted plates. Size bars represent 25μm. (C) Histogram of colony diameter size quantification of cell lines embedded in soft agar. Results are the mean ± S.E.M. of 3 separate experiments, n>30 images were taken per sample. ***, p<0.001.

Figure 3.3 Reduced BRM chromatin remodeling activity increased cell motility

(A) Representative micrographs of Control MCF10A (Ctrl) and K749R ATPase-deficient BRM-expressing MCF10A cells (K749R) at times 0, 6, 9 and 12 hours after artificial wound was made. Time 0h is low magnification, scale bar represents 100μm. Times 6, 9, and 12 hours represent high magnification, scale bar represents 25μm. (B) Histogram of percent wound closure between Ctrl and K749R cells over 12 hours of observation. Results are the mean ± S.E.M. of 6 separate experiments, n>30 scratch images per sample. ***, p<0.001.

Figure 3.4 Loss of BRM associated with upregulation of tumor promoting genes

RNA from MCF10A cells expressing BRM-specific hairpins were analyzed, normalized to Scramble shRNA controls and thresholded to 1.5 fold change as previously described [46]. A total of 186 genes were altered with BRM knockdown in MCF10A cells (see Table 3.2 Supplemental Table). Specific genes of interest were highlighted: Hormone dependent genes, reactive stromal genes, and ECM remodeling genes.

Figure 3.5 BRM was reduced and associated with poor clinical prognosis in human breast cancers

Kaplan-Meier analysis of the probability that patient would remain relapse-free (upper panels) or survive (lower panels) after therapy in the 295 breast cancer patients in the NKI data set [85]. The patients were stratified according to their lymph node (LN) status, estrogen receptor (ER) status or the histological grades of breast cancer. In each group, the patients were grouped into quartiles according to the expression levels of BRM. The log-rank test is used to calculate the *P* values.

Figure 3.6 Preliminary findings on BRM levels in the Murine Breast Cancer model MMTV-Neu

Top panel: Low magnification micrographs of Wild type (WT) and MMTV-Neu mouse mammary tissues stained for BRM expression. Scale bar represents 100μm. Bottom panel: High magnification micrographs of normal and tumor mouse mammary tissues stained for BRM expression. Scale bar represents 25 μm.

Figure 3.7 Preliminary Findings on BRM levels in human breast cancer samples

Top panel: Low magnification micrographs of normal human breast tissue (reductive mammoplasty); ductal carcinoma *in situ* (DCIS) breast tissue and

invasive ductal carcinomas (IDC) breast tissue stained for BRM expression. Scale bar represents 100μm. Bottom panel: High magnification micrographs of human normal, DCIS and IDC mammary tissues stained for BRM expression. Scale bar represents 25 μm.

Table 3.1 Microarray Analysis of Genes Altered in BRM-Deficient non-malignant MECs

RNA from MCF10A cells expressing BRM-specific hairpins were analyzed, normalized to Scramble shRNA control cells and thresholded to 1.5 fold change as previously described . A total of 186 genes were altered with BRM knockdown in MCF10A cells (see Appendix V for complete list of genes). Specific genes of interest were highlighted: Hormone-dependent genes, Reactive stromal genes and ECM remodeling genes.

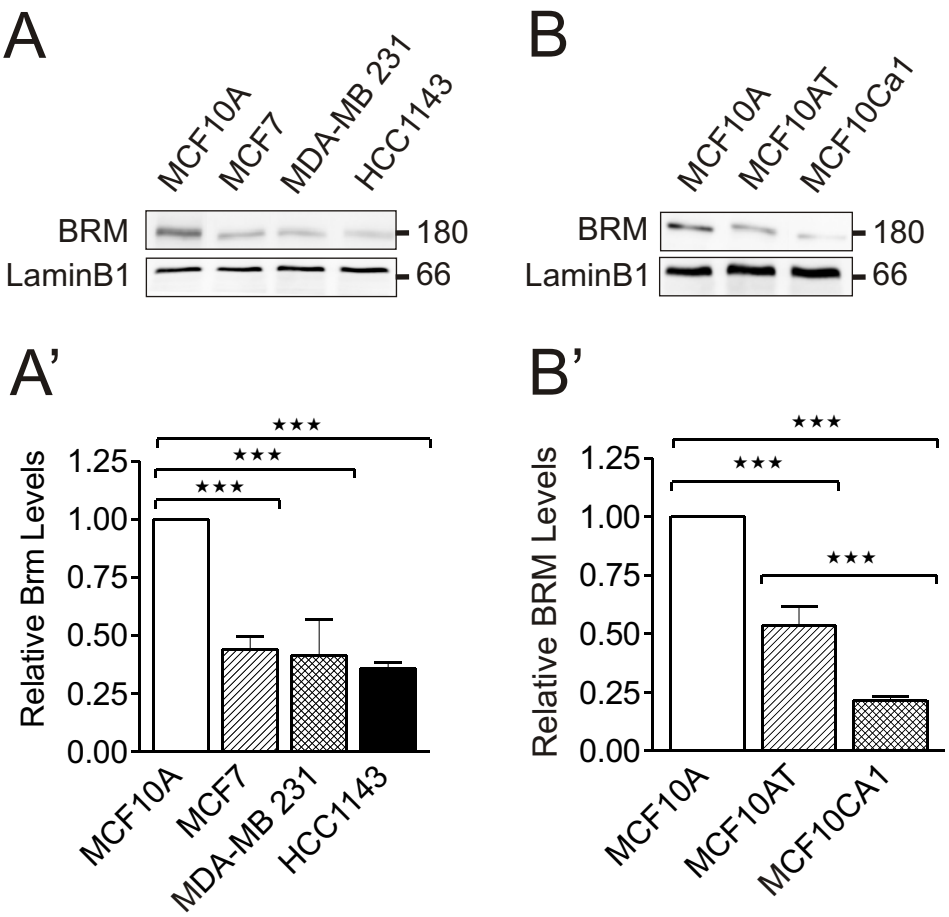

Figure 3.1 Reduced BRM levels correlated with malignant behavior in human breast cancer cell lines

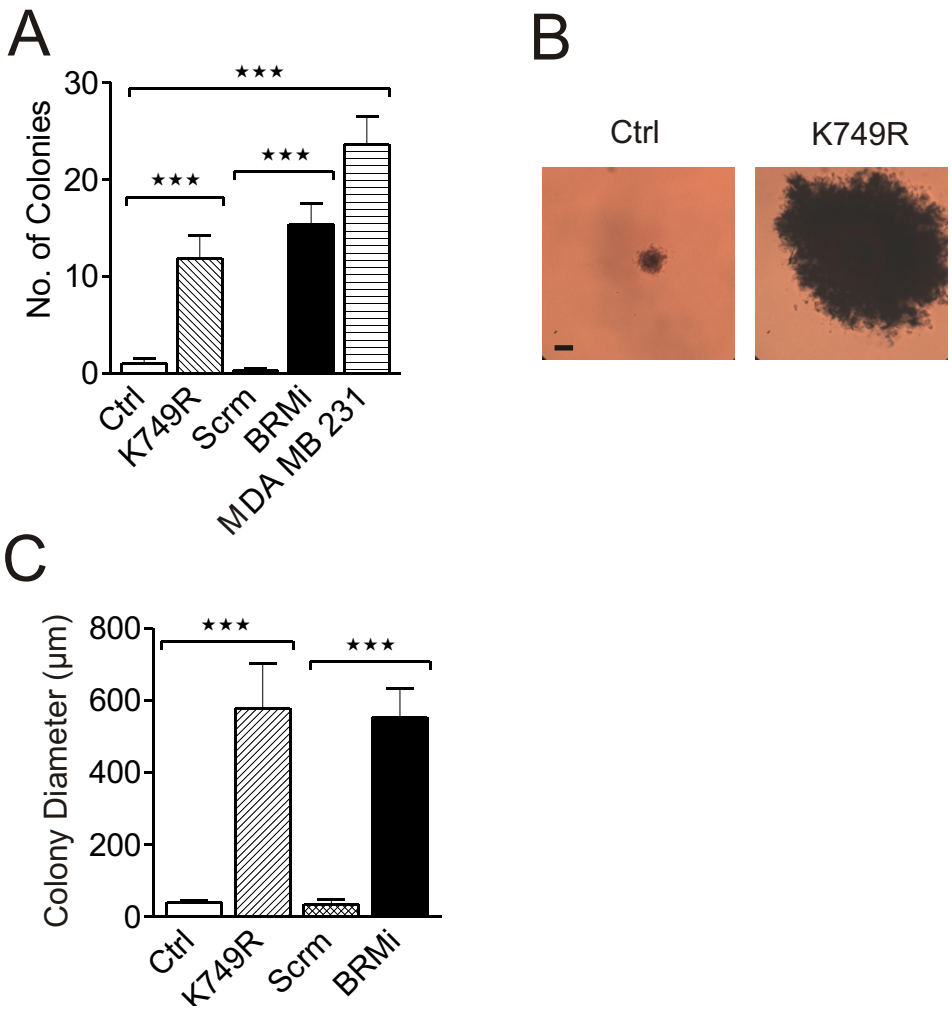

Figure 3.2 Absence of BRM and/or its remodeling activity promoted anchorage independent growth and survival

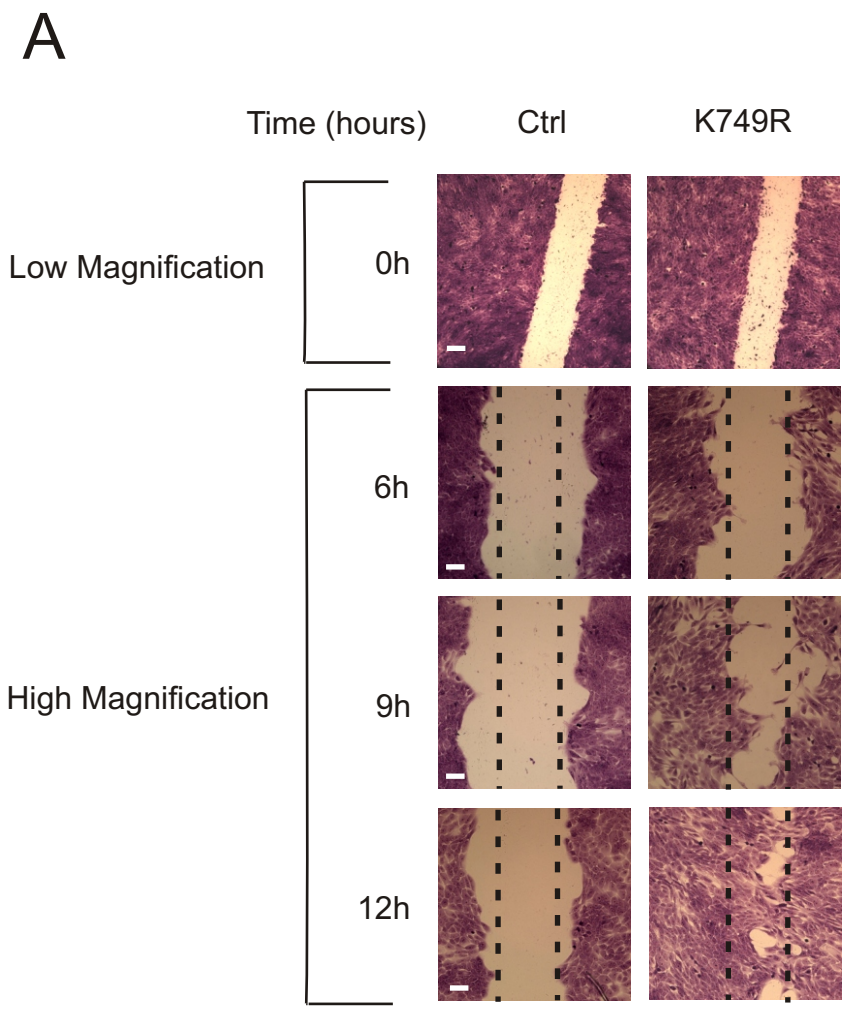

Figure 3.3 Reduced BRM chromatin remodeling activity increased cell motility

B

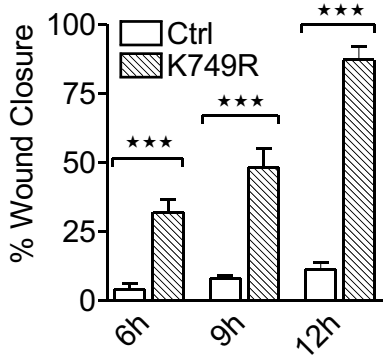

Figure 3.3 Reduced BRM chromatin remodeling activity increased cell motility

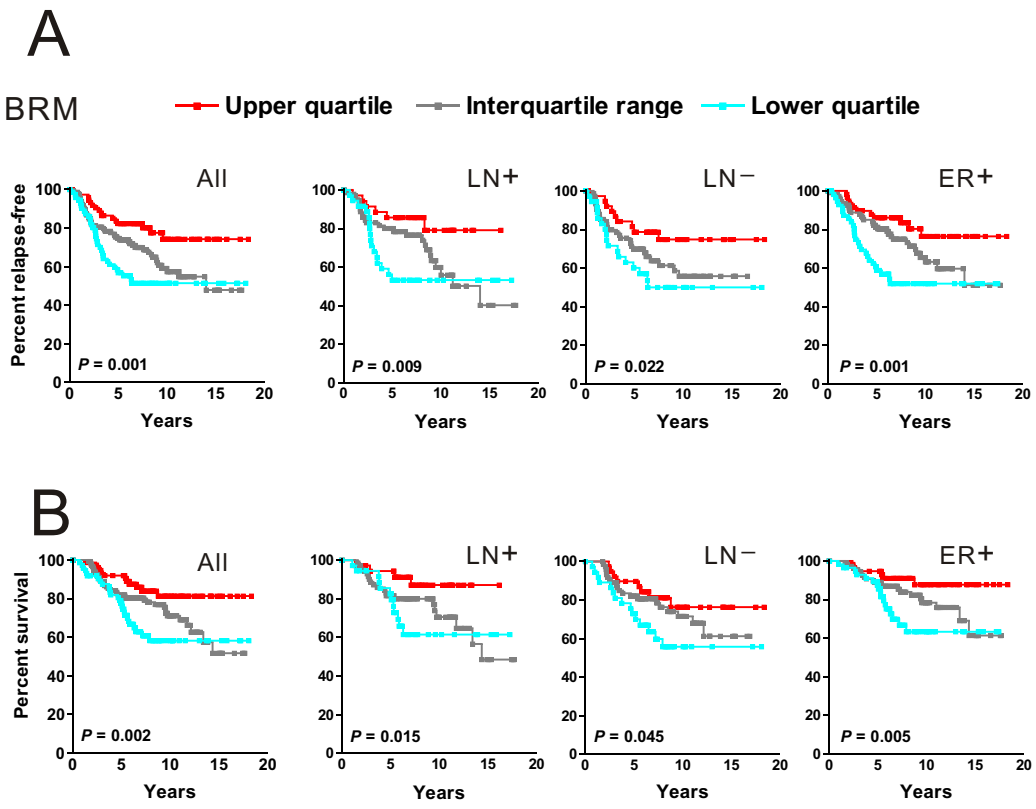

Figure 3.4 BRM was reduced and associated with poor clinical prognosis in human breast cancers

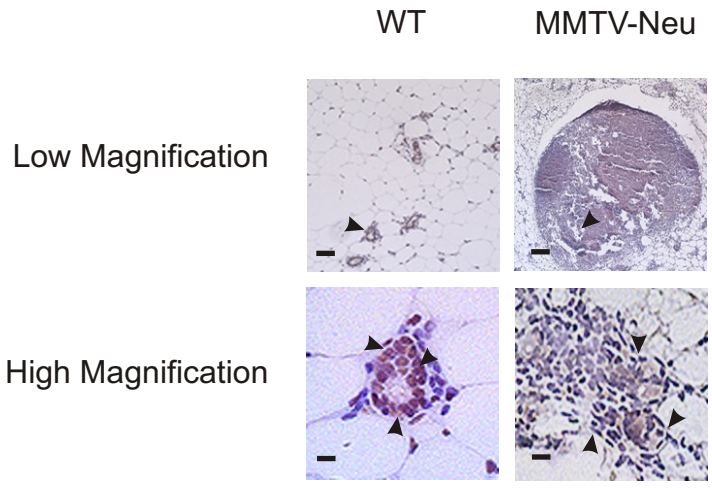

Figure 3.5 Preliminary findings on BRM levels in the Murine Breast Cancer model MMTV-Neu

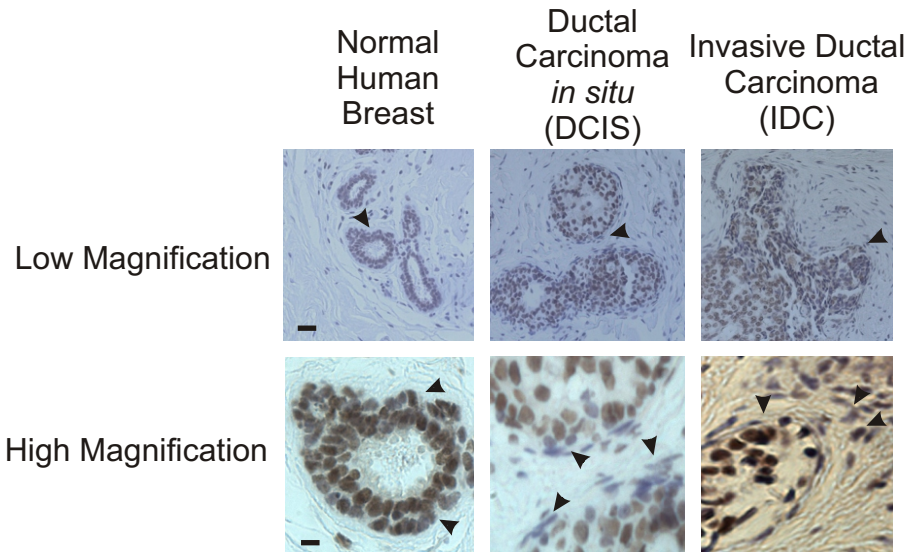

Figure 3.6 Preliminary findings on BRM levels in human breast cancer samples

Gene Symbol	Gene Description	Fold Change (BRMi)
Hormone Dependent Genes		
AHR	Aryl Hydrocarbon Receptor	-1.77
KLK5	Kallikrein-related peptidase 5	-1.91
HIPK3	Androgen receptor-interacting nuclear protein kinase	-1.82
Reactive Stromal Genes		
FN1	Fibronectin 1	2.13
VIM	Vimentin	1.97
SNA12	Snail homolog 2 (Drosophila)	2.03
ITGA5	Integrin alpha 5	1.71
TGFβ1	Transforming growth factor beta induced 1	1.64
ECM Remodeling Genes		
MMP2	Gelatinase A, 72kDa gelatinase, 72kDa type IV Collagenase	1.62
NID2	Nidogen 2 (Osteonidogen)	1.72
CLDN8	Claudin 8	-2.34
LOXL2	Lysyl-oxidase like protein 2	1.84
Chromatin Remodeling Genes		
SMARCA2	SWI/SNF Brahma (BRM)	-1.94

Table 3.1 Microarray Analysis of Genes Altered in BRM-Deficient Non-malignant MECs

Chapter Four
Conclusions and Future Directions

Chapter 4:

Conclusions and Future Directions

Summary

Mammary epithelial cell (MEC)-extracellular matrix (ECM) interactions are critical for normal breast tissue development, differentiation and homeostasis by engaging a repertoire of ECM adhesion receptors including integrins to activate signaling processes that control MEC differentiation, proliferation and survival [1-4]. Malignant progression alters MEC responsiveness to ECM cues and is highlighted by the observation that the expression of integrins is altered during breast tumor progression [5-11]. The molecular basis for altered integrins in breast tumors and the regulation of integrin changes during malignant transformation are less understood.

The goal of my thesis is to test the hypothesis that oncogene-dependent transformation promotes breast tumor progression through regulating changes in ECM responsiveness via α5 integrin through targeting of the SWI/SNF chromatin remodeling protein BRM.

Oncogenic targeting of SWI/SNF BRM regulates α5 integrin to promote a tumor phenotype

The central finding of this study is that oncogenic signaling depended upon increased α5β1 integrin-fibronectin (FN) interactions to drive mammary epithelial cell (MEC) growth and survival and promoted a premalignant phenotype (Figure 2.1). Consistently, overexpression of α5 integrin in non-malignant MECs in the context of its ligand, fibronectin, was sufficient to disrupt acinar morphogenesis and promoted MEC growth and survival to form filled lumen structures in 3D cultures (Figure 2.1). I implicated the SWI/SNF chromatin remodeling protein BRM in the transcriptional regulation of α5 integrin-driven MEC growth and survival in 3D assays (Figure 2.2, Figure 2.3, and Figure 2.5). I observed that BRM protein levels were decreased in oncogenically transformed MECs and that re-expression of wild type BRM in these cells promoted the formation of growth arrested, hollow acinar structures phenotypically similar to those formed by non-malignant MECs (Figure 2.2, Figure 2.6). Overall these studies underscore the reciprocal relationship between oncogenic transformation and altered ECM responsiveness via α5 integrin and implicate oncogene-driven downregulation of the SWI/SNF chromatin modeling protein BRM as a mediator of these interactions.

Role of ECM Responsiveness in breast tumors

In Chapter 2, I identified α5 integrin as a key regulator of ECM responsiveness in transformed MECs. Notably, expression of α5 integrin and fibronectin are largely absent in normal adult mammary tissue and their aberrant expression is associated with breast tumor progression and metastasis and also correlates with decreased survival of breast cancer patients [25, 26]. The findings in my thesis bolster support and add to the growing body of literature that implicates α5β1 integrin in the pathogenesis of cancers [12-17].

Importantly, the molecular basis for α5 integrin upregulation in breast tumors is less than understood. In Chapter 2, I demonstrated that oncogene-dependent transformation depends on α5β1 integrin-FN interactions to support MEC survival in the absence of basement membrane ligation (I.e., luminal filling) thereby promoting a pre-malignant phenotype (Figure 2.1). Similarly, human breast cancer cells upregulate α6β4 integrin-laminin 5 interactions to enhance MEC survival [18]. Do tumors enhance MEC-ECM interactions to support their own survival in adverse conditions, such as detachment from the basement membrane? My results suggest that oncogene-dependent effects are potentially linked to releasing tumor cells from ECM restriction of the malignant phenotype by increasing α5 integrin levels (Figure 2.1).

The limitations of these results are first, I only examined the role of α5 integrin in two transformed breast cancer cell lines. To more broadly examine the dependence of MECs on elevated α5 integrin signaling to promote a malignant phenotype, one could also perform similar studies from Figure 2.1 on breast cancer cell lines that form phenotypically diverse structures in 3D as defined by Kenny *et al*., “Mass:” MCF-7, T47-D; “Grape-like:” SK-BR-3 and MDA-MB-468, and “Stellate:” BT-549, MDA-MB-231[19]. Furthermore, since α5 integrin is upregulated in pancreatic, lung, skin and other cancers, one could also examine the importance of this signaling in the development of these cancer types to determine if this is a conserved mechanism for tumor promotion.

Second, I cannot rule out the possibility that overexpression of other FN binding integrins such as αvβ6 or αvβ3 can elicit that same response in MECs [20]. In α5 integrin null mouse embryos and in culture studies, fibronectin matrix assembly still occurs in the absence of this subunit suggesting that other α subunits are able to partially compensate α5 integrin loss[21]. To address this deficiency, experiments similar to those performed in figure 2.1 could be done, along with an experiment examining shRNA-mediated knockdown of αv integrin in transformed MECs in 3D cultures. Furthermore, in addition to ruling out αv integrin involvement, I also need to address the specific activity of α5 integrin in promoting MEC growth and survival.

To specifically test the relationship between MEC growth and survival and α5 integrin expression, one could knockdown α5 integrin levels in transformed MECs and observe the phenotypic behavior of these cells in 3D culture assays. If α5 integrin knockdown is not able to suppress the 3D transformed phenotype, these results suggest that FN-driven signaling itself may be more important to promoting MEC growth and survival in transformed cells and that other α subunits can compensate for the loss of α5 integrin in this model.

How could α5 integrin be mediating cell survival in transformed MECs?
I believe activated extracellular signal–related kinase (ERK) signaling is a tractable target of α5β1 integrin-FN induced MEC survival since elevated ERK signaling is associated with oncogenic transformation and inhibition of the pro-apoptotic protein Bim in MECs [22-25]. Furthermore, Bim expression is reduced in breast cancer cell lines and tissues however the mechanism behind its regulation remains unclear [23-25]. I propose that increasing α5β1 integrin-FN interactions promotes MEC survival and luminal filling in 3D cultures through elevated ERK signaling and suppression of Bim. To address this question, ERK signaling and Bim expression in MECs with increased α5β1 integrin-FN interactions would first be examined. Inhibition of ERK signaling through pharmacological inhibitors (PD98059) would correlate with luminal clearance in 3D cultures and re-expression of pro-apoptotic Bim in oncogenically transformed MECs.

Multiple signaling proteins in addition to ERK are activated downstream of Ras/RTK signaling such as p38 Mitogen-Activated Protein Kinase (MAPK) and JNK (c-Jun N-terminal Kinase) [26, 27]. If ERK signaling is not responsible for α5β1 integrin-FN induced MEC survival in 3D cultures, I propose that the α5 integrin transcript levels of BRM-knockdown and transformed MECs treated with pharmacological inhibitors targeting these alternative signaling cascades (PD169316, and SP600125 respectively) be examined.

These findings would be important to the breast cancer field, as current strategies for treating breast cancer rely heavily upon inducing apoptosis to eradicate tumor cells thus furthering our understanding of these cell survival/cell death decisions could assist in the development of novel anti-cancer treatments strategies [28, 29]

BRM as a regulator of α5 integrin

In Chapter 2, I found that reduced expression and/or activity of a chromatin remodeling protein, BRM, increased α5 integrin mRNA, protein and cell surface levels (Figure 2.2). The regulation of α5 integrin gene transcription however, appears to be a key mechanism for the control of α5β1 surface expression [30, 31]. The correlative relationship I discovered between chromatin remodeling and regulation of α5 integrin expression, suggests a higher level of complexity exists in integrin subunit regulation. This is consistent with a previous study that found that loss of SWI/SNF BRG-1 activity increases bulk protein levels of α5 integrin and αv integrin in human fibroblasts [32].

The limitations of my experimental findings are that I never examined direct transcriptional regulation of α5 integrin by BRM. To address this question, I would first examine the binding of BRM to the α5 integrin proximal promoter regions through use of a serial deletion truncation series, each region to query would contain a CpG island, lack a TATA and CCAAT box and contain consensus binding sites for ETS, SP1, AP-2 or AP-1 transcription factors [33, 34].

Based on my findings that BRM played a repressive role in α5 integrin transcriptional activity (Chapter 2), one might predict BRM to be present at this promoter site in control cells and absent upon induction of BRM shRNA. If this is true, re-expression of BRM in BRM-deficient oncogenically transformed MECs would show binding of BRM to the relevant α5 integrin promoter site and lack of this binding in empty vector transfected BRM-deficient oncogenically transformed MECs.

Two alternative hypotheses could explain results contrary to my expected results above. First, BRM is required to repress α5 integrin expression but is no longer required once repression has been achieved. This might explain an absence of BRM association with the promoter in both control and induced BRM shRNA cells. In this case, a time course examining BRM re-expression in transformed MECs (i.e. repression of α5 integrin) may demonstrate a temporary binding of BRM on the α5 integrin promoter.

Second, the molecular mechanisms governing α5 integrin expression have not been fully elucidated and may require further exploration and the relationship between BRM chromatin remodeling and α5 integrin transcriptional activation may be indirect. For example, BRM could normally function to transcriptionally activate α5 integrin transcriptional repressors, therefore the downregulation of BRM would release α5 integrin from a state of transcriptional repression. Forkhead transcription factors, Cox-2 inhibitors, and activated peroxisome

proliferator-activated receptor-γ (PPARγ) pathways are known to suppress α5 integrin transcripts and would serve as the starting point to explore these questions [35-38]. Alternatively, one could perform ChIP-chip [39] and ChIP-Seq [40-42] assays. These are two established tools to examine genome-wide protein–DNA interactions and histone modifications, thereby building a comprehensive and high-resolution map for DNA-binding proteins of interest.

Exploring the role of BRM in breast tumor progression

Chapter 3 studies showed that BRM knockdown enhanced MEC motility and anchorage independent growth and microarray analysis of these knockdown cells confirmed an upregulation of genes known to promote breast tumor motility and invasion, such as snail-1 and vimentin (Figure 3.2, Table 3.1; [43, 44]). Furthermore, analysis of published microarrays from breast cancer patients supported my hypothesis that BRM expression is relevant to breast tumor progression since patients with the lowest BRM expression had the highest incidence of tumor recurrence and morbidity (Figure 3.4). To explore the possibility that BRM could promote tumor progression and enhance tumor progression I began examination of BRM levels in murine and human mammary glands at different disease states.

My preliminary results suggested that BRM expression may be reduced *in vivo* (Figure 3.5, Figure 3.6). However, I fully appreciate that these studies are quite preliminary since my studies examined an extremely limited sample size and so caution must be taken in interpreting these results. Nevertheless, these data collectively suggests that perhaps decreased BRM levels may contribute to breast tumor progression.

Role of BRM in breast tumor invasion

My preliminary work suggested that decreased BRM levels in non-malignant MECs enhanced motility and increase anchorage independent growth, common behavioral traits of breast tumor cells (Chapter 3; [45]). While acquiring anchorage independent growth is not necessarily indicative of MEC invasion or tumorigenic behaviors, previous reports suggest it may represent promotion of a pre-malignant phenotype [46].

To address these questions, one could determine if BRM knockdown promotes MEC invasion behavior through ECM-coated Boyden Chamber invasion assays and further in *in vivo* xenotransplant studies. If reduced BRM expression enhances MEC invasive behavior, one could next examine the possible relationship between ECM degrading enzymes, matrix metalloproteinases (MMPs) and BRM expression through gel zymograms, the degradation and release of fluorescein or radio-labeled ECM substrates and the detection of MMP activity through enzyme immunoassays [47-49]. One would also need to analyze

MMP transcript levels in these MECs as well. MMP inhibitors, such as SB-3CT or 5a could be used to study this functional link, however, due to their lack of specificity for MMP-9, shRNA-mediated knockdown of MMP-9 would be most appropriate for these experiments [50, 51]. Furthermore, MMP-9 could be a potential transcriptional target of BRM chromatin remodeling activity; this relationship could be initially examined via chromatin Immunoprecipitation studies of the MMP promoter site [52].

Interestingly, enhancing α5β1 integrin-FN interactions increases the expression of MMP-9, in human lung cancer cells [53]. Consistent with this finding, inhibition of α5 integrin blocks MMP-9 activity in ovarian cancer cells and overexpression of ErbB2 increases the expression of α5 integrin and MMP-9 in human breast cancer cells [13, 54]. MMP-9 expression levels, along with other MMP family members, correlate with breast tumor progression and current clinical trials are underway to target their activity [55-65]. However, the lack of specificity of these inhibitors and the exact mechanisms of MMP transcriptional regulation and localized activity is hampering these efforts. Therefore, studying the transcriptional regulation of matrix-degrading enzymes via interactions between cancer cells and the ECM is important to the study of breast tumor invasion, metastasis and angiogenesis and warrants further investigation [60, 66].

Role of BRM in ECM Responsiveness in vivo

In Chapter 3, I found that BRM expression may be decreased in murine and human breast cancer samples. To strengthen these preliminary findings, one would need to examine a much larger sample size of mouse and human mammary glands for each condition in order to reach statistical significance and draw any further conclusions [67].

In addition to furthering my preliminary examination of BRM in mouse and human breast tissues, I also have yet to explore the relevance of BRM in the developing mammary gland *in vivo*. In addition to receiving cues from the microenvironment, the behavior of normal and malignant MECs is regulated by neighboring cells, stromal cells, soluble factors and physical forces which are variables not included in the parameters of my 3D rBM morphogenesis assays[11]. Therefore, in order to more faithfully recapitulate the histological complexity of the normal breast and breast cancers, one would need to examine whole animal systems of breast gland development and tumorigenesis.

In parallel to previous reports on $BRM^{-/-}$ mice in lung cancer and prostate cancer models, one could first explore the phenotypic characteristics of the developing mammary gland in $BRM^{-/-}$ mice [68, 69]. Specifically, one could examine the expression of α5 integrin, FN and branching morphogenesis at the various stages of mammary gland development: 3 weeks of age (pre-puberty), 5 weeks of age (puberty), 10 weeks of age (sexual maturity), early (9–12 days) and late

(18–21 days) pregnancy, and lactation (7–10 days) [70-72]. α5β51 integrin and FN levels are unique in mouse mammary gland development, as their expression during peri-puberty- and pregnancy-induced proliferation stages is significantly increased [73-76]. Therefore, I hypothesize that examination of mammary glands from $BRM^{-/-}$ mice would reveal early onset and sustained expression of α5β51 integrin and FN during mammary gland development, disrupted branching morphogenesis and the presence of uncontrolled proliferation, or hyperplastic lesions, similar to those found in the lung and prostate of these $BRM^{-/-}$ transgenic mice [69, 77]. Based upon my data on BRM activity in the regulation of ECM responsiveness and the fact that $BRM^{-/-}$ null mice do not form tumors, I hypothesize that the loss of BRM primes or sensitizes the developing mammary gland microenvironment to enhance tumor formation in the presence of carcinogenic agents or activating oncogenic mutations[78].

Last, one could probe for specific splice variants of FN produced in the mammary glands of $BRM^{-/-}$ mice. There is precedent for BRM-directed splicing activity as shown for the CD44 and E-Cadherin adhesion receptor transcripts in cervical cancer cells[79]. Fibronectin (FN) has three segments, which can be alternatively spliced at the mRNA level: EDA (extra domain A), EDB (extra domain B) and IIICS (type III homology connecting segment) regions.

The splicing patterns of these segments are developmentally regulated and are tissue- and cell-type specific, and their expression is very limited in normal adult tissues and is implicated in tumor progression [80]. These studies are important to determining the mechanism by which BRM chromatin remodeling activity could regulate or contribute to changes in ECM responsiveness during breast cancer progression.

Remaining Questions

Mechanism of BRM Repression in Breast Tumors

My studies showed that MECs with enhanced RTK or Ras signaling displayed reduced levels of BRM expression chromatin remodeling activity (Chapter 2 and Chapter 3). With further investigations on BRM and other SWI/SNF subunit involvement in cancers underway, an underlying question is how is BRM lost during tumor progression? Sequence analysis of BRM in 10 BRM-deficient cell lines did not reveal any mutations or other alterations to explain its silencing [68, 81, 82]. However, the BRM locus region is a common site for loss of heterozygosity in many human cancers [83-86]). As treatment of cancer cell lines deficient in BRM with broad class HDAC inhibitors revealed re-expression of BRM, this suggests that epigenetic silencing may regulate BRM expression [68, 87].

To begin to address whether methylation of BRM occurs during tumorigenesis, I identified two putative sites in the BRM locus for methylation analysis (i.e., methylation-specific PCR, bisulfite sequencing) (Figure 4.1 [88-90]). Complete sequence analysis of the BRM gene and validation of all putative sites for methylation will present a formidable task due to its large number of exons (>34) and the resulting size of its mRNA (~5.5 kb) (http://cpgislands.usc.edu/cpg.aspx).

Promoter methylation may not be the only mechanism underlying suppression of BRM. Alternatively, I speculate that regulation of BRM expression could occur directly through oncogene-dependent signaling during breast tumor progression. Interestingly, kinase phosphorylation events, by an unidentified kinase protein, abolish BRM protein levels during mitosis and treatment of cells with a broad spectrum phosphatase inhibitor reactivates SWI/SNF BRM expression and remodeling activity [91, 92]. Moreover, activated ERK signaling, through enhanced oncogenic signally, can dramatically alter gene transcription and promote cell growth and survival of MECs [25, 93, 94] . To test the hypothesis that enhanced kinase signaling in oncogenically transformed MECs via ERK downregulates BRM expression, one needs to first address whether Ras and ErbB2-transformed MECs modulate transcript levels of BRM (I only examined bulk protein levels).

Application of RTK-Integrin pathway inhibitors could be utilized to target specific kinases and determine which oncogenic signals are involved in driving down BRM levels in MECs. Furthermore, thirteen putative MAPK phosphorylation sites exist in the BRM locus and one could mutate and examine BRM transcript level changes in oncogenically transformed MECs [91, 92].

Role of SWI/SNF BRM Accessory Factors

Overall the relative abundance and combinatorial assembly of SWI/SNF accessory subunits are elegantly compared with a chromatin remodeling "language" wherein the subunit "letters" can be assembled into at least 288 distinct words, each with possible alternative cellular outcomes [95]. It is apparent in human cancer that disease-associated misspellings can contribute to disease initiation, progression and metastasis. Furthermore, the SWI/SNF accessory subunits are thought to dictate the specificity of SWI/SNF complex targeting and activity [96-98]. Scant evidence currently exists to determine whether these accessory SWI/SNF subunits contribute to tumor progression and the current work presented here cannot rule out SWI/SNF subunit cooperation.

To this end, I would begin to explore and identify key SWI/SNF accessory subunits in the regulation of MEC growth and survival in 3D morphogenesis assays through use of shRNA-mediated knockdown of SWI/SNF accessory units, of which BAF60a, BAF155, BAF170 and BAF57 have been generated and verified in lung cancer epithelial cells (see Appendix III).

α5 Integrin as a Clinical Therapeutic Target

My overall observations revealed that α5β1 integrin supported MEC tumor growth *in vitro* and offered α5β1 integrin as a potential target for the development of anti-breast cancer therapies. These findings add to the growing body of literature that implicates α5β1 integrin in the pathogenesis of many cancers, including breast cancer [12-17]. For example, in murine lung cancer cells, shRNA targeting of α5 integrin decreases tumor cell migration, proliferation and anchorage-independent growth [99]. Furthermore, knockdown of α5 integrin in these tumor cells decreases tumor burden and reduces the number of metastatic lesions in murine xenotransplant studies [99]. Unfortunately, α5 integrin- or FN-null mouse models do not allow for the examination of mammary gland or breast tumor development as they both result in embryonically lethal phenotypes [100, 101]. However, if one was to further explore the anti-tumor effects of α5 integrin in breast cancer models, orthotopic transplant studies using α5 integrin-shRNA transformed MECs or the generation of tissue specific transgenic mice would prove to be useful.

Recently, SJ479, a small molecule α5 integrin antagonist that affects angiogenesis through decreased adhesion and migration, also inhibits tumor cell proliferation and decreases anchorage independent growth of malignant glioma cells [102]. Other targeting strategies such as RGD peptides coupled with polyethylenimine (PEI) spacer molecules, phages displaying RGD-containing

peptides, and a polymeric form of fibronectin (sFN), among other agents, are currently an area of intense investigation [103-108]. Unfortunately, much of this work is being carried out in models that are unrelated to breast cancers. Importantly, one of the major challenges facing oncologists is the high degree of breast cancer recurrence, such as resistance to Trastuzumab, an ErbB2-targeted therapy [109, 110]. However, the mechanisms that control Trastuzumab resistance remain poorly understood. I demonstrate that ErbB2 signaling depends upon α5β1 integrin-FN interactions to support MEC growth and survival and therefore presents a potential novel therapeutic target in the treatment of ErbB2-positive breast tumors. Together, these observations emphasize the overall need to test anti-α5β1 integrin agents in breast cancer models as well.

Final Conclusions

In this study I provide evidence to support the hypothesis that oncogene-driven MECs rely on enhanced α5β1 integrin-FN interactions to support MEC growth and survival and promote a pre-malignant phenotype in 3D cultures and implicate BRM chromatin remodeling activity in the regulation of tumor-driven ECM responsiveness changes (Chapter 2). Furthermore, I have shown that abrogation of BRM in MECs enhanced cell motility and anchorage independent growth and upregulated a gene program associated with breast tumor progression (Chapter 3).

Whether BRM is a *bona fide* tumor suppressor in breast cancers and whether targeting the re-expression of BRM in breast tumors is a viable therapeutic target remains an area of active research. Nevertheless, regaining ECM responsiveness in breast tumor cells by manipulating chromatin is without precedent and forms the foundation for future investigations into the epigenetic mechanisms governing ECM responsiveness and may lead to the discovery of novel molecular targets in the treatment of breast cancer.

References

1. Lin, C.Q. and M.J. Bissell, *Multi-faceted regulation of cell differentiation by extracellular matrix.* FASEB J, 1993. **7**(9): p. 737-43.
2. Roskelley, C.D. and M.J. Bissell, *The dominance of the microenvironment in breast and ovarian cancer.* Semin Cancer Biol, 2002. **12**(2): p. 97-104.
3. Shapiro, T.J. and P.M. Clark, *Breast cancer: what the primary care provider needs to know.* Nurse Pract, 1995. **20**(3): p. 36, 39-40, 42 passim.
4. Gumbiner, B.M., *Cell adhesion: the molecular basis of tissue architecture and morphogenesis.* Cell, 1996. **84**(3): p. 345-57.
5. Jacks, T. and R.A. Weinberg, *Taking the study of cancer cell survival to a new dimension.* Cell, 2002. **111**(7): p. 923-5.
6. Huang, S. and S. Chakrabarty, *Regulation of fibronectin and laminin receptor expression, fibronectin and laminin secretion in human colon cancer cells by transforming growth factor-beta 1.* Int J Cancer, 1994. **57**(5): p. 742-6.
7. Chakrabarty, S., et al., *Elevated serum levels of transforming growth factor-alpha in breast cancer patients.* Cancer Lett, 1994. **79**(2): p. 157-60.
8. Desgrosellier, J.S. and D.A. Cheresh, *Integrins in cancer: biological implications and therapeutic opportunities.* Nat Rev Cancer. **10**(1): p. 9-22.
9. Petersen, O.W., et al., *Differentiation and cancer in the mammary gland: shedding light on an old dichotomy.* Adv Cancer Res, 1998. **75**: p. 135-61.

10. Streuli, C.H. and M.J. Bissell, *Expression of extracellular matrix components is regulated by substratum.* J Cell Biol, 1990. **110**(4): p. 1405-15.

11. Ronnov-Jessen, L., O.W. Petersen, and M.J. Bissell, *Cellular changes involved in conversion of normal to malignant breast: importance of the stromal reaction.* Physiol Rev, 1996. **76**(1): p. 69-125.

12. Murillo, C.A., P.G. Rychahou, and B.M. Evers, *Inhibition of alpha5 integrin decreases PI3K activation and cell adhesion of human colon cancers.* Surgery, 2004. **136**(2): p. 143-9.

13. Sawada, K., et al., *Loss of E-cadherin promotes ovarian cancer metastasis via alpha 5-integrin, which is a therapeutic target.* Cancer Res, 2008. **68**(7): p. 2329-39.

14. Hsu, S.L., et al., *Proteolysis of integrin alpha5 and beta1 subunits involved in retinoic acid-induced apoptosis in human hepatoma Hep3B cells.* Cancer Lett, 2001. **167**(2): p. 193-204.

15. Morozevich, G.E., et al., *Implication of alpha5beta1 integrin in invasion of drug-resistant MCF-7/ADR breast carcinoma cells: a role for MMP-2 collagenase.* Biochemistry (Mosc), 2008. **73**(7): p. 791-6.

16. Maschler, S., et al., *Tumor cell invasiveness correlates with changes in integrin expression and localization.* Oncogene, 2005. **24**(12): p. 2032-41.

17. Spangenberg, C., et al., *ERBB2-mediated transcriptional up-regulation of the alpha5beta1 integrin fibronectin receptor promotes tumor cell survival under adverse conditions.* Cancer Res, 2006. **66**(7): p. 3715-25.

18. Zahir, N., et al., *Autocrine laminin-5 ligates alpha6beta4 integrin and activates RAC and NFkappaB to mediate anchorage-independent survival of mammary tumors.* J Cell Biol, 2003. **163**(6): p. 1397-407.

19. **Kenny, P.A., Lee. G.Y., Myers, C.A., Neve, R.M., Semeiks, J.R., Spellman, P.T., Lorenz, K., Lee, E.H., Barcellos-Hoff, M., Peterson, O.W., Gray, J.W., and Bissell, M.J.**, *The morphologies of breast cancer cell lines in three-dimensional assays correlate with their profiles of gene expression.* Mol Oncol, 2007. **1**(1): p. 84-96.

20. Busk, M., R. Pytela, and D. Sheppard, *Characterization of the integrin alpha v beta 6 as a fibronectin-binding protein.* J Biol Chem, 1992. **267**(9): p. 5790-6.

21. Yang, J.T. and R.O. Hynes, *Fibronectin receptor functions in embryonic cells deficient in alpha 5 beta 1 integrin can be replaced by alpha V integrins.* Mol Biol Cell, 1996. **7**(11): p. 1737-48.

22. Muthuswamy, S.K., et al., *ErbB2, but not ErbB1, reinitiates proliferation and induces luminal repopulation in epithelial acini.* Nat Cell Biol, 2001. **3**(9): p. 785-92.

23. Wen, Y.Y., et al., *The expression of SIAH1 is downregulated and associated with Bim and apoptosis in human breast cancer tissues and cells.* Mol Carcinog.

24. Reginato, M.J., et al., *Bim regulation of lumen formation in cultured mammary epithelial acini is targeted by oncogenes.* Mol Cell Biol, 2005. **25**(11): p. 4591-601.

25. Reginato, M.J., et al., *Integrins and EGFR coordinately regulate the pro-apoptotic protein Bim to prevent anoikis.* Nat Cell Biol, 2003. **5**(8): p. 733-40.

26. Yarden, Y. and M.X. Sliwkowski, *Untangling the ErbB signalling network.* Nat Rev Mol Cell Biol, 2001. **2**(2): p. 127-37.

27. Marais, R. and C.J. Marshall, *Control of the ERK MAP kinase cascade by Ras and Raf.* Cancer Surv, 1996. **27**: p. 101-25.

28. Bihani, T., et al., *Dissecting the senescence-like program in tumor cells activated by Ras signaling.* J Biol Chem, 2007. **282**(4): p. 2666-75.

29. Dlamini, Z., Z. Mbita, and T. Ledwaba, *Can targeting apoptosis resolve the cancer saga?* Future Oncol, 2005. **1**(3): p. 339-49.

30. Larouche, K., et al., *Expression of the alpha 5 integrin subunit gene promoter is positively regulated by the extracellular matrix component fibronectin through the transcription factor Sp1 in corneal epithelial cells in vitro.* J Biol Chem, 2000. **275**(50): p. 39182-92.

31. Gingras, M.E., et al., *Regulation of the integrin subunit alpha5 gene promoter by the transcription factors Sp1/Sp3 is influenced by the cell density in rabbit corneal epithelial cells.* Invest Ophthalmol Vis Sci, 2003. **44**(9): p. 3742-55.

32. Hill, D.A., et al., *Inducible changes in cell size and attachment area due to expression of a mutant SWI/SNF chromatin remodeling enzyme.* J Cell Sci, 2004. **117**(Pt 24): p. 5847-54.

33. Gingras, M.E., et al., *Differential binding of the transcription factors Sp1, AP-1, and NFI to the promoter of the human alpha5 integrin gene dictates its transcriptional activity.* Invest Ophthalmol Vis Sci, 2009. **50**(1): p. 57-67.

34. Fu, J., et al., *Promoter regulation of the visinin-like subfamily of neuronal calcium sensor proteins by nuclear respiratory factor-1.* J Biol Chem, 2009. **284**(40): p. 27577-86.

35. Han, S., et al., *Activation of peroxisome proliferator-activated receptor beta/delta (PPARbeta/delta) increases the expression of prostaglandin E2 receptor subtype EP4. The roles of phosphatidylinositol 3-kinase and CCAAT/enhancer-binding protein beta.* J Biol Chem, 2005. **280**(39): p. 33240-9.

36. Lee, B.H. and E. Ruoslahti, *alpha5beta1 integrin stimulates Bcl-2 expression and cell survival through Akt, focal adhesion kinase, and Ca2+/calmodulin-dependent protein kinase IV.* J Cell Biochem, 2005. **95**(6): p. 1214-23.

37. Morelli, C., et al., *Akt2 inhibition enables the forkhead transcription factor FoxO3a to have a repressive role in estrogen receptor alpha transcriptional activity in breast cancer cells.* Mol Cell Biol. **30**(3): p. 857-70.

38. Han, S., et al., *Fibronectin stimulates human lung carcinoma cell growth by inducing cyclooxygenase-2 (COX-2) expression.* Int J Cancer, 2004. **111**(3): p. 322-31.

39. Barski, A., et al., *High-resolution profiling of histone methylations in the human genome.* Cell, 2007. **129**(4): p. 823-37.

40. Johnson, D.S., et al., *Genome-wide mapping of in vivo protein-DNA interactions.* Science, 2007. **316**(5830): p. 1497-502.

41. Robertson, G., et al., *Genome-wide profiles of STAT1 DNA association using chromatin immunoprecipitation and massively parallel sequencing.* Nat Methods, 2007. **4**(8): p. 651-7.

42. Mikkelsen, T.S., et al., *Genome-wide maps of chromatin state in pluripotent and lineage-committed cells.* Nature, 2007. **448**(7153): p. 553-60.

43. McInroy, L. and A. Maatta, *Down-regulation of vimentin expression inhibits carcinoma cell migration and adhesion.* Biochem Biophys Res Commun, 2007. **360**(1): p. 109-14.

44. Olmeda, D., et al., *Snail silencing effectively suppresses tumour growth and invasiveness.* Oncogene, 2007. **26**(13): p. 1862-74.

45. Hanahan, D. and R.A. Weinberg, *The hallmarks of cancer.* Cell, 2000. **100**(1): p. 57-70.

46. Bian, J., et al., *Suppression of in vivo tumor growth and induction of suspension cell death by tissue inhibitor of metalloproteinases (TIMP)-3.* Carcinogenesis, 1996. **17**(9): p. 1805-11.

47. Snoek-van Beurden, P.A. and J.W. Von den Hoff, *Zymographic techniques for the analysis of matrix metalloproteinases and their inhibitors.* Biotechniques, 2005. **38**(1): p. 73-83.

48. Jinga, D.C., Blidaru, A., Condrea, I., Ardeleanu, C., Dragomir, C., Szegli, G., Stefanescu, M., Matache, C. , *MMP-9 and MMP-2 gelatinases and TIMP-1 and TIMP-2 inhibitors in breast cancer: correlations with prognostic factors.* J Cell Mol Med, 2007. **10**(2): p. 499-510.

49. Tam, E.M., et al., *Characterization of the distinct collagen binding, helicase and cleavage mechanisms of matrix metalloproteinase 2 and 14 (gelatinase A and MT1-MMP): the differential roles of the MMP hemopexin c domains and the MMP-2 fibronectin type II modules in collagen triple helicase activities.* J Biol Chem, 2004. **279**(41): p. 43336-44.

50. Nyormoi, O., L. Mills, and M. Bar-Eli, *An MMP-2/MMP-9 inhibitor, 5a, enhances apoptosis induced by ligands of the TNF receptor superfamily in cancer cells.* Cell Death Differ, 2003. **10**(5): p. 558-69.

51. Rao, J.S., Bhoopathi, P., Chetty, C., Gujrati, M., Sajani, L.S., *MMP-9 SiRNA Induced Senescence Resulting In Inhibition of Medulloblastoma Growth via p16INK4A and MAPK Pathway.* Cancer Res, 2007. **67**(10): p. 4956-4964.

52. Chicoine, E., et al., *Evidence for the role of promoter methylation in the regulation of MMP-9 gene expression.* Biochem Biophys Res Commun, 2002. **297**(4): p. 765-72.

53. Han, S., et al., *Fibronectin increases matrix metalloproteinase 9 expression through activation of c-Fos via extracellular-regulated kinase and phosphatidylinositol 3-kinase pathways in human lung carcinoma cells.* J Biol Chem, 2006. **281**(40): p. 29614-24.

54. Kim, I.Y., et al., *Overexpression of ErbB2 induces invasion of MCF10A human breast epithelial cells via MMP-9.* Cancer Lett, 2009. **275**(2): p. 227-33.

55. Greene, G.F., et al., *Correlation of metastasis-related gene expression with metastatic potential in human prostate carcinoma cells implanted in nude mice using an in situ messenger RNA hybridization technique.* Am J Pathol, 1997. **150**(5): p. 1571-82.

56. Haas, T.L. and J.A. Madri, *Extracellular matrix-driven matrix metalloproteinase production in endothelial cells: implications for angiogenesis.* Trends Cardiovasc Med, 1999. **9**(3-4): p. 70-7.

57. Kleiner, D.E. and W.G. Stetler-Stevenson, *Matrix metalloproteinases and metastasis.* Cancer Chemother Pharmacol, 1999. **43 Suppl**: p. S42-51.

58. Chang, C. and Z. Werb, *The many faces of metalloproteases: cell growth, invasion, angiogenesis and metastasis.* Trends Cell Biol, 2001. **11**(11): p. S37-43.

59. Baker, E.A., et al., *Expression of proteinases and inhibitors in human breast cancer progression and survival.* Mol Pathol, 2002. **55**(5): p. 300-4.

60. Deryugina, E.I. and J.P. Quigley, *Matrix metalloproteinases and tumor metastasis.* Cancer Metastasis Rev, 2006. **25**(1): p. 9-34.

61. Erlichman, C., et al., *Phase I study of the matrix metalloproteinase inhibitor, BAY 12-9566.* Ann Oncol, 2001. **12**(3): p. 389-95.

62. Rudek, M.A., et al., *Phase I clinical trial of oral COL-3, a matrix metalloproteinase inhibitor, in patients with refractory metastatic cancer.* J Clin Oncol, 2001. **19**(2): p. 584-92.

63. Rosemurgy, A., et al., *Marimastat in patients with advanced pancreatic cancer: a dose-finding study.* Am J Clin Oncol, 1999. **22**(3): p. 247-52.

64. Macaulay, V.M., et al., *Phase I study of intrapleural batimastat (BB-94), a matrix metalloproteinase inhibitor, in the treatment of malignant pleural effusions.* Clin Cancer Res, 1999. **5**(3): p. 513-20.

65. Falardeau, P., et al., *Neovastat, a naturally occurring multifunctional antiangiogenic drug, in phase III clinical trials.* Semin Oncol, 2001. **28**(6): p. 620-5.

66. Bergers, G. and L.E. Benjamin, *Tumorigenesis and the angiogenic switch.* Nat Rev Cancer, 2003. **3**(6): p. 401-10.

67. Land, C.E., *Statistical limitations in relation to sample size.* Environ Health Perspect, 1981. **42**: p. 15-21.

68. Glaros, S., et al., *The reversible epigenetic silencing of BRM: implications for clinical targeted therapy.* Oncogene, 2007. **26**(49): p. 7058-66.

69. Shen, H., et al., *The SWI/SNF ATPase Brm is a gatekeeper of proliferative control in prostate cancer.* Cancer Res, 2008. **68**(24): p. 10154-62.

70. Schedin, P., T. Mitrenga, and M. Kaeck, *Estrous cycle regulation of mammary epithelial cell proliferation, differentiation, and death in the Sprague-Dawley rat: a model for investigating the role of estrous cycling in*

mammary carcinogenesis. J Mammary Gland Biol Neoplasia, 2000. **5**(2): p. 211-25.

71. Schedin, P., et al., *Fibronectin fragments induce MMP activity in mouse mammary epithelial cells: evidence for a role in mammary tissue remodeling.* J Cell Sci, 2000. **113 (Pt 5)**: p. 795-806.
72. Bemis, L.T. and P. Schedin, *Reproductive state of rat mammary gland stroma modulates human breast cancer cell migration and invasion.* Cancer Res, 2000. **60**(13): p. 3414-8.
73. Silberstein, G.B., *Postnatal mammary gland morphogenesis.* Microsc Res Tech, 2001. **52**(2): p. 155-62.
74. Deugnier, M.A., et al., *Myoepithelial cell differentiation in the developing mammary gland: progressive acquisition of smooth muscle phenotype.* Dev Dyn, 1995. **204**(2): p. 107-17.
75. Koukoulis, G.K., et al., *Immunohistochemical localization of integrins in the normal, hyperplastic, and neoplastic breast. Correlations with their functions as receptors and cell adhesion molecules.* Am J Pathol, 1991. **139**(4): p. 787-99.
76. Suzuki, R., et al., *Proliferation and differentiation in the human breast during pregnancy.* Differentiation, 2000. **66**(2-3): p. 106-15.
77. Reisman, D.N., et al., *Loss of BRG1/BRM in human lung cancer cell lines and primary lung cancers: correlation with poor prognosis.* Cancer Res, 2003. **63**(3): p. 560-6.

78. Reyes, J.C., et al., *Altered control of cellular proliferation in the absence of mammalian brahma (SNF2alpha).* EMBO J, 1998. **17**(23): p. 6979-91.

79. Batsche, E., M. Yaniv, and C. Muchardt, *The human SWI/SNF subunit Brm is a regulator of alternative splicing.* Nat Struct Mol Biol, 2006. **13**(1): p. 22-9.

80. Matsumoto, E., et al., *Expression of fibronectin isoforms in human breast tissue: production of extra domain A+/extra domain B+ by cancer cells and extra domain A+ by stromal cells.* Jpn J Cancer Res, 1999. **90**(3): p. 320-5.

81. Mizutani, T., et al., *Maintenance of integrated proviral gene expression requires Brm, a catalytic subunit of SWI/SNF complex.* J Biol Chem, 2002. **277**(18): p. 15859-64.

82. Bourachot, B., M. Yaniv, and C. Muchardt, *Growth inhibition by the mammalian SWI-SNF subunit Brm is regulated by acetylation.* EMBO J, 2003. **22**(24): p. 6505-15.

83. Eiriksdottir, G., et al., *Loss of heterozygosity on chromosome 9 in human breast cancer: association with clinical variables and genetic changes at other chromosome regions.* Int J Cancer, 1995. **64**(6): p. 378-82.

84. Neville, L., et al., *Fragile X mental retardation syndrome: DNA diagnosis and carrier detection in New Zealand families.* N Z Med J, 1995. **108**(1009): p. 404-6.

85. Sarkar, A., et al., *Dynamics of chromosome compaction during mitosis.* Exp Cell Res, 2002. **277**(1): p. 48-56.

86. Sabah, M., et al., *Loss of p16INK4A expression is associated with allelic imbalance/loss of heterozygosity of chromosome 9p21 in microdissected synovial sarcomas.* Virchows Arch, 2005. **447**(5): p. 842-8.

87. Reisman, D., *Therapeutic targeting of Brahma by HDAC inhibitors.* Cancer Biol Ther, 2007. **6**(7): p. 997-8.

88. Fraga, M.F. and M. Esteller, *DNA methylation: a profile of methods and applications.* Biotechniques, 2002. **33**(3): p. 632, 634, 636-49.

89. El-Maarri, O., *Methods: DNA methylation.* Adv Exp Med Biol, 2003. **544**: p. 197-204.

90. Wong, H.L., et al., *Rapid and quantitative method of allele-specific DNA methylation analysis.* Biotechniques, 2006. **41**(6): p. 734-9.

91. Muchardt, C., et al., *The hbrm and BRG-1 proteins, components of the human SNF/SWI complex, are phosphorylated and excluded from the condensed chromosomes during mitosis.* EMBO J, 1996. **15**(13): p. 3394-402.

92. Sif, S., et al., *Mitotic inactivation of a human SWI/SNF chromatin remodeling complex.* Genes Dev, 1998. **12**(18): p. 2842-51.

93. Guo, W. and F.G. Giancotti, *Integrin signalling during tumour progression.* Nat Rev Mol Cell Biol, 2004. **5**(10): p. 816-26.

94. Boudreau, N., C. Myers, and M.J. Bissell, *From laminin to lamin: regulation of tissue-specific gene expression by the ECM.* Trends Cell Biol, 1995. **5**(1): p. 1-4.

95. Wu, J. and M. Grunstein, *25 years after the nucleosome model: chromatin modifications.* Trends Biochem Sci, 2000. **25**(12): p. 619-23.

96. Halliday, G.M., et al., *SWI/SNF: a chromatin-remodelling complex with a role in carcinogenesis.* Int J Biochem Cell Biol, 2009. **41**(4): p. 725-8.

97. Trotter, K.W. and T.K. Archer, *Nuclear receptors and chromatin remodeling machinery.* Mol Cell Endocrinol, 2007. **265-266**: p. 162-7.

98. Reisman, D., S. Glaros, and E.A. Thompson, *The SWI/SNF complex and cancer.* Oncogene, 2009. **28**(14): p. 1653-68.

99. Roman, J., et al., *{alpha}5{beta}1 Integrin Expression is Essential for Tumor Progression in Experimental Lung Cancer.* Am J Respir Cell Mol Biol.

100. Yang, J.T., H. Rayburn, and R.O. Hynes, *Embryonic mesodermal defects in alpha 5 integrin-deficient mice.* Development, 1993. **119**(4): p. 1093-105.

101. George, E.L., et al., *Defects in mesoderm, neural tube and vascular development in mouse embryos lacking fibronectin.* Development, 1993. **119**(4): p. 1079-91.

102. Maglott, A., et al., *The small alpha5beta1 integrin antagonist, SJ749, reduces proliferation and clonogenicity of human astrocytoma cells.* Cancer Res, 2006. **66**(12): p. 6002-7.

103. Garanger, E., D. Boturyn, and P. Dumy, *Tumor targeting with RGD peptide ligands-design of new molecular conjugates for imaging and therapy of cancers.* Anticancer Agents Med Chem, 2007. **7**(5): p. 552-8.

104. Ruoslahti, E., *Integrins as signaling molecules and targets for tumor therapy.* Kidney Int, 1997. **51**(5): p. 1413-7.

105. Kunath, K., et al., *Integrin targeting using RGD-PEI conjugates for in vitro gene transfer.* J Gene Med, 2003. **5**(7): p. 588-99.

106. Khalili, P., et al., *A non-RGD-based integrin binding peptide (ATN-161) blocks breast cancer growth and metastasis in vivo.* Mol Cancer Ther, 2006. **5**(9): p. 2271-80.

107. Ramakrishnan, V., et al., *Preclinical evaluation of an anti-alpha5beta1 integrin antibody as a novel anti-angiogenic agent.* J Exp Ther Oncol, 2006. **5**(4): p. 273-86.

108. Ricart, A.D., et al., *Volociximab, a chimeric monoclonal antibody that specifically binds alpha5beta1 integrin: a phase I, pharmacokinetic, and biological correlative study.* Clin Cancer Res, 2008. **14**(23): p. 7924-9.

109. Wang, S.E., et al., *HER2 kinase domain mutation results in constitutive phosphorylation and activation of HER2 and EGFR and resistance to EGFR tyrosine kinase inhibitors.* Cancer Cell, 2006. **10**(1): p. 25-38.

110. Pegram, M.D., et al., *Rational combinations of trastuzumab with chemotherapeutic drugs used in the treatment of breast cancer.* J Natl Cancer Inst, 2004. **96**(10): p. 739-49.

Figure Legends

Figure Legend

Figure 4.1 Predicted CpG Islands in human SMARCA2 (BRM) Gene

Using the CpG island methylation site searcher tool (http://cpgislands.usc.edu/), I identify two putative sites for methylation in the BRM sequence that could be queried in future studies.

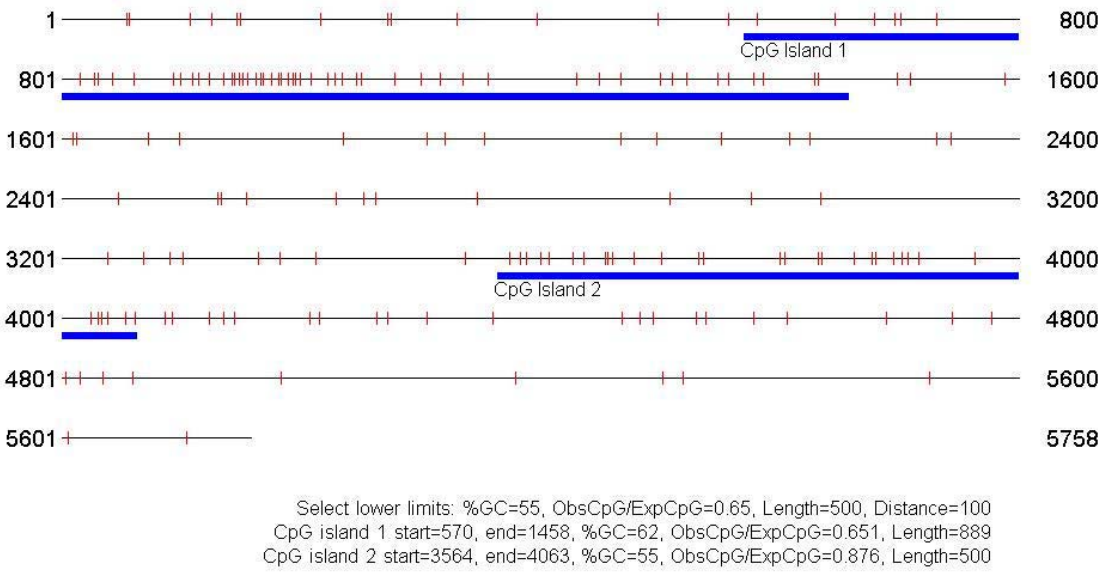

Figure 4.1 Predicted CpG Islands in human SMARCA2 (BRM) Gene

Chapter Five
Addendum

Statement of Contribution

The work entitled “SWI/SNF Chromatin Remodeling Enzyme ATPases Promote Cell Proliferation in Normal Mammary Epithelial Cells,” currently in press for the Journal of Cellular Physiology contains work and substantial scientific input from Kathleen M. Stewart. Specifically, Kathleen mentored and worked side by side with the primary author Dr. Nathalie Cohet for one week in the Spring of 2006 and also for one month in the Summer of 2008 in order to instruct Dr. Cohet on 3D culturing, cryosectioning, immunostaining, RNA and protein purification techniques along with frequent email and phone communications since 2005 on the passaging/culturing of mammary epithelial cells and general Weaver laboratory assays.

ORIGINAL ARTICLE JCP-09-0610 (22072)

Journal of Cellular Physiology

SWI/SNF[Q1] Chromatin Remodeling Enzyme ATPases Promote Cell Proliferation in Normal Mammary Epithelial Cells

NATHALIE COHET,[1] KATHLEEN M. STEWART,[2] RAJINI MUDHASANI,[1] ANANTHI J. ASIRVATHAM,[1] CHANDRASHEKARA MALLAPPA,[1] KAREN M. IMBALZANO,[1] VALERIE M. WEAVER,[2] ANTHONY N. IMBALZANO,[1]* AND JEFFREY A. NICKERSON[1]*

[1]*Department of Cell Biology, University of Massachusetts Medical School, Worcester, Massachusetts*

[2]*Department of Surgery, Center for Bioengineering and Tissue Regeneration, University of California at San Francisco, San Francisco, California*

The ATPase subunits of the SWI/SNF chromatin remodeling enzymes, Brahma (BRM) and Brahma-related gene 1 (BRG1), can induce cell cycle arrest in BRM and BRG1 deficient tumor cell lines, and mice heterozygous for Brg1 are pre-disposed to breast tumors, implicating loss of BRG1 as a mechanism for unregulated cell proliferation. To test the hypothesis that loss of BRG1 can contribute to breast cancer, we utilized RNA interference to reduce the amounts of BRM or BRG1 protein in the nonmalignant mammary epithelial cell line, MCF-10A. When grown in reconstituted basement membrane (rBM), these cells develop into acini that resemble the lobes of normal breast tissue. Contrary to expectations, knockdown of either BRM or BRG1 resulted in an inhibition of cell proliferation in monolayer cultures that was enhanced in three-dimensional rBM culture. This inhibition was strikingly enhanced in three-dimensional rBM culture, although some BRM-depleted cells were later able to resume proliferation. Cells did not arrest in any specific stage of the cell cycle; instead, the cell cycle length increased by approximately 50%. Thus, SWI/SNF ATPases promote cell cycle progression in nonmalignant mammary epithelial cells.

J. Cell. Physiol. 9999: 1–12, 2010.

The mammalian SWI/SNF complexes are a family of chromatin-remodeling enzymes that regulate gene expression by disrupting histone—DNA contacts in an ATP-dependent manner (Imbalzano et al., 1994; Kwon et al., 1994). The complexes are evolutionarily conserved in eukaryotes and contain either Brahma (BRM) or Brahma-related gene 1 (BRG1) as the central ATPase subunit (Khavari et al., 1993; Muchardt and Yaniv, 1993; Wang et al., 1996). SWI/SNF enzyme complexes include other proteins known as BRG1 and BRM-associated factors (BAFs) that can modulate the activity of the ATPase subunits and might provide gene-specific recruitment (Wang et al., 1996). The BRM and BRG1 proteins are highly similar, with a sequence identity of 74% in humans, and they display similar enzymatic properties (Khavari et al., 1993; Muchardt and Yaniv, 1993; Chiba et al., 1994; Phelan et al., 1999; Sif et al., 2001). Both are involved in developmental processes in plants, invertebrates, and vertebrates (reviewed in de la Serna et al., 2006; Kwon and Wagner, 2007). Despite these similarities, the two alternative ATPase subunits can serve different functions in the regulation of differentiation, transcriptional control, and other important cell processes (Reyes et al., 1998; Bultman et al., 2000; Kadam and Emerson, 2003).

BRG1 and BRM are important for cell cycle arrest. Reintroduction of BRG1 or BRM into deficient tumor cell lines induces cell cycle arrest and a "flat cell" phenotype by a mechanism requiring RB family members (Dunaief et al., 1994; Strober et al., 1996; Trouche et al., 1997; Zhang et al., 2000; Strobeck et al., 2000b). RB and BRM (or BRG1) cooperate to repress E2F1-mediated activation (Trouche et al., 1997; Wang et al., 2002) and repress levels of CDK2, cyclin A, and cyclin E (Strobeck et al., 2000a,b; Coisy et al., 2004; Roberts and Orkin, 2004). BRM can compensate for BRG1 loss in RB signaling pathways, suggesting a redundancy between the two factors in this mechanism of cell cycle control (Reisman et al., 2002; Strobeck et al., 2002).

Approximately 10% of mice heterozygous for Brg1 develop tumors, mostly mammary carcinomas (Bultman et al., 2008). This study and earlier work (Bultman et al., 2000) firmly established BRG1 as a tumor suppressor in vivo. Although Brm deficient mice do not present with tumors, depending on the strain background, they can be physically larger, with an increased tissue and organ size because of increased proliferation (Reyes et al., 1998). In addition, immortalized fibroblasts derived from Brm-deficient mouse embryos have a delayed and shorter S-phase, and a prolonged mitosis (Coisy-Quivy et al., 2006). Together, these previous studies indicate that BRG1 and BRM are negative regulators of cell cycle progression in culture and are likely to decrease proliferation in vivo. A logical prediction from this literature would be that the loss of BRG1 or BRM should lead to the loss of growth control, to hyperplasia, and to cancer progression.

Additional Supporting Information may be found in the online version of this article.

Contract grant sponsor: National Cancer Institute; Contract grant number: PO1 CA82834.

*Correspondence to: Anthony N. Imbalzano and Jeffrey A. Nickerson, Department of Cell Biology, University of Massachusetts Medical School, Lake Avenue North, Worcester, MA 01655. E-mail: anthony.imbalzano@umassmed.edu; jeffrey.nickerson@umassmed.edu

Received 14 December 2009; Accepted 16 December 2009

Published online in Wiley InterScience (www.interscience.wiley.com.). 00 Month 2010. DOI: 10.1002/jcp.22072

The MCF-10A line immortalized spontaneously in culture from primary cells taken from a patient with fibrocystic disease (Soule et al., 1990). The MCF-10A line has a stable, near-diploid karyotype (Soule et al., 1990; Yoon et al., 2002), but has lost the p16 locus (Yaswen and Stampfer, 2002; Debnath et al., 2003). The cells express wild type p53 (Merlo et al., 1995; Debnath et al., 2003). MCF-10A cells cultured in three-dimensional reconstituted basement membrane (rBM) culture develop important features of normal breast tissue by a program of proliferation, cell cycle arrest, apical—basolateral polarization, and apoptosis to create a luminal space (Debnath et al., 2002, 2003; Underwood et al., 2006). In addition, cell nuclei of mammary epithelial cells forming acini in three-dimensional rBM culture recapitulate the architecture of mammary epithelial cells in tissue (Lelievre et al., 1998).

To address the function of the SWI/SNF ATPases in normal mammary epithelial cells, we generated MCF-10A cells with inducible knockdowns of either BRG1 or BRM. The depletion of either ATPase subunit decreased the rate of cell proliferation without inducing a complete cell growth arrest in monolayer culture. The decrease in proliferation was amplified in three-dimensional rBM culture. Further analysis demonstrated that the length of the cell cycle increased after depletion of either SWI/SNF ATPase, indicating a role for BRG1 and BRM as positive regulators of cell cycle progression.

Materials and Methods

Cell culture

MCF-10A cells from the Karmanos Cancer Institute (Detroit, MI) were maintained in monolayer as described (Debnath et al., 2003).

Doxycycline-inducible BRG1 and BRM knockdowns

Generation of vectors. Lentiviral vectors were from the D. Trono lab (www.tronolab.unige.ch) and obtained from Addgene[Q2]: pLV-tTRKRAB-Red encoding the TetR-KRAB regulator, pLVTHM, for cloning the shRNA, the packaging vector pCMV-dR8.91 and the Envelope vector pMD2.G. The shRNA sequences for BRG1 and BRM were from previously designed siRNAs (Rosson et al., 2005). Annealed oligonucleotides were cloned in the pSUPER.retro.puro vector then inserted between the EcoRI/ClaI sites of pLVTHM to express the shRNA under the control of the H1 promoter. The first forward sequence was 5′-GATCCCCGTGCGACATGTCTGCGCTG TTCAAGACACAGCGCAGACATGTCGCACTTTTTGGAAA-3′ where the underlined sequence is specific for the BRG1 ATPase domain. The second forward sequence was 5′-GATCCCCGTCTGAAGATCGTGCTGCTTTCAAGAGAAG-CAGCACGATCTTCAGACTTTTTGGAAA-3′ where the underlined sequence is specific for the BRM ATPase domain. The control scrambled (SCRAM) forward sequence was 5′-ATCCCCCAGTTA-CTAGACGCGATCGTTCAAGAGACGATCGCGTCTAGTAACT-GTTTTTA-3′.

For the double BRG1 and BRM knockdown, a new shBRM lentivector was engineered with Gateway® Technology (Invitrogen[Q3]). The cassette tetO-H1-shBRM was removed from the pLVTHM and cloned in the Entry vector pENTR1A-no ccdB (a gift of Eric Campeau) used to transfer the shBRM expression cassette into a lentiviral destination vector. We used the promoter-less lentiviral destination vector pLenti 2X Puro DEST, clone #w16.1 (E. Campeau), which contains elements that allow packaging of the construct and a puromycin resistance marker for selection of stably transduced cells (Campeau et al., 2009). The LR Recombination Reaction was performed by using the Gateway LR clonase™ II enzyme Mix (Invitrogen).

Lentivirus production. 5×10^6 293T cells were seeded in a 10 cm dish and transfected the following day with the Lipofectamine® 2000 reagent (Invitrogen). Viral supernatants were collected and 0.45 μm filtered at 48 and 72 h post-transfection, then stored at −80°C.

Transduction of MCF-10A cells. MCF-10A cells at 75% confluence were incubated for 16 h with lentivirus (LV) diluted in growth media containing 8 μg/ml polybrene. The next day the viruses were removed, the cells were rinsed twice with PBS, and fresh media were added. Cells were passed twice before FACS sorting. To induce shRNA-GFP expression, Doxycycline was used at 0.01—0.5 μg/ml.

Cell sorting

To obtain a population of cells expressing the shRNA and GFP under doxycycline control, the cells were FACS-sorted twice. The first sort was of uninduced cells and selected dsRED-positive cells that constitutively expressed the tTR-KRAB protein coupled to the dsRed marker (constitutive expression). The second sort was performed 2 days after doxycycline induction and selected both dsRED- and GFP-positive cells that expressed both shRNA and GFP after doxycycline induction. Cells were FACS selected prior to every experiment.

Western blot analysis

Whole cell extracts were prepared from MCF-10A cells in monolayer culture after trypsinization and two washes with 5 ml of cold 1× PBS. Then, cells were lysed in 100 μl Laëmmli lysis buffer (1% SDS, 0.04 M Tris—HCl pH 6.8, 6% glycerol, 0.003% bromophenol blue, 0.015 M β-mercaptoethanol) for every 10^6 cells, boiled for 5 min, and stored at −80°C. Proteins were separated on 7.5% SDS—PAGE, transferred to a nitrocellulose membranes, and detected with primary antibodies and ECL detection (Amersham[Q4]). The antibodies used were: BRG1 (dilution 1:1000, anti-serum; de La Serna et al., 2000), BRM (dilution 1:1000, Abcam[Q5], ab15597), PI3Kinase p85, H-SH2 domain (dilution 1:1000, Upstate[Q6], cat. no. 06-496), GFP (dilution 1:1000, Roche[Q7], cat. no. 1814460), p21 Waf1/Cip1(12D1) Rabbit mAb (dilution 1:1000, Cell Signaling[Q8], 2947S), p53 (dilution 1:1000, Cell Signaling, 9282), phospho-p53 (Ser15) (dilution 1:1000, Cell Signaling, 9284S), phospho-p53 (Ser46) (dilution 1:1000, Cell Signaling, 2521S), phospho-p53 (Ser 20) (dilution 1:1000, Cell Signaling, 9287S), cyclin A (BF683) mouse mAb (dilution 1:1000, Cell Signaling, 4656), mTOR (dilution 1:1000, Millipore[Q9], 04-385), phospho-mTOR (Ser 2448) (dilution 1:1000, Millipore, 09-213), p70 S6 kinase (S6K) (dilution 1:1000, Millipore, 06-926).

Proliferation assays

Direct cell counting. Cells were grown 2 days in the presence (pre-induction) or absence of doxycycline (0.05 or 0.1 μg/ml) prior to seeding in a 12-well plate (4,000 cells/well) with or without doxycycline. Cells were counted daily after trypsin treatment using either a hemacytometer or a Z1 Coulter counter.

DNA quantification using the Cyquant cell proliferation kit (Invitrogen). Cells were seeded in a 96-well plate at different densities in triplicate. One plate was prepared per day for the time course. Cell growth was stopped by removing the medium and freezing the plate immediately with storage at −80°C. The kit uses a proprietary green fluorescent dye, Cyquant® GR dye, which exhibits strong fluorescence enhancement when bound to DNA. Fluorescence was measured using a fluorescence microplate reader. A reference standard curve (with cell numbers from 50 to 50,000 cells) was used to convert fluorescence values into cell numbers.

Immunofluorescent staining of monolayer cultures

Monolayer cultures were prepared following the methods of Wagner et al. (2003). Before mounting coverslips with Prolong Gold (Invitrogen), cells were stained with DAPI (2 μg/ml) and DRAQ5 (Alexis[Q10], 1:5,000) DNA dyes in PBS for 5 min at room temperature then washed once with PBS.

Phospho-histone H3 (serine 10) antibody was from Upstate Millipore. All the secondary antibodies (Alexa Fluor® 488 or 568 conjugated) were from Molecular Probes[Q11]. For the observation of expressed fluorescent proteins, cells on coverslips were washed in PBS and directly fixed in 4% paraformaldehyde in CSK for 50 min, rinsed in TBS—0.05% Tween-20, and stained with DAPI and DRAQ5.

BrdU incorporation assay

Cell cycle length of non-synchronized MCF-10A cells was measured by labeling cells with bromodeoxyuridine (BrdU). 2×10^5 cells were plated on a coverslip in each well of a 6-well dish. At time 0, BrdU was added to the culture medium to a final concentration of 20 μM. At each time point (1, 5, 10, and 15 h of BrdU incorporation) cells were washed twice with cold DPBS, permeabilized with 0.5% Triton X-100 in CSK buffer for 3 min, and fixed with 4% formaldehyde in CSK buffer for 20 min. All steps were performed on ice. Then cells were washed thrice with PBS-0.5% Tween 20 for 10 min each at room temperature. DNA was denatured by 2 N HCl for 30 min at 37°C, followed by two washes with PBS. All antibodies were diluted in TBS-1. Coverslips were incubated with anti-BrdU (clone BU-33, Sigma[Q12], 1:400) for 1 h at 37°C or overnight at 4°C. The second antibody was goat anti-mouse IgG1 coupled to Alexa Fluor 568 (Invitrogen, 1:2,000). After each antibody incubation, cells were rinsed thrice in PBS containing 0.05% Tween 20 for 10 min each at room temperature. Before mounting coverslips with Prolong Gold (Invitrogen), cells were stained with DAPI (2 μg/ml) and DRAQ5 (Alexis, 1:5,000) diluted in PBS for 5 min at room temperature before a last wash with PBS. Images of 10 fields were taken at low magnification and BrdU-positive cells were counted in each field with ImageJ. A linear regression was applied to extrapolate the time needed for 100% to incorporate BrdU. This time is the cell cycle length.

mRNA analysis

RNA was isolated from MCF-10A monolayer culture using Trizol (Invitrogen) and reverse transcribed. The cDNA was amplified using the Qiagen HotStarTaq Master Mix kit (Qiagen[Q13], #203445) containing 0.1 μg of specific primers and SYBR green. RT-PCR and real-time PCR were performed using procedures previously described (Ohkawa et al., 2006). Primers for measuring GAS5 RNA levels were CAG TGT GGC TCT GGA TAG CA (forward) and TTA AGC TGG TCC AGG CAA GT (reverse).

Three-dimensional culture of MCF-10A cells on reconstituted basement membrane

MCF-10A cells were cultured in either Reduced Growth Factor Matrigel without phenol red (lot#11346, BD Biosciences) or Non-Reduced Growth Factor Matrigel with phenol red (lot#22704, BD Biosciences[Q14]) following the procedures of Debnath et al. (2003). Briefly, for overlay cultures, cells were prepared for three-dimensional rBM culture by growing to 20—30% confluency in monolayer and seeding in a single cell suspension on 100 μl of matrigel in a 35 mm well at 7,000—15,000 cells/well or on 40 μl matrigel in a 8-well chamber slide at 5,000 cells/well. Cells in rBM were grown in assay media (Debnath et al., 2003) containing 2% horse serum, 5 ng/ml EGF, and 2% Matrigel. All cultures were incubated at 37°C in a 5% CO_2 humidified incubator for up to 20 days. Media was replaced every 2—4 days. Morphology was observed every 2 days via phase contrast microscopy. Acinar size was determined from phase contrast micrographs. Two diameters were measured per acinus with ImageJ software. The minimum number of measured acini per sample was 15.

Cell counting in rBM culture

Three-dimensional cultures were incubated for 30—40 min in 37°C incubator with 0.25% trypsin—EDTA. As soon as the Matrigel was dissolved, the acinar cell suspension was centrifuged 5 min at 1,000 rpm, the supernatant was discarded and the pellet was resuspended with 0.05% trypsin—EDTA then put back in the dish for incubation at 37°C. When a single cell suspension was observed, trypsin activity was stopped with resuspension media (DMEM/F12 containing 20% horse serum and antibiotics) and cells were counted by trypan blue exclusion in a hemocytometer, or without trypan blue with an automatic cell counter.

Results

Inducible knockdown of SWI/SNF ATPase subunits in MCF-10A human mammary epithelial cells

We engineered the conditional expression of a short hairpin (sh) sequence targeting BRG1 (Rosson et al., 2005) in the human breast epithelial cell line, MCF-10A (Soule et al., 1990). A doxycyclin-inducible LV (Wiznerowicz and Trono, 2003) stably introduced the shRNA gene into MCF-10A cells. Two lentiviral constructs were used. The first expressed the tTR-KRAB transactivator and dsRed (LV-tetR-KRAB-dsRed), whereas the second expressed the shRNA and GFP under tTR-KRAB transcriptional repression (LV-shBRG1i-GFP). We used two different strategies of lentiviral infection without noting any significant difference in outcome. In some experiments, cells were modified in one step by a double infection with both LVs. In other experiments, cells were engineered by sequential infection, first with LV-tetR-KRAB-dsRed and, after sorting for dsRed fluorescence, with LV-shBRG1i-GFP. Pools of cells were FACS sorted for dsRed fluorescence and doxycycline-induced GFP fluorescence, without a requirement for cloning or drug selection (Fig. S1).

This inducible knockdown system was used both in monolayer culture and in three-dimensional culture in rBM. As expected, cultures maintained in the absence of doxycycline constitutively expressed dsRED, which marks cells also expressing the TetR-KRAB repressor (Fig. 1). This repressor prevents expression of the GFP marker and the shRNA, which are both encoded by the second virus. Addition of doxycycline-induced expression of both GFP and the shRNA. Because of the molecular and functional similarity between BRG1 and the other SWI-SNF ATPase subunit, BRM, we also generated MCF-10A cells with an inducible BRM knockdown using the same lentiviral vector system. The control vector conditionally expressed a scrambled sequence shRNA.

We evaluated the efficiency of the BRG1 and BRM knockdown by Western blotting (Fig. 2). Protein lysates were obtained from cells expressing the BRG1 shRNA, (BRG1i), the BRM shRNA (BRMi), or the scrambled sequence control shRNA (SCRAM), with or without induction with 0.01 μg/ml doxycycline in monolayer culture for 3 days. As shown in Figure 2A, the protein level of BRG1 was efficiently knocked down in BRG1i cells (compare lanes 4 and 5), but was not decreased in the BRMi cells (compare lanes 6 and 7). Similarly, BRM levels (Fig. 2B) were not decreased in BRG1i cells but were greatly reduced in BRMi cells, demonstrating the specificity of each shRNA. GFP expression was monitored as an additional marker of doxycycline induction. Protein levels were measured by quantification of Western blot signals. The knockdown of BRG1 protein in BRG1i cells was determined to be 75%, whereas the knockdown of BRM was 90% in BRMi cells, with minor variations between experiments. Optimizing this inducible system, we determined that 48 h were needed to get maximal protein decrease (Fig. S2) at an optimal concentration of doxycycline of between 0.01 and 0.05 μg/ml (Fig. S3). We also noticed a small but consistent increase in the amount of BRM protein in the BRG1i cell line (Fig. 2B, compare lanes 4 and 5) and a similar small but reproducible increase in the amount of BRG1 in BRMi cells (Fig. 2A, compare lanes 6 and 7). These observations suggest a compensation effect in protein levels of the two SWI/SNF ATPase subunits BRG1 and BRM.

One concern with siRNA technology is the capacity of dsRNA to trigger a non-specific interferon response in some cellular systems (Bridge et al., 2003; Diebold et al., 2003; Sledz et al., 2003). The inclusion of the scrambled sequence SCRAM controls in every experiment controlled for these effects, but to further validate the system, we directly measured the level of mRNAs coding for the interferon response genes IFITM1, MX1, and OAS1. The results showed that the interferon response

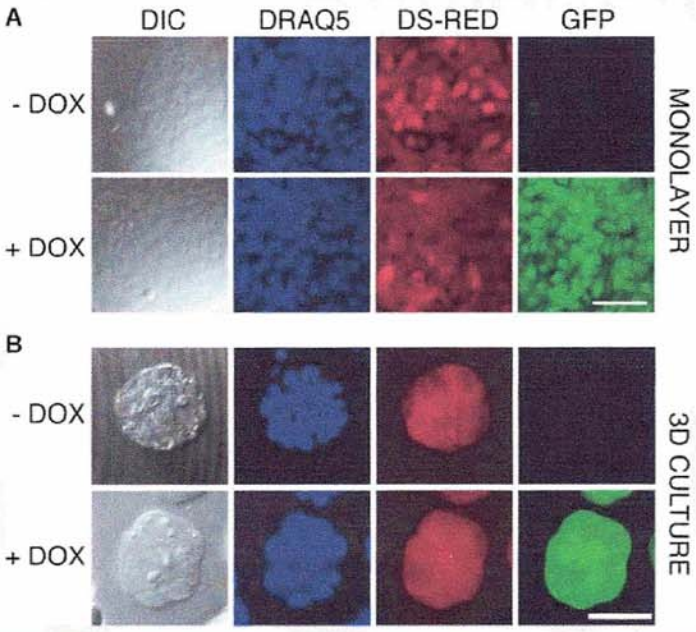

Fig. 1. Doxycycline-inducible shRNA expression in MCF-10A cells. In this system, dsRED and the TET-KRAB regulator are constitutively expressed from the same vector whereas GFP fluorescence is expressed only after doxycycline induction of the shRNA targeting BRG1. Cells were sorted after 2 days of doxycycline induction (0.1 μg/ml). Then, after 5 days of culture without doxycycline, cells were seeded on coverslips and induced or not with 0.05 μg/ml doxycycline for 3 days before fixing with formaldehyde and staining nuclei with DRAQ5. Confocal image stacks, shown here for the MCF-10A-SCRAM control cell line), were collected for both monolayer (panel 1A, scale bar = 100 μm) and 3D culture (panel 1B, scale bar = 50 μm.). The micrographs of the acinus (panel B) were maximum intensity projections. Confocal settings were held constant so that linear quantitative comparisons could be made between samples with and without doxycycline induction.

was not activated by any of the shRNAs in this experimental system (data not shown).

BRG1 or BRM knockdown impedes the early proliferation stage of MCF-10A acinus formation

Normal MCF-10A mammary epithelial cells, when cultured in three-dimensional rBM culture, reproduce important features of normal breast tissue in a well-characterized temporal and spatial program (Petersen et al., 1992; Weaver et al., 1995, 1997, 2002; Debnath et al., 2002, 2003). An initial stage of proliferation produces loosely connected groups of cells and is followed by cell cycle arrest. Acini form from these groups of cells by basal deposition of a basement membrane and luminal clearance of cells not apposing the basement membrane. Malignant changes in cells alter this program of development in rBM culture with the formation of structures having an altered morphology, loss of cell cycle arrest, and basement membrane-independent cell survival (Imbalzano et al., 2009).

To determine whether the depletion of BRG1 caused these malignant alterations in acinar development, we cultured wild type MCF-10A human mammary epithelial cells, BRG1i cells expressing the doxycycline-inducible shRNA targeting BRG1, and control SCRAM cells in three-dimensional rBM culture. These cells were pre-induced with doxycycline 2 days before being plated on a layer of rBM with an overlay of 2% rBM in culture medium and were maintained in culture for 18 days (Debnath et al., 2003). Twenty-four hours after establishing these overlay cultures, the cells from all three cell lines (wild-type MCF-10A, BRG1i, and SCRAM) had attached to the rBM. After 2 days, all the cell lines formed spherical masses of cells. The diameter of these structures was measured. As shown in Figure 3A—C, from 4 days of culture, the size of the multicellular structures of BRG1i cells expressing the shBRG1 after doxycycline induction were smaller than the structures formed from non-induced BRG1i cells or from controls (SCRAM and wild type MCF-10A). This size difference increased with time in culture (Fig. 3D,E). Dead cells were rare as determined by dye-exclusion. Cell counting, performed after digestion of the extracellular matrix and dissociation of the cell masses, revealed a dramatic decrease in proliferation (Fig. 3C).

BRMi cells with a doxycycline-inducible knockdown of BRM and control SCRAM cells were grown in three-dimensional rBM culture, with conditions matched to the BRG1 knockdown experiments. As illustrated in Figure 4A, the BRMi cells expressing the shBRM with doxycycline gave smaller multicellular masses than the uninduced BRMi without doxycycline and the SCRAM control cells. These changes were clear from day 4 in culture. The diameter (Fig. 4B) and the size distribution (Fig. 4C) of the multicellular structures were determined. In the early proliferation stage of differentiation (day 0 to day 8), the MCF-10A cells expressing the shBRM (+doxycycline) recapitulated the striking decrease in proliferation observed previously with the BRG1 knockdown

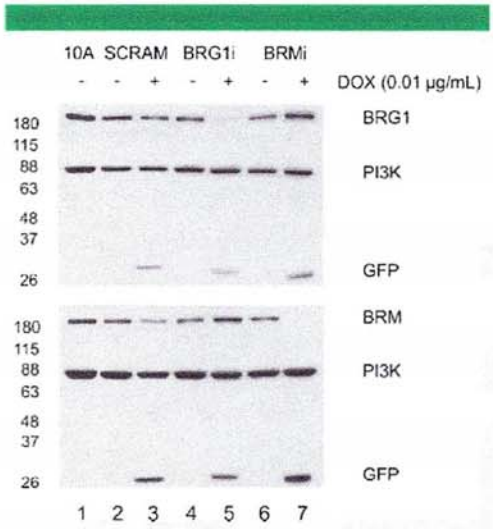

Fig. 2. Doxycycline-inducible knockdown of BRG1 and BRM in MCF-10A cells. Total protein was extracted from cells treated or not for 3 days with 0.01 μg/ml doxycycline. BRG1 (A), BRM (B) and GFP protein expression were examined by Western blotting. The protein of 0.5 × 10^5 cells per lane was separated by SDS—PAGE (7.5%) and probed with the indicated antibodies. PI3 kinase was the loading control.

MCF-10A cells. An analysis of size distributions (Fig. 4C, compare fraction of acini with a diameter <40 μm) showed a larger fraction of small multicellular structures after BRM knockdown than was observed in the controls from day 4 to day 11. However, unlike BRG1i cells, the difference in size between BRMi cells induced to deplete BRM and uninduced cells decreased with time in culture (see Fig. 4A after day 8). A subset of cells escaped from the growth defect and formed multicellular structures that were larger than normal acini. Subsequent work has established that these escaping structures have developed a tumor like phenotype via altered integrin expression (V. M. Weaver, manuscript in preparation[Q15]).

BRG1 and BRM knockdown decreases proliferation in monolayer culture

To ascertain whether growth in three-dimensional rBM culture was required for this unexpected decrease in proliferation after BRM or BRG1 depletion, we grew the same cell lines with or without doxycycline induction in monolayer culture. After 2 days of pre-induction, we seeded the different cell lines at the same density in 12-well dishes. Each day from day 2 to day 6, cells were trypsinized and counted. A 50% decrease in cell number was observed four or five days after seeding (Fig. 5A), roughly matching the 4-day delay observed in three-dimensional culture (see Figs. 3 and 4).

To more precisely quantify the proliferation decrease after BRG1 or BRM knockdown, we used a second method that was more robust and sensitive than simple cell counting, eliminated the need for trypsinization, and allowed larger numbers of replicates of each sample. This method measured the density of adherent cells using a dye that fluoresces strongly when bound to cellular nucleic acids, and confirmed the previous results obtained from cell counting. There was a 50% proliferation decrease by day 5 after BRG1 or BRM knockdown (Fig. 5B).

To eliminate the possibility that BRG1 knockdown was only causing the detachment of cells, we manually counted the unattached cells suspended in the culture medium during the 5 days of the proliferation assay. Viability was measured by trypan blue exclusion. There was no increase in the number of detached live or dead cells after knockdown. We also examined whether cellular senescence might explain the reduced proliferation. ββ-Galactosidase staining marks senescent cells (Dimri et al., 1995) and we observed no increase in ββ-galactosidase-positive cells after knockdown. We also stained the cell cultures with toluidine blue to observe cell morphology and detect structural changes characteristic of senescent or apoptotic cells. No changes were observed that were characteristic of senescence or programmed cell death.

A decrease of proliferation without complete arrest might be due to an abnormal stimulation of cell contact inhibition. A delay of 4 days for a proliferation decrease to become significant might be explained by this hypothesis. Induction of contact inhibition depends on cell density and might need some time after cell seeding to develop (Nelson and Chen, 2003; Liu et al., 2006; Gray et al., 2008). To determine whether contact inhibition was involved in the decrease of cell proliferation after BRG1 or BRM knockdown, we plated the cell lines on glass coverslips in 6-well plates. After 5 days of doxycycline induction, we immunostained the cells with an antibody that specifically recognizes the mitosis-specific serine 10 phosphorylation of histone H3 (Fig. 6A) (Ajiro et al., 1983; Ajiro and Nishimoto, 1985; Shibata et al., 1990; Goto et al., 1999; Wei et al., 1999; Li et al., 2005; Eberlin et al., 2008). The fraction of cells in mitosis and the location of those mitotic cells within the epithelial colonies were measured (Fig. 6). The overall percentage of cells in mitosis was low, as would be expected after 5 days in culture, but the number of mitotic cells after BRG1 or BRM knock down was reduced ($P < 0.05$) relative to the uninduced control (Fig. 6B). This confirmed the growth inhibition caused by BRG1 or BRM depletion using a third method, and showed that the decrease in proliferation was not caused by a mitotic arrest.

The localization of mitotic cells was scored according to whether they were inside the colony, crowded by other cells, or whether they were at the edge of the colony. As seen in Figure 6A—C, mitotic cells were preferentially located at the edges of colonies. Quantification (Fig. 6C) was consistent with previous studies reporting contact inhibition in MCF-10A cells (Liu et al., 2006). The percent of mitotic cells inside the colonies was about 20% and this was not significantly changed by knockdown of either BRG1 or BRM. Taken together these data are inconsistent with the hypothesis that a decrease in cell proliferation after BRG1 or BRM knockdown was caused by the hyper-activation of cell contact inhibition.

Reduction of BRG1 or BRM levels lengthens the cell cycle

FACS sorting of propidium iodide- and DAPI-stained cells showed no significant changes in the fraction of cells in each phase of the cell cycle after reduction of BRG1 or BRM levels. To measure the length of the cell cycle, we performed a time course experiment after pulse labeling cells with BrdU (Fig. 7). BrdU is only incorporated into DNA during S-phase, so we were able to measure the cell cycle length of each cell line by counting the fraction of BrdU positive cells at different times after pulse labeling. Using a linear regression method, we extrapolated the results to 100% incorporation, which corresponded to the time needed for one complete cell cycle (Fig. 7A). The normal cell cycle length of wild-type MCF-10A cells, control SCRAM cells, and uninduced BRG1 and BRM

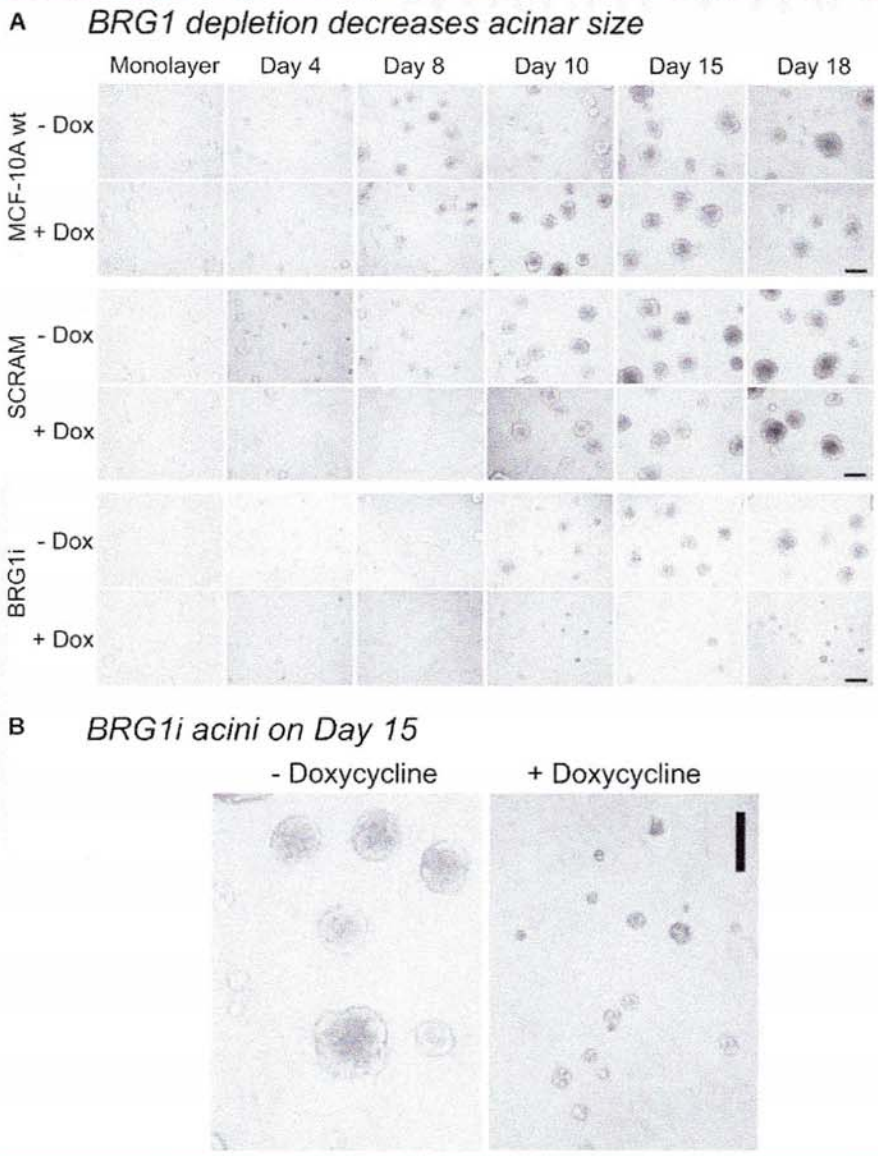

Fig. 3. Decreased proliferation after BRG1 knockdown in rBM culture. A: MCF-10A cells were seeded with or without doxycycline in Matrigel. The micrograph for day 0 shows the initial monolayer culture. Every 2 days, media with or without doxycycline were replaced and phase contrast micrographs were taken. Decreased proliferation was observed from day 4 in MCF-10A cells expressing the shRNA targeting BRG1 (+doxycycline). Size bar: 150 mm. B: Representative micrographs of MCF-10A BRG1i acini grown in the presence or absence of doxycycline for 15 days. These pictures were among those used to make the measurements of acinar diameter presented in part D. Size bar: 150 μm. C: The three-dimensional Matrigel cultures were trypisinized to obtain a single cell suspension at different times after seeding (days 4 and 9). Then, cells were counted both using a hemacytometer with trypan blue to detect dead cells, and with an automatic cell counter. The asterisk indicates that no increase of trypan blue positive dead cells was detected in the BRG1i cells grown with doxycycline. D: Median acinar diameter during differentiation. For each cell sample, the median acinus size was calculated ($n \geq 10$ acini with 2 measurements of diameter for each acinus). Statistical analysis was by a Student's t-test. The comparisons had a high degree of statistical significance ($^{**}P \leq 0.01$). E: Size distribution of acini. The percentage of acini with a diameter smaller than 22 μm, contained in the interval 22—65 μm, 65—110 μm, or greater than 110 μm were calculated.

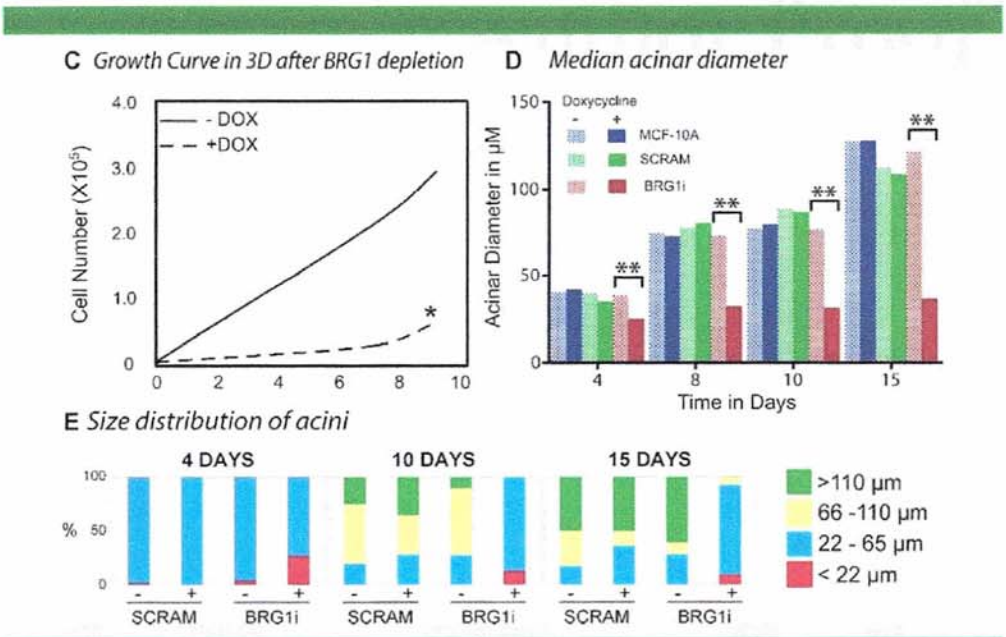

Fig. 3. ***(Continued)***

knockdown cells (no doxycycline) was 18—22 h (Fig. 7A, B). The induced BRG1 and BRM knockdown cells exhibited a longer cell cycle of 31—32 h. We concluded that an extra 10—14 h were needed to complete one cell cycle for MCF-10A cells depleted for either BRG1 or BRM and, consequently, that BRG1 and BRM regulate cell cycle length.

A BRG1-BRM double knockdown is lethal

The reciprocal increase of BRM protein level in BRG1 knockdown MCF-10A cells and an increase in BRG1 levels in BRM knockdown cells (Fig. 2) implicates a compensatory mechanism for these two ATPase subunits. This suggests that a more severe phenotype might result from knocking down both BRM and BRG1. To evaluate this, we created a double knockdown in MCF-10A cells. MCF-10A cells with a doxycycline-inducible knockdown of BRG1 were infected with a LV expressing both shRNA targeting BRM and a puromycin resistance gene. After adding doxycycline and puromycin to the media, most of these cells died and the remaining drug-resistant cells did not show the expected decrease in BRM protein. Presumably, the drug treatment conditions selected for cells that escaped BRM knockdown. As a control, MCF-10A cells expressing only the TetR-KRAB regulator were infected under the same conditions. After selection and doxycycline induction, there was minimal cell death and these cells showed the expected BRM knockdown (data not shown).

Upregulation of GAS5 in cells depleted for BRM

To address the mechanisms reducing proliferation rates in MCF10-A cells with reduced BRG1 or BRM, a number of cell cycle regulators were examined. Most of these were not altered after BRG1 or BRM knockdown.

One difference observed was in the levels of GAS5 in BRM, but not BRG1, deficient cells. GAS5 is an alternatively spliced, long non-coding RNA with several snoRNAs in its introns (Coccia et al., 1992; Muller et al., 1998; Smith and Steitz, 1998; Raho et al., 2000). Overexpression of specific GAS5 transcripts can induce cell cycle arrest in some cell lines and sensitize cells to apoptotic signals (Mourtada-Maarabouni et al., 2008, 2009). GAS5 was reported to be down-regulated in breast cancer-derived cell lines (Mourtada-Maarabouni et al., 2009). Q-PCR using primers for regions of GAS5 common to all splice variants showed that GAS5 levels were up-regulated in BRM depleted MCF-10A cells, but not BRG1 depleted cells (Fig. 8). Pathways converging on GAS5 are not yet known, but our data establish a correlation between the overexpression of a noncoding RNA that can negatively regulate cell cycle progression and the decreased proliferation of MCF-10A cells after BRM reduction.

Cyclin A has been implicated in cell cycle control by BRG1 during RB-mediated cell cycle arrest (Strobeck et al., 2000b; Zhang et al., 2000) and is a direct target of BRM in some cells (Coisy et al., 2004). We observed no differences in the expression level of cyclin A in either BRG1 or BRM deficient MCF10-A cells (Fig. S4A). The mTOR pathway can also affect cell cycle progression via control of translation (Ma and Blenis, 2009). Western blot analysis of mTOR, phopho-mTOR, and the mTOR downstream target, p70 S6K, showed no changes due to BRG1 or BRM depletion (Fig. S4B).

A recent report indicated that BRG1 depletion activated p53 in several tumor cell lines (Naidu et al., 2009). We examined total p53 and serine-15 phosphorylated p53 protein levels in BRG1- and BRM-depleted MCF10-A cells by Western blot, but observed no increase (Fig. S4C) as might be expected if the p53 pathway were activated.

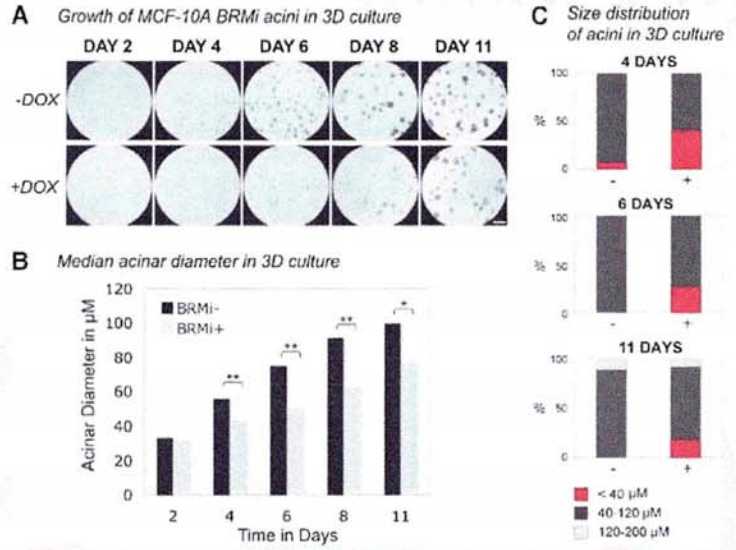

Fig. 4. MCF-10A cells induced to knock down BRM formed acini with a more variable median size in rBM culture. A: MCF-10A cells with an inducible BRM knockdown or control scrambled shRNA were seeded in Matrigel overlay culture. Cultures were fed every 2 days with medium containing 0.05 µM doxycycline or medium without doxycycline. Every 2 days phase contrast micrographs were taken of the live cultures. Smaller acini were observed from day 4 in the MCF-10A cells expressing the shRNA targeting BRMi (+doxycycline). No differences in size were observed in MCF-10A cells expressing scrambled shRNA in the presence or absence of doxycycline (data not shown). Size bar: 250 µm Most acini were smaller after the induced knockdown of BRM, but a few acini were able to escape this decrease in proliferation. B: For each cell line and condition, the median acinar diameter was calculated from micrographs including the one in part A. Two measurements of diameter were averaged for each acinus and more than 24 acini were measured for each sample and time point. Statistical analysis was by a Student's t-test. The comparisons marked with one asterisk were significant ($P < 0.05$) and those marked with two asterisks were highly significant ($P \leq 0.01$). **: The size distribution of acini in 3D culture is shown for the data of parts A and B. The percent of acini with a diameter inferior to 40 µm, contained in the interval 40—120 µm, and contained in the interval 120—200 µm were calculated.

Discussion

BRG1 and BRM depletion reduces proliferation in MCF-10A mammary epithelial cells

We knocked down BRG1 and BRM in MCF-10A cells, an immortalized but largely normal mammary epithelial cell line (Soule et al., 1990; Yoon et al., 2002). Grown in three-dimensional rBM culture, MCF-10A cells form acini that resemble structures in normal breast tissue (Debnath et al., 2002). Contrary to expectations, we did not observe an increased rate of proliferation in either monolayer or three-dimensional rBM culture. rBM cultures of breast tumor-derived cells (Weaver et al., 1997) or of malignant cells engineered from MCF-10A cells (Miller et al., 1993; Dawson et al., 1996; Strickland et al., 2000; Santner et al., 2001) form larger, disorganized structures without proliferation arrest or lumen formation (Imbalzano et al., 2009). BRG1 depleted MCF-10A cells did not have a tumor-like phenotype. Instead, the cells grew more slowly in monolayer culture and, in rBM culture, they failed to expand or form acini. MCF-10A cells with reduced BRM levels also proliferated more slowly on average in both monolayer and for the first 6 days in three-dimensional rBM culture.

Multiple methods confirmed the decrease in proliferation of both BRG1 and BRM knockdown MCF-10A cells. In monolayer culture, cells having reduced levels of BRG1 or BRM did not arrest in any specific phase of the cell cycle. BrdU incorporation kinetics definitively showed that cells having reduced levels of BRG1 or BRM simply took longer to traverse the cell cycle. The conclusions that can be reached from these studies are that BRG1 and BRM act as positive regulators of cell cycle progression and BRG1 is required for acinus formation in three-dimensional rBM culture.

MCF-10A cells expressing shRNA targeting either BRG1 or BRM showed nearly identical decreases in proliferation and increases in cell cycle length in monolayer culture. However, the cells remained proliferative, which suggests that either protein is sufficient to support some proliferation. The proteins are similar structurally and, while some functions are unique to one or the other ATPase (Kadam and Emerson, 2003), there are also circumstances where the one ATPase can compensate for the absence of the other (Reyes et al., 1998; Strobeck et al., 2002). Given that cells died when we attempted to knock down both BRG1 and BRM, and that in the absence of one protein the levels of the other increased (Fig. 2), we propose that either BRG1 or BRM is necessary to promote cell proliferation and that the cells undergo some form of compensation to increase the levels of the remaining protein when the other is knocked down.

Recently, two reports have established a BRG1 requirement for cell proliferation. These reports differ from the present study in the cell types examined, which suggests that the function of BRG1, and likely BRM, is cell context dependent. In several tumor cell lines with wild type p53, the depletion of BRG1, but not the depletion of BRM, led to activation of p53 and cell senescence (Naidu et al., 2009). In contrast, our results are

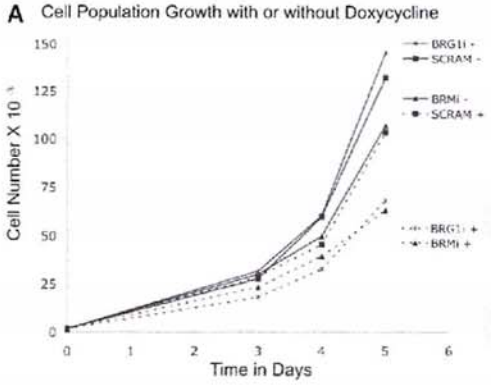

B Relative Cell Numbers with or without Doxycycline

Cells	± Dox	Time in Days 0	3	4	5
MCF-10A wt	-	100	100	100	100
MCF-10A wt	+	100	111 ± 13	105 ± 11	124 ±27
MCF-10A SCRAM	-	100	100	100	100
MCF-10A SCRAM	+	100	119 ± 17	130 ± 11	101 ± 11
MCF-10A BRG1i	-	100	100	100	100
MCF-10A BRG1i	+	100	71 ± 5	49 ± 12	48 ±9
MCF-10A BRMi	-	100	100	100	100
MCF-10A BRMi	+	100	71 ± 5	67 ± 8	50 ± 9

Fig. 5. The knockdown of BRG1 slowed proliferation in MCF-10A cells grown in monolayer culture. A: Growth curves for MCF-10A cells after BRG1 or BRM shRNA knockdown, or expressing a scrambled sequence shRNA (SCRAM). Cells were pre-incubated for 2 days with 0.05 μg/ml doxycycline (+) before being seeded in a 12-well dish at 1,500 cells per well at day 0. Control cells (−) were not treated with doxycycline and did not express the shRNA. Cells were trypsinized and then counted each day from day 2 to day 5. B: Cell proliferation was measured every day by quantifying DNA (Cyquant kit) in parallel with the cell counting of part A. The decrease of proliferation was quantified by calculating the ratio (%) of the cell number with doxycycline to the cell number of the matched doxycycline-free control.

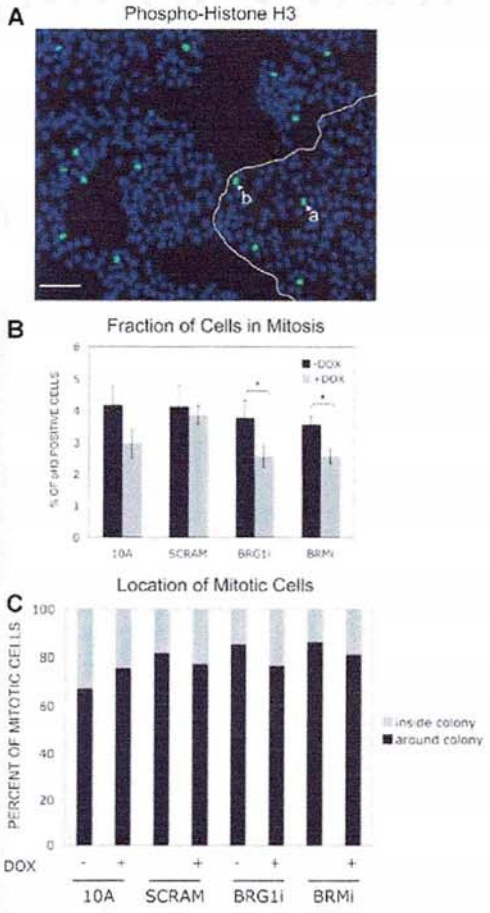

Fig. 6. The knockdown of BRG1 or of BRM reduced the percentage of cells MCF-10A cells in monolayer culture that were in mitosis. A: In this micrograph, nuclei are stained blue with DAPI and mitotic cells are identified by immunostaining for serine 10 phosphorylated Histone H3 (green) Size bar: 100 mm. The number of mitotic cells was determined, along with their position in the colonies. For example, on this picture, the white arrows show one peripheral (a) and one internal mitotic (b) cell. B: This histogram compares the percentage of mitotic cells at all positions within colonies after 7 days in the presence or absence of doxycycline. The asterisk indicates a difference that had statistical significance ($P \leq 0.05$). C: The position of mitotic cells in MCF-10A monolayer colonies was scored from micrographs including that of part A. The compiled data quantify the percentage of mitotic cells at the periphery of the colony and the percentage at interior positions. For each cell sample, n ≥ 2,000 cells.

in a non-tumorigenic cell and do not implicate the p53 pathway. A second study using adult fibroblasts from mice that are deficient for Brm and/or Brg1 showed that the absence of Brg1, but not the absence of Brm, decreased genome integrity, leading to aberrant mitoses and decreased proliferative capacity (Bourgo et al., 2009). In contrast, our results implicate both BRG1 and BRM in promoting cell proliferation.

Efforts to address the mechanisms responsible for decreased proliferation showed that neither the p53 nor the mTOR pathways were altered in BRG1 or BRM knockdown MCF-10A cells. We did find that BRM, but not BRG1, deficient cells contained elevated levels of the large non-coding RNA, GAS5. GAS5 is an inhibitor of cell cycle progression, but is also reported to sensitize cells to apoptotic signaling (Mourtada-Maarabouni et al., 2009). We observed no apoptosis after BRM knockdown. The correlation between cell cycle length and elevated GAS5 RNA was observed only for BRM-deficient MCF-10A cells, despite the similar decrease in cell proliferation rate observed after BRG1 knockdown. The mechanisms by which BRG1 and BRM alter cell cycle progression may be different.

BRG1 in breast cancer progression

There are numerous links between BRG1, BRM, and cancer. While Brg1 null mice are embryonic lethal, heterozygous Brg1

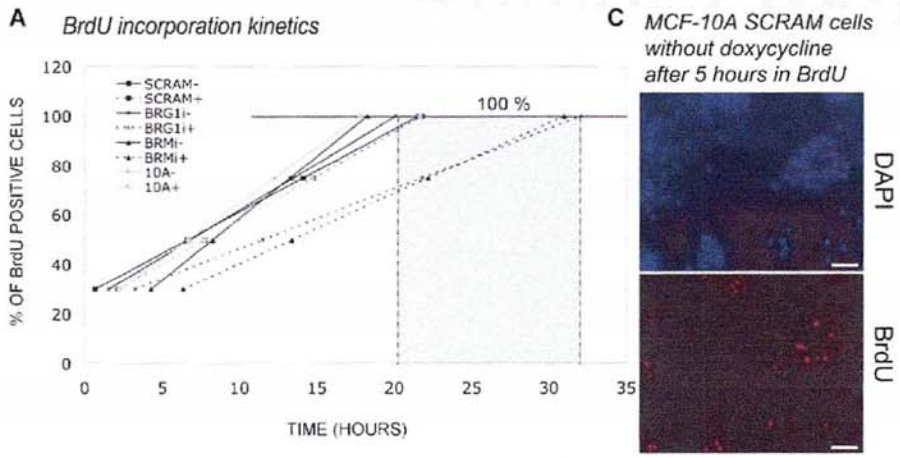

B Time in hours needed to label 30, 50, 75 and 100 % of cells with BrdU

% BrdU +	10A-	10A+	SCRAM-	SCRAM+	BRG1i-	BRG1i+	BRMi-	BRMi+
30	2.3	2.2	0.7	2.1	1.5	3.2	4.3	6.3
50	6.7	7.7	6.6	7.7	6.8	11.5	8.2	13.4
75	12.2	14.7	14.1	14.8	13.5	21.7	13.2	22.2
100	17.8	21.6	21.6	21.8	20.1	32.0	18.2	31.0

Fig. 7. The knockdown of BRG1 or of BRM increased the length of the cell cycle as determined by pulse labeling with BrdU. A: Cell cycle length was measured from a time course of BrdU incorporation. The graph plots the percent of BrdU positive cells as a function of time in hours. A linear extrapolation to the time when 100% of cells were BrdU-positive cells calculated the mean length of a single cell cycle. B: Calculated according to the linear regression method, the time in hours needed for 30%, 50%, 75% and 100% of cells to become BrdU-positive. C: A representative micrograph from which the measurements of parts A and B were made shows MCF-10A cells with the SCRAM control shRNA in absence of doxycycline after 5 h in BrdU. The number of BrdU positive cells (lower) and the number of total cells (upper, DAPI fluorescence) were counted. Seven fields were analyzed for each group in each of two independent experiments.

mice have an increased susceptibility to epithelial tumors of the breast (Bultman et al., 2000, 2008). Tissue-specific knockout of one Brg1 allele in the lung potentiates tumor formation in an induced carcinogenesis model (Glaros et al., 2008). In contrast,

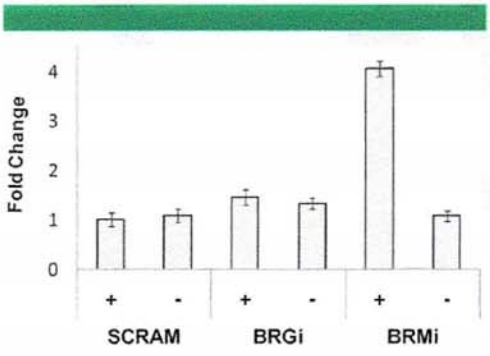

Fig. 8. Overexpression of GAS5 RNA in BRM, but not BRG1, deficient cells. Real-time PCR analysis of GAS5 RNA levels in each cell line. The data represent the mean plus or minus a standard deviation for three independent experiments.

Brm null mice are viable and do not have increased tumor rates, a result attributed to compensation for Brm loss by elevated levels of Brg1 (Reyes et al., 1998). In addition, the knockout of Brm does not cause additional tumors in Brg1+/− mice (Bultman et al., 2008). Despite the lack of tumor formation in Brm null mice, the levels and localization of BRM have prognostic value in staging human lung tumors (Reisman et al., 2003; Fukuoka et al., 2004).

Our results strongly suggest that, at least in normal mammary epithelial cells, reduction of BRG1 or BRM protein levels does not cause a loss of proliferation control leading to accelerated growth. These are different results than those obtained in prior studies using tumor cells, where loss of BRG1/BRM accelerates proliferation. This transformation-specific difference might be due to additional genetic lesions accumulating in cancer cells prior to loss of BRG1 or BRM function.

In conclusion, both BRG1 and BRM are positive regulators of normal mammary cell cycle progression. Despite previous studies indicating that loss of one Brg1 allele predisposes mice to breast tumors, significant reduction of BRG1 levels in normal but immortalized human mammary epithelial cells does not promote properties associated with tumor or transformed cells. This suggests that reduction of BRG1 levels is not sufficient for mammary epithelial cell transformation. BRG1 is required for acinus formation in three-dimensional rBM culture, a model system that recapitulates many aspects of normal breast tissue development. These results are consistent

with previous observations that functional SWI/SNF ATPases are necessary for the development and differentiation of many tissue types (reviewed in de la Serna et al., 2006). We propose that SWI/SNF ATPases, and BRG1 in particular, contribute to normal cell growth and differentiation, whereas the contribution of BRG1 deficiency to oncogenesis requires additional genetic changes.

Acknowledgments

This work was funded by the National Cancer Institute (PO1 CA82834). We thank Eric Campeau (UMass Medical School) for contributing LV vectors, including the pLenti 2X Puro DEST vector of his design, and for his advice and support. Timothy Pasek provided valuable technical assistance. Samisubbu Naidu and Elliott Androphy provided helpful discussion and antibodies, and Jean Underwood generously provided microscopy support. Core facilities were subsidized by Diabetes Endocrinology Research Center grant P30 DK32520.

Literature Cited

Ajiro K, Nishimoto T. 1985. Specific site of histone H3 phosphorylation related to the maintenance of premature chromosome condensation. Evidence for catalytically induced interchange of the subunits. J Biol Chem 260:15379–15381.

Ajiro K, Nishimoto T, Takahashi T. 1983. Histone H1 and H3 phosphorylation during premature chromosome condensation in a temperature-sensitive mutant (tsBN2) of baby hamster kidney cells. J Biol Chem 258:4534–4538.

Basle[OCR] LS. 1860. Examination of sputum from a case of cancer of the pharynx and the adjacent parts. Arch Med (London) 2:44.

Bourgo RJ, Siddiqui H, Fox S, Solomon D, Sansam CG, Yaniv M, Muchardt C, Metzger D, Chambon P, Roberts CW, Knudsen ES. 2009. SWI/SNF-Deficiency Results[OCR] in aberrant chromatin organization, mitotic failure, and diminished proliferative capacity. Mol Biol Cell.

Bridge AJ, Pebernard S, Ducraux A, Nicoulaz AL, Iggo R. 2003. Induction of an interferon response by RNAi vectors in mammalian cells. Nat Genet 34:263–264.

Bultman S, Gebuhr T, Yee D, La Mantia C, Nicholson J, Gilliam A, Randazzo F, Metzger D, Chambon P, Crabtree G, Magnuson T. 2000. A Brg1 null mutation in the mouse reveals functional differences among mammalian SWI/SNF complexes. Mol Cell 6:1287–1295.

Bultman SJ, Herschkowitz JI, Godfrey V, Gebuhr TC, Yaniv M, Perou CM, Magnuson T. 2008. Characterization of mammary tumors from Brg1 heterozygous mice. Oncogene 27:460–468.

Campeau E, Ruhl VE, Rodier F, Smith CL, Rahmberg BL, Fuss JO, Campisi J, Yaswen P, Cooper PK, Kaufman PD. 2009. A versatile viral system for expression and depletion of proteins in mammalian cells. PLoS ONE 4:e6529.

Chiba H, Muramatsu M, Nomoto A, Kato H. 1994. Two human homologues of *Saccharomyces cerevisiae* SWI2/SNF2 and *Drosophila brahma* are transcriptional coactivators cooperating with the estrogen receptor and the retinoic acid receptor. Nucleic Acids Res 22:1815–1820.

Coccia EM, Cicala C, Charlesworth A, Ciccarelli C, Rossi GB, Philipson L, Sorrentino V. 1992. Regulation and expression of a growth arrest-specific gene (gas5) during growth, differentiation, and development. Mol Cell Biol 12:3514–3521.

Coisy M, Roure V, Ribot M, Philips A, Muchardt C, Blanchard JM, Dantonel JC. 2004. Cyclin A repression in quiescent cells is associated with chromatin remodeling of its promoter and requires Brahma/SNF2alpha. Mol Cell 15:43–56.

Coisy-Quivy M, Disson O, Roure V, Muchardt C, Blanchard JM, Dantonel JC. 2006. Role for Brm in cell growth control. Cancer Res 66:5069–5076.

Dawson PJ, Wolman SR, Tait L, Heppner GH, Miller FR. 1996. MCF10AT: a model for the evolution of cancer from proliferative breast disease. Am J Pathol 148:313–319.

de La Serna IL, Carlson KA, Hill DA, Guidi CJ, Stephenson RO, Sif S, Kingston RE, Imbalzano AN. 2000. Mammalian SWI—SNF complexes contribute to activation of the hsp70 gene. Mol Cell Biol 20:2839–2851.

de la Serna IL, Ohkawa Y, Imbalzano AN. 2006. Chromatin remodelling in mammalian differentiation: lessons from ATP-dependent remodellers. Nat Rev Genet 7:461–473.

Debnath J, Mills KR, Collins NL, Reginato MJ, Muthuswamy SK, Brugge JS. 2002. The role of apoptosis in creating and maintaining luminal space within normal and oncogene-expressing mammary acini. Cell 111:29–40.

Debnath J, Muthuswamy SK, Brugge JS. 2003. Morphogenesis and oncogenesis of MCF-10A mammary epithelial acini grown in three-dimensional basement membrane cultures. Methods 30:256–268.

Diebold SS, Montoya M, Unger H, Alexopoulou L, Roy P, Haswell LE, Al-Shamkhani A, Flavell R, Borrow P, Reis e Sousa C. 2003. Viral infection non-plasmacytoid dendritic cells into high interferon producers. Nature 424:324–328.

Dimri GP, Lee X, Basile G, Acosta M, Scott G, Roskelley C, Medrano EE, Linskens M, Rubelj I, Pereira-Smith O., et al. 1995. A biomarker that identifies senescent human cells in culture and in aging skin in vivo. Proc Natl Acad Sci USA 92:9363–9367.

Dunaief JL, Strober BE, Guha S, Khavari PA, Alin K, Luban J, Begemann M, Crabtree GR, Goff SP. 1994. The retinoblastoma protein and BRG1 form a complex and cooperate to induce cell cycle arrest. Cell 79:119–130.

Eberlin A, Grauffel C, Oulad-Abdelghani M, Robert F, Torres-Padilla ME, Lambrot R, Spehner D, Ponce-Perez L, Wurtz JM, Stote RH, Kimmins S, Schultz P, Dejaegere A, Tora L. 2008. Histone H3 tails containing dimethylated lysine and adjacent phosphorylated serine modifications adopt a specific conformation during mitosis and meiosis. Mol Cell Biol 28:1739–1754.

Farrants AK. 2008. Chromatin remodelling and actin organisation. FEBS Lett 582:2041–2050.

Feoli F, Paesmans M, Van Eeckhout P. 2008. Fine needle aspiration cytology of the breast: impact of experience on accuracy, using standardized cytologic criteria. Acta Cytol 52:145–151.

Fukuoka J, Fujii T, Shih JH, Dracheva T, Meerzaman D, Player A, Hong K, Settnek S, Gupta A, Buetow K, Hewitt S, Travis WD, Jen J. 2004. Chromatin remodeling factors and BRM/BRG1 expression as prognostic indicators in non-small cell lung cancer. Clin Cancer Res 10:4314–4324.

Giardina C, Renzulli G, Serio G, Caniglia DM, Lettini T, Ferri C, D'Eredita G, Ricco R, Delfino VP. 1996. Nuclear morphometry in node-negative breast carcinoma. Anal Quant Cytol Histol 18:374–382.

Glaros S, Cirrincione GM, Palanca A, Metzger D, Reisman D. 2008. Targeted knockout of BRG1 potentiates lung cancer development. Cancer Res 68:3689–3696.

Goto H, Tomono Y, Ajiro K, Kosako H, Fujita M, Sakurai M, Okawa K, Iwamatsu A, Okigaki T, Takahashi T, Inagaki M. 1999. Identification of a novel phosphorylation site on histone H3 coupled with mitotic chromosome condensation. J Biol Chem 274:25543–25549.

Gray DS, Liu WF, Shen CJ, Bhadriraju K, Nelson CM, Chen CS. 2008. Engineering amount of cell-cell contact demonstrates biphasic proliferative regulation through RhoA and the actin cytoskeleton. Exp Cell Res 314:2846–2854.

Haroske G, Dimmer V, Friedrich K, Meyer W, Thieme B, Theissig F, Kunze KD. 1996. Nuclear image analysis of immunohistochemically stained cells in breast carcinomas. Histochem Cell Biol 105:479–485.

Hill DA, Chiosea S, Jamaluddin S, Roy K, Fischer AH, Boyd DD, Nickerson JA, Imbalzano AN. 2004. Inducible changes in cell size and attachment area due to expression of a mutant SWI/SNF chromatin remodeling enzyme. J Cell Sci 117:5847–5854.

Imbalzano AN, Kwon H, Green MR, Kingston RE. 1994. Facilitated binding of TATA-binding protein to nucleosomal DNA. Nature 370:481–485.

Imbalzano KM, Tatarkova I, Imbalzano AN, Nickerson JA. 2009. Increasingly transformed MCF-10A cells have a progressively tumor-like phenotype in three-dimensional basement membrane culture. Cancer Cell Int 9:7.

Kadam S, Emerson BM. 2003. Transcriptional specificity of human SWI/SNF BRG1 and BRM chromatin remodeling complexes. Mol Cell 11:377–389.

Khavari PA, Peterson CL, Tamkun JW, Crabtree GR. 1993. BRG1 contains a conserved domain of the SWI2/SNF2 family necessary for normal mitotic growth and transcription. Nature 366:170–174.

Kwon CS, Wagner D. 2007. Unwinding chromatin for development and growth: a few genes at a time. Trends Genet 23:403–412.

Kwon H, Imbalzano AN, Khavari PA, Kingston RE, Green MR. 1994. Nucleosome disruption and enhancement of activator binding by a human SW1/SNF complex. Nature 370:477–481.

Lelievre SA, Weaver VM, Nickerson JA, Larabell CA, Bhaumik A, Petersen OW, Bissell MJ. 1998. Tissue phenotype depends on reciprocal interactions between the extracellular matrix and the structural organization of the nucleus. Proc Natl Acad Sci USA 95:14711–14716.

Li DW, Yang Q, Chen JT, Zhou H, Liu RM, Huang XT. 2005. Dynamic distribution of Ser-10 phosphorylated histone H3 in cytoplasm of MCF-7 and CHO cells during mitosis. Cell Res 15:120–126.

Liu WF, Nelson CM, Pirone DM, Chen CS. 2006. E-cadherin engagement stimulates proliferation via Rac1. J Cell Biol 173:431–441.

Ma XM, Blenis J. 2009. Molecular mechanisms of mTOR-mediated translational control. Nat Rev Mol Cell Biol 10:307–318.

Marshall PN. 1983. Papanicolaou staining—A review. Microsc Acta 87:233–243.

Merlo GR, Basolo F, Fiore L, Duboc L, Hynes NE. 1995. p53-dependent and p53-independent activation of apoptosis in mammary epithelial cells reveals a survival function of EGF and insulin. J Cell Biol 128:1185–1196.

Miller FR, Soule HD, Tait L, Pauley RJ, Wolman SR, Dawson PJ, Heppner GH. 1993. Xenograft model of progressive human proliferative breast disease. J Natl Cancer Inst 85:1725–1732.

Mourtada-Maarabouni M, Hedge VL, Kirkham L, Farzaneh F, Williams GT. 2008. Growth arrest in human T-cells is controlled by the non-coding RNA growth-arrest-specific transcript 5 (GAS5). J Cell Sci 121:939–946.

Mourtada-Maarabouni M, Pickard MR, Hedge VL, Farzaneh F, Williams GT. 2009. GAS5, a non-protein-coding RNA, controls apoptosis and is downregulated in breast cancer. Oncogene 28:195–208.

Muchardt C, Yaniv M. 1993. A human homologue of *Saccharomyces cerevisiae* SNF2/SWI2 and *Drosophila* brm genes potentiates transcriptional activation by the glucocorticoid receptor. EMBO J 12:4279–4290.

Muller AJ, Chatterjee S, Teresky A, Levine AJ. 1998. The gas5 gene is disrupted by a frameshift mutation within its longest open reading frame in several inbred mouse strains and maps to murine chromosome 1. Mamm Genome 9:773–774.

Naidu SR, Love IM, Imbalzano AN, Grossman SR, Androphy EJ. 2009. The SWI/SNF chromatin remodeling subunit BRG1 is a critical regulator of p53 necessary for proliferation of malignant cells. Oncogene 28:2492–2501.

Nelson CM, Chen CS. 2003. VE-cadherin simultaneously stimulates and inhibits cell proliferation by altering cytoskeletal structure and tension. J Cell Sci 116:3571–3581.

Ohkawa Y, Marfella CG, Imbalzano AN. 2006. Skeletal muscle specification by myogenin and Mef2D via the SWI/SNF ATPase Brg1. EMBO J 25:490–501.

Petersen OW, Ronnov-Jessen L, Howlett AR, Bissell MJ. 1992. Interaction with basement membrane serves to rapidly distinguish growth and differentiation pattern of normal and malignant human breast epithelial cells. Proc Natl Acad Sci USA 89:9064–9068.

Phelan ML, Sif S, Narlikar GJ, Kingston RE. 1999. Reconstitution of a core chromatin remodeling complex from SWI/SNF subunits. Mol Cell 3:247–253.

Raho G, Barone V, Rossi D, Philipson L, Sorrentino V. 2000. The gas 5 gene shows four alternative splicing patterns without coding for a protein. Gene 256:13–17.

Reisman DN, Strobeck MW, Betz BL, Sciarlotta J, Funkhouser W Jr, Murchardt C, Yaniv M, Sherman LS, Knudsen ES, Weissman BE. 2002. Concomitant down-regulation of BRM and BRG1 in human tumor cell lines: differential effects on RB-mediated growth arrest vs CD44 expression. Oncogene 21:1196–1207.

Reisman DN, Sciarrotta J, Wang W, Funkhouser WK, Weissman BE. 2003. Loss of BRG1/BRM in human lung cancer cell lines and primary lung cancers: correlation with poor prognosis. Cancer Res 63:560–566.

Reyes JC, Barra J, Muchardt C, Camus A, Babinet C, Yaniv M. 1998. Altered control of cellular proliferation in the absence of mammalian brahma (SNF2alpha). EMBO J 17:6979–6991.

Roberts CW, Orkin SH. 2004. The SWI/SNF complex—Chromatin and cancer. Nat Rev Cancer 4:133–142.

Rosson GB, Bartlett C, Reed W, Weissman BE. 2005. BRG1 loss in MiaPaCa2 cells induces an altered cellular morphology and disruption in the organization of the actin cytoskeleton. J Cell Physiol 205:286–294.

Santner SJ, Dawson PJ, Tait L, Soule HD, Eliason J, Mohamed AN, Wolman SR, Heppner GH, Miller FR. 2001. Malignant MCF10CA1 cell lines derived from premalignant human breast epithelial MCF10AT cells. Breast Cancer Res Treat 65:101–110.

Shibata K, Inagaki M, Ajiro K. 1990. Mitosis-specific histone H3 phosphorylation in vitro in nucleosome structures. Eur J Biochem 192:87–93.

Sif S, Saurin AJ, Imbalzano AN, Kingston RE. 2001. Purification and characterization of mSin3A-containing Brg1 and hBrm chromatin remodeling complexes. Genes Dev 15:603–618.
Sledz CA, Holko M, de Veer MJ, Silverman RH, Williams BR. 2003. Activation of the interferon system by short-interfering RNAs. Nat Cell Biol 5:834–839.
Smith CM, Steitz JA. 1998. Classification of gas5 as a multi-small-nucleolar-RNA (snoRNA) host gene and a member of the 5'-terminal oligopyrimidine gene family reveals common features of snoRNA host genes. Mol Cell Biol 18:6897–6909.
Soule HD, Maloney TM, Wolman SR, Peterson WD Jr, Brenz R, McGrath CM, Russo J, Pauley RJ, Jones RF, Brooks SC. 1990. Isolation and characterization of a spontaneously immortalized human breast epithelial cell line, MCF-10. Cancer Res 50:6075–6086.
Strickland LB, Dawson PJ, Santner SJ, Miller FR. 2000. Progression of premalignant MCF10AT generates heterogeneous malignant variants with characteristic histologic types and immunohistochemical markers. Breast Cancer Res Treat 64:235–240.
Strobeck MW, Fribourg AF, Puga A, Knudsen ES. 2000a. Restoration of retinoblastoma mediated signaling to Cdk2 results in cell cycle arrest. Oncogene 19:1857–1867.
Strobeck MW, Knudsen KE, Fribourg AF, DeCristofaro MF, Weissman BE, Imbalzano AN, Knudsen ES. 2000b. BRG-1 is required for RB-mediated cell cycle arrest. Proc Natl Acad Sci USA 97:7748–7753.
Strobeck MW, Reisman DN, Gunawardena RW, Betz BL, Angus SP, Knudsen KE, Kowalik TF, Weissman BE, Knudsen ES. 2002. Compensation of BRG-1 function by Brm: Insight into the role of the core SWI-SNF subunits in retinoblastoma tumor suppressor signaling. J Biol Chem 277:4782–4789.
Strober BE, Dunaief JL, Guha [illegible], Goff SP. 1996. Functional interactions between the hBRM/hBRG1 transcriptional activators and the pRB family of proteins. Mol Cell Biol 16:1576–1583.
Trouche D, Le Chalony C, Muchardt C, Yaniv M, Kouzarides T. 1997. RB and hbrm cooperate to repress the activation functions of E2F1. Proc Natl Acad Sci USA 94:11268–11273.
Underwood JM, Imbalzano KM, Weaver VM, Fischer AH, Imbalzano AN, Nickerson JA. 2006. The ultrastructure of MCF-10A acini. J Cell Physiol 208:141–148.
Wagner S, Chiosea S, Nickerson JA. 2003. The spatial targeting and nuclear matrix binding domains of SRm160. Proc Natl Acad Sci USA 100:3269–3274.
Wang W, Xue Y, Zhou S, Kuo A, Cairns BR, Crabtree GR. 1996. Diversity and specialization of mammalian SWI/SNF complexes. Genes Dev 10:2117–2130.
Wang S, Fusaro G, Padmanabhan J, Chellappan SP. 2002. Prohibitin co-localizes with Rb in the nucleus and recruits N-CoR and HDAC1 for transcriptional repression. Oncogene 21:8388–8396.
Weaver VM, Howlett AR, Langton-Webster B, Petersen OW, Bissell MJ. 1995. The development of a functionally relevant cell culture model of progressive human breast cancer. Semin Cancer Biol 6:175–184.
Weaver VM, Petersen OW, Wang F, Larabell CA, Briand P, Damsky C, Bissell MJ. 1997. Reversion of the malignant phenotype of human breast cells in three-dimensional culture and in vivo by integrin blocking antibodies. J Cell Biol 137:231–245.
Weaver VM, Lelievre S, Lakins JN, Chrenek MA, Jones JC, Giancotti F, Werb Z, Bissell MJ. 2002. beta4 integrin-dependent formation of polarized three-dimensional architecture confers resistance to apoptosis in normal and malignant mammary epithelium. Cancer Cell 2:205–216.
Wei Y, Yu L, Bowen J, Gorovsky MA, Allis CD. 1999. Phosphorylation of histone H3 is required for proper chromosome condensation and segregation. Cell 97:99–109.
Wiznerowicz M, Trono D. 2003. Conditional suppression of cellular genes: lentivirus vector-mediated drug-inducible RNA interference. J Virol 77:8957–8961.
Yaswen P, Stampfer MR. 2002. Molecular changes accompanying senescence and immortalization of cultured human mammary epithelial cells. Int J Biochem Cell Biol 34:1382–1394.
Yoon DS, Wersto RP, Zhou W, Chrest FJ, Garrett ES, Kwon TK, Gabrielson E. 2002. Variable levels of chromosomal instability and mitotic spindle checkpoint defects in breast cancer. Am J Pathol 161:391–397.
Zhang HS, Gavin M, Dahiya A, Postigo AA, Ma D, Luo RX, Harbour JW, Dean DC. 2000. Exit from G1 and S phase of the cell cycle is regulated by repressor complexes containing HDAC-Rb-hSWI/SNF and Rb-hSWI/SNF. Cell 101:79–89.
Zink D, Fischer AH, Nickerson JA. 2004. Nuclear structure in cancer cells. Nat Rev Cancer 4:677–687.

Q1: Author: The Journal's copyeditors have taken care to format your authorship according to journal style (First name, Middle Initial, Surname). In the event a formatting error escaped their inspection, or there was insufficient information to apply journal style, please take a moment to review all author names and sequences to ensure the accuracy of the authorship in the published article. Please note that this information will also affect external indexes referencing this paper (e.g., PubMed).

Q2: Author: Please provide complete location.

Q3: Author: Please provide complete location.

Q4: Author: Please provide complete location.

Q5: Author: Please provide complete location.

Q6: Author: Please provide complete location.

Q7: Author: Please provide complete location.

Q8: Author: Please provide complete location.

Q9: Author: Please provide complete location.

Q10: Author: Please provide complete location.

Q11: Author: Please provide complete location.

Q12: Author: Please provide complete location.

Q13: Author: Please provide complete location.

Q14: Author: Please provide complete location.

Q15: Author: Please update.

Q16: Author: Please provide citations in the text for the following references: Beale, 1860, Farrants, 2008, Feoli et al., 2008, Giardina et al., 1996, Haroske et al., 1996, Hill et al., 2004, Marshall, 1983, Zink et al., 2004.

Q17: Author: Please provide the volume number and page range.

Q18: Author: Please provide the first name (initials) of the author.

Statement of Contribution

The following review and supporting figures for the working manuscript entitled, “Extracellular Matrix at a Glance,” contained contributions made by Kathleen M. Stewart, specifically, work pertaining to Aging and Fibrosis changes in the stroma and compilation of ECM mutations and murine mouse models.

The Extracellular Matrix at a Glance

Christian Frantz[1], Kathleen M. Stewart[1]and Valerie M. Weaver[1, 2, 3]

[1]Department of Surgery and Center for Bioengineering and Tissue Regeneration, University of California San Francisco, San Francisco, CA 94143
[2]Department of Anatomy and Bioengineering and Therapeutic Sciences, Eli and Edythe Broad Center of Regeneration Medicine and Stem Cell Research and Helen Diller Family Comprehensive Cancer Center, University of California San Francisco, San Francisco, CA 94143

[3]Address correspondence to:

Valerie M. Weaver
University of California, San Francisco
Center for Bioengineering and Tissue Regeneration
Department of Surgery
513 Parnassus Avenue, S1364C-0456
San Francisco, CA 94143
Email: Valerie.Weaver@ucsfmedctr.org
Telephone: (415) 476-3826
Fax: (415) 476-3985

In all tissues and organs, the extracellular matrix (ECM), composed of water, proteins and polysaccharides, provides scaffolding for the present cellular component. The composition and enzymes present in the ECM is determined by the cells contained within and in contact with the matrix itself (fibroblasts, epithelial cells etc.). It is a dynamic structure, constantly remodeled by enzymatic and non-enzymatic reactions and by post-translational modifications of its components. The ECM plays many important roles, it provides the mechanical properties of the organs (tensile and compressive strength and elasticity), protection (provides buffering to maintain extracellular homeostasis and retains water) and organization (binding of growth factors and interaction with cell-surface receptors controls cell behavior). Each of these roles (mechanical, protection and organization) can vary greatly from one tissue to another (lungs vs. skin vs. bones for example) or from one pathological state of the tissue to another (normal epithelial ECM vs. tumor ECM for example). The molecular and cellular composition of the ECM is also tissue specific and changes during pathological conditions. In this Cell Science at a Glance article, we will first describe briefly the major molecular components of the ECM and then compare the ECM of normal tissues vs. pathologically modified tissue ECMs (aged tissue, wounded or fibrotic tissue and tumor tissue). We will focus on the cellular and molecular composition, on the topology, mechanical properties and post-translational modifications, on the signaling factors involved in ECM remodeling and induced cellular responses and on forces exerted in the different ECMs. For a purpose of clarity and article size limitation, we will focus mainly on the stroma

of epithelial tissues (glands, lungs, skin etc.). We will finally discuss the recent use of synthetic extracellular matrices that provide a more physiologically relevant three dimensional environment from which to study cellular biology and the potential applications of these three dimensional substrata in regenerative medicine research.

Molecular component of the ECM

The matrix is composed of two main classes of macromolecules: glycosaminoglycans (GAGs) which are formed from unbranched polysaccharide chains that are covalently linked to protein in the form of proteoglycans and fibrous proteins, including collagens, elastins, fibronectins and laminins [Alberts B et al, 2002]. A summary of some ECM components and their structure can be found in panel 1 of the poster. Mouse models have been established for most of these molecules, displaying a range in the severity of phenotypes, but also demonstrating the importance of the ECM in tissue and organ formation (summarized in table 1). Glycosaminoglycans fill most of the extracellular space in the form of hydrated gels. They are unbranched polysaccharide chains composed of repeating disaccharide units (sulfated *N*-aceltylglucosamine or *N*-acetylgalactosamine and glucuronic or iduronic acid) and form four main groups: hyaluronic acid, chondroitin sulfate, heparan sulfate and keratan sulfate (Iozzo and Murdoch). They are extremely hydrophilic, thus adopt highly extended conformations and form hydrogels, enabling the matrix to withstand compressive forces. Except for hyaluronic acid, all GAGs form covalent bonds to a core

protein in the form of proteoglycans (Iozzo and Murdoch). Core proteins and attached GAG chains can vary greatly, giving rise to unlimited heterogeneity. For example, aggrecan, a large proteoglycan has over 100 GAG chains while decorin has only a single GAG chain. They have a wide range of function: perlecan act as sieves in the kidney, decorin, biglycan and lumican can bind to collagen fibers (Iozzo and Murdoch). Proteoglycans in general can bind and store growth factors at the proximity of the cell plasma membrane.

Amongst the fibrous proteins composing the ECM, collagen is the most abundant, constituting almost 30% of the total protein mass in multicellular animals. Collagens provide ECM structure and tensile strength. Additionally, collagens are involved in cell adhesion, chemotaxis, and migration, and play an important role in development (ref). Most of the collagen is secreted by fibroblasts. At least 27 collagen types have been identified in vertebrates (Myllyharju and Kivirikko). A collagen molecule is long, stiff and forms a triple-stranded helix. They assemble in supramolecular complexes such as fibrils and networks, depending on the type of collagen (see panel 1) and can have tissue specific distribution. Fibrous collagens form the collagen fibril bundles in the stroma while network collagens are part of the basement membrane. Collagen synthesis involves many enzymatic post-translational modifications (Myllyharju and Kivirikko) consisting mainly in proline and lysine hydroxylation, lysine glycosylation and cleavage of N and C-terminal propeptides. After cleavage, collagen fibrils are strengthened by covalent crosslinking between lysine residues of the constituent collagen molecules by lysyl oxidases (LOX) (Myllyharju and

Kivirikko; Robins). Fibroblasts, by exerting tension on the matrix, organize collagen fibrils into sheets and cables and influence alignment of collagens fibers. Collagen fibers are usually a heterogeneous mix of different types of collagens, with one type of collagen being the most predominant. Collagen is also associated with elastins.

One other major fibrous ECM protein is elastin. Elastin fibers provide recoil to tissues that undergo repeated stretch and its stretch is limited by its association with collagen fibrils. Secreted tropoelastin fibers assemble in fibers and become highly crosslinked to one another between lysines by LOX. Elastin fibers are covered by glycoproetic microfibrils, mainly fibrillins, which are essential for the fiber's integrity.

A third fibrous protein, fibronectin (FN) organizes the matrix and help cells to attach to it. FN is secreted in the form of a dimer joined by two C-terminal disulfide bonds. FN has several binding sites, to other FN dimers, collagen, heparin and cell surface integrin receptors (Pankov and Yamada). Cell surface binding of soluble FN dimers is essential for its assembly into longer fibrils. Cell contraction through the actomyosin cytoskeleton and the resulting integrin clustering promotes FN fibril assembly by exposing cryptic binding sites allowing them to bind one another (Leiss et al.; Mao and Schwarzbauer; Vakonakis and Campbell).

FN is additionally important for cell migration during development. Contrary to fibronectin's molecular properties, other extracellular matrix proteins like tenascins can act as anti-adhesive molecule during cell migration (Chiquet-Ehrismann).

The matrix forms a basement membrane (BM) at the interface between the epithelium and the stroma or connective tissue. The BM is a thin and flexible specialized extracellular matrix underlying all epithelia and is secreted by the cells that rest upon it (LeBleu et al., 2007). The BM is mainly composed of type IV collagen, the heparan sulfate proteoglycan perlecan and the glycoproteins laminin and nidogen/entactin. For reasons of concision, this review will mainly focus on the ECM underlying the BM, forming the interstitial stroma.

The stromal ECM is modified dramatically during aging, wound healing and tumorigenesis. In the following paragraphs, we will discuss the changes occurring to the composition, topology, mechanical properties and signaling events in the ECM during these processes.

ECM of a normal epithelial tissue under tissue homeostasis

In a normal healthy epithelium, epithelial cells adopt an apical-basal polarity, with the basal side in contact with the BM and a lumen at the apical side. The stroma contains fibroblasts and infiltrated leukocytes. Fibroblasts are the major cells of the stroma. They secrete and reorganize the components of the stromal ECM, mainly collagen type I, elastin, fibronectin and GAGs (hyaluronic acid, decorin, tenascin etc…). The ECM is kept under tensional homeostasis and

is compliant in nature, formed by a meshwork of relaxed collagen type I and elastin fibers, and fibrillar fibronectin, all of which are embedded in a glycosaminoglycan chain hydrogel (Bosman and Stamenkovic, 2003). The matrix resists tensile (via collagen and elastin fibers) and compressive (via the hydrated GAGs network) stresses. Binding of proteoglycans to collagen fibers can modify its mechanical properties (Scott, 2003). Even in a normal tissue, the ECM is in a dynamic process of continuous remodeling. Metalloproteinases (MMPs) secreted by fibroblasts participate in this process by degrading all of the components of the ECM (Mott and Werb, 2004). However, to maintain tissue homeostasis, MMP activity is balanced by tissue inhibitors of metalloproteinases (TIMPs) (Malemud, 2006). Other stromal enzymes like LOXs and transglutaminases also retain a low activity level, keeping collagen and elastin fibers in a relaxed state (Bolognia). Growth factors can be found bound to proteoglycans (for example syndecans and heparan sulfate bind FGF and decorin bind TGF-) (Macri et al., 2007; Murakami et al., 2008). These growth factors are released when the matrix is remodeled and can activate resident fibroblasts. Under pathological conditions (*ie* aging, wounding or cancer) the ECM composition, topology and mechanical properties are modified in specific manners.

Aged Tissue

When tissue ages, gaps begin to appear between epithelial cells due to reduction or complete loss of cadherins, catenins, occludins and other junctional proteins (Akintola et al., 2008; Bolognia, 1995; Lapiere, 1990) and the BM is degraded and becomes thinner (Callaghan and Wilhelm, 2008). Stromal fibroblasts can become senescent (growth arrest, altered functions and resistant to apoptotic signals) (Krtolica and Campisi, 2003). Senescent fibroblasts show increased expression of FN, MMPs (MMP-2, -3 and -9 specifically), EGF-like growth factors (ie heregulin), cytokines (IL-1 , -6 and -8) and plasminogen activator inhibitor (PAI) (Krtolica and Campisi, 2002). Additionally, mitochondrial-related reactive oxygen species (ROS) are produced and present in the ECM (Untergasser et al., 2005). The cytokines released induce infiltration of leukocytes. Secretion of MMPs, PAI and ROS leads to the degeneration of the elastin network, decreased total amount of GAGs (with however an increase in the ration of decorin (Nomura)), partial degradation of collagen fibers (Calleja-Agius et al., 2007) and to a thinning of the BM (Callaghan and Wilhelm, 2008). In an aging tissue, collagen fibers become inappropriately cross-linked via glycation, lipid oxidation byproducts and UV-induced cross-linking in the skin (Robins). These changes in the amount of collagen cross-linking and degradation of ECM proteins alter the tensile properties of the tissue by stiffening the ECM even if it contains less collagen and elastin fibers. The increased stiffness of the stroma exerts forces on the aged epithelium and on the weak BM, which is now less resistant to the stromal pressure. The combination of stiffened matrix and

presence of senescent fibroblasts has been shown to promote the development of age-related epithelial cancers (Krtolica and Campisi, 2002; Paszek and Weaver, 2004; Sprenger et al., 2008). Stiffened matrix is also found in wounded, fibrotic tissue and in tissue surrounding tumors.

Wounded and fibrotic tissue

Acute injury activates the fibrogenic machinery to induce wound healing. The BM is disrupted, epithelial cells loose their apical-basal polarity and cell-cell contacts, and may undergo epithelial-to-mesenchymal transition (EMT) and migrate to close the wound (Kisseleva and Brenner; Schafer and Werner). Fibroblasts migrate into the wound, where they proliferate and produce large amounts of ECM proteins. Vascular damage due to injury leads to inflammation of the tissue and fibrosis. Macrophages, neutrophils and lymphocytes infiltrate the ECM surrounding the damaged site. Cytokines (TGF- and CTGF) liberated by recruited macrophages and apoptotic parenchymal cells induces the generation of myofibroblasts, the primary source of collagens during wound healing (De Wever et al.; Desmouliere et al., 2004; Kisseleva and Brenner; Schafer and Werner). Multiple sources of myofibroblasts have been identified: resident fibroblasts, cells having undergone EMT and fibrocytes recruited from the bone marrow (Desmouliere et al., 2004; Kisseleva and Brenner). These myofibroblasts undergo apoptosis once the wound is resolved. Activated myofibroblasts induce production and deposition of collagen types I and III, fibronectin and hyaluronic acid. Enhanced contractile forces produced by

myofibroblasts induce the formation of larger, more rigid collagen bundles, which are additionally cross-linked and strengthened by the activity of lysyl-oxidases [REF]. An additionnal source of TGF- is ECM-bound TGF- released by increased MMP expression. It is now well known that TGF- can lead to epithelial-to-mesenchymal transition (EMT) of epithelial cells and induce migration to resolve the wound. In the absence of continuous injury, the induced fibrosis is reversed. Under chronic tissue damage, the matrix is continuously produced and remodeled by collagen and TGF- autoactivated myofibroblasts, TIMP production is prevalent over MMPs, and the vasculature is remodeled (Kisseleva and Brenner, 2008). Matrix remodeling and cross-linking during wound repair and fibrosis leads to reduced mechanical stability, decreased tensile strength and elasticity in scarred tissues (Schafer and Werner). Dividing and migrating cells at the edge of a wound exert a compression force on the underlying stroma. This force is countered by a reciprocal resistance force by the stiffened stroma, additionally stiffened by contraction forces exerted by migrating cells and myofibroblasts (Paszek and Weaver, 2004). These forces could participate in preventing the wound to resolve and therefore induce chronic fibrosis.

Tumor tissue

Tumors have been compared to wounds that do not heal (Dvorak; Schafer and Werner). A tumor can be formed from proliferating transformed epithelial cells that lose their apical-basal polarity and their cell-cell junctions. They eventually can become metastatic. In the tumor stroma, stromal fibroblasts can differentiate by the same mechanisms described for the wound stroma. These differentiated fibroblasts have been classified in four cell types: peritumoral fibroblasts, reactive stromal fibroblasts, cancer-associated fibroblasts and myofibroblasts (De Wever et al., 2008). Additionally, inflammatory cells, immunocytes and macrophages are infiltrating the stromal ECM in large quantities (Tan and Coussens, 2007). Similar to fibrosis, myofibroblasts deposit increasing quantities of collagen type I, III and IV, elastin, fribronectin, tenascin, and proteoglycans (fibrillin, decorin, biglycan, lumican, fibromodulin etc…) and producing growth factors (TGF-β, FGF, VEGF…) surrounding the tumor and leading to a desmoplasmic stroma (De Wever et al., 2008; Desmouliere et al., 2004). In the tumor stroma, collagen and elastin fibers are reoriented and cross-linked to form larger, more rigid bundles and the fibronectin meshwork is denser. Increased cross-linking is due to elevated expression of LOX and transglutaminases (Erler and Weaver, 2009). The ECM surrounding the tumor stiffens, resulting in reduced elasticity. Importantly, it is now clear that matrix stiffening enhances tumor cell survival, migration and growth and increases tumor angiogenesis (Erler and Weaver; Erler and Weaver, 2009; Paszek and Weaver; Paszek et al.). MMPs are released and activated by tumor cells and

myofibroblasts (De Wever et al.), resulting in pockets of compliancy within the heterogeneous tumor. MMP proteolysis releases and activates ECM-embedded growth factors such as VEGF bound to heparin sulfate proteoglycans and TGF- bound to fibrillin and decorin (Bosman and Stamenkovic, 2003). VEGF enhances vascular permeability and promotes new vessel growth while TGF- induces differentiation of fibroblasts into myofibroblasts. TGF- also serves as a chemoattractant for inflammatory cells and stimulates the production of FN and collagen by myofibroblasts, which in turn produce more TGF- . Recruited macrophages, in addition to producing ROS, also produce TGF- and PDGF. Many chemokines/growth factors (PDGF, EGF, bFGF, TGF- …) are produced by tumor cells and these all contribute to activation of myofibroblasts (De Wever et al.). As a consequence of all these ECM transformations, the “force map” of a tumor ECM is drastically different from the ECM in normal healthy tissue: proliferating transformed epithelium is exerting a chronic incremental compression force on the BM and the surrounding stromal tissue; these forces are countered by a reciprocal resistance force by the stiffened stroma, additionally stiffened by contraction forces exerted by migrating cells and myofibroblasts and by liquid pressure from leaky blood vessels (Paszek MJ and Weaver VM, 2004).

Perspectives: Synthetic extracellular matrices

Publications describing and applying synthetic extracellular matrices to biological research has increased exponentially, with powerful applications in the field of regenerative medicine. Critical features needed for these matrices to be biocompatible, to be able to be used as an ECM scaffold are: to support host cell attachment via integrins, to be degradable by MMPs and to have appropriate biomechanical properties (Badylak; Lutolf and Hubbell; Rosso et al.; Zisch et al.). These matrices should be adjustable to a specific biological environment to obtain cell- and tissue-specificity. Panel 2 describes a few examples of now commonly used naturally derived and semi-synthetic matrices. Matrigel®, derived from Engelbreth-Holm-Swarm mouse carcinoma, mimics the BM. It has been used in two- and three-dimensional cell cultures, in tissue explants, in tissue engineering using stem cells and in tissue transplant studies (Kleinman and Martin, 2005). Other intact ECM scaffolds have been harvested from various tissues (small intestine, skin, pancreas etc…) and are available for clinical use (an extensive list of these ECM materials can be found in (Badylak)). One of the most widely used and characterized is derived from porcine small intestinal submucosa (SIS). Purified components of the ECM, for example collagen (type I, fibronectin, fibril and hyaluronic acid) have also been used (Rosso et al.). The advantage of these purified matrices is that the biochemical and mechanical properties can be controlled. Additionally, HA can be functionalized, cross-linked with gelatin for example, to sustain cell adhesion (Serban et al., 2008). Semi-synthetic matrices have also been developed utilizing the inherent properties of

peptides to self assemble or the properties of poly(ethylene glycol) (PEG) macromers to form 3D hydrated networks. PEG hydrogels can be engineered to sustain cell adhesion (Lutolf and Hubbell, 2005) to be degradable by MMPs (Ehrbar et al., 2007) and to covalently incorporate growth factors (Zisch et al.). Recently, peptide-based hydrogels have emerged as a suitable tool to mimic the ECM (Ulijn and Smith). Peptide-amphiphiles, capable of self assembly, have been used to mimic the collagen triple helix super secondary structure (Smith and Ma). Like PEG gels, these peptide gels can be designed to be cleaved by specific enzymes (Ulijn and Smith). Finally, functionalized polyacrylamide gels cross-linked with Matrigel, collagen type I or fibronectin can be used as an easy tool to mimic various tissue compliancies and ECM microenvironments (Johnson et al.; Pelham and Wang). Collectively these new advances in matrix biology have allowed for major progress in regenerative medicine and stem cell biology (Daley et al.), and these synthetic matrices permit substantial breakthroughs in celllular biology through the application of three-dimensional cell culture systems that are closer to physiological conditions [debnath, Bissell etc], and through the ability of creating micropatterned surfaces facilitating the understanding of how adhesive (cell-ECM adhesion), structural (cell shape) and mechanical cues (force associated with ECM interactions) regulate cell fate (Kandere-Grzybowska et al.; Pirone and Chen).

References

Akintola, A. D., Crislip, Z. L., Catania, J. M., Chen, G., Zimmer, W. E., Burghardt, R. C. and Parrish, A. R. (2008). Promoter methylation is associated with the age-dependent loss of N-cadherin in the rat kidney. *Am J Physiol Renal Physiol* **294**, F170-6.

Badylak, S. F. (2007). The extracellular matrix as a biologic scaffold material. *Biomaterials* **28**, 3587-93.

Bolognia, J. L. (1995). Aging skin. *Am J Med* **98**, 99S-103S.

Bosman, F. T. and Stamenkovic, I. (2003). Functional structure and composition of the extracellular matrix. *J Pathol* **200**, 423-8.

Callaghan, T. M. and Wilhelm, K. P. (2008). A review of ageing and an examination of clinical methods in the assessment of ageing skin. Part 2: Clinical perspectives and clinical methods in the evaluation of ageing skin. *Int J Cosmet Sci* **30**, 323-32.

Calleja-Agius, J., Muscat-Baron, Y. and Brincat, M. P. (2007). Skin ageing. *Menopause Int* **13**, 60-4.

Chiquet-Ehrismann, R. (2004). Tenascins. *Int J Biochem Cell Biol* **36**, 986-90.

Daley, W. P., Peters, S. B. and Larsen, M. (2008). Extracellular matrix dynamics in development and regenerative medicine. *J Cell Sci* **121**, 255-64.

De Wever, O., Demetter, P., Mareel, M. and Bracke, M. (2008). Stromal myofibroblasts are drivers of invasive cancer growth. *Int J Cancer* **123**, 2229-38.

Desmouliere, A., Guyot, C. and Gabbiani, G. (2004). The stroma reaction myofibroblast: a key player in the control of tumor cell behavior. *Int J Dev Biol* **48**, 509-17.

Dvorak, H. F. (1986). Tumors: wounds that do not heal. Similarities between tumor stroma generation and wound healing. *N Engl J Med* **315**, 1650-9.

Ehrbar, M., Rizzi, S. C., Schoenmakers, R. G., Miguel, B. S., Hubbell, J. A., Weber, F. E. and Lutolf, M. P. (2007). Biomolecular hydrogels formed and degraded via site-specific enzymatic reactions. *Biomacromolecules* **8**, 3000-7.

Erler, J. T. and Weaver, V. M. (2009). Three-dimensional context regulation of metastasis. *Clin Exp Metastasis* **26**, 35-49.

Iozzo, R. V. and Murdoch, A. D. (1996). Proteoglycans of the extracellular environment: clues from the gene and protein side offer novel perspectives in molecular diversity and function. *Faseb J* **10**, 598-614.

Johnson, K. R., Leight, J. L. and Weaver, V. M. (2007). Demystifying the effects of a three-dimensional microenvironment in tissue morphogenesis. *Methods Cell Biol* **83**, 547-83.

Kandere-Grzybowska, K., Campbell, C., Komarova, Y., Grzybowski, B. A. and Borisy, G. G. (2005). Molecular dynamics imaging in micropatterned living cells. *Nat Methods* **2**, 739-41.

Kisseleva, T. and Brenner, D. A. (2008). Mechanisms of fibrogenesis. *Exp Biol Med (Maywood)* **233**, 109-22.

Kleinman, H. K. and Martin, G. R. (2005). Matrigel: basement membrane matrix with biological activity. *Semin Cancer Biol* **15**, 378-86.

Krtolica, A. and Campisi, J. (2002). Cancer and aging: a model for the cancer promoting effects of the aging stroma. *Int J Biochem Cell Biol* **34**, 1401-14.

Krtolica, A. and Campisi, J. (2003). Integrating epithelial cancer, aging stroma and cellular senescence. *Adv Gerontol* **11**, 109-16.

Lapiere, C. M. (1990). The ageing dermis: the main cause for the appearance of 'old' skin. *Br J Dermatol* **122 Suppl 35**, 5-11.

LeBleu, V. S., Macdonald, B. and Kalluri, R. (2007). Structure and function of basement membranes. *Exp Biol Med (Maywood)* **232**, 1121-9.

Leiss, M., Beckmann, K., Giros, A., Costell, M. and Fassler, R. (2008). The role of integrin binding sites in fibronectin matrix assembly in vivo. *Curr Opin Cell Biol* **20**, 502-7.

Lutolf, M. P. and Hubbell, J. A. (2005). Synthetic biomaterials as instructive extracellular microenvironments for morphogenesis in tissue engineering. *Nat Biotechnol* **23**, 47-55.

Macri, L., Silverstein, D. and Clark, R. A. (2007). Growth factor binding to the pericellular matrix and its importance in tissue engineering. *Adv Drug Deliv Rev* **59**, 1366-81.

Malemud, C. J. (2006). Matrix metalloproteinases (MMPs) in health and disease: an overview. *Front Biosci* **11**, 1696-701.

Mao, Y. and Schwarzbauer, J. E. (2005). Fibronectin fibrillogenesis, a cell-mediated matrix assembly process. *Matrix Biol* **24**, 389-99.

Mott, J. D. and Werb, Z. (2004). Regulation of matrix biology by matrix metalloproteinases. *Curr Opin Cell Biol* **16**, 558-64.

Murakami, M., Elfenbein, A. and Simons, M. (2008). Non-canonical fibroblast growth factor signalling in angiogenesis. *Cardiovasc Res* **78**, 223-31.

Myllyharju, J. and Kivirikko, K. I. (2004). Collagens, modifying enzymes and their mutations in humans, flies and worms. *Trends Genet* **20**, 33-43.

Nomura, Y. (2006). Structural change in decorin with skin aging. *Connect Tissue Res* **47**, 249-55.

Pankov, R. and Yamada, K. M. (2002). Fibronectin at a glance. *J Cell Sci* **115**, 3861-3.

Paszek, M. J. and Weaver, V. M. (2004). The tension mounts: mechanics meets morphogenesis and malignancy. *J Mammary Gland Biol Neoplasia* **9**, 325-42.

Paszek, M. J., Zahir, N., Johnson, K. R., Lakins, J. N., Rozenberg, G. I., Gefen, A., Reinhart-King, C. A., Margulies, S. S., Dembo, M., Boettiger, D. et al. (2005). Tensional homeostasis and the malignant phenotype. *Cancer Cell* **8**, 241-54.

Pelham, R. J., Jr. and Wang, Y. (1997). Cell locomotion and focal adhesions are regulated by substrate flexibility. *Proc Natl Acad Sci U S A* **94**, 13661-5.

Pirone, D. M. and Chen, C. S. (2004). Strategies for engineering the adhesive microenvironment. *J Mammary Gland Biol Neoplasia* **9**, 405-17.

Robins, S. P. (2007). Biochemistry and functional significance of collagen cross-linking. *Biochem Soc Trans* **35**, 849-52.

Rosso, F., Marino, G., Giordano, A., Barbarisi, M., Parmeggiani, D. and Barbarisi, A. (2005). Smart materials as scaffolds for tissue engineering. *J Cell Physiol* **203**, 465-70.

Schafer, M. and Werner, S. (2008). Cancer as an overhealing wound: an old hypothesis revisited. *Nat Rev Mol Cell Biol* **9**, 628-38.

Scott, J. E. (2003). Elasticity in extracellular matrix 'shape modules' of tendon, cartilage, etc. A sliding proteoglycan-filament model. *J Physiol* **553**, 335-43.

Serban, M. A., Scott, A. and Prestwich, G. D. (2008). Use of hyaluronan-derived hydrogels for three-dimensional cell culture and tumor xenografts. *Curr Protoc Cell Biol* **Chapter 10**, Unit 10 14.

Smith, L. A. and Ma, P. X. (2004). Nano-fibrous scaffolds for tissue engineering. *Colloids Surf B Biointerfaces* **39**, 125-31.

Sprenger, C. C., Plymate, S. R. and Reed, M. J. (2008). Extracellular influences on tumour angiogenesis in the aged host. *Br J Cancer* **98**, 250-5.

Tan, T. T. and Coussens, L. M. (2007). Humoral immunity, inflammation and cancer. *Curr Opin Immunol* **19**, 209-16.

Ulijn, R. V. and Smith, A. M. (2008). Designing peptide based nanomaterials. *Chem Soc Rev* **37**, 664-75.

Untergasser, G., Madersbacher, S. and Berger, P. (2005). Benign prostatic hyperplasia: age-related tissue-remodeling. *Exp Gerontol* **40**, 121-8.

Vakonakis, I. and Campbell, I. D. (2007). Extracellular matrix: from atomic resolution to ultrastructure. *Curr Opin Cell Biol* **19**, 578-83.

Zisch, A. H., Lutolf, M. P. and Hubbell, J. A. (2003). Biopolymeric delivery matrices for angiogenic growth factors. *Cardiovasc Pathol* **12**, 295-310.

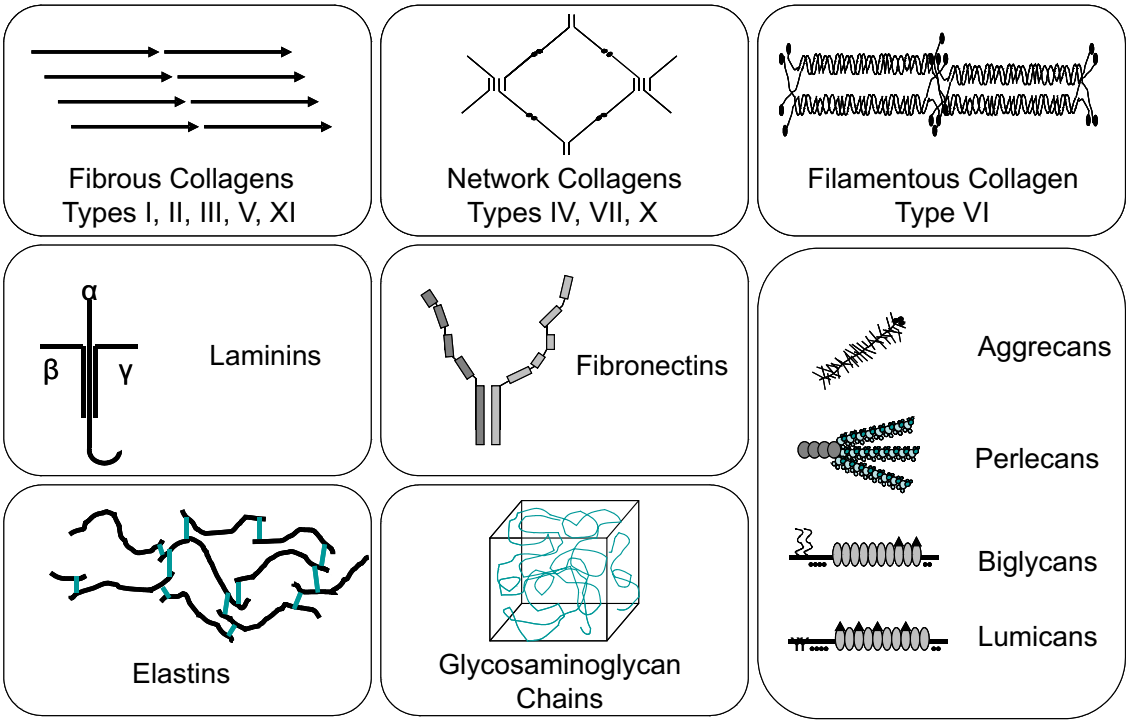

Figure 5.1 ECM Components

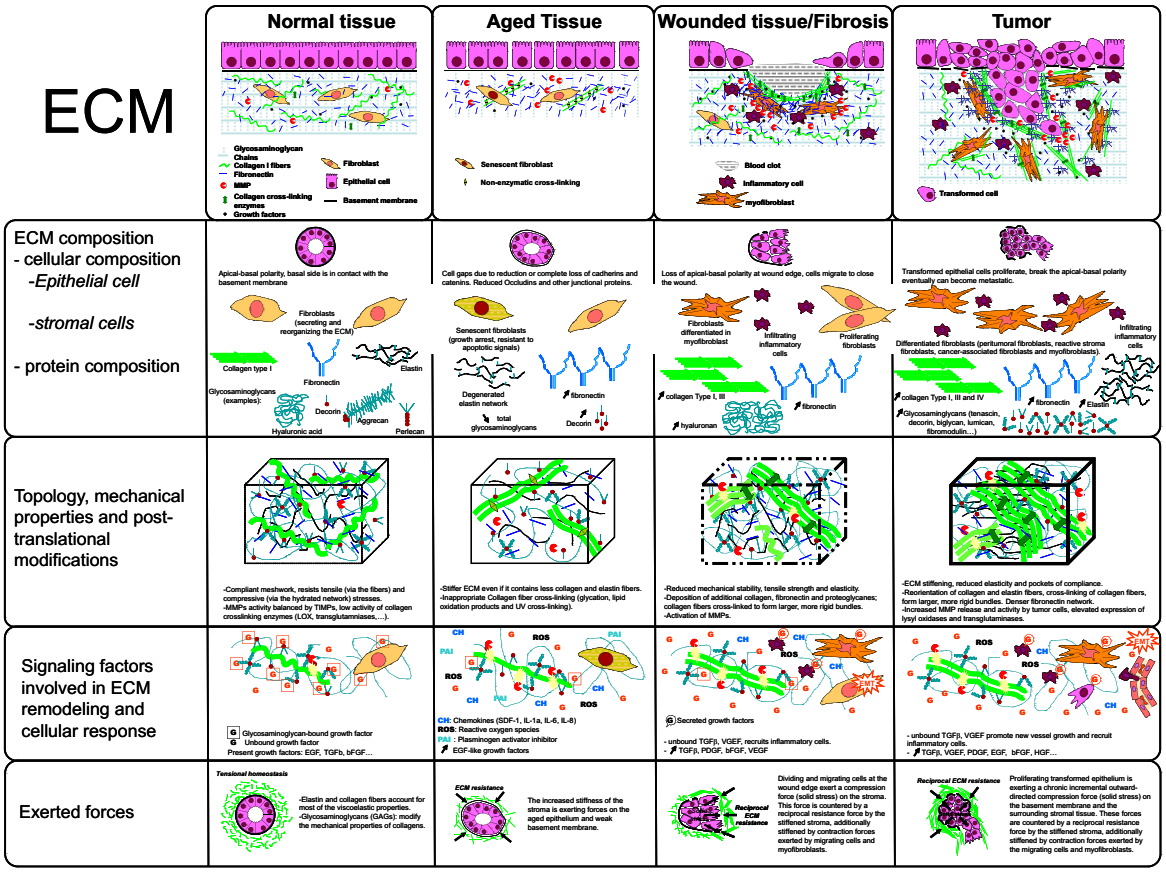

Figure 5.2 ECM Changes at a glance.

Unpublished Methods

3D Start to Finish Protocol

SOLUTIONS

1.5X Cytoskeleton Extraction Buffer (40mL)

1.2mL 5M NaCl

18mL 1M sucrose

600ul 1M PIPES pH6.7

2mL 100mM MgCl2

18.2mL ddH2O

adjust pH to 6.7 with 1N NaOH, store at 4ºC

Protease Inhibitors (per 1.2mL 1X Extraction Buffer)

12ul 0.5M EDTA

2.4ul 1mg/mL

2.4ul 1mg/mL

1.26ul 10mg/mL E-64

1.2ul 1M NaF

1.2ul 2mg/mL Pepstatin

12ul 100mM Benzamidine

8ul 125mM Na orthovanidate

12ul 100mM Pefabloc SC-

7.5X DMEM:F12 (per 100uL)

75ul 10X DMEM

7.5ul 1M HEPES ph= 7.5-8.0

15ul 6% sodium bicarbonate solution

2.5ul ddH2O

2% Paraformaldehyde (quick method)—need for both 3D methods

For 50mL:

Add 25mL ddH20 to a 50mL conical tube

Add 1g Paraformaldehyde powder (stored at 4 degrees)

Warm in the microwave for 10 seconds, swirl, heat 10 seconds more (DO NOT BOIL!!!)

Add 5ul 2N NaOH

Warm again carefully until dissolved to a clear liquid

Add 5mL 10X PBS

Add 20mL ddH20

PH to 7.3-7.5

Store in a dark glass at 4 degrees

PBS / Glycine (10X Stock) –need for both 3D methods

1.3 M NaCl (sodium chloride)

70 mM Na_2HPO_4 (sodium phosphate)

35mM NaH_2PO_4 (potassium phosphate monobasic)

1M Glycine

- add ingredients, bring up to 500mL in ddH_2O and stir until dissolved

- sterile filter into 500mL jar

- *dilute to 1X with ddH_2O for use*

Sucrose 1M stock (34.23%):

-makes 50 mL; can store at –20˚C and thaw at 37˚C when ready to use

-17.12 g Sucrose (Ultra Pure; ICN Biomedicals Cat# 821713)

-add ~45 mL ddH_20

-stir until dissolved

Sucrose 30%:

-makes 10 mL; can store at –20˚C and thaw at 37˚C when ready to use

-5.26 mL 1M Sucrose

-1 mL 10X PBS

-3.74 mL ddH_20

Sucrose 18%:

-makes 10 mL; can store at –20˚C and thaw at 37˚C when ready to use

-8.78 mL 1M Sucrose

-1 mL 10X PBS

-236 µL ddH_20

0.5 % Gelatin

Prepare a stock of 2% (w/v) gelatin in ddH2O: 0.8g of gelatin (Type A from Porcine skin 300 Bloom Sigma Cat.# G-2500) in 40mL ddH2O in a polypropylene tube. Gelatin will not dissolve fully until autoclaved. Dilute this stock to 0.5% in ddH2O and then add in 0.05% (w/v) chromium potassium sulfate.

10X IF Buffer (500ml)—need for both 3D methods

38g NaCl

9.38g Na2HPO4

2.07g NaH2PO4

2.5g NaN3

5g BSA

10ml Triton-X 100

2.5ml Tween-20

Total 3D Embedment of MCF-10A Cells

1. Split cells 1 day prior to embedment, preferably 30-40% confluency to ensure cells are actively dividing/integrins presented etc
2. Day of embedment, aspirate media, rinse 1x with PBS, rinse 1x with 0.05% Trypsin EDTA, aspirate and add small volume of 0.05% trypsin EDTA and incubate 5-8' in 37 C incubator
3. While cells are trypsinizing, pull out matrigel and bring into hood on ICE
4. For 96-well cultures, spread 10-20ul underlay Matrigel, place in 37C incubator for 15-20' to polymerize
5. In the meantime, resuspend cells in 20% DHS, count with hemacytometer and make the appropriate adjustments to volume or take aliquot, spin 5' 1000rpm, most often, put amount of cells needed in 1.5ml eppendorf tube and spin down TAKE NOTE of position of tube since pellet will not be visible (want 6-10,000 cells per well depending on experiment) –Note: if you want RNA/protein err on the higher side, if you want to do more imaging in phase contrast during growth, use lower range so you don't have interference of other colonies/achieve single colonies during imaging)
6. Place tube of cells directly into the ice, aspirate media carefully out of tube, leaving approximately 20-30ul of media behind
7. Flick cells gently for 3-5 sec to enable easier resuspension

8. Quickly add appropriate volume of ICE cold matrigel (30-60ul per well; if you want to make cryoblocks, more volume = more to cut, painting technique can get away with 30ul) and resuspend pellet of cells on ICE without creating any bubbles (draw from bottom, add to top method)
9. Add 60ul of matrigel + cells to each 96-well
10. Place TC plate at 37C incubator for 15-20 min to polymerize
11. Add ~200ul of MCF-10A 2-D growth media gently to the side of each well
12. Refeed cultures every 2 days with growth media (make in large quantity and use for entire experiment, using new media/fresh EGF will affect cell growth curves)

Cryosectioning/Immunostaining of 3D Cultures:

1. Using a cryostat (as cold as you can get it, -33 preferable), cut 6 micron sections of 3D tissue blocks and transfer sections to the gelatin-coated paraffin ring on charged microscope slides (Fisher #12-550-34).
2. Dehydrate samples 2-4hr RT covered or keep slides at –80 until needed
3. Rehydrate slides for 30'-1hr with 1x IF at RT
4. Incubate sections in blocking buffer (room temperature; 1 hour) Block is 10% goat sera or whatever your secondary antibody was generated in (we've used donkey as well), 1/100 anti mouse F(ab) to block non-specific binding to the mouse-derived Matrigel--all diluted in 1X IF
5. Incubate sections in primary antibody + block at 4°C overnight in a humidified chamber.

6. Next morning, allow samples to warm up to RT before removing primary antibody.
7. CAREFULLY wash sections in 1x IF buffer, RT 3x 15' each wash (no rocking needed)
8. Incubate in secondary antibody plus 1ug/ml DAPI (Sigma Cat# D9542-1mg) in IF buffer + block at RT for 45' keeping slides under foil/covered
9. Wash sections in 1x IF buffer, RT 3x 15' each wash
10. Aspirate residual and mount sections with ProLong Gold (Invitrogen Cat #P36930) mounting media with 22x50mm Corning Cover glass (Cat #12-531E)
11. Leave under foil to dry at RT overnight or until hard set
12. Best to visualize as soon as possible, can keep 1 week 4C
13. Store long term at -20°C.

Painting Method of 3D Processing

1. Allow cultures to grow until desired length of time, if other wells are continuing to grow, do procedure below in sterile Laminar Flow Hood.
2. Add ~15ul of Matrigel in a thin coat to either a 4/ 8-well chamber slide (or for cost issues, I've starting using 18mm coverglass (VWR Cat#16004-300CS) in 12-well dishes), spread over ICE to get an even, thin underlay, allow to polymerize at RT or 37C for 5-10 minutes

3. Place 50ul per 4-well chamber slide of fresh matrigel into a separate tube and keep on ICE
4. Aspirate media from 3D cultures.
5. Using a cut pipette tip or large bore pipette tip, dislodge matrigel from edges, gently dissociate matrigel from well by squishing with tip in a gentle circular motionuntil you can pick up matrigel in pipette tip
6. Add this culture to your fresh matrigel tube and mix gently by dispensing to the bottom of the tube and drawing from the top, continuously until color is uniform without generation of air bubbles! (i.e. your fresh matrigel will be bright pink/red your older matrigel will be more orange in color)
7. Place tube immediately back on ICE, if you do get bubbles you can quickly spin on countertop and then immediately place the tube back on ICE!
8. Add ~0-60ul of this new matrigel + cell mixture to each chamber slide by tilting the chamberslide at an almost vertical angle, so that when you slowly dispense the matrigel starting at the top of the chamberslide, gravity will carry each drop down the slide, try NOT to touch or disrupt the thin underlay of matrigel at all as this will affect how your cells lay/images after immunostaining
9. Allow chamber slides to polymerize 15-20’ at 37 degrees
10. In the meantime prepare fixation solution
11. Continue Immunostaining protocol as outlined below

12. At the end of IF protocol, either remove chamberslide top or for 18mm coverslips, using a bent syringe to loosen the coverslip and tweezers, inverst coverslips onto mounting media on top of a microscope slide

Processing 3-D cultures for Cryosectioning:

Make 96-Well Cryomolds prior to extraction:

1. Turn heat block to 95 C
2. Casting molds are .65ml eppendorf tubes with both the lids and bottoms cut off with a razor blade
3. Rinse pre-used molds with lots and lots of h2o to remove any excess OCT
4. Blow airline through each tube to thoroughly dry
5. Place medium weigh boat with a couple chips of paraffin a top the heat block and let melt
6. Place eppendorf tubes top-side down (smooth side) into paraffin weigh boat
7. Pick up each eppendorf and blow lightly on the tube while spinning the tube in your hands, keeping the tube vertical so that you don't blow the wax up into the insides of the tube, if you do, keep a pair of sharp tweezers handy, to scrape the inside out of any paraffin as this will cause your cultures/solutions to stick

8. Once the paraffin has dried on the outside lip of the tube (a grayish white translucent color), place paraffin side down onto 22mm glass --it may be tacky enough to stick a little
9. Put two eppendorf tube casting molds per coverslip
10. Place the coverslip back onto the heat block for ~1', you will see the paraffin melt around the mold and turn clear
11. Carefully pick up coverslip, sometimes tweezers help and place on bench to harden at RT
12. Keep these casting molds in 10cm TC dish until needed

Day of Extraction:

Processing Timepoints:

1. Begin by processing all 'extraction' samples.
2. Using a p20 set at 8ul fitted with a tip, which has been cut at the end (cut tip), squish around the matrigel in the well and carefully transfer it to a non-stick/low retention tube (Phenix Cat#MAX-815S)
3. Add 5ul of fresh matrigel (use a cut tip) to each tube and mix by flicking with your finger. AVOID bubbles, quickly spin on table top centrifuge if bubbles occur
4. Place tubes at 37ºC and allow to gel.
5. In the meantime, prepare your 1x Cytoskeleton Extraction Buffer and add fresh Protease Inhibitors as well as 0.5% peroxide/carbomyl free triton X-100 (sigma cat#X-100-PC, located at -20ºC). You will need 300ul per sample.

6. Gently add 300ul of extraction buffer to each tube by tilting the tube and dripping it down the side.
7. Incubate this at RT for 30 minutes.
8. After 15 minutes, prepare your 'non-extracted' samples.
9. Transfer to a non-stick tube, mix in 5ul of fresh matrigel (use a cut tip), and allow to gel at 37ºC.
10. Once the extraction is over, aspirate off the extraction buffer mixture and gently wash each sample with **1X PBS/Glycine** by tilting the tube and dripping it down the side, inverting once and then decanting off.
11. Remove 'non-extraction' samples from the incubator and process with 'extracted' samples from this point on.
12. To each tube, add 7.33ul of **ICE COLD 7.5X DMEM:F12+HEPES+sodium bicarbonate** as well as 47.67 collagen I (use a cut tip) and mix gently by pipetting up and down (use a cut tip/this mixing step is VERY important…if you do not mix well your sections later on will not have a consistent number of cells!). Again, if bubbles occur, spin quickly <1sec to remove bubbles
13. Transfer this mixture to a labeled **sectioning mold**.
14. Place each sectioning mold on a PCR block inverted onto ice in an ice bucket with a lid. Be sure not to a level higher than that of the block or overnight the ice will melt and contaminate your samples with water!
15. To each sectioning mold add ~350ul of **2% paraformaldehyde ICE COLD** and allow to fix overnight at 4ºC.

The next day:

Change Ice if needed, the rest of the steps will be performed atop the same ICE cold PCR block

Do 3X10 minute blocking steps in 1X PBS/Glycine

Remove PBS/Glycine, add ICE COLD 18% sucrose in PBS for 3h at RT in ice bucket

3X brief 1X PBS/Glycine washes

3 hour incubation in 30% sucrose in 1X PBS

3X brief 1X PBS/Glycine washes

Embed samples in OCT:

Prepare powdered dry ice by smashing it with a rubber hammer in a large ice tray. Aspirate 1X PBS/Glycine and replace with a small dab of OCT (fill up sectioning mold ~1/3 full).

Place these on the powdered dry ice and freeze.

Use a 1mL serological pipette snapped in half, to pop out the cast into a labeled 1.5mL eppendorf tube.

Store at -80ºC until ready to section.

To reuse sectioning molds:

OCT is water soluble, so simply by soaking and then rinsing several times in water you can reuse your sectioning molds. Simply prepare them as you originally did.

MTT Adhesion Assay Solutions

Stock: 5mg/ml in PBS (store 4 in foil)

12.5mg MTT(4 silver chem. Box 2)

2.5ml sterile PBS

- Vortex well

- can sterile filter

Working: 1:10 in DMEM:F12

1200ML stock soln

10800ML DMEM:F12

-Pipet up & down to mix

After 2hr, aspirate MTT soln

-check for purple cells unbder phase first

Add 100ul DMSO / well

Incubate 37c 5-10 min

Pipet up and down gently & add 65ul to a well ea of 96 well plate

Read on plate reader

-MTT button (preprogrammed for 550-630nm)

-saved in Temp folder->save to floppy.txt

-export to Excel

Rinse ea. Well w/500ul DPBS

Block ea well (not TCPS) w/BSA for 30+ min

-1 left on until during 5min 1m M MnCL2 incubation

Trypsinize cells ~12 min (0.25%)

Resusp in 20% DHS

Count Cells

Spin Down 5min 1000rpm

Resuspend to 330,000 cells/ml in DHS free Growth Me

Split into 2x15mL conical tubes ea. w/2ml of cells for each tube (1 @ a time) add 20ul 100mm MnClz (1mm final) for 5 min-flick to mix

Plate one cell type @ a time across the rows 250ul / well → 82500 cells/well (can plate more next time)

Tap plate on sides x 3 / side to spread out

Incubate 20min at 37c

Rinse w/250ul DPBS

Add MTT working soln (175ul) to ea wll for 2hr @37c.

DNA isolation from tails (modified from T. Jacks Protocol)

1. Place each tail in a clean eppendorf tube
2. Add 500µl tail lysis buffer containing Proteinase K to each tube (15µl PK:mL buffer)
3. Incubate o/n at 50-60C
4. Add 250µl saturated NaCl (5M)
5. Shake vigorously (~20 times), incubate on ice 10 min
6. Spin at low speed (5000 rpm), 10 min, 4C
7. Decant supernatant into new eppendorf
8. Add 650µl isopropanol and invert to mix. Incubate at RT for 5min
9. Recover DNA by centrifuging at RT, max speed, 10 min
10. Wash with 70% ethanol
11. Invert and dry at 55C, 5 min
12. Resuspend in 200µl water
13. Incubate for 30 min at 37C

Tail lysis buffer

1M Tris pH 8.0	5ml
5M NaCl	10ml
0.5M EDTA pH 8.0	10ml
10% SDS	25ml
H2O	450ml

FACS Protocol

NOTES: Give yourself at least 8 hrs. before your FACS appointment to complete this protocol! This estimated time is for 36 samples. All dishes should be at the same confluence. You should have the following # of tubes *per cell type:*

2 Blank: cells only

2 NSB: cells and 2° Ab ONLY (need 2 for each kind of 2° Ab used)

2 Cells with both 1° Ab and 2° Ab

The night before:

Prepare 50 ml 1% BSA/DPBS: 500 mg BSA in 50 ml DPBS. Sterile filter and store at 4°C.

The day of FACS analysis…

1. Set Sorval centrifuge in cell culture room to 0-4°C

2. Trypsinize cells. Resuspend in ice cold DMEM:F12 and transfer to a 15-ml tube

4. Spin down: 1200rpm/5min/0-4°C/Sorval RT7

5. Aspirate supernatant. Resuspend pellet in 10 ml of DPBS (ice cold)

7. Count and adjust cells to $1x10^6$ cells/ml in DPBS

8. Spin down: 1200 rpm/5min/0-4°C/Sorval RT7

9. Resuspend pellet in 1% BSA/DPBS @ $1x10^6$ cells/ml (or > $5x10^5$ cells/ml) and transfer to a 14ml polypropylene round-bottom tube (Falcon #352059)

The total volume should be equal to (1ml * # of tubes for that cell type)

Make sure to have a uniform single cell suspension. Keep tubes on ice!

10. Rock very gently on ice for 30 min – 1 hour (Blocking step)

11. Aliquot 1ml to each of 5ml polypropylene round-bottom 12x75 mm tubes (Falcon #352063)

12. Spin down: 1200 rpm/5min/0-4°C (don't need to do this if adding 1° Ab directly to blk buffer, but if you want to conserve the antibody, then spin down and use a minimum of 200µl Ab solution)

13. Add 200µl 1° Ab solution per tube (usually 1:100 dilution in 1% BSA/DBPS) and incubate on ice for 1 hour, swirling every 10 min. OR rock back and forth somehow.

14. Wash 3X by spinning down 1200 rpm/5min/0-4°C and resuspending in 1 ml ice cold DPBS.

15. After the last wash, resuspend in 200µl ice cold 2° Ab solution and incubate on ice for 1 hour, swirling every 10 min. OR rock back and forth somehow (usually 1:100 dilution in 1% BSA/DBPS).

16. Wash 3X by spinning down 1200 rpm/5min/0-4°C and resuspend in 1 ml ice cold DPBS.

17. After last wash, transfer cell suspension from each tube to a FACS tube (5ml polystyrene round-bottom tube 12x75mm Falcon #352058)

18. Keep on ice and carry to FACS.

When at the FACScan, you only need to measure each tube once. Count 10,000 cells per sample.

Protocol for Quantifying Proteins

Solutions and Supplies:

BCA Protein Assay Reagent Kit (pierce #23227)

BCA protein standards

1 XPBS

96 well microtiter Plate

Pierce BCA Protein Assay

1. Into a 96 well microtiter plate, load 25 ul per well of the BCA standards into columns 1 + 2 in order of decreasing concentration from lanes A to H (usually make the following concentrations of the standards: 0.4, 0.36, 0.32, 0.24, 0.2, and 0.12 and 0 mg/ml BSA). There ends up being four 0 mg/ml BSA wells (1 G, IH,2G, 2 H)

2. Pipet 45 ul of 1 X PBS in lane t\ columns 3-X according to the number of samples being tested. (usually duplicates of the samples are run).

3. Pipet 5 ul of each protein lysate per well (Lane t\ columns 3-X).

4. Also 5 ul of a control sample for background (SDS, RIP A., or the lysis buffer, etc.) in the last column after the sample.

5.Mix 1 part Reagent B to 50 parts Reagent A from the BCA Kit. Adding 200 ul of solution to each well, so if using 8O wells = 16 mL of solution (mix 17mL just to be sure there is enough)

a. Example for 17 mL Reagent solution,
b. 17/51 = 333 uL reagent B
c. 17ml-0.333 ml = 16.67 mL Reagent A

6. Pipet 200 ul of Reagent solution to each well.

7. Cover entire plate (use the clear, sticky 96-well plate covers and incubate 35 minutes at 37 C.

8.Using plate reader: Hit "Read" Button. The desired assays = #47. If this assay is not displayed in the LED then punch in the number 47. Hit enter. Punch in the number of samples (96, or 8O, etc). Hit enter. Then put the plate in the holder as directed and hit "Read".

9. Obtain printout and use results to determine protein concentration. Data is given as ug protein/well.

Preparation of Lentivirus

The following protocol is adequate to generate enough virus to infect up to one 60 mm dish at 1.6 ml per dish or a- couple of 35 mm dishes or 4 to 6 wells of a 12 well plate.

1: Trypsinize 60 mm stock dish of 293T cells grown in 10% donor horse seruml90% high glucose DMEM/supplemented with 2 mM L-glutamine and PeniStrep (near confluent dish is about 1 x 107 cells). Plate 1.2 xl 06 cells in a gelatin coated 35 mm dish in 1.6 ml of medium. Do this late afternoon to early evening on the day before transfection .

2. Sometime (at least a couple of hours before transfection) remove 0.8 ml of media from the dish and replace with 0.8 mll0% fetal bovine serum 190% high glucose DMEMIsupplemented with 2 mM L-glutamine and Pen/Strep. Prepare to do transfection late in the afternoon to early evening.

3. About 1/2 hour before transfection mix in a sterile 1.5 ml eppendorftube:

3.25 ug recombinant lentiviral proviral vector

2.43 ug psP AX2 packaging vector

0.97 ug pMD2.G vector (VSVG)

sterile ddH20 to 81 ul.

Add 81ul 2xHBSS and mix well~ by tapping the tube. Let stand 5 minutes at room temperature.

Add 10.13 ul CaCl2, and mix well by tapping the tube. Let stand 25 minutes at room temperature.

Add to plate dropwise dispersing the drops over the surface of the plate. Gently shake plate back and forth to mix and disperse the precipitate. Return to the incubator and leave overnight.

4. In the morning following transfection aspirate media from plate and add carefully (ie dropwise) 1.6 ml of 10% donor horse serum/90% high glucose DMEM/supplemented with 2 mM L-glutamine and PeniStrep. Return to incubator (37°C) 36 hr to 60 hr. (36 hr takes you to the evening of the next day and allows you to do an overnight infection of the target cells. 48 hours takes you to the morning two days later and allows you to do the infection for 8 hours during the day. 60 hours takes you approximately until the evening 2 days later and allows you to do an infection overnight. I would recommend either 48 or 60 hours although you will probably get a decent virus by 36 hours).

Purification of DNA from Agarose Gels

Author: Johnathon Lakins

Last Edited 911 0/2007

Purpose

Agarose Gel Solubilization\DNA Silica Binding Buffer

4 M Guanidinium Isothiocyanate

0.5 M Potassium Acetate-Acetic Acid pH =4.7-4.9

Diatomaceous Earth Slurry

0.75 g Diatomaceous Earth (Sigma D3877) (washed in ddH20 and resin fines removed) in 5 ml of

ddH20

Resin Wash Buffer

80% Isopropanol

Elution Buffer (placed at 50°C to 55°C)

1 mM Tris-HCl, pH = 8.2 to 8.5 at Room Temperature

5 mMNaCl

1. To agarose gel slice add 3 volumes (3 times in volume the weight of the agarose slice ... .if you use thin

preparative gels 500 microliters is more than sufficient) agarose gel solubilization buffer and mix by inversion at room temperature until gel slice is dissolved.

2. Resuspend Diatomaceous Earth Slurry by vortexing and then remove 30 to 50 microliters and add to solubilized agarose slice (FINES HAVE BEEN REMOVED

TO PREVENT COLUMN FROM BEING BLOCKED BUT DIATOMACEOUS EARTH SEDIMENTS F AIRL Y QUICKLY (ORDER OF MINUTES)
SO TAKE ALIQUOT QUICKLY AFTER RESUSPENSION).

3. Mix by inverting several times over 2 to 5 minutes at room temperature.

4. Load into Promega minicolumn in a 2 ml collecting tube using successive 0.2 ml aliquots and spinning
briefly at 1200 rpm in microfuge at room temperature (DO NOT SPIN AT ANY HIGHER SPEED OR FOR MUCH LONGER THAN IT TAKES TO SPIN OUT LIQIUD OTHERWISE YOU CAN DRY THE RESIN AND LOSE THE DNA).

6. Wash diatomaceous earth one time with 0.15 ml agarose gel solubiliztion buffer and after with four successive 0.2 ml washes using 80% isopropanol spinning briefly at 1200 rpm in microfuge at room temperature.

7. After last wash spin full speed (10,000 rpm on Janna's fuge) in a microfuge at room temperature for at least 2
minutes to dry diatomaceous earth (diatomaceous earth at this grade goes from dark brown when wet to a light
sandy brown when dry). DNA WILL NOT ELUTE EFFICIENTLY UNLESS DIATOMACEOUS EARTH IS DRY.

RNA Isolation from 3D Cultures

1. Make 4M Guanidium Thiocynate/25mm Na Citrate, pH 7.0/0.5% N-Lauryl Sarcosine(GTC)
2. Before prep add 100mM final BME (70ul/ 10mL GTC)
3. Add GTC directly to Matrigel. Use 300ul per 100ul Matrigel or 600ul per 60mm dish. 600ul is max volume per epitube. (can store at -20C)
4. Add 1/10 volume (60ul) 2M acetic acid pH 4 to acidify GTC (turns yellow)
5. Vortex well, make sure matrigel is fully dissolved
6. Add 1 volume (600ul) of phenol saturated w/0.1M Citric acid pH 4.3
7. Vortex to mix thoroughly
8. Add 2/10 (120ul) original volume of 49:1 Chloroform:Isoamyl alcohol
9. DO NOT VORTEX. Mix by inverting quickly 15-20X
10. Ice for 15 min
11. Spin at 5,000g, 30 min, 4C
12. Remove aqueous phase to new tube
13. Add ½ original volume (300ul) 1.2M NaCl/0.8M Trisodium citrate in depc H2O
14. Add ½ original volume (300ul) isopropanol
15. Incubate RT, 15 min (can store at 4C)
16. Spin 30 min, 14K, 4C
17. Wash with 75% ETOH in depc H2O 2X
18. Air dry 5-10 min, dissolve in DEPC H2O, take OD spec

'Scratch' Assay

For each strain you wish to test, plan to use 2 wells of a six well plate. Prior to plating, turn over your 6 well plate and draw a vertical line down the center of each plate. On each line draw 5 horizontal lines down your original line. Plate your cells such that they will all reach ~85% confluency at the same time.

Early in the morning when your cells have reached 85% confluency, use a lOOul pipette tip to 'scratch' a line down the center of each well using your vertical line as a guide. At this point you will note cells floating above this line. To ensure that these do not simply plate down and appear as 'migrated' cells, change the media at this time. Place cells at 37°C for an hour to allow recovery time. At this time, take photos at each of your five points in each welL This is your time zero. Allow cells to incubate for another 6-8 hours (or longer, use your best judgement).

At this point you can take pictures at each of your five points. Additionally, you may want to allow the cells to recover for another hour, wash them once with DPBS and then fix them at -20°C wi~h ice cold MeO~At this point you can use a PAP pen to outline a few pomts in each dish (along your lme) and stain for DAPI (to look for mitotic indices- an indicator of proliferation) and activated FAK (an indicator of migration). It is up to you to decide how you want to score your assay, but if you use all of these tips as you go along, you will have enough data to score the assay many different ways.

Soft Agar Assay

Anchorage independent growth was assessed using a soft agar assay (Wang et al., 1998). Duplicate wells of a 6 well polystyrene tissue culture dish were coated with a 1.5 mL underlay containing 1% melted agarose (diluted in sterile water) diluted 1:1 with 2X growth media. This mixture was polymerized at room temperature for at least 10 minutes while the target cells were prepared. 100,000 cells were added to a mixture containing 3 mL 2X growth medium combined with 3 mL melted 0.7 % agarose (dissolved in sterile water) which was cooled to 40 ºC. 1.5 mL of cell/agarose mixture was gently placed on top of the 0.5% agarose/1X growth media underlay and polymerized in the incubator for 15 minutes. Growth media was gently added on top of the embedded cells and replaced every two days. Total number of colonies were counted and measured in three 3D visual planes per well after 14 days of growth at 10X magnification under a light microscrope.

Solutions

10X PBS/Glycine

38g NaCl (FW 58.44) 1.3M

4.97g Na2HPO4 (FW 141.96)0.07M

2.4 g NaH2PO4 (FW 137.99) 0.035 M

37.5g Glycine (FW 75.07) 1M

-Fill to 500ml with dd H20, sterile filter if desired

10x IF

38g NaCl (FW 58.44) 1.3M

4.97g Na2HPO4 (FW 141.96)0.07M

2.4 g NaH2PO4 (FW 137.99) 0.035 M

2.5g NaN3

5g BSA

10ml Triton-X 100

2.5ml Tween-20

-Fill to 500ml dd H20

10x Transfer Buffer

30.29 g Tris HCl (FW 121.14g) 0.25M

144.13g Glycine (FW 75.07g) 1.92M

-Fill to 1L ddH20 do not adjust pH

10x Running Buffer

30.275g Tris

144.1g Glycine

10ml of 10% SDS

Fill to make 1L with dd H20

10X TBS

12.114g Tris

78.894 g NaCl

Fill to 1L with dd H20

5X SDS-PAGE Sample Buffer (makes 10ml)

2.5 ml of 1M Tris (pH= 6.8)

5ml glycerol

2ml 10% SDS

o.5ml 0.05% Bromophenol Blue

(add 50ul/ml of 2-BME fresh)

1X TAE

38.72g Tris

9.136ml Glacial Acetic Acid

16 ml EDTA

Fill to 8L ddH20

1x TRANSFER BUFFER

100 ml 10x Transfer Buffer

200 ml Methanol (fresh)

10ml of 10% SDS (if desired) to final conc of 0.1% SDS

-Fill to 1L ddH20 and keep at 4C

0.2% TBST

100ml 10x TBS

2ml Tween-20

-Fill to 1L ddH20

RIPA

20mM Tris pH 8.0 (stock is 1.5M) 1.3ml

137mM NaCl (5M stock) 2.74ml

10% glycerol ---10ml glycerol

1% IGEPAL –1ml

0.1% SDS ---1ml

0.5% deoxycholate –0.5g

2mM EDTA (0.5M stock) 400ul

-Fill to 100ml ddH20

2YT (1L)

16g Tryptone

10g Yeast Extract

5g NaCl

In 500ml Erlenmeyer flask add 250ml of 2YT, and add 15g/L of Agar (3.75g)

Add stir bar and autoclave; In the meantime warm up a water bath to 60C

Add flask to water bath and allow to cool to 60C (1-2h); Add drugs and stir briefly

Pour plates near open flame.

STRIP Protocol for Nitrocellulose membranes

Protocol:

- Incubate the membrane to strip for 10 min at 50°C in « STRIP buffer»

(rotate the membrane in a glass hybridization tube with buffer in a hybridization oven, or in a closed container in a warm bath with gentle agitation)

- Wash the membrane thoroughly with ddH20 in a container with agitation. In general, I do a quick wash then wash several times (it is important to change H20 often) at least 1 hour. But if you are pressed for time, you can verify the pH of the ddH20 and stop when the pH is around 7.

« STRIP buffer» :

700 uL B-mercapto-ethanol

20 mL SDS 10 %

12,5 mL Tris-HCl 0,5 M pH 6,8

66,8 mL ddH20 (qsp 100 mL)

Note: The STRIP buffer can be used 3 times before to trash.

Antibody	Company	Catalog #	Clone	Host	Dilution for IF	IHC	WB	FACS
α2 integrin	BD Biosciences	555669	12F1	Ms				1:100
α2 integrin (function blocking)	Millipore	MAB1988	10G11	Ms	2-20μg/ml for inhibition		1:250	
α3 integrin	Millipore	ab1920		Rb	1:100		1:300	1:100
α3 integrin	Millipore	MAB1952	PIB5	Ms				0.111111111
α5 integrin	Hybridoma		BIIGII	Rt	Neet 1:1			Neet 1:1
α5 integrin	Millipore	ab1928		Rb			1:100	
α5 integrin (function blocking)	Millipore	MAB1956Z	P1D6	Ms	2-20μg/ml			
α6 integrin (CD49f)	BD Transduction	555734	GoH3	Rt	1:100		1:300	1:100
αv integrin	Chemicon	MAB1953Z	M9	Ms			1:250	1:100
β1 integrin	Hybridoma		TS2/16	Ms	Neet 1:1			Neet 1:1
β1 integrin	Hybridoma		AIIBII	Rt	1:776 (2.5μg/ml)			1:776 (2.5μg/ml)
β4 integrin	Hybridoma		3E1	Ms	Neet 1:1			Neet 1:1
β-catenin	Sigma	C2006		Rb	1:1000			
BRM	Reisman			Rb	1:1000 (Cyto extraction)	1:1000	1:1000	
BRG1	Imbalzano			Rb			1:50	
Caspase-3	Cell Signaling	9661		Rb	1:100			
Fibronectin	BD Biosciences	610077	10	Ms	1:100		1:50	
Fibronectin (function blocking)	Millipore	MAB88916	3E3	Ms	2-20μg/ml			
Ki-67	BD Transduction	610968	35	Ms	1:100 (Cyto extraction)	1:50		
Lamin B1	Santa Cruz	sc-30264		Gt			1:1000	
Laminin 5	Marinkovich		BM165	Ms	1:100 (350μg/ml)			

Appendix I. List of Antibodies: source, applications and working dilutions.

Gene Name	NCBI Accession Number	Forward Primer	Reverse Primer	Product Length (bp)
18S rRNA	M10098	CGGCTACCACATCCAAGGAA	GCTGGAATTACCGCGGCT	187
α2 Integrin (ITGA2)	NM_002203	AGCCACCAAATTAGCAGGTG	TGTGGTCCATCTGCATCCTA	193
α3 Integrin (ITGA3)	NM_02204	GCCTGCCAAGCTAATGAGAC	CACCAGCAGAGTGAGGATCA	192
α5 Integrin (ITGA5)	NM_02205	AGCCTCAGAAGGAGGAGGAC	GGTTAATGGGTGATTGGTG	186
αV Integrin (ITGAV)	NM_002210	CACCAGCAGTCAGAGAGATGGA	ACAACTGGCCCAACATCTTC	224
BRM (SMARCA2)	NM_003070.3	AGCAGCCAGATGAGTGACCT	TCTCTTCGGTTTCCTGCCTA	217
BRG-1 (SMARCA4)	NM_001128849.1	AGGCAAAATCCAGAAGCTGA	CGCTTGTCCTTCTTCTGGTC	165
Collagen Type1, α1 (COL1a1)	NM_000088	CCTGGATGCCATCAAAGTCT	AATCCATCGGTCATGCTCTC	153
Fibronectin 1 (FN-1)	NM_ 212482	CAGTGGGAGACCTCGAGAAG	GTCCCTCGGAACATCAGAAA	169
Laminin-5,γ2 chain (LAMC2)	NM_005562	GGCTGGTCTTACTGGAGCAG	ACATCAGCCAGAATCCCATC	154

Appendix II. List of Q RT-PCR Target Sequences and Product Length

BRM shRNA sequences	
target length:	23mer
target seq:	**AAGCTGACTCAGGTCTTGAACAC**
extended seq w/o AA:	**GCTGACTCAGGTCTTGAACACtcac**
antisense	**gtgaGTGTTCAAGACCTGAGTCAGC**
Bulged sense	**GCTGACTCAGATCTTGAAAACtcac**
sense oligo	5'- cttgtggaaaggacgaaacaccGCTGACTCAGATCTTGAAAACtcacttcaagagagtgaGTGTTCAAGACCTGAGTCAGCttttt<u>ctgcag</u>tttt - 3'
rev. oligo hBrm #3	aaaactgcagaaaaaGCTGACTCAGGTCTTGAACACtcactctcttgaagtgaGTTTTCAAGATCTGAGTCAGCggtgtttcgtcctttccacaag
~85% KD	: homologous to hBrm isoform a & b
	: target seq. Only match 8 nucleotide to Brg1

target seq:	**AAGGAGGTGCTAAGACACTTATG**
extended seq w/o AA:	**GGAGGTGCTAAGACACTTATGaaca**
antisense	**tgttCATAAGTGTCTTAGCACCTCC**
Bulged sense	**GGAGGTGCTACGACACTTCTGaaca**
sense oligo	5'- cttgtggaaaggacgaaacaccGGAGGTGCTACGACACTTCTGaacattcaagagatgttCATAAGTGTCTTAGCACCTCCttttt<u>ctgcag</u>tttt - 3'
rev. oligo hBrm #4	aaaactgcagaaaaaGGAGGTGCTAAGACACTTATGaacatctcttgaatgttCAGAAGTGTCGTAGCACCTCCggtgtttcgtcctttccacaag
~90% KD	: homologous to hBrm isoform a & b
	: target seq. Only matched 9 nucleotide with Brg1

target seq:	AAGCGCTATTGAATATTGCAATC
extended seq w/o AA:	GCGCTATTGAATATTGCAATCtata
antisense	tataGATTGCAATATTCAATAGCGC
Bulged sense	GCGCTATTGAcTATTGCAcTCtata
sense oligo	5'- cttgtggaaaggacgaaacaccGCGCTATTGAcTATTGCAcTCtatattcaagagatataGATTGCAATATTCAATAGCGCttttt<u>ctgcag</u>tttt - 3' 5'- cttgtggaaaggacgaaacaccGCGCT**(delta A)**TTGAcTATTGCAcTCtatattcaagagatataGATTGCAATATTCAATAGCGCttttt<u>ctgcag</u>tttt - 3'
delta A mutation RO shBrm 3'UTR #5	aaaactgcagaaaaaGCGCTATTGAATATTGCAATCtatatctcttgaatataGAgTGCAATAgTCAATAGCGCggtgtttcgtcctttccacaag
~98% KD	

Appendix III Supplementary shRNA Sequences targeting BRM and BAF subunits

Sequence information for all BRM and BAF subunit shRNA targeting sequences, **% KD** indicates validation of knockdown by western blot (So, A., and Yamamoto, K., unpublished observations).

BRM shRNA sequences	
target seq:	AAGTGTACTTAATCTTTGCTTTC
extended seq w/o AA:	GTGTACTTAATCTTTGCTTTCtttg
antisense	caaaGAAAGCAAAGATTAAGTACAC
Bulged sense	GTGTACTTAAcCTTTGCTcTCtttg
sense oligo	5'- cttgtggaaaggacgaaacaccGTGTACTTAAcCTTTGCTcTCtttgttcaagagacaaaGAAAGCAAAGATTAAGTACACtttttctgcagtttt - 3'
RO shBrm 3'UTR #6	aaaactgcagaaaaaGTGTACTTAATCTTTGCTTTCtttgtctcttgaacaaaGAgAGCAAAGgTTAAGTACACggtgtttcgtcctttccacaag
~97% KD	

target seq:	AAGTCATAAGCCTGAGGCAAATA
extended seq w/o AA:	GTCATAAGCCTGAGGCAAATAaaat
antisense	atttTATTTGCCTCAGGCTTATGAC
Bulged sense	GTCATAAGCCgGAGGCAAgTAaaat
sense oligo	5'- cttgtggaaaggacgaaacaccGTCATAAGCCgGAGGCAAgTAaaatttcaagagaatttTATTTGCCTCAGGCTTATGACtttttctgcagtttt - 3'
RO shBrm 3'UTR #7	aaaactgcagaaaaaGTCATAAGCCTGAGGCAAATAaaattctcttgaaatttTAcTTGCCTCcGGCTTATGACggtgtttcgtcctttccacaag
~86% KD	

BAF60a shRNA sequences	
target length:	21mer
target seq:	AAGGACAACACCAGAATGAAG
extended seq w/o AA:	GGACAACACCAGAATGAAGagggtc
antisense	gaccctCTTCATTCTGGTGTTGTCC
Bulged sense	GGACAACACCgGAATGAAtagggtc
sense oligo	5'- cttgtggaaaggacgaaacaccGGACAACACCgGAATGAAtagggtcttcaagagagaccctCTTCATTCTGGTGTTGTCCtttttctgcagtttt - 3'
RO shBaf60a #5	aaaactgcagaaaaaGGACAACACCAGAATGAAGagggtctctcttgaagaccctaTTCATTCcGGTGTTGTCCggtgtttcgtcctttccacaag
~78% KD	

Appendix III. Supplementary shRNA Sequences targeting BRM and BAF subunits (Continued)

BAF60a shRNA sequences	
target seq:	AAGACACCTGTTATCCTCTTC
extended seq w/o AA:	GACACCTGTTATCCTCTTCtttcac
antisense	gtgaaaGAAGAGGATAACAGGTGTC
Bulged sense	GACACCTGTTcTCCTCTTatttcac
sense oligo	5'- cttgtggaaaggacgaaacaccGACACCTGTTcTCCTCTTatttcacttcaagagagtgaaaGAAGAGGATAACAGGTGTCttttt<u>ctgcag</u>tttt - 3'
<u>RO shBaf60a #6</u>	aaaactgcagaaaaaGACACCTGTTATCCTCTTCtttcactctcttgaagtgaaatAAGAGGAgAACAGGTGTCggtgtttcgtcctttccacaag
~78.5% KD	

target seq:	AAGACAGCTTGTTATGACATT
extended seq w/o AA:	GACAGCTTGTTATGACATTgatgtt
antisense	aacatcAATGTCATAACAAGCTGTC
Bulged sense	GACAGCTTGTcATGACATagatgtt
sense oligo	5'- cttgtggaaaggacgaaacaccGACAGCTTGTcATGACATagatgtttcaagagaaacatcAATGTCATAACAAGCTGTCttttt<u>ctgcag</u>tttt - 3'
<u>RO shBaf60a #8</u>	aaaactgcagaaaaaGACAGCTTGTTATGACATTgatgtttctcttgaaaacatctATGTCATgACAAGCTGTCggtgtttcgtcctttccacaag
77% KD	

BAF170 shRNA sequences	
target length:	20mer
target seq:	GGCTGGTGAAAGGTGTTTAT
extended seq w/o AA:	GGCTGGTGAAAGGTGTTTATacaag
antisense	cttgtATAAACACCTTTCACCAGCC
Bulged sense	GGCTGGTGAAcGGTGTTTcTacaag
sense oligo	5'- cttgtggaaaggacgaaacaccGGCTGGTGAAcGGTGTTTcTacaagttcaagagacttgtATAAACACCTTTCACCAGCCttttt<u>ctgcag</u>tttt - 3'
<u>Baf170 3'UTR #1</u>	aaaactgcagaaaaaGGCTGGTGAAAGGTGTTTATacaagtctcttgaacttgtAgAAACACCgTTCACCAGCCggtgtttcgtcctttccacaag
86% KD	

Appendix III. Supplementary shRNA Sequences targeting BRM and BAF subunits (Continued)

BAF170 shRNA sequences	
target seq:	GGTGTTTATACAAGGTTCTA
extended seq w/o AA:	GGTGTTTATACAAGGTTCTAttaac
antisense	gttaaTAGAACCTTGTATAAACACC
Bulged sense	GGTGTTTATAgAAGGTTCaAttaac
sense oligo	5'- cttgtggaaaggacgaaacaccGGTGTTTATAgAAGGTTCaAttaacttcaagagagttaaTAGAACCTTGTATAAACACCttttt<u>ctgcag</u>tttt - 3'
<u>shBaf170 3'UTR #3</u>	aaaactgcagaaaaaGGTGTTTATACAAGGTTCTAttaactctcttgaagttaaTtGAACCTTcTATAAACACCggtgtttcgtcctttccacaag
88% KD	

BAF57 shRNA Sequences	
target seq:	CCGCGTACCTTGCTTACATAA
extended seq with +G	GCCGCGTACCTTGCTTACATAAatg
antisense	catTTATGTAAGCAAGGTACGCGGC
sense oligo	5'- cttgtggaaaggacgaaacaccGCCGCGTACCTTGCTTACATAAatgttcaagagacatTTATGTAAGCAAGGTACGCGGCttttt<u>ctgcag</u>tttt - 3'
<u>RO Baf57 #2</u>	aaaactgcagaaaaaGCCGCGTACCTTGCTTACATAAatgtctcttgaacatTTATGTAAGCAAGGTACGCGGCggtgtttcgtcctttccacaag
73% KD	

BAF155 shRNA Sequences	
target length:	23mer
target seq:	AAGGAACTCACTTGGCAGTCAGA
extended seq w/o AA:	GGAACTCACTTGGCAGTCAGAgcat
antisense	atgcTCTGACTGCCAAGTGAGTTCC
Bulged sense	**GGAACTCACTaGGCAGTCtGAgcat**
sense oligo	5'- cttgtggaaaggacgaaacaccGGAACTCACTaGGCAGTCtGAgcatttcaagagaatgcTCTGACTGCCAAGTGAGTTCCttttt<u>ctgcag</u>tttt - 3'
<u>RO Baf155 3'UTR #1</u>	aaaactgcagaaaaaGGAACTCACTTGGCAGTCAGAgcattctcttgaaatgcTCaGACTGCCtAGTGAGTTCCggtgtttcgtcctttccacaag
72% KD	

Appendix III. Supplementary shRNA Sequences targeting BRM and BAF subunits (Continued)

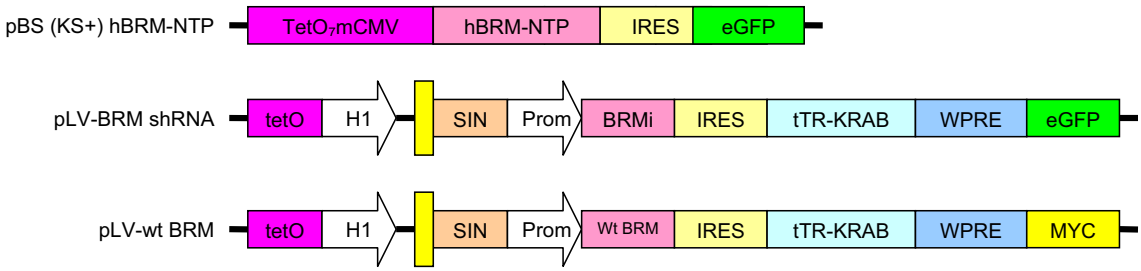

Appendix IV. Diagram of BRM Constructs Utilized

Full methodology of construct and virus production are included in methods for Chapters 2 and 3 respectively.

Gene Symbol	Fold change	Regulation	Gene Description
C20orf69	1.61	down	chromosome 20 open reading frame 69
RNU5E	1.62	down	RNA, U5E small nuclear
CYP4Z1	1.61	down	cytochrome P450, family 4, subfamily Z, polypeptide 1
IFI44L	1.92	up	interferon-induced protein 44-like
IFI44	1.63	up	interferon-induced protein 44
PHGDH	2.37	down	phosphoglycerate dehydrogenase
RASSF5	2.02	down	Ras association (RalGDS/AF-6) domain family member 5
C20orf69	1.61	down	chromosome 20 open reading frame 69
SNORA61	1.70	up	small nucleolar RNA, H/ACA box 61 | chromosome 1 open reading frame 79
SLC6A9	1.91	down	solute carrier family 6 (neurotransmitter transporter, glycine), member 9
RNU5F	1.63	up	RNA, U5F small nuclear
F3	1.90	up	coagulation factor III (thromboplastin, tissue factor)
SNORD47|GAS5	1.62	up	small nucleolar RNA, C/D box 47 | growth arrest-specific 5
SNORD78	2.42	up	small nucleolar RNA, C/D box 78
SNORD44	1.89	up	small nucleolar RNA, C/D box 44
SNORD75	1.89	up	small nucleolar RNA, C/D box 75
	1.87	down	hypothetical protein LOC100129443 | KIAA0040
LEMD1	2.21	down	LEM domain containing 1
PFKP	1.71	up	phosphofructokinase, platelet
VIM	1.97	up	vimentin
C20orf69	1.61	down	chromosome 20 open reading frame 69
SGPL1	1.61	down	sphingosine-1-phosphate lyase 1
PAPSS2	1.65	up	3'-phosphoadenosine 5'-phosphosulfate synthase 2
	1.81	up	
PNLIPRP3	1.80	down	pancreatic lipase-related protein 3
LIPA	1.85	up	lipase A, lysosomal acid, cholesterol esterase (Wolman disease)
BNIP3	1.80	up	BCL2/adenovirus E1B 19kDa interacting protein 3
HIPK3	1.82	down	homeodomain interacting protein kinase 3
CD82	1.61	down	
	1.61	down	chromosome 20 open reading frame 69
CARS	1.65	down	cysteinyl-tRNA synthetase
TCN1	2.01	down	transcobalamin I (vitamin B12 binding protein, R binder family)

SNORD30	1.99	up	small nucleolar RNA, C/D box 30
	1.82	up	
TMPRSS13	1.69	down	transmembrane protease, serine 13
MARS	1.62	down	methionyl-tRNA synthetase
GLIPR1	1.76	up	GLI pathogenesis-related 1 (glioma)
MYBPC1	1.79	down	myosin binding protein C, slow type
TCP11L2	2.52	down	t-complex 11 (mouse)-like 2
MGP	2.78	down	matrix Gla protein
ITGA5	1.71	up	integrin, alpha 5 (fibronectin receptor, alpha polypeptide)
	1.75	up	
ALDH1L2	2.25	down	aldehyde dehydrogenase 1 family, member L2
STX2	1.65	up	syntaxin 2
CCNA1	2.68	down	cyclin A1
MIPEP	1.69	down	mitochondrial intermediate peptidase
POSTN	1.90	up	periostin, osteoblast specific factor
PCK2	1.84	down	phosphoenolpyruvate carboxykinase 2 (mitochondrial)
SMOC1	1.75	down	SPARC related modular calcium binding 1
SERPINA5	1.89	down	serpin peptidase inhibitor, clade A
SERPINA3	1.81	down	serpin peptidase inhibitor, clade A
CRIP2	1.68	down	cysteine-rich protein 2
NID2	1.72	up	nidogen 2 (osteonidogen)
DIO2	2.14	up	deiodinase, iodothyronine, type II
GCNT3	2.67	down	glucosaminyl (N-acetyl) transferase 3, mucin type
GRAMD2	1.61	down	GRAM domain containing 2
	2.49	down	
	1.69	up	
GPT2	2.37	down	glutamic pyruvate transaminase (alanine aminotransferase) 2
MMP2	1.62	up	matrix metallopeptidase 2
MT2A	1.74	up	metallothionein 2A
MT1L	1.65	up	metallothionein 1L (gene/pseudogene)
MT1E	2.14	up	metallothionein 1E
MT1DP	1.75	up	metallothionein 1D (pseudogene)
MT1F	1.83	up	metallothionein 1F
MT1X	1.87	up	metallothionein 1X
GPR56	1.73	down	G protein-coupled receptor 56

	1.64	down	
HSD11B2	2.24	down	hydroxysteroid (11-beta) dehydrogenase 2
GAN	1.76	down	giant axonal neuropathy (gigaxonin)
	1.79	down	chromosome 20 open reading frame 69
PPL	1.66	down	periplakin
NUPR1	2.57	down	nuclear protein 1
MT1G	1.97	up	metallothionein 1G
PLLP	1.60	down	plasma membrane proteolipid (plasmolipin)
AARS	1.69	down	alanyl-tRNA synthetase
MLKL	1.63	up	mixed lineage kinase domain-like
CDRT1	2.04	down	CMT1A duplicated region transcript 1
LOC201229	1.62	down	
PECAM1	1.99	down	platelet/endothelial cell adhesion molecule (CD31 antigen)
	1.78	down	
CASP14	2.19	up	caspase 14, apoptosis-related cysteine peptidase
UCA1	2.00	up	urothelial cancer associated 1
	5.41	up	
ZNF114	1.87	up	zinc finger protein 114
	1.61	down	chromosome 20 open reading frame 69
AP1M2	1.64	down	adaptor-related protein complex 1, mu 2 subunit
	1.70	up	
KLK5	1.91	down	kallikrein-related peptidase 5
TMC4	1.71	down	transmembrane channel-like 4
ATP6V1B1	2.18	down	ATPase, H+ transporting, lysosomal
MTHFD2	1.62	down	methylenetetrahydrofolate dehydrogenase
CYBRD1	1.70	down	cytochrome b reductase 1
AOX1	1.80	up	aldehyde oxidase 1
	1.71	down	
	1.68	down	
	1.63	down	
	2.01	up	
ZEB2	1.64	up	zinc finger E-box binding homeobox 2
ABCA12	1.69	down	ATP-binding cassette, sub-family A (ABC1), member 12
FN1	2.13	up	fibronectin 1
EPHA4	1.83	up	EPH receptor A4

PER2	1.94	down	period homolog 2 (Drosophila)
TRIB3	1.98	down	tribbles homolog 3 (Drosophila)
MT1P3|MT1JP	1.68	up	metallothionein 1 pseudogene 3 | metallothionein 1J (pseudogene)
TSHZ2	1.80	down	teashirt zinc finger homeobox 2
SDCBP2	1.71	down	syndecan binding protein (syntenin) 2
SLC4A11	1.66	down	solute carrier family 4, sodium borate transporter, member 11
CLDN8	2.34	down	claudin 8
PXK	1.63	down	PX domain containing serine/threonine kinase
GRAMD1C	1.68	down	GRAM domain containing 1C
	1.64	down	
DKFZP	1.61	down	similar to hypothetical protein LOC284701
	2.00	down	
CCDC80	1.95	up	coiled-coil domain containing 80
FSTL1	2.02	up	follistatin-like 1
CCDC58	1.62	up	coiled-coil domain containing 58
PLOD2	1.82	up	procollagen-lysine, 2-oxoglutarate 5-dioxygenase 2
GNB4	1.64	up	guanine nucleotide binding protein (G protein), beta polypeptide 4
BCL6	1.66	down	B-cell CLL/lymphoma 6 (zinc finger protein 51)
CLDN1	1.64	down	claudin 1
CCR2	1.63	down	chemokine (C-C motif) receptor 2 | chemokine (C-C motif) receptor 2-like
	1.79	down	
MT2A	1.86	up	metallothionein 2A
TMPRSS	1.84	up	transmembrane protease, serine 11E2 | metallothionein 2A
AREG	1.94	up	amphiregulin (schwannoma-derived growth factor)
AREG	2.06	up	amphiregulin (schwannoma-derived growth factor)
RXFP1	2.01	down	relaxin/insulin-like family peptide receptor 1
TLR1	1.69	down	toll-like receptor 1
	1.64	up	
SLC7A11	3.26	down	solute carrier family 7, (cationic amino acid transporter, y+ system)
IL7R	3.66	up	interleukin 7 receptor
SKP2	1.65	up	S-phase kinase-associated protein 2 (p45)
IL31RA	1.61	up	interleukin 31 receptor A
F2R	1.84	up	coagulation factor II (thrombin) receptor
TGFBI	1.64	up	transforming growth factor, beta-induced, 68kDa
SPINK6	1.77	up	serine peptidase inhibitor, Kazal type 6

C20orf69	1.61	down	chromosome 20 open reading frame 69
	1.62	down	membrane-associated ring finger (C3HC4) 11
HMGCS1	2.31	up	3-hydroxy-3-methylglutaryl-Coenzyme A synthase 1 (soluble)
F2RL2	1.64	up	coagulation factor II (thrombin) receptor-like 2
C5orf13	2.27	up	chromosome 5 open reading frame 13
HBEGF	1.69	down	heparin-binding EGF-like growth factor
CD14	1.66	down	
LOC644714	1.89	down	
MICB	1.66	up	MHC class I polypeptide-related sequence B
NT5E	1.90	up	5'-nucleotidase, ecto (CD73)
TREM1	2.04	up	triggering receptor expressed on myeloid cells 1
GPR110	1.76	down	G protein-coupled receptor 110
C6orf138	1.76	down	chromosome 6 open reading frame 138
LAMA4	1.70	up	laminin, alpha 4
	1.70	down	
AHR	1.77	down	aryl hydrocarbon receptor
	1.62	down	
SNORA22	1.80	down	small nucleolar RNA, H/ACA box 22
CD36	3.13	up	
SERPINE1	2.36	up	serpin peptidase inhibitor, clade E
PRKAR2B	2.05	down	protein kinase, cAMP-dependent, regulatory, type II, beta
IFRD1	1.88	down	interferon-related developmental regulator 1
CPA4	2.41	up	carboxypeptidase A4
	1.61	down	chromosome 20 open reading frame 69
AGR2	3.13	down	anterior gradient homolog 2 (Xenopus laevis)
IGFBP3	1.76	up	insulin-like growth factor binding protein 3
PDK4	1.70	down	pyruvate dehydrogenase kinase, isozyme 4
SLC25A13	1.88	up	solute carrier family 25, member 13 (citrin)
ASNS	4.47	down	asparagine synthetase
AZGP1	3.66	down	alpha-2-glycoprotein 1, zinc-binding
JHDM1D	1.63	down	jumonji C domain containing histone demethylase
ATP6V0D2	1.76	down	ATPase, H+ transporting, lysosomal 38kDa, V0 subunit d2
POP1	1.83	up	processing of precursor 1, ribonuclease P/MRP
	1.61	down	
LOXL2	1.84	up	lysyl oxidase-like 2

STC1	2.17	up	stanniocalcin 1
SNAI2	2.03	up	snail homolog 2 (Drosophila)
FABP4	3.11	up	fatty acid binding protein 4, adipocyte
CCNE2	1.76	up	cyclin E2
HAS2	1.68	up	hyaluronan synthase 2
FBXO32	2.45	down	F-box protein 32
SMARCA2	**1.94**	**down**	**SWI/SNF related, matrix associated,regulator of chromatin**
PSAT1	2.52	down	phosphoserine aminotransferase 1
SNORD36B	1.74	up	ribosomal protein L7a
MT1G	1.89	up	metallothionein 1G
	1.70	down	
GK|GK3P	1.74	down	glycerol kinase | glycerol kinase 3 pseudogene
TSC22D3	1.71	down	TSC22 domain family, member 3
C20orf69	1.62	down	chromosome 20 open reading frame 69
C20orf69	1.61	down	chromosome 20 open reading frame 69

Table 3.2 Complete Microarray Analysis of Genes Altered in BRM-deficient non-malignant MECs

UCSF Library Release

Publishing Agreement

It is the policy of the University to encourage the distribution of all theses, dissertations, and manuscripts. Copies of all UCSF theses, dissertations, and manuscripts will be routed to the library via the Graduate Division. The library will make all theses, dissertations, and manuscripts accessible to the public and will preserve these to the best of their abilities, in perpetuity.

Please sign the following statement:

I hereby grant permission to the Graduate Division of the University of California, San Francisco to release copies of my thesis, dissertation, or manuscript to the Campus Library to provide access and preservation, in whole or in part, in perpetuity.

Author Signature

4/19/2010

Date